

Proceedings of the  
**Forty-First**  
**DOE Solar Photochemistry**  
**P.I. Meeting**

Gaithersburg Marriott Washingtonian Center  
Gaithersburg, Maryland  
June 3-5, 2019

Chemical Sciences, Geosciences, and Biosciences Division  
Office of Basic Energy Sciences  
Office of Science  
U.S. Department of Energy

## FOREWORD

The 41<sup>st</sup> Department of Energy Solar Photochemistry Principal Investigators' Meeting, sponsored by the Chemical Sciences, Geosciences, and Biosciences Division of the Office of Basic Energy Sciences, is being held June 3-5, 2019 at the Washingtonian Marriott in Gaithersburg, Maryland. These proceedings include the meeting agenda, abstracts of the formal presentations and posters, and a list of participants.

The Solar Photochemistry Program supports fundamental, molecular-level research on solar energy capture and conversion in the condensed phase and at interfaces. This conference is the annual meeting of the grantees who conduct research with support from this Program. The gathering is intended to facilitate the exchange of ideas and foster collaboration among these researchers.

The meeting this year features an invited presentation by Harry Atwater, Director of the Joint Center for Artificial Photosynthesis (JCAP). JCAP is the Department of Energy's Fuels from Sunlight Energy Innovation Hub, a multi-investigator research and development center that was established in 2010 and renewed in 2015. Its mission is currently focused on creating a scientific foundation for the solar-driven conversion of carbon dioxide into renewable transportation fuels. Prof. Atwater will tell us about recent JCAP discoveries and research accomplishments.

I would like to express my thanks to Justin Johnson who continues to spend part of his time as a detailee for the Solar Photochemistry Program, assisting with numerous critical behind-the-scenes tasks. Special appreciation also goes to Teresa Crockett of the Office of Basic Energy Sciences and Connie Lansdon of the Oak Ridge Institute for Science and Education for their assistance with logistics for this meeting. Finally, I am grateful to all of the participants in this meeting who have contributed so much to the continued success of the Solar Photochemistry Program.

Chris Fecko  
Chemical Sciences, Geosciences,  
and Biosciences Division  
Office of Basic Energy Sciences

## TABLE OF CONTENTS

<b>Foreword</b> .....	ii
-----------------------	----

<b>Program</b> .....	xii
----------------------	-----

### Abstracts of Oral Presentations

#### Session I – Opening Session

Pathways to Selective and Efficient Carbon Dioxide Reduction <u>Harry A. Atwater</u> .....	1
---	---

#### Session II – Electron Transfer and Proton-Coupled Electron Transfer

A Bigger, Better Inverted Region <u>John R. Miller</u> , Richard A. Holroyd, Andrew R. Cook, Norihiko Takeda, Tomoyasu Mani, Marshall D. Newton, Matthew J. Bird, and Hung-Cheng Chen.....	3
---	---

Proton-Coupled Electron Transfer Drives Grothuss-Type Proton Transfer in Artificial Photosynthesis Devens Gust, <u>Thomas A. Moore</u> , and <u>Ana L. Moore</u> .....	6
---	---

Hydrogen Bonding Interactions in Photoinduced PCET <u>Dmitry E. Polyansky</u> , Sergei V. Lyamar, Mehmed Z. Ertem, and Gerald F. Manbeck.....	8
--	---

#### Session III – Molecular Chromophores and Catalysts

Model Dyes for Study of Electron Transfer Processes at Metal Oxide Semiconductor Interfaces <u>E. Galoppini</u> , <u>R. A. Bartynski</u> , L. Gundlach, A. Teplyakov, R. Harmer, H. Fan, S. Rangan, J. Vierek, J. Nieto-Pescador, and B. Abraham .....	11
---	----

Molecular Modules for Photochemical and Catalytic Function in Artificial Photosynthesis <u>Karen L. Mulfort</u> , Lars Kohler, Dugan Hayes, Ryan G. Hadt, Jens Niklas, Oleg G. Poluektov, Lin X. Chen, and David M. Tiede .....	14
--	----

Aryl Ether Weak Donor-Based Dyes as Strong Photoinduced Oxidants Roberta R. Rodrigues, Adithya Peddapuram, and <u>Jared H. Delcamp</u> .....	17
---	----

## Session IV – Supramolecular Assemblies

Photoacid Dye-Sensitized Solar Energy Conversion using Water as a Protonic Semiconductor Leanna Schulte, Simon Luo, Rylan Kautz, Joseph Cardon, William White, and <u>Shane Ardo</u> .....	18
Organic, Nanoscale, and Self-Assembled Structures Relevant to Solar Energy Conversion <u>Michael J. Therien</u> .....	20
Microsecond Charge Separation Lifetimes in Semiconducting Single-Walled Carbon Nanotube Heterojunctions <u>Jeff Blackburn</u> , Hyun Suk Kang, Dana Sulas, Andrew Ferguson, Justin Johnson, and Garry Rumbles .....	23

## Session V – Singlet Fission and Triplet Dynamics

Ultrafast Vibrational Nano-Thermometers to Probe Triplet Separation vs. Relaxation during Singlet Fission Eric R. Kennehan, Grayson S. Doucette, and <u>John B. Asbury</u> .....	28
Triplet Energy Transduction in Designed Chromophore Architectures Melissa K. Gish, Nadia V. Korovina, Marissa Martinez, Natalie A. Pace, Nicholas Pompetti, Matthew C. Beard, and <u>Justin C. Johnson</u> .....	32
Singlet Fission in Nanocrystal-Molecule Hybrid Structures Zhiyuan Huang and <u>Ming Lee Tang</u> .....	36
Quantum Interferences among Dexter Energy Transfer Pathways Shuming Bai, Peng Zhang, Spiros S. Skourtis, and <u>David N. Beratan</u> .....	38

## Session VI – Bioinspired/Biohybrid Approaches

Modular Nanoscale and Biomimetic Assemblies for Photocatalytic Hydrogen Generation <u>Kara L. Bren</u> , <u>Todd D. Krauss</u> , and <u>Ellen M. Matson</u> .....	40
Photochemical N <sub>2</sub> Reduction by Nanoparticle-Nitrogenase Complexes Katherine A. Brown, Jesse Ruzicka, Hayden Kallas, Bryant Chica, David W. Mulder, <u>John W. Peters</u> , Gordana Dukovic, <u>Lance C. Seefeldt</u> , and <u>Paul W. King</u> .....	43

## Session VII – Semiconductor Nanoparticles for Solar Energy Conversion

Controlling the Optical and Electrical Properties of QDs, QD assemblies, and QD Films for Solar Energy Conversion Daniel Kroupa, Haipeng Lu, Noah Bronstein, Yong Yan, Nathan Neale, Elisa Miller, Mike Carroll, Marissa Martinez, Arthur J. Nozik, Justin C. Johnson, and <u>Matthew C. Beard</u> .....	45
Hot-Carrier Dynamics in Quantum Dots Manipulated by Spin-Exchange Auger Interactions Rohan Singh, Wenyong Liu, Jaehoon Lim, Istvan Robel, and <u>Victor I. Klimov</u> .....	50
Time-Domain Atomistic Studies of Far-from-Equilibrium Dynamics in Nanoscale Materials for Solar Energy Harvesting <u>Oleg V. Prezhdo</u> .....	52
Metal-Tipped and Electrochemically Wired Semiconductor Nanocrystals: Modular Constructs for Directed Charge Transfer Jeffry Pyun, S. Scott Saavedra, and <u>Neal R. Armstrong</u> .....	57

## Session VIII – Semiconductor Photoelectrodes

Modulation of Photoinduced Charge Transfer at the Semiconductor Interface Rebecca Scheidt, Elizabeth Kerns, Greg Samu, and <u>Prashant V. Kamat</u> .....	59
Molecular Level Functionalization, Atomically Thin Photoelectrodes, and Protective Coatings Based on Two-Dimensional Materials Ellen X. Yan, Annelise C. Thompson, Burton H. Simpson, Miguel A. Cabán-Acevedo, Kimberly M. Papadantonakis, Bruce S. Brunschwig, and <u>Nathan S. Lewis</u> .....	63
Photoexcited Charge Carrier Dynamics at Photocatalytic Semiconductor/liquid Interfaces Zed Xu, Haotian Shi, Bingya Hou, Fengyi Zhao, Tim Lian, and <u>Stephen B. Cronin</u> .....	65
Investigating Ultrafast Dynamics in Solid-State Photocatalytic and Photovoltaic Materials Using Time-Resolved Mössbauer Spectroscopy Cali Antolini, Melissa A. Smith, Jacqueline Escolastico, Nathan Girard, Xiaoyi Zhang, E. Ercan Alp, <u>Benjamin T. Young</u> , and <u>Dugan Hayes</u> .....	67

## Session IX – Heterogeneous Solar Fuels Catalysts

Tracking Structures in Solar Fuels Catalysis: In-situ X-ray Characterization of Interfacial Water-Splitting Molecular and Thin-Film Catalysts <u>David M. Tiede</u> , Gihan Kwon, Alex B. F. Martinson, Tae Wu Kim, Emily Sprague-Klein, Karen L. Mulfort, Oleg G. Poluektov, and Lin X. Chen.....	69
---	----

Nanoscale Probing of Carrier-Selective Catalyst-Semiconductor Contacts in Water-Splitting Photoelectrodes  
Shannon W. Boettcher, Forrest Laskowski, Michael Nellist, Jingjing Qui, Sebastian Oener, and Adrian Gordon.....72

Proton-Coupled Electron Transfer Studies of Homogeneous and Heterogeneous Energy Conversion Catalysts  
Daniel G. Nocera .....75

### **Session X – Building Systems for Generating Solar Fuels**

Exploring the Synergy between Semiconductor Surfaces and Molecular Catalysts for Efficient Solar CO<sub>2</sub> Reduction  
Peipei Huang, Sebastian Pantovich, Ethan Jarvis, Christine A. Caputo, and Gonghu Li..79

Nanostructured Solar Fuel Systems  
Pengtao Xu, Yugang C. Li, Zhifei Yan, Jeremy L. Hitt, Tian Huang, John R. Swierk, Nicholas S. McCool, Christopher L. Gray, and Thomas E. Mallouk.....81

Charge Transport and Catalytic Mechanisms for Coupling Visible Light Driven CO<sub>2</sub> Reduction and H<sub>2</sub>O Oxidation across Ultrathin Oxide Membrane  
Heinz Frei.....84

### **Abstracts of Poster Presentations**

1. Crystal Packing and Singlet Fission Rates  
Paul I. Dron, Dean Antic, Christopher M. Pochas, Eric A. Buchanan, Andrew J. Chomas, Zdenek Havlas, Alexandr Zaykov, and Josef Michl.....88
2. Size Dependent Plasmon Induced Hot Electron Transfer in CdS-Au Nanorods  
Tianquan Lian.....89
3. Toward More Stable Water Oxidation Catalysts: Progress in Measurement and Synthesis  
Aaron G. Nash, Colton Breyer, Brett D. Vincenzini, Thomas Chi Cao, Dale Chatfield, Diane K. Smith, Douglas B. Grotjahn .....90
4. Photoredox Catalysts Involving Square Planar Cyclotetrapyridyl-type Ligands and Their Synthesis Using Metal Template Methodology  
Lanka Wickramasinghe, Liubov Lifshits, Elamparuthi Ramasamy, Ramesh Deshmukh and Randolph P. Thummel .....91

5. Nanoelectrode as a Light Guide for Photoelectrochemical Imaging and Collision Experiments Je Hyun Bae, Alexander Nepomnyashchii, Qian Wang, Xiang Wang, and <u>Michael V. Mirkin</u> .....	92
6. Revealing Oxidation Mechanisms onto Semiconductor Surfaces Xueqiang Zhang, Tadashi Ogitsu, Brandon C. Wood, Tuan Anh Pham, and <u>Sylwia Ptasinska</u> .....	93
7. Tuning 2D MoS <sub>2</sub> and WS <sub>2</sub> Catalytic Activity and Optoelectronic Properties Hanyu Zhang, Jeremy R. Dunklin, Obadiah G. Reid, Sanjini U. Nanayakkara, Seok Joon Yun, Young Hee Lee, Tong Sun, Xiang Wang, Jun Liu, Chuanxiao Xiao, Michael V. Mirkin, Jeffrey L. Blackburn, and <u>Elisa M. Miller</u> .....	94
8. Collaboration between Experiment and Theory for Design of Panchromatic Dyes Shin Hee Lee, Adam J. Matula, Gongfang Hu, Jennifer L. Troiano, Christopher J. Karpovich, <u>Victor S. Batista</u> , <u>Gary W. Brudvig</u> , <u>Robert H. Crabtree</u> and <u>Charles A. Schmuttenmaer</u> .....	95
9. Electronic and Vibrational Coherence in Heterogeneous Electron Transfer <u>Lars Gundlach</u> , Elena Galoppin, Baxter Abraham, Zhengxin Li, Hao Fan, and Ryan Harmer .....	96
10. Symmetry Breaking Charge Transfer for Rapid, Long-Lived Charge Separation <u>Mark Thompson</u> , <u>Stephen Bradforth</u> , Mike Kellogg, Ali Akil, and Laura Estergreen.....	97
11. MOFs as Scaffolds for Light-Harvesting and Solar Energy Conversion: Fundamental Studies of Energy and Charge Transport <u>Joseph T. Hupp</u> .....	98
12. C-H Bond Formation with CO <sub>2</sub> : Toward Carbon Neutral Fuel Production <u>Louise A. Berben</u> , Natalia D. Loewen, and Cody R. Carr.....	99
13. Dynamics of Liquid and Solid-State Copper Complex Electron Transfer and Transport Tea-Yon Kim, Austin L. Raithel, Yujue Wang and <u>Thomas W. Hamann</u> .....	100
14. Electron/hole Selectivity in Organic Semiconductor Contacts for Solar Energy Conversion Kira Egelhofer, Ellis Roe, and <u>Mark C. Lonergan</u> .....	101
15. Electrochemically and Plasmonically Modifying the Interfacial Thermodynamics, Excitonic and Charge Transfer Kinetics of 2D Transition Metal Dichalcogenides for (Photo)electrochemical Catalysis G. Michael Carroll, Jeremy Dunklin, Aaron Rose, Hanyu Zhang, Elisa M. Miller, Nathan R. Neale, and <u>Jao van de Lagemaat</u> .....	102

16. Escape and Recombination of Delocalized Charge in Nonpolar Media Jack Burke, Madison Jilek, Jake Keiper, and <u>Matthew Bird</u> .....	103
17. State Mixing Determines the Fate of the Multiexciton State in Singlet Fission <u>Michael R. Wasielewski</u> .....	104
18. Integrated Synthetic, Computational, Spectroelectrochemical Study of Polyoxometalate Water Oxidation Catalyst-Based Photoanodes <u>Craig L. Hill</u> , <u>Tianquan Lian</u> , and <u>Djamaladdin G. Musaev</u> .....	105
19. Ligand Control of Nanocrystal Band Energetics David P. Morgan and <u>David F. Kelley</u> .....	106
20. Spatial and Temporal Imaging of Energy Transport in Two-Dimensional Heterostructures Long Yuan, Daria D. Blach, Shubin Deng, and <u>Libai Huang</u> .....	107
21. Advances in Controlling and Studying Semiconductor/Electrolyte Interfaces: Electrodeposition of Protective Layers on p-InGaP <sub>2</sub> and Operation of Semiconductor Ultramicroelectrodes under Accumulation Conditions Mitchell Lancaster and <u>Stephen Maldonado</u> .....	108
22. Fundamental Studies on DSPEC for Water Splitting Lei Wang, Renato N. Sampaio, Gerald F. Manbeck, Dmitry E. Polyansky, and <u>Javier J. Concepcion</u> .....	109
23. Slow Charge Transfer from Pentacene Triplet States to Molecular Acceptors at the Optimal Driving Force Natalie Pace, Justin Johnson, <u>Garry Rumbles</u> , and Obadiah Reid.....	110
24. Sensitized Photocurrents on Single Crystal Semiconductors from Quantum Confined Semiconducting Carbon Nanotubes and Perovskite Quantum Dots: Hot Injection and Possible Multiple Excitons from Sub-bandgap Illumination Kevin Watkins, Lenore Kubie, Yuqi Shi, and <u>Bruce Parkinson</u> .....	111
25. Transport and Excitations in the Photoanode of a Dye-Sensitized Solar Cell <u>Frances Houle</u> and Thomas Cheshire .....	112
26. Probing Excited State Pathways by Coherent Vibrational Motions in Light Conversion Model Pt Dimer Complexes Using Femtosecond Optical Spectroscopy and X-ray Scattering Pyosang Kim, Denis Leshchev, Subhangi Roy, Andrew Valentine, Antonio A. Lopez, Felix N. Castellano, Xiaosong Li, and <u>Lin X. Chen</u> .....	113

27. Insights into the Reaction Coordinate for MLCT-state Deactivation: Using Vibronic Coherence to Inform Synthetic Design Bryan C. Paulus, Sara L. Adelman, Lindsey L. Jamula, and <u>James K. McCusker</u> .....	114
28. Surface Photovoltage Studies on Inorganic Tandem Photocatalysts for Overall Water Splitting <u>Frank E. Osterloh</u> .....	115
29. New Chromophores for Bookending the Near Ultraviolet and Near Infrared Regions: “Blue” BODIPYs and Annulated Bacteriochlorins <u>David F. Bocian</u> , <u>Dewey Holten</u> , <u>Christine Kirmaier</u> , and <u>Jonathan S. Lindsey</u> .....	116
30. Controlling Singlet Fission by Molecular Contortion <u>X.-Y. Zhu</u> and <u>C. Nuckolls</u> .....	117
31. Toward Photo-induced Water Oxidation by Dual-Function Metal Organic Frameworks Shaoyang Lin, Arnab Chakraborty, Shaunak Shaikh, Bradley Gibbons, and <u>Amanda Morris</u> .....	118
32. Combined Theoretical and Experimental Investigations of Atomic Doping to Enhance Photon Absorption and Carrier Transport of LaFeO <sub>3</sub> Photocathodes Garrett P. Wheeler, Valentin Baltazar, Tyler Smart, Andjela Radmilovic, Yuan Ping, and <u>Kyoung-Shin Choi</u> .....	119
33. Thermochemical Guidelines for Designing Efficient H <sub>2</sub> Evolution or Selective CO <sub>2</sub> Reduction Catalysts & First Stable and Selective Synthetic Electrocatalyst for Reversible CO <sub>2</sub> /HCO <sub>2</sub> <sup>-</sup> Conversion Bianca Ceballos, Drew Cunningham, Caitlin Hanna, Zachary Thammavongsy, Reyna Velasquez, Andrew Luu, and <u>Jenny Y. Yang</u> .....	120
34. Theoretical Limits of Multiple Exciton Generation and Singlet Fission Tandem Devices for Solar Water Splitting Marissa Martinez, <u>Arthur J. Nozik</u> , and Matthew C. Beard .....	121
35. Polarizability and Low-Frequency Vibrations in Electron-Transfer Reactions <u>D. V. Matyushov</u> and M. D. Newton .....	122
36. Two Dimensional Electronic Vibrational (2DEV) Spectroscopy and Quantum Light Spectroscopy <u>G.R. Fleming</u> , Eric Wu, Eric Arsenault, Pallavi Bhattacharyya and Kaydren Orcutt .....	123
37. Z-Scheme Solar Water Splitting via Self-Assembly of Photosystem I-Catalyst Hybrids in Thylakoid Membranes <u>Lisa M. Utschig</u> , Sarah R. Soltau, Karen L. Mulfort, Jens Niklas, and Oleg G. Poluektov .....	124

38. Determination of Vibrational Motions Driving Photoinduced Electron Transfer Reactions in Molecular Crystals and Organic Thin Films Christopher C. Rich, Kajari Bera, Alyssa A. Cassabaum, and <u>Renee R. Frontiera</u> .....	125
39. Charge Separation and Triplet Exciton Formation Pathways in Small-Molecule Bulk Heterojunction Blends as Studied by Time-Resolved EPR Spectroscopy <u>Oleg G. Poluektov</u> , Jens Niklas, Karen L. Mulfort, Lin X. Chen, David M. Tiede, and Kristy L. Mardis.....	126
40. Halide Substitution Modulates Screening in Lead Halide Perovskites Casey L. Kennedy, Andrew H. Hill, and <u>Erik M. Grumstrup</u> .....	127
41. Roles of Triethanolamine in Photochemical CO <sub>2</sub> Reduction with [Ru(dmb) <sub>2</sub> (CO) <sub>2</sub> ] <sup>2+</sup> and Ru(II)-Ru(II) Supramolecular Systems R. N. Sampaio, D. C. Grills, D. E. Polyansky, and <u>E. Fujita</u> .....	128
42. Extremes in Photophysical Behavior from Re(I) MLCT Excited States Hala Atallah, Chelsea M. Taliaferro, Joseph M. Favale, and <u>Felix N. Castellano</u> .....	129
43. Kinetic Dispersion and Lateral Interactions Detected in Ferrocene-Modified Amorphous Carbon Electrodes Arise from Inherent Disorder in Carbon Materials <u>Jillian L. Dempsey</u> , Debanjan Dhar, Brittany Huffman, Matthew Lockett, and Catherine McKenas .....	130
44. Development of Robust Plasmonic and Excitonic Nanostructures for Investigation of Energy Conversion Dynamics in Hybrid Plexcitonic Model Systems Christopher W. Leishman, Nikunj Kumar Visaveliya, Kara Ng <sup>1</sup> , Pooja Gaikwad, Amedee des Georges, Alexander Govorov, and <u>Dorthe M. Eisele</u> .....	131
45. Mechanistic Studies of Synergistic Metal-Ligand Cooperativity Promoted by a Ligand-Based Redox Couple <u>David C. Grills</u> , Mehmed Z. Ertem, and Etsuko Fujita .....	132
46. Molecular Photoelectrocatalysts for Hydrogen Evolution Bethany M. Stratakes, Tianfei Liu, Dean Bass, and <u>Alexander J. M. Miller</u> .....	133
47. Coherences in Photoinduced Electron Transfer Reaction: A Mechanistic Insight Shahnawaz Rafiq, Bo Fu, and <u>Gregory D. Scholes</u> .....	134
48. Precise Mechanisms of CO <sub>2</sub> to CO Conversion Catalyzed by Iridium(III) Phenyl-Pyridine Photo- and Electrocatalysts <u>Gerald F. Manbeck</u> , Mehmed Z. Ertem, Dmitry E. Polyansky, and Etsuko Fujita .....	135
49. Electron Transfer Dynamics in Efficient Molecular Solar Cells Andrew Maurer, Eric Piechota, Victoria Davis, and <u>Gerald J. Meyer</u> .....	136

50. Surface Chemistry and Heterogeneous Processes in Solar-Driven Pyridine-Catalyzed CO <sub>2</sub> Reduction Denis Potapenko, Ari Gilman, and <u>Bruce E. Koel</u> .....	137
51. Coherent Energy and Charge Transport Processes in Photovoltaic Dendritic Molecular Systems Probed in Solution and in the Solid State <u>T. Goodson III</u> .....	138
52. Energetic Effects of Hybrid Organic/Inorganic Interfacial Architecture on Nanoporous Black Silicon Photoelectrodes Ryan T. Pekarek, Steven T. Christensen, Jun Liu, and <u>Nathan R. Neale</u> .....	139
53. Mechanistic Investigation of Oxygen Atom Transfer Pathway for Ru-based Water Oxidation Catalysts <u>Mehmed Z. Ertem</u> and Javier J. Concepcion .....	140

**41<sup>st</sup> DOE SOLAR PHOTOCHEMISTRY  
P.I. MEETING**

**June 3-5, 2019**

**Washingtonian Marriott  
Gaithersburg, MD**

**PROGRAM**

**Monday Morning, June 3**

7:30 a.m. Breakfast

**SESSION I  
Opening Session**

8:30 a.m. News from DOE-BES Chemical Sciences, Geosciences, and Biosciences Division  
**Bruce Garrett and Chris Fecko**, DOE Office of Basic Energy Sciences

9:00 a.m. *Invited Presentation from the Joint Center for Artificial Photosynthesis*  
Pathways to Selective and Efficient Carbon Dioxide Reduction  
**Harry A. Atwater**, California Institute of Technology

10:00 a.m. Break

**SESSION II  
Electron Transfer and Proton-Coupled Electron Transfer**  
Amanda Morris, Chair

10:30 a.m. A Bigger, Better Inverted Region  
**John R. Miller**, Brookhaven National Laboratory

11:00 a.m. Proton-Coupled Electron Transfer Drives Grotthuss-Type Proton Transfer in  
Artificial Photosynthesis  
**Thomas A. Moore and Ana L. Moore**, Arizona State University

11:30 a.m. Hydrogen Bonding Interactions in Photoinduced PCET  
**Dmitry E. Polyansky**, Brookhaven National Laboratory

12:00 p.m. Working Lunch (*Discussions about morning scientific presentations*)

## Monday Afternoon, June 3

### **SESSION III** **Molecular Chromophores and Catalysts** Mark Thompson, Chair

- 3:00 p.m. Model Dyes for Study of Electron Transfer Processes at Metal Oxide Semiconductor Interfaces  
**Elena Galoppini and Robert A. Bartynski**, Rutgers University
- 3:30 p.m. Molecular Modules for Photochemical and Catalytic Function in Artificial Photosynthesis  
**Karen Mulfort**, Argonne National Laboratory
- 4:00 p.m. Aryl Ether Weak Donor-Based Dyes as Strong Photoinduced Oxidants  
**Jared H. Delcamp**, University of Mississippi
- 4:15 p.m. Break

### **SESSION IV** **Supramolecular Assemblies** Tim Lian, Chair

- 4:45 p.m. Photoacid Dye-sensitized Solar Energy Conversion using Water as a Protonic Semiconductor  
**Shane Ardo**, University of California, Irvine
- 5:00 p.m. Organic, Nanoscale, and Self-Assembled Structures Relevant to Solar Energy Conversion  
**Michael J. Therien**, Duke University
- 5:30 p.m. Microsecond Charge Separation Lifetimes in Semiconducting Single-walled Carbon Nanotube Heterojunctions  
**Jeff Blackburn**, National Renewable Energy Laboratory

## Monday Evening, June 3

- 6:00 p.m. Working Dinner (*Discussions about afternoon presentations*)
- 7:30 p.m. Posters (*Odd numbers*)

## Tuesday Morning, June 4

7:30 a.m. Breakfast

### **SESSION V** **Singlet Fission and Triplet Dynamics** Renee Frontiera, Chair

8:30 a.m. Ultrafast Vibrational Nano-Thermometers to Probe Triplet Separation vs. Relaxation during Singlet Fission  
**John B. Asbury**, Pennsylvania State University

9:00 a.m. Triplet Energy Transduction in Designed Chromophore Architectures  
**Justin C. Johnson**, National Renewable Energy Laboratory

9:30 a.m. Singlet Fission in Nanocrystal-Molecule Hybrid Structures  
**Ming Lee Tang**, University of California, Riverside

9:45 a.m. Quantum Interferences among Dexter Energy Transfer Pathways  
**David N. Beratan**, Duke University

10:00 a.m. Break

### **SESSION VI** **Bioinspired/Biohybrid Approaches** Gary Brudvig, Chair

10:30 a.m. Modular Nanoscale and Biomimetic Assemblies for Photocatalytic Hydrogen Generation  
**Kara L. Bren, Todd D. Krauss, and Ellen M. Matson**, University of Rochester

11:15 a.m. Photochemical N<sub>2</sub> Reduction by Nanoparticle-Nitrogenase Complexes  
**John W. Peters**, Washington State University  
**Lance C. Seefeldt**, Utah State University  
**Paul W. King**, National Renewable Energy Laboratory

12:00 p.m. Working Lunch (*Discussions about morning scientific presentations*)

## **Tuesday Afternoon, June 4**

3:00 p.m. Solar Photochemistry Program Information  
**Chris Fecko**, DOE Office of Basic Energy Sciences

### **SESSION VII** **Semiconductor Nanoparticles for Solar Energy Conversion** Xiaoyang Zhu, Chair

3:30 p.m. Controlling the Optical and Electrical Properties of QDs, QD assemblies, and QD films for Solar Energy Conversion  
**Matthew C. Beard**, National Renewable Energy Laboratory

4:00 p.m. Break

4:30 p.m. Hot-Carrier Dynamics in Quantum Dots Manipulated by Spin-Exchange Auger Interactions  
**Victor I. Klimov**, Los Alamos National Laboratory

5:00 p.m. Time-Domain Atomistic Studies of Far-from-Equilibrium Dynamics in Nanoscale Materials for Solar Energy Harvesting  
**Oleg V. Prezhdo**, University of Southern California

5:30 p.m. Metal-Tipped and Electrochemically Wired Semiconductor Nanocrystals: Modular Constructs for Directed Charge Transfer  
**Neal R. Armstrong**, University of Arizona

## **Tuesday Evening, June 4**

6:00 p.m. Working Dinner (*Discussions about afternoon presentations*)

7:30 p.m. Posters (*Even numbers*)

## Wednesday Morning, June 5

7:30 a.m. Breakfast

### **SESSION VIII** **Semiconductor Photoelectrodes** Tom Hamann, Chair

8:30 a.m. Modulation of Photoinduced Charge Transfer at the Semiconductor Interface  
**Prashant V. Kamat**, Notre Dame University

9:00 a.m. Molecular Level Functionalization, Atomically Thin Photoelectrodes, and Protective Coatings Based on Two-Dimensional Materials  
**Nathan S. Lewis**, California Institute of Technology

9:30 a.m. Photoexcited Charge Carrier Dynamics at Photocatalytic Semiconductor/liquid Interfaces  
**Stephen B. Cronin**, University of Southern California

9:45 a.m. Investigating Ultrafast Dynamics in Solid-State Photocatalytic and Photovoltaic Materials Using Time-Resolved Mössbauer Spectroscopy  
**Benjamin T. Young**, Rhode Island College  
**Dugan Hayes**, University of Rhode Island

10:00 a.m. Break

### **SESSION IX** **Heterogeneous Solar Fuels Catalysts** Nate Neale, Chair

10:30 a.m. Tracking Structures in Solar Fuels Catalysis: In-situ X-ray Characterization of Interfacial Water-Splitting Molecular and Thin-Film Catalysts  
**David M. Tiede**, Argonne National Laboratory

11:00 a.m. Nanoscale Probing of Carrier-Selective Catalyst-Semiconductor Contacts in Water-Splitting Photoelectrodes  
**Shannon W. Boettcher**, University of Oregon

11:30 a.m. Proton-Coupled Electron Transfer Studies of Homogeneous and Heterogeneous Energy Conversion Catalysts  
**Daniel G. Nocera**, Harvard University

12:00 p.m. Working Lunch (*Discussions about morning scientific presentations*)

**Wednesday Afternoon, June 5**

**SESSION X**  
**Building Systems for Generating Solar Fuels**  
Frank Osterloh, Chair

- 1:15 p.m. Exploring the Synergy between Semiconductor Surfaces and Molecular Catalysts for Efficient Solar CO<sub>2</sub> Reduction  
**Christine A. Caputo and Gonghu Li**, University of New Hampshire
- 1:45 p.m. Nanostructured Solar Fuel Systems  
**Thomas E. Mallouk**, Pennsylvania State University
- 2:15 p.m. Charge Transport and Catalytic Mechanisms for Coupling Visible Light Driven CO<sub>2</sub> Reduction and H<sub>2</sub>O Oxidation across Ultrathin Oxide Membrane  
**Heinz Frei**, Lawrence Berkeley National Laboratory
- 2:45 p.m. Closing Comments  
**Chris Fecko**, DOE Office of Basic Energy Sciences
- 3:00 p.m. Adjourn

# Pathways to Selective and Efficient Carbon Dioxide Reduction

Harry A. Atwater  
Joint Center for Artificial Photosynthesis  
California Institute of Technology  
Pasadena, CA 91125

The Joint Center for Artificial Photosynthesis (JCAP) is an integrated, multi-institutional partnership with a mission to develop the scientific framework for achieving highly selective and efficient generation of solar fuels from sunlight, carbon dioxide and water. JCAP's current project plan is guided by three primary milestones:

1. Discovery and understanding of highly selective catalytic mechanisms for carbon dioxide reduction and oxygen evolution under mild conditions of temperature and pressure, informing the design of overall solar-energy-to-fuels components for key processes including light capture, energy transfer, electron transport and charge separation.
2. Discovery of electrocatalytic and photoelectrocatalytic materials and useful light-absorber photoelectrodes, followed by integration. This is required to design and construct components for test-bed prototypes that demonstrate selective, efficient CO<sub>2</sub> reduction into hydrocarbon fuels at full solar flux.
3. Demonstration, in JCAP test-bed prototypes, of artificial photosynthetic carbon dioxide reduction components and oxygen evolution components that exceed natural photosynthesis in efficiency and rival it in selectivity.

The JCAP research portfolio spans (photo) electrocatalysis mechanisms, accelerated materials discovery using both high throughput and directed methods, materials integration, and testbed prototypes combines common themes including integration of theory and experiment, as well as development and use of advanced *in situ* and *operando* experimental techniques at the national user facilities.

At present, a major thematic focus of the mechanistic theory and experimental effort is the understanding of C-C coupling, and the environmental factors that can impart selectivity in catalysis, as summarized by the mechanistic pathway diagram in Figure 1. Another area of focused effort is to

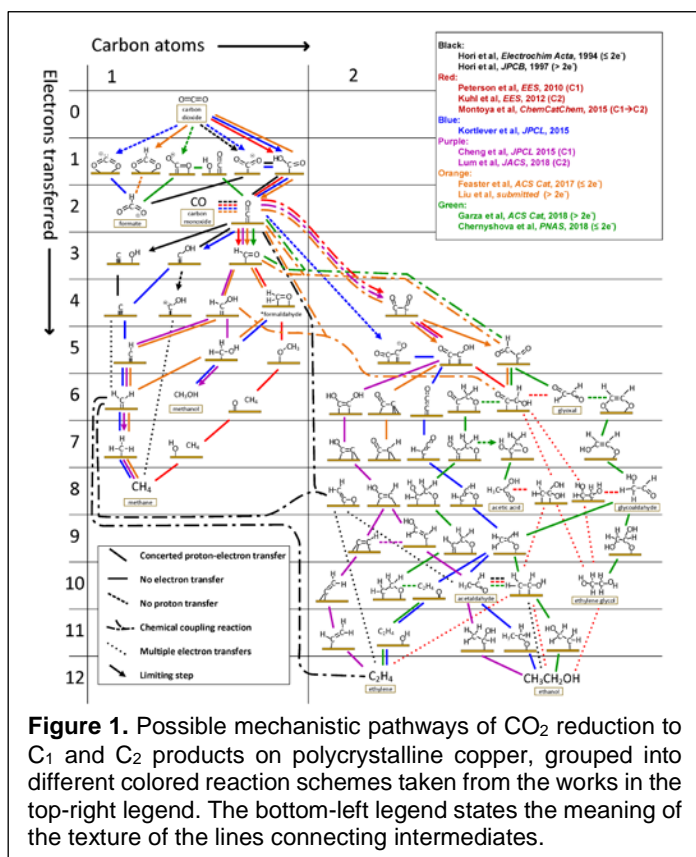


**Figure 1.** Possible mechanistic pathways of CO<sub>2</sub> reduction to C<sub>1</sub> and C<sub>2</sub> products on polycrystalline copper, grouped into different colored reaction schemes taken from the works in the top-right legend. The bottom-left legend states the meaning of the texture of the lines connecting intermediates.

identify a way to breaking the scaling relationships that constrain the relative activity and partial current densities for different products, which scale in proportion to the reactant binding energies on metal surfaces, but whose ratios typically cannot be varied widely to achieve high selectivity for a single or a few specified products. The electrocatalysis mechanisms effort includes surface science experiments that probe the atomic scale surface morphology and composition of catalysts, including *operando* X-ray diffraction and spectroscopy measurements as well as electrochemical scanning tunneling microscopy. This is complemented by first-principles theory that responds to the observations made by experimentalists. Several of JCAP's theorists have been able to map the activation energy landscape for electrochemical CO<sub>2</sub> reduction, and recently also for CO reduction, on transition metal heterogeneous catalyst surfaces, for both singular orientation surfaces as well as on stepped surfaces, and have been able to generate quantitative agreement with experiments.

Mechanistic efforts in photocatalysis include both the i) development and use of advanced computational techniques for understanding the resonant optical absorption in metals and semiconductors and ii) ultrafast absorption spectroscopy to characterize generation of electron and hole excited state distributions and the decay processes for 'hot' carriers and iii) model electrochemical experiments of production distributions focused on fundamental understanding of how light illumination can be used to alter or tailor CO<sub>2</sub> reduction selectivity and activity.

Materials discovery work spans electrocatalysts for CO<sub>2</sub> reduction and water oxidation, light absorbers for photoanodes and photocathodes, photoelectrocatalysts and protection layers. CO<sub>2</sub> reduction electrocatalyst materials discovery activities can be broadly classified into i) efforts aimed at understanding how to use surface structure, alloy composition and functionalization to direct selectivity, particularly towards dicarbon productions, on copper and copper alloys, including nanoparticle and oxide-derived Cu and ii) non-copper based single-atom center catalysts (e.g., Ni-N-doped graphene), and framework materials (e.g., Al-doped MOFs). Progress has also been made in development of acid-stable oxygen evolution catalysts composed of non-precious metals.

In the area of photocatalysis and light absorbers, JCAP's combined theory/experiment high throughput materials discovery initiative, in an effort focused on bismuth oxide iron tungstate materials, has found a material with the largest photovoltage for stable catalytically active wide bandgap semiconductor materials. A separate materials discovery effort has focused on photocathodes has utilized first-principles theoretical methods to screen for candidate nanostructured metal alloy, metal chalcogenide and metal oxide structures with optimal bandgaps and band edges that also satisfy stability criteria at the working pH conditions.

JCAP integration efforts have focused on expanding the portfolio and operating range of metal oxide protective coatings for photoanodes, as well as interfacial charge transfer dynamics and efficiency. Interface researchers have created high-throughput and directed methods for discovery and characterization of integrated material assemblies by combining catalysts and metal oxide photoanode materials.

JCAP's modeling simulation and test-bed effort has used multiphysics models to compare the performance of testbed prototypes with widely varying configurations, including both dark and light-driven gas-diffusion electrode (GDE) architectures and related membrane-electrode assemblies against traditional planar bulk aqueous electrolyte cells.

## A Bigger, Better Inverted Region

John R. Miller<sup>1</sup>, Richard A. Holroyd<sup>1</sup>, Andrew R. Cook<sup>1</sup>, Norihiko Takeda<sup>1</sup>, Tomoyasu Mani<sup>1,2</sup>,  
Marshall D. Newton,<sup>1</sup> Matthew J. Bird<sup>1</sup> and Hung-Cheng Chen<sup>1</sup>

<sup>1</sup>Chemistry Division, Brookhaven National Laboratory, Upton, NY 11973

<sup>2</sup>Chemistry Department, University of Connecticut, Storrs, CT 06269

The principal theme of this talk will explore the idea that we can more deeply understand the inverted region of the Marcus Theory and use to it control and improve energy conversion. Here we focus on the role of electronic coupling between diffusing donor and acceptor molecules as might be found in fluid solutions or in solid films with diffusing excitons. Figure 1 depicts bimolecular electron transfer (ET) rate constants,  $k_{et}$ , for large and small electronic couplings, using eq 1 combined with the Waite expression,  $k_{Bi}^{-1} = k_{ET}^{-1} + k_d^{-1}$  to include the rate of diffusion,  $k_d$ . Figure 1's two calculated curves differ only in electronic coupling,  $H_{da}$ , having identical dependence on  $\Delta G^\circ$ , in the Franck-Condon-weighted density of states, FCWD.

$$k_{ET} = \frac{2\pi}{\hbar} |H_{da}(r)|^2 \text{FCWD} \quad (1)$$

For small electronic couplings highly-exoergic ET, typical for charge recombination (CR) reactions,  $k_{et}$  is slowed three decades by the inverted effect. But with large electronic couplings (red curve) CR is barely slowed and is almost as fast as moderately exoergic charge separation (marked CS); there is a long, flat region with rates at the diffusion-controlled limit. The blue curve is clearly desirable to favor CS over CR. We will discuss tests of how realistic this idealized example is and how we might lean to exert control over electronic couplings to achieve conditions like those of the blue curve in Figure 1. We seek to understand how the inverted region is often absent and sometimes present.

Figure 2 shows how we can get rid of the flat region by increasing the diffusion coefficient a few decades by making one reactant the solvated electron ( $e_s^-$ ) in high-mobility liquids tetramethylsilane (TMS) and isooctane (Iso). The reaction studied here is  $e_s^- + \text{Stilbene} \rightarrow \text{Stilbene}^*$ . Highly mobile electrons in TMS and Iso diffuse at least 1000 times faster than molecular diffusion, letting us escape the diffusion-controlled limit. Further the free energy change can be adjusted *continuously* over an  $\sim 200$  meV range by increasing pressure which raises the energy of  $e_s^-$ . The much higher diffusion-controlled limit lets us see an inverted region for most of the TMS points (blue). That inverted region ends and the rates increase when  $-\Delta G^\circ$  reaches the  $\sim 0.85$  eV energy

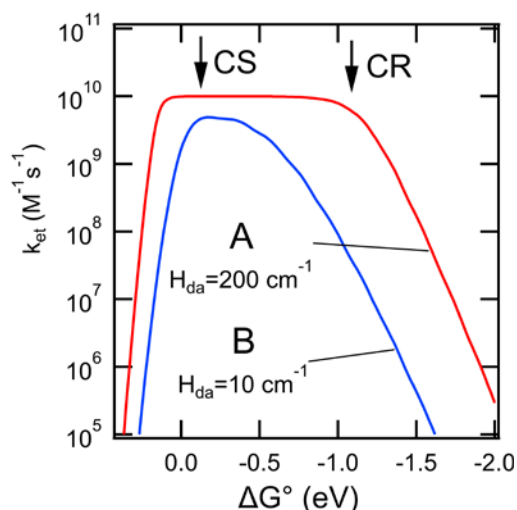


**Figure 1.** Bimolecular electron transfer rate constants vs. driving force for  $D=10^{-5}$  cm<sup>2</sup>/s.

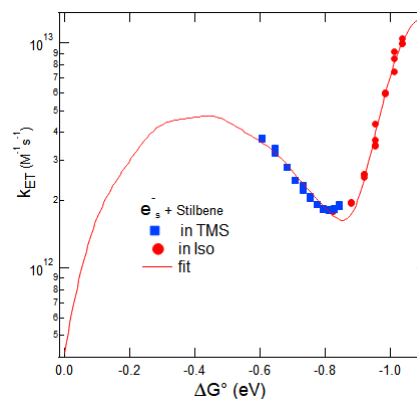


**Figure 2** Rate constants for electron attachment to t-Stilbene in TMS and Isooctane.

of the first excited state of the product, Stilbene\*. Indeed this technique is frequently limited because radical anions are open-shell species which often have low-lying excited states that prevent observation of much larger inverted regions for many molecules. Highly mobile electrons give us insight into underlying principles governing free energy relations for electron transfer but may not be directly relevant solar energy conversion in molecular systems.

Figure 3 displays one of the rare examples of the inverted region for bimolecular electron transfer. This data does not use high-mobility species; the reactants are radical anions of quaterthiophene ( $T_4$ ) or poly-3-decylthiophene (P3DT). The fit curves interpret the enhanced inverted region for P3DT as a result of reduced electronic couplings. There is still a “flat region” for which rates are controlled by diffusion, but some data points escape it. This data, though less dramatic, seems to be an example of the principle illustrated in Figure 1. We will discuss why smaller electronic couplings might be expected for the reactions of P3DT.

If reduced electronic couplings,  $H_{da}$ , enhance the inverted region, we want to learn: How do we reduce  $H_{da}$ ? We will discuss first the simple effects of size (and delocalization): bigger is better (smaller  $H_{da}$ ). We will also discuss what we call size-mismatch, which we implicate in Figure 3, and symmetry mismatch. These effects are potentially of great importance but amazingly have been little studied. Let's change that!

Conjugated polymers which delocalize charges and excitons have slipped some form their former place in the sun, but given the right breakthroughs, retain potential to provide an important, perhaps the important alternative for thin, flexible, deployable and *potentially* efficient solar energy capture. We will describe results that investigate these using pulse radiolysis to understand the dependence of free energies of delocalized charges and excitons on lengths of the chains in which they reside. We can replace a widely-used empirical  $1/n$ , description by one rooted in simple thermodynamic concepts.

We will also describe results finding very high charge mobility along conjugated polymer chains and note how high mobilities could assist in more efficient organic photovoltaics. These findings implicate polarity of the medium as an important factor in determining charge mobilities along conjugated chains and lead us to speculate that this factor may even be more important than control of dihedral angles.

The experimental results described above use the radiation chemistry technique of pulse radiolysis, which is a strong complement to photoexcitation methods. Pulse radiolysis also provides new insight into energetics of charge transfer via novel determinations of redox potentials of molecules through chemical equilibria.

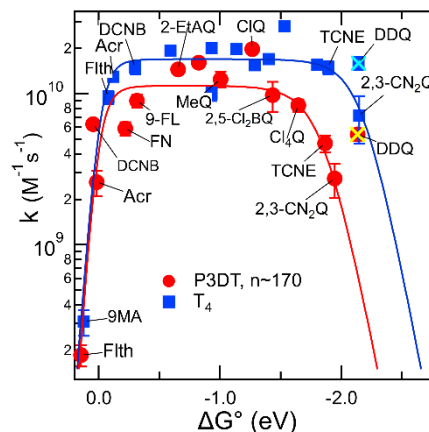


Figure 3 Rate constants for electron transfer to varied acceptors from anions of P3DT or  $T_4$  ( $n=4$ ) in THF solution.

## DOE Solar Photochemistry Sponsored Publications 2016-2019

1. Cook, A. R.; Asaoka, S.; Li, X.; Miller, J. R. "Electron Transport with Mobility,  $\mu > 86 \text{ Cm}^2/\text{Vs}$ , in a 74 Nm Long Polyfluorene", *J. Phys. Chem. Lett.*, **2019**, *10*, 171-175.
2. Burke, J. H.; Bird, M. J. "Energetics and Escape of Interchain-Delocalized Ion Pairs in Nonpolar Media", *Adv. Mater.*, **2019**, *31*.
3. Cook, A. R.; Valasek, M.; Funston, A. M.; Poliakov, P.; Michl, J.; Miller, J. R. "p-Carborane Conjugation in Radical Anions of Cage-Cage and Cage-Phenyl Compounds", *J. Phys. Chem. A*, **2018**, *122*, 798-810.
4. Chen, H. C.; Sreearunothai, P.; Cook, A. R.; Asaoka, S.; Wu, Q.; Miller, J. R. "Chain Length Dependence of Energies of Electron and Triplet Polarons in Oligofluorenes", *J. Phys. Chem. C*, **2017**, *121*, 5959-5967.
5. Chen, H. C.; Cook, A. R.; Asaoka, S.; Boschen, J. S.; Windus, T. L.; Miller, J. R. "Escape of Anions from Geminate Recombination in THF Due to Charge Delocalization", *PCCP*, **2017**, *19*, 32272-32285.
6. Bird, M. J.; Iyoda, T.; Bonura, N.; Bakalis, J.; Ledbetter, A. J.; Miller, J. R. "Effects of Electrolytes on Redox Potentials through Ion Pairing", *J. Electroanal. Chem.*, **2017**, *804*, 107-115.
7. Bird, M. J.; Bakalis, J.; Asaoka, S.; Sirringhaus, H.; Miller, J. R. "Fast Holes, Slow Electrons, and Medium Control of Polaron Size and Mobility in the Da Polymer F8BT", *J. Phys. Chem. C*, **2017**, *121*, 15597-15609.
8. Wu, Q.; Zaikowski, L.; Kaur, P.; Asaoka, S.; Gelfond, C.; Miller, J. R. "Multiply Reduced Oligofluorenes: Their Nature and Pairing with THF-Solvated Sodium Ions", *J. Phys. Chem. C*, **2016**, *120*, 16489-16499.
9. Hack, J.; Grills, D. C.; Miller, J. R.; Mani, T. "Identification of Ion-Pair Structures in Solution by Vibrational Stark Effects", *J. Phys. Chem. B*, **2016**, *120*, 1149-1157.
10. Craig, P. R.; Havlas, Z.; Trujillo, M.; Rempala, P.; Kirby, J. P.; Miller, J. R.; Noll, B. C.; Michl, J. "Electronic Spectra of the Tetraphenylcyclobutadienecyclopentadienylnickel(II) Cation and Radical", *J. Phys. Chem. A*, **2016**, *120*, 3456-3462.

# Proton-Coupled Electron Transfer Drives Grotthuss-Type Proton Transfer in Artificial Photosynthesis

Devens Gust, Thomas A. Moore and Ana L. Moore  
School of Molecular Sciences  
Arizona State University  
Tempe, AZ, 85287-1604

In photosystem II, tyrosine Z ( $Y_z$ ) functions as a redox relay between the photo-oxidized primary donor ( $P680^{+}$ ) and the oxygen-evolving complex, the  $Mn_4O_5Ca$  catalyst where water oxidation takes place. The oxidation of  $Y_z$  by  $P680^{+}$  occurs with the transfer of the phenolic proton of  $Y_z$  to its hydrogen-bonded histidine (His190) partner in an iconic proton-coupled electron transfer (PCET) process.

Benzimidazole-phenol (BIP see Figure 1, reduced on left, oxidized on right) and several of its derivatives have been designed to mimic the behavior of the  $Y_z$ -His190 pair. The phenol is a model of  $Y_z$ , and the benzimidazole models His190. Changes in the protonation state of the system upon oxidation of the phenol can be clearly detected by infrared spectroelectrochemistry (IRSEC). With a simple BIP, proton transfer from the phenol to the imidazole takes place upon oxidation of the phenol; this is known as an electron-proton transfer (EPT) process (Figure 1). When a second proton acceptor, either an amino (Figure 2) or imino (Figure 3) group is added to the BIPs, the electrochemical oxidation of the phenol becomes a one-electron, two-proton transfer, an E2PT process. Interestingly, from theory we know that due to the change in  $\Delta pK_a$  between the imino and amino groups, oxidation of the phenol in BIPs with imino substituents occurs at  $\sim 300$  mV higher potential than with the amino-BIPs. IRSEC results demonstrate that the basicity of the

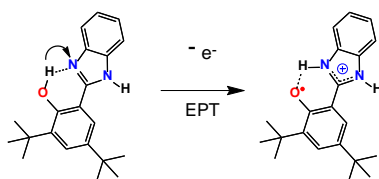


Figure 1

imino nitrogen of *N*-phenylimino-substituted BIPs can be controlled by the electron donating/withdrawing properties of R groups at the *para*-position of the *N*-phenylimino group, (Figure 3). Proton transfer to the imino group, (the E2PT process) takes place with sufficiently strong electron-donating groups, e.g.  $R = -OCH_3$  substitution. But when the imine basicity is reduced, e.g., with  $R = -CN$ , an EPT product is dominant with the formation of the benzimidazolium ion like in Figure 1. Thus, the mechanism and consequently the extent of proton translocation along the H-bond network, either  $\sim 1.6$  Å or  $\sim 6.4$  Å, can be controlled through structural design.

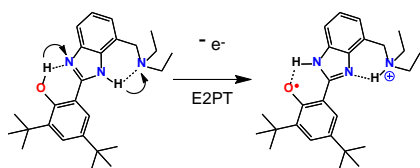


Figure 2

Elaborating on this theme, E3PT and E4PT systems are being designed and studied. By linking high potential porphyrin derivatives to the BIP-based EnPT systems the oxidation and proton translocation processes can be photochemically driven.

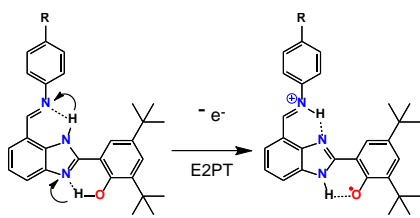


Figure 3

IRSEC results demonstrate that the basicity of the imino nitrogen of *N*-phenylimino-substituted BIPs can be controlled by the electron donating/withdrawing properties of R groups at the *para*-position of the *N*-phenylimino group, (Figure 3). Proton transfer to the imino group, (the E2PT process) takes place with sufficiently strong electron-donating groups, e.g.  $R = -OCH_3$  substitution. But when the imine basicity is reduced, e.g., with  $R = -CN$ , an EPT product is dominant with the formation of the benzimidazolium ion like in Figure 1. Thus, the mechanism and consequently the extent of proton translocation along the H-bond network, either  $\sim 1.6$  Å or  $\sim 6.4$  Å, can be controlled through structural design.

Elaborating on this theme, E3PT and E4PT systems are being designed and studied. By linking high potential porphyrin derivatives to the BIP-based EnPT systems the oxidation and proton translocation processes can be photochemically driven. Preliminary studies of the first such systems will be presented. Aims of this study include determining how many proton transfers can be associated with a single oxidation event and constructing Grotthuss-type proton wires where proton transport across lipid bilayers to generate proton-motive force is accomplished in conjunction with redox reactions. Linking charge separation and photodriven electron transfer to the

generation of proton currents opens a new strategy in the design of artificial photosynthetic systems.

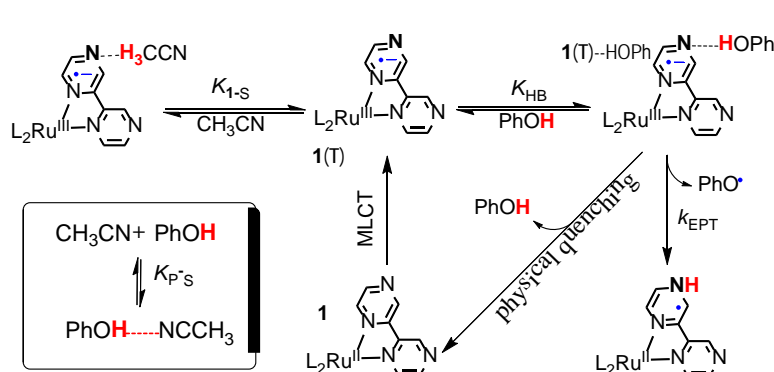
### DOE Solar Photochemistry Sponsored Publications 2017-2019

1. Watson, B. L.; Moore, T. A.; Moore, A. L.; Gust, D., Synthesis of a Novel Building Block for the Preparation of Multi-Chromophoric Sensitizers for Panchromatic Dye-Sensitized Solar Cells. *Dyes Pigm.* **2017**, *136*, 893-897.
2. Llansola-Portoles, M. J.; Gust, D.; Moore, T. A.; Moore, A. L., Artificial Photosynthetic Antennas and Reaction Centers. *C. R. Chim.* **2017**, *20*, 296-313.
3. Ho, J.; Kish, E.; Mendez-Hernandez, D. D.; WongCarter, K.; Pillai, S.; Kodis, G.; Niklas, J.; Poluektov, O. G.; Gust, D.; Moore, T. A.; Moore, A. L.; Batista, V. S.; Robert, B., Triplet-Triplet Energy Transfer in Artificial and Natural Photosynthetic Antennas. *Proc. Natl. Acad. Sci. U. S. A.* **2017**, *114*, E5513-E5521.
4. Finkelstein-Shapiro, D.; Fournier, M.; Méndez-Hernández, D. D.; Guo, C.; Calatayud, M.; Moore, T. A.; Moore, A. L.; Gust, D.; Yarger, J. L., Understanding Iridium Oxide Nanoparticle Surface Sites by Their Interaction with Catechol. *Phys. Chem. Chem. Phys.* **2017**, *19*, 16151-16158.
5. Koepf, M.; Bergkamp, J. J.; Teillout, A.-L.; Llansola-Portoles, M. J.; Kodis, G.; Moore, A. L.; Gust, D.; Moore, T. A., Design of Porphyrin-Based Ligands for the Assembly of [d-Block Metal : Calcium] Bimetallic Centers. *Dalton Trans.* **2017**, *46*, 4199-4208.
6. Huynh, M. T.; Mora, S. J.; Villalba, M.; Tejada-Ferrari, M. E.; Liddell, P. A.; Cherry, B. R.; Teillout, A.-L.; Machan, C. W.; Kubiak, C. P.; Gust, D.; Moore, T. A.; Hammes-Schiffer, S.; Moore, A. L., Concerted One-Electron Two-Proton Transfer Processes in Models Inspired by the Tyr-His Couple of Photosystem II. *ACS Cent. Sci.* **2017**, *3*, 372-380.
7. Gacek, D. A.; Moore, A. L.; Moore, T. A.; Walla, P. J., Two-Photon Spectra of Chlorophylls and Carotenoid-Tetrapyrrole Dyads. *J. Phys. Chem. B* **2017**, *121* (43), 10055-10063.
8. Mora, S. J.; Odella, E.; Moore, G. F.; Gust, D.; Moore, T. A.; Moore, A. L., Proton-Coupled Electron Transfer in Artificial Photosynthetic Systems. *Acc. Chem. Res.* **2018**, *51* (2), 445-453.
9. WongCarter, K.; Llansola-Portoles, M. J.; Kodis, G.; Gust, D.; Moore, A. L.; Moore, T. A., Light Harvesting, Photoregulation, and Photoprotection in Selected Artificial Photosynthetic Systems. In *Light Harvesting in Photosynthesis*, Croce, R.; van Grondelle, R.; van Amerongen, H.; van Stokkum, I., Eds. CRC Press: Boca Raton, Florida, 2018, Chapter 21, pp 485-510.
10. Odella, E.; Mora, S. J.; Wadsworth, B. L.; Huynh, M. T.; Goings, J. J.; Liddell, P. A.; Groy, T. L.; Gervaldo, M.; Sereno, L. E.; Gust, D.; Moore, T. A.; Moore, G. F.; Hammes-Schiffer, S.; Moore, A. L., Controlling Proton-Coupled Electron Transfer in Bioinspired Artificial Photosynthetic Relays. *J. Am. Chem. Soc.* **2018**, *140* (45), 15450-15460.
11. Tejada-Ferrari, M. E.; Brown, C. L.; Coutinho, G. C. C. C.; Gomes de Sá, G. A.; Palma, J. L.; Llansola-Portoles, M. J.; Kodis, G.; Mujica, V.; Ho, J.; Gust, D.; Moore, T. A.; Moore, A. L., Electronic Structure and Triplet-Triplet Energy Transfer in Artificial Photosynthetic Antennas. *Photochem. Photobiol.* **2019**, *95*, 211-219.

## Hydrogen Bonding Interactions in Photoinduced PCET

Dmitry E. Polyansky, Sergei V. Lyamar, Mehmed Z. Ertem, and Gerald F. Manbeck  
 Chemistry Division, Energy & Photon Sciences Directorate  
 Brookhaven National Laboratory  
 Upton, NY 11973-5000

Proton-coupled electron transfer (PCET) reactions play an important role in natural and artificial photosynthetic transformations, by providing low energy pathways in charge separation, charge transport and redox catalysis. It has been demonstrated that hydrogen-bonding (HB)



Scheme 1. General mechanism of a photochemical reaction between complex and phenols, invoking the complex-phenol ( $K_{HB}$ ), complex-solvent ( $K_{1-s}$ ), and phenol-solvent ( $K_{p-s}$ ) H-bonding pre-equilibria.

between donor and acceptor molecules has a profound effect on the kinetics of a PCET process. However, when HB interactions involve transient species, such as transition metal complexes in their MLCT excited states, the HB equilibrium (e.g.,  $K_{HB}$  in the Scheme 1) must be extracted from excited state lifetime or luminescence measurements. Our recent work demonstrates that only a rigorously derived kinetic model which explicitly includes all HB interactions involving a metal complex, quencher, and a solvent molecule can accurately describe the reactivity between a photo-excited Ru polypyridine complex containing an uncoordinated H-bonding site and an HB acidic solute (e.g., phenol).<sup>6</sup> Our kinetic model clearly shows that the separation of the HB equilibrium constant,  $K_{HB}$ , and the reaction rate constant,  $k_{EPT}$  (where EPT stands for electron-proton transfer, a subset of PCET where a proton and an electron are transferred via concerted pathway) can be achieved only in the range where  $K_{HB}[\text{PhOH}] \gg 1$ , and the Stern-Volmer dependence approaches a plateau. However, all reports of EPT reactions between phenol type donors and metal complexes in their MLCT excited states have not demonstrated significant saturation of quenching plots thereby preventing an accurate determination of equilibrium and rate constants. We determined that for most phenolic quenchers this limitation arises from a combination of two factors: low  $K_{HB}$  values along with insufficient PhOH solubility and high quenching efficiencies ( $k_{EPT}$  values) that makes the excited state lifetime immeasurably small at relatively low [PhOH], well before the  $K_{HB}[\text{PhOH}] \gg 1$  condition is satisfied.

In order to alleviate these limitations, we have developed a new approach for evaluation of  $K_{HB}$  using halogenated alcohols as HB surrogates of phenolic quenchers.<sup>1</sup> This approach is based on the similarity of the H-bond donating capacities of alcohols and phenols on the Abraham HB acidity scale. We have shown that in a series of halogenated alcohols (ROH) with varying HB acidities a linear correlation exists between the free energy of hydrogen bond formation in 1(T)-HOR exciplexes and the HB acidities  $\alpha_2^H$  of ROH donors (alcohols or *p*-substituted phenols) as

shown in Figure 1. This correlation allows an accurate prediction of HB equilibrium constants in systems where they cannot be measured directly. It was also found that the decay of an H-bonded exciplex always involves a physical quenching pathway concurrent with the electron-proton transfer. Depending upon the EPT driving force ( $\Delta G_{\text{EPT}}$ ), the contribution of this pathway to the observed overall quenching varies from insignificant for high  $\Delta G_{\text{EPT}}$ , to dominant at low driving forces.<sup>1</sup>

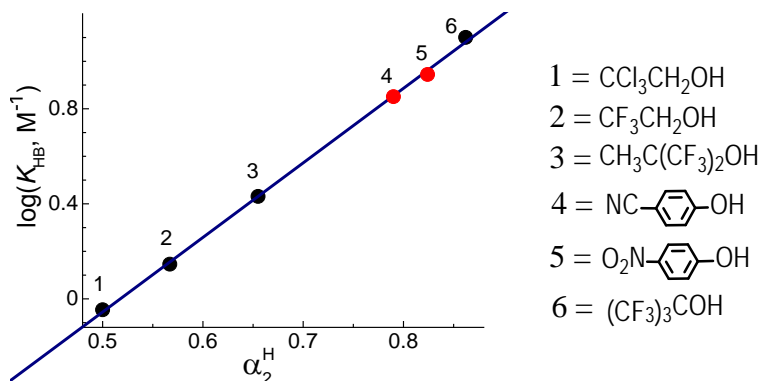


Figure 1. Dependence of  $\log K_{\text{HB}}$  upon HB acidity of alcohols (1-3, and 6) and phenols (4 and 5).

We have applied aforementioned models to mechanistic investigation of PCET between several Ru polypyridine complexes containing H-bond accepting sites and a series of *p*-substituted phenols.<sup>3</sup> It was demonstrated that the Hammett  $\sigma_p$  provides a common descriptor for analyzing the observed reactivity in terms of free energy correlations, since all phenol's thermochemical properties bearing on the quenching mechanism (H-bonding and Brønsted acidities, O-H bond dissociation free energy, and the phenoxyl radical reduction potential) linearly correlate with  $\sigma_p$ . It was found that while for the less acidic phenols the log of bimolecular rate coefficients ( $k_q^{\text{obs}}$ ) for quenching of the triplet MLCT excited states by phenols linearly correlates with  $\sigma_p$ , appreciable deviations from linearity are observed for more acidic phenols (Figure 2). This pattern is attributed to a transition of the quenching mechanism from an EPT to a proton transfer (PT); the latter becomes predominant for the most acidic phenols in acetonitrile, but not in dichloromethane. This assertion is supported by a detailed thermochemical analysis, which also excludes the quenching pathways involving electron transfer from phenols with or without deprotonation of phenols to the solvent, either concerted or

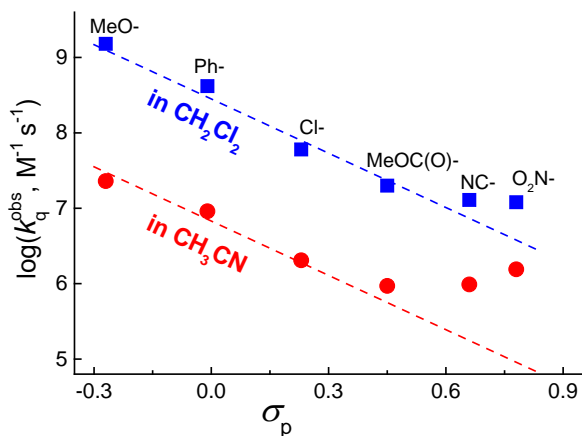


Figure 2. Hammett  $\sigma_p$  correlations of  $\log k_q^{\text{obs}}$  in  $\text{CH}_2\text{Cl}_2$  (blue squares) and MeCN (red circles).

sequential.<sup>3</sup>

Our future work will aim at mechanistic studies of photo-driven and thermal PCET reactions in intra- or intermolecular HB donor-acceptor pairs. We will particularly focus on obtaining accurate thermodynamic and kinetic parameters for oxidation of proton-electron donors using pulse radiolysis in organic solvents and using these parameters for validating theoretical models for PCET reactions.

## DOE Solar Photochemistry Sponsored Publications 2016-2019

1. Lymar, S. V.; Manbeck, G. F.; Polyansky, D. E. "Hydrogen Bonding between Hydroxylic Donors and MLCT-Excited Ru(bpy)<sub>2</sub>(bpz)<sup>2+</sup> Complex: Implications for Photoinduced Electron-Proton Transfer" *Chem. Commun.*, **2019**, DOI: 10.1039/C9CC01896D.
2. Hsieh, Y. C.; Betancourt L. E.; Senanayake, S. D.; Enyuan, H; Zhang, Y.; Xu, W. Q.; Polyansky, D. E., "Modification of CO<sub>2</sub> Reduction Activity of Nanostructured Silver Electrocatalysts by Surface Halide Anions" *ACS Appl. Energy Mater.* **2019**, 2, 102–109.
3. Lymar, S. V.; Ertem, M. Z.; Lewandowska-Andralojc, A.; Polyansky, D. E. "Solvent-Dependent Transition from Concerted Electron-Proton to Proton Transfer in Photoinduced Reactions between Phenols and Polypyridine Ru Complexes with Proton-Accepting Sites" *Dalton Trans.*, **2018**, 47, 15917-15928.
4. Shimoda, T.; Morishima, T.; Kodama, K.; Hirose, T.; Polyansky, D. E.; Muckerman, J.T.; Fujita, E. "Photocatalytic CO<sub>2</sub> Reduction by Trigonal Bipyramidal Cobalt(II) Polypyridyl Complexes: Nature of Cobalt(I) and Cobalt(0) Complexes upon Their Reactions with CO<sub>2</sub>, CO and Proton" *Inorg. Chem.* **2018**, 57, 5486-5498.
5. Grills, D. C.; Polyansky, D. E.; Fujita, E. "Application of Pulse Radiolysis to Mechanistic Investigations of Catalysis Relevant to Artificial Photosynthesis" *ChemSusChem* **2017**, 10, 4359 - 4373.
6. Lymar, S. V.; Ertem, M. Z.; Lewandowska-Andralojc, A.; Polyansky, D. E. "Role of Hydrogen Bonding in Photoinduced Electron-Proton Transfer from Phenols to a Polypyridine Ru Complex with a Proton-Accepting Ligand" *J. Phys. Chem. Lett.* **2017**, 8, 4043-4048.
7. Thuy-Duong, N.-P.; Liu, Z.; Luo, S.; Gamalski, A. D.; Vovchok, D.; Xu, W.; Stach, E. A.; Polyansky, D. E.; Fujita, E.; Rodriguez, J. A.; Senanayake, S. D. "Unraveling the Hydrogenation of TiO<sub>2</sub> and Graphene Oxide/TiO<sub>2</sub> Composites in Real Time by in Situ Synchrotron X-ray Powder Diffraction and Pair Distribution Function Analysis" *J. Phys. Chem. C* **2016**, 120, 3472-3482.
8. Nguyen-Phan, T. D.; Luo, S.; Vovchok, D.; Llorca, J.; Graciani, J.; Sanz, J. F.; Sallis, S.; Xu, W. Q.; Bai, J. M.; Piper, L. F. J.; Polyansky, D. E.; Fujita, E.; Senanayake, S. D.; Stacchiola, D. J.; Rodriguez, J. A. "Visible Light-Driven H<sub>2</sub> Production over Highly Dispersed Ruthenia on Rutile TiO<sub>2</sub> Nanorods" *ACS Catal.* **2016**, 6, 407-417.
9. Nguyen-Phan, T. D.; Luo, S.; Vovchok, D.; Llorca, J.; Sallis, S.; Kattel, S.; Xu, W. Q.; Piper, L. F. J.; Polyansky, D. E.; Senanayake, S. D.; Stacchiola, D. J.; Rodriguez, J. A. "Three-dimensional ruthenium-doped TiO<sub>2</sub> sea urchins for enhanced visible-light-responsive H<sub>2</sub> production" *Phys. Chem. Chem. Phys.* **2016**, 18, 15972-15979.

## Model Dyes for Study of Electron Transfer Processes At Metal Oxide Semiconductor Interfaces

E. Galoppini,<sup>a</sup> R. A. Bartynski,<sup>b</sup> L. Gundlach,<sup>c,d</sup> A. Teplyakov<sup>d</sup>  
 R. Harmer,<sup>a</sup> H. Fan,<sup>a</sup> S. Rangan,<sup>b</sup> J. Vierek,<sup>b</sup> J. Nieto-Pescador<sup>c</sup>, B. Abraham<sup>d</sup>

<sup>a</sup>Chemistry Department, Rutgers University-Newark, Newark, NJ 07102;

<sup>b</sup>Department of Physics and Astronomy, Rutgers University-New Brunswick, Piscataway, NJ

08854 <sup>c</sup>Department of Physics and Astronomy, University of Delaware, Newark, DE 19716

<sup>d</sup>Department of Chemistry and Biochemistry, University of Delaware, Newark, DE 19716

Electron transfer at the interface between a photoactive molecule (a chromophore or a photocatalyst) and a large-bandgap nanostructured metal oxide semiconductor (TiO<sub>2</sub> and ZnO either single crystal or nanostructured) remains at the center of intense research in solar energy conversion including photocatalysis, solar fuels, photovoltaics, and artificial photosynthesis. More broadly, the properties and processes at the chromophore/semiconductor interface impact research in molecular electronics and other fields where heterogeneous electron transfer (HET) plays a central role. An enduring challenge is the ability to attain control of the chromophore/semiconductor interface at the molecular level. This research aims at achieving this with a combination of organic synthesis (Galoppini) surface science (Bartynski), theory and ultrafast spectroscopies in collaboration with the Gundlach group. The presentation will address the development of “functional” bridging units (**Fig. 1**) to (a) control the *energy level alignment* of molecules on nanostructured or single crystal inorganic semiconductors using permanent dipoles and (b) to probe *vibronic and electronic coupling* to the semiconductor acceptor states in HET processes. Our progress in both areas will be discussed.

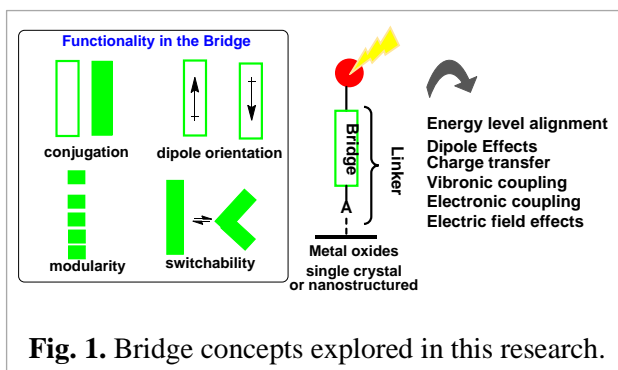
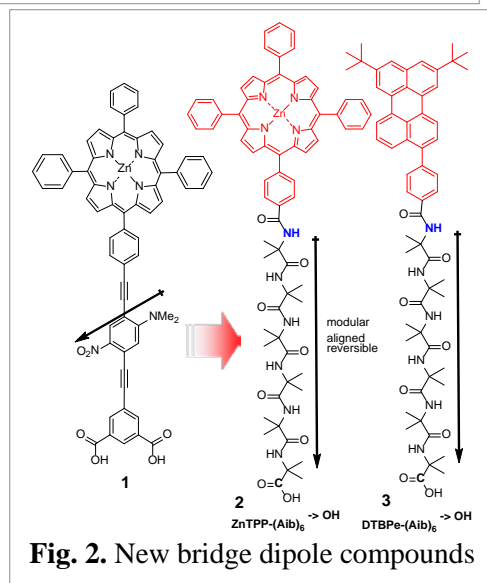


**Fig. 1.** Bridge concepts explored in this research.

(a) A key goal is to tune the energy alignment of the levels of an adsorbed chromophore-containing molecule with respect to the valence and conduction bands of the oxide semiconductor. Based on our previous successful work involving rigid-rod porphyrins like **1** in **Fig. 2a**, we are now attempting to increase the effect of the dipole layer by using helical (Aib)<sub>n</sub> peptides as dipole units, as shown in **Fig. 2b**. When adsorbed on the oxide surface, the peptide N → C dipole layer offsets the electrostatic potential at the chromophore from that of the oxide, thereby achieving the desired relative shift of the energy levels. The helical peptide dipole effect has been observed on metal surfaces by Tanaka, Maran et.al, providing an useful precedent to the proposed work. We will describe the design and synthesis



of helical (Aib)<sub>n</sub> oligopeptides linkers capped with ZnTPP and DTBPe chromophores. The dipole direction reversal was attained by switching the position of the head group on the (Aib)<sub>n</sub> chain with respect to the anchor group. To date we have prepared, purified, and fully characterized four compounds: ZnTPP-(Aib)<sub>6</sub>→OH (**2**), ZnTPP-(Aib)<sub>6</sub>←OH, DTBPe-(Aib)<sub>6</sub>→OH (**3**) and DTBPe-(Aib)<sub>6</sub>←OH where the arrow indicates the direction of the N to C dipole of the peptide with respect to the surface.

Their study in solution and bound to nanostructured TiO<sub>2</sub> and single crystal TiO<sub>2</sub>(110) surfaces is in progress. To characterize the energy level shifts that dipole containing linkers induce on chromophore head groups, when bound to crystal TiO<sub>2</sub>(110), we developed, and applied to the molecules of **Fig. 2**, (i) a new method to create uniform thick films for molecular characterization via electron spectroscopy, (ii) a single crystal surface solution sensitization technique that minimizes molecular contamination, and (iii) new computational codes that produce an appropriately weighted density of electronic states which improves the assignment of spectral features to molecular orbitals. **Fig. 3** shows experimental results for the TiO<sub>2</sub>(110) surface after solution sensitization with reference compound **1**. The valence band spectrum is well described by the weighted DOS, and the XPS core levels yield the expected C/N ratio indicating non-dissociative adsorption and no appreciable contamination. Peptide **2** yielded different results that will be discussed in the talk.

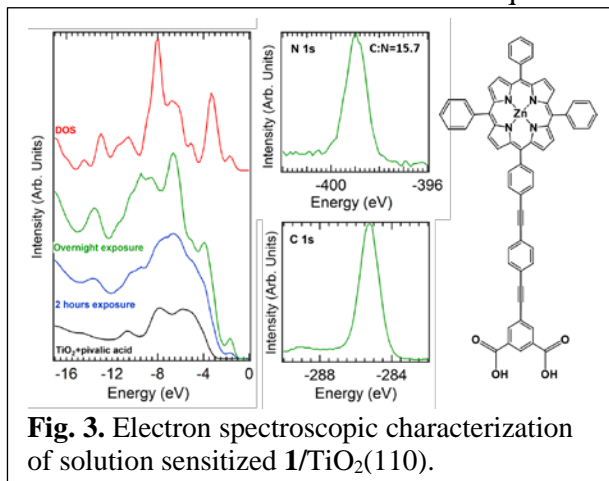


**Fig. 3.** Electron spectroscopic characterization of solution sensitized **1**/TiO<sub>2</sub>(110).

(b) As part of our collaboration with the Gundlach group, we are developing new di-*t*-butylperylene (DTBPe) chromophores with bridge/anchor group combinations and with one or two linker units, **Fig.4,ac** designed to tune vibronic and electronic coupling to acceptor states for an in-depth study of coherence in heterogeneous charge transfer. Second, with the Gundlach and Teplyakov groups we developed a stepwise click methodology for the functionalization of ZnO nanorods that prevents etching, as schematically illustrated in **Fig.4,b**. Since the ZnO nanorod surface is highly ordered, the DTBPe/ZnO interface prepared by click will be an excellent substrate. This versatile methodology will be employed for single crystal surfaces (Bartynski). Studies of perylene derivative **DTBPe-Ph-COOH** on both the TiO<sub>2</sub>(110) and ZnO(0001), show excellent agreement with electronic structure calculations and indicate that the chromophore's HOMO and LUMO lie within the energy gap of the peptide (Aib)<sub>6</sub> indicating that dipole-induced shifts owing to the linker group in compound **3** in **Fig.2** should be easily measured.

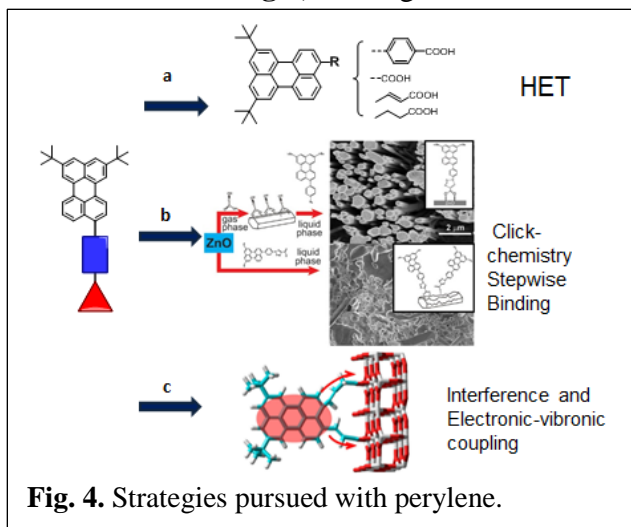


**Fig. 4.** Strategies pursued with perylene.

## DOE Solar Photochemistry Sponsored Publications 2017-2019

1. *Vibronic Effects in the Ultrafast Interfacial Electron Transfer of Perylene Sensitized TiO<sub>2</sub> Surfaces* Oliboni, Robson; Yan, Han; Fan, Hao; Abraham, Baxter; Avenoso, Joseph; Galoppini, Elena; Batista, Victor; Gundlach, Lars; Rego, Luis *J. Phys. Chem. C* Manuscript ID jp-2019-02106y, **2019** submitted, in revision.
2. *Comparison of ZnO surface modification with gas-phase propiolic acid at high and medium vacuum conditions* Mahsa Konh, Chuan He, Zhengxin Li, Shi Bai, Elena Galoppini, Lars Gundlach, Andrew V. Teplyakov *Journal of Vacuum Science* **2018**, A 36, 041404 DOI: [10.1116/1.5031945](https://doi.org/10.1116/1.5031945)
3. *Vibrational Spectroscopy on Photoexcited Dye-Sensitized Films via Pump-Degenerate Four-Wave Mixing* Abraham, Baxter; Fan, Hao; Galoppini, Elena; Gundlach, Lars *J. Phys. Chem. A* **2018**, 122, 2039-2045 DOI: [10.1021/acs.jpca.7b10652](https://doi.org/10.1021/acs.jpca.7b10652)
4. *Morphology-Preserving Sensitization of ZnO Nanorod Surfaces via Click-Chemistry* Chuan He, Baxter Abraham, Hao Fan, Ryan Harmer, Zhengxin Li, Elena Galoppini, Lars Gundlach, and Andrew V. Teplyakov *J. Phys. Chem. Lett.* **2018**, 9, 768-772. DOI: [10.1021/acs.jpcllett.7b03388](https://doi.org/10.1021/acs.jpcllett.7b03388).
5. *Adsorption Geometry and Energy Level Alignment at the PTCDA/TiO<sub>2</sub> (110) Interface*, S Rangan, C Ruggieri, R Bartynski, JI Martínez, F Flores, J Ortega, *J. Phys. Chem. B* **2018**, 122, 534-542.
6. *Unveiling universal trends for the energy level alignment in organic/oxide interfaces,* J.I. Martínez, F. Flores, J. Ortega, S. Rangan, C.M. Ruggieri, and R.A. Bartynski, *Physical Chemistry Chemical Physics* **2017**, 19, 24412-24420.

## Molecular modules for photochemical and catalytic function in artificial photosynthesis

Karen L. Mulfort, Lars Kohler, Dugan Hayes, Ryan G. Hadt, Jens Niklas, Oleg G. Poluektov, Lin X. Chen, David M. Tiede

Division of Chemical Sciences and Engineering  
Argonne National Laboratory  
Lemont, IL 60439

This program investigates the underlying chemical, physical, and electronic properties of molecular chromophores and catalysts which are capable of coupling one-electron photoinduced excited states to multi-electron charge accumulation and ultimately, the multi-electron redox catalysis required for solar energy conversion. Molecular modules enable an unparalleled opportunity to understand, with very high resolution, how even very minor changes to the molecular structure influence photochemical and catalytic activity. Therefore, a highlight of this program is the close interaction of directed synthesis with high-resolution physical characterization of the ground and excited states using techniques including transient optical spectroscopy, multi-frequency EPR, X-ray absorption spectroscopy, and X-ray scattering. This talk will describe our group's progress in the design and discovery of modular, molecular architectures for artificial photosynthesis, specifically recent work on 1) driving directional electron transfer from Cu(I)diimine photosensitizer modules and 2) mapping the impact of structure on activity in Co(II)poly(pyridyl) H<sub>2</sub> catalyst modules. We anticipate that these studies will inform the design of advanced photocatalyst architectures based on molecular modules.

*CuHETPHEN chromophore modules.* The visible-light accessible metal-to-ligand charge transfer (MLCT) states of Cu(I)diimine complexes suggest that they may be viable replacements for benchmark [Ru(2,2'-bipyridine)<sub>3</sub>]<sup>2+</sup>-type photosensitizers. To access greater structural diversity and synthetic versatility than what is typically available with homoleptic Cu(I)diimine complexes, we have synthesized and fully characterized the ground and excited states of several heteroleptic Cu(I)bis(1,10-phenanthroline) (CuHETPHEN) model complexes (Figure 1). As previously observed for the

more common homoleptic Cu(I)bis(phenanthroline) complexes, modification of the phenanthroline ligand sterics adjacent to the Cu(I) center dramatically influences the excited state lifetime, allowing us to tune the <sup>3</sup>MLCT lifetime across orders of magnitude. These studies benchmarking the thermodynamic and kinetic properties of model CuHETPHEN complexes provide the foundational knowledge required for their integration into photocatalyst architectures.

Given the asymmetric coordination environment possible with CuHETPHEN complexes, we are particularly interested in understanding how to drive *directional* photoinduced electron transfer from these molecular modules. To investigate this question, we synthesized four CuHETPHEN dyads with the well-known molecular electron acceptor 1,4,5,8-naphthalene-diimide (NDI) covalently bound to either the blocking ligand (2,9-dimesityl-1,10-phenanthroline) or the

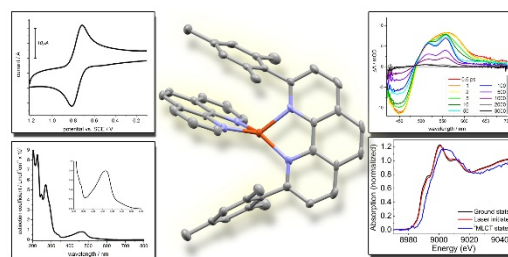


**Figure 1.** Single crystal structure of a CuHETPHEN complex and characterization: cyclic voltammety, UV-Vis absorption spectroscopy, ultrafast transient optical spectroscopy, and Cu K-edge X-ray transient absorption.

secondary ligand (1,10-phenanthroline or 2,9-dimethyl-1,10-phenanthroline) (Figure 2). Analysis of the ultrafast transient absorption spectra demonstrates that charge transfer proceeds with strong directional preference, and that complete formation of the charge-separated state is up to 35 times faster when NDI is linked to the blocking ligand. Also, in the coordinating polar solvent acetonitrile, the charge-separated state of the dyads is stabilized by the large structural distortion observed in the Cu(II) state, resulting in dramatically longer lifetimes for dyads with minimal substitution about the copper center. This work using model electron acceptors establishes a set of design principles we will use to connect more challenging electron acceptors (i.e. proton reduction catalysts) to molecular chromophores based on the CuHETPHEN platform.

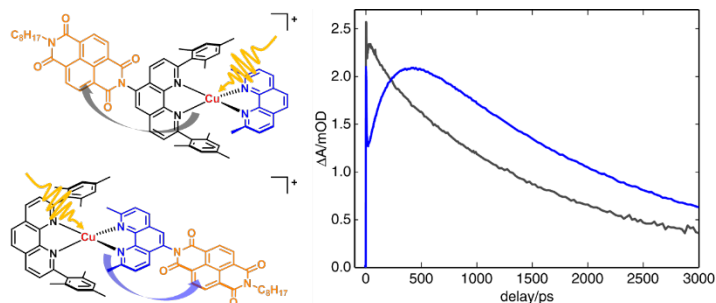


**Figure 2.** Left: chemical structure of CuHETPHEN-NDI dyads with NDI linked to blocking ligand (top) and secondary ligand (bottom). Right: Comparison of kinetics of charge separation following 400 nm excitation to form  $\text{NDI}^{\cdot-}$  in  $\text{CH}_3\text{CN}$ . Gray trace of CuHETPHEN with NDI on blocking ligand, blue trace of NDI on secondary ligand.

*Co(II)tetra(pyridyl) catalyst modules.* To complement our group's research on molecular modules that perform visible light absorption and direct photoinduced charge separation, we have recently pursued the design and mechanistic evaluation of new molecular, macrocyclic Co(II) catalysts for aqueous  $\text{H}_2$  generation (Figure 3). These catalysts were designed to incorporate redox-active bipyridine groups that are linked by nitrogen groups, both components that can participate in electron and proton transfer steps in the catalytic cycle. In comparing two molecular catalysts that differ by only one linking nitrogen, single crystal analysis reveals a profound impact on the molecular geometry, which in turn influences their relative catalytic activity. Photocatalysis measurements show that both catalysts are highly active for aqueous proton reduction at moderate pH levels, with the closed macrocycle reaching almost  $2 \times 10^4$  turnovers of  $\text{H}_2$  when photo-driven by  $[\text{Ru}(2,2'\text{-bipyridine})_3]^{2+}$  using ascorbate as an electron relay and a phosphine compound as the terminal electron donor. Measurements of the electrocatalytic activity were used to investigate key steps in the mechanism of proton reduction, and from a detailed analysis of these experiments, we propose a mechanism for catalytic proton reduction to  $\text{H}_2$  that involves both intramolecular proton and electron transfer steps between the macrocycle ligand to the cobalt center. This work demonstrates the vital role of the second coordination sphere in the catalytic cycle, and places these relatively simple complexes on the pathway toward molecular catalysts that mimic the valuable features of enzymatic catalysis.

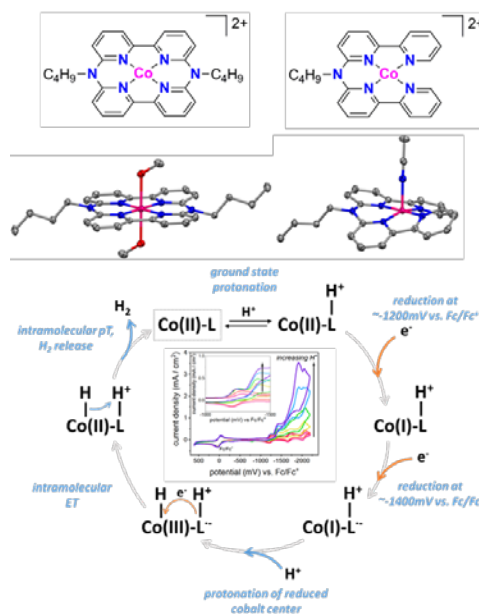


**Figure 3.** Top: chemical and single crystal structures of molecular Co(II)tetra(pyridyl)  $\text{H}_2$  catalysts. Bottom: proposed mechanism for proton reduction by new Co(II)tetra(pyridyl) catalysts.

## DOE Solar Photochemistry Sponsored Publications 2016-2019

1. L. Kohler, K. L. Mulfort. Photoinduced electron transfer kinetics of linked Ru-Co photocatalyst dyads. *J. Photochem. Photobiol. A*, **2019**, 373, 59-65. (Dr. Rajendra Rathore Memorial Issue)
2. L. Kohler, J. Niklas, R. C. Johnson, M. Zeller, O. G. Poluektov, K. L. Mulfort. Molecular cobalt catalysts for H<sub>2</sub> generation with redox activity and proton relays in the second coordination sphere. *Inorg. Chem.*, **2019**, 58, 1697-1709.
3. D. Hayes, L. Kohler, L. X. Chen, K. L. Mulfort. Ligand mediation of vectorial charge transfer in Cu(I)diimine chromophore—acceptor dyads. *J. Phys. Chem. Lett.*, **2018**, 9, 2070-2076.
4. D. Hayes, L. Kohler, R. G. Hadt, X. Zhang, C. Liu, K. L. Mulfort, L. X. Chen. Electron and energy relays along excited state pathways in supramolecular dinuclear complexes revealed by ultrafast optical and X-ray transient absorption spectroscopy. *Chem. Sci.*, **2018**, 9, 860-875.
5. L. Kohler, R. G. Hadt, D. Hayes, L. X. Chen, K. L. Mulfort. Synthesis, structure, and excited state kinetics of heteroleptic Cu(I) complexes with a new sterically demanding phenanthroline ligand. *Dalton Trans.*, **2017**, 46, 13088-13100.
6. K. L. Mulfort. Interrogation of cobaloxime-based supramolecular photocatalyst architectures. *Comptes Rendus Chimie*, **2017**, 20, 221-229.
7. D. Moonshiram, A. Guda, L. Kohler, A. Picon, S. Guda, C. S. Lehmann, X. Zhang, S. Southworth, K. L. Mulfort. Mechanistic evaluation of a nickel proton reduction catalyst using time-resolved X-ray absorption spectroscopy. *J. Phys. Chem. C*, **2016**, 120, 20049-20057.
8. K. L. Mulfort, L. M. Utschig. Modular homogeneous chromophore-catalyst assemblies, *Acc. Chem. Res.*, **2016**, 49, 835-843.
9. L. Kohler, D. Hayes, J. Hong, T. J. Carter, M. L. Shelby, K. A. Fransted, L. X. Chen, K. L. Mulfort. Synthesis, structure, ultrafast kinetics, and light-induced dynamics of CuHETPHEN chromophores. *Dalton Trans.*, **2016**, 45, 9871-9883.
10. J. Huang, Y. Tang, K. L. Mulfort, X. Zhang. The direct observation of charge separation dynamics in CdSe quantum dots/cobaloxime hybrids. *Phys. Chem. Chem. Phys.*, **2016**, 18, 4300-4303.

## Aryl Ether Weak Donor-Based Dyes as Strong Photoinduced Oxidants

Roberta R. Rodrigues, Adithya Peddapuram, and Jared H. Delcamp  
Department of Chemistry and Biochemistry  
University of Mississippi  
University, MS 38677

The overall goal of this project is to design a series of organic dyes with oxidation potentials varying from ~1-2 V versus NHE to analyze the effects of electron transfer agent potentials on the duration of charge separation at a metal oxide interface. Dyes are needed which are strongly oxidizing that can efficiently transfer electrons at an interface for a number of applications and to probe recombination rates as potentials are separated further in energy from a metal oxide conduction band potential. This current abstract focuses on a dye design which has increased the oxidation potential to 1.7 V from 1.0 V where many organic dyes based on ubiquitous aryl amines are found. Weakly donating aryl ether groups were used in conjunction with the electron deficient  $\pi$ -bridges, thienopyrroledione (pictured below) and benzothiadiazole. The dyes were studied via computation, cyclic voltammetry in solution and on  $\text{TiO}_2$ , absorption spectroscopy in solution and on  $\text{TiO}_2$ , time-correlated single photon counting experiments to probe electron transfer rates to  $\text{TiO}_2$ , and in dye-sensitized solar cell devices with several techniques to probe electron transfer efficiencies and durations. The devices focus on the use of  $\text{Fe}(\text{bpy})_3^{3+/2+}$  as a redox shuttle with a high oxidation potential (~1.4 V versus NHE) to demonstrate the strongly oxidizing nature of these dyes. In addition to the high oxidation potential of  $\text{Fe}(\text{bpy})_3^{3+/2+}$  and the reversible reduction/oxidation potentials of this complex, computational studies reveal a relatively low reorganization energy upon electron transfer. This low energy is attractive for probing kinetics without requiring a large overpotential for electron transfer. Future studies will focus on the use of transient absorption spectroscopy to probe the duration of charge separation at both the  $\text{TiO}_2$ -dye interface and at the  $\text{TiO}_2$ -redox shuttle interface to better understand the kinetics of this system. Additionally, future dye designs are being pursued to increase the oxidation potential to values  $\geq 2.0$  V versus NHE through  $\pi$ -bridge selection and weaker donor group designs.

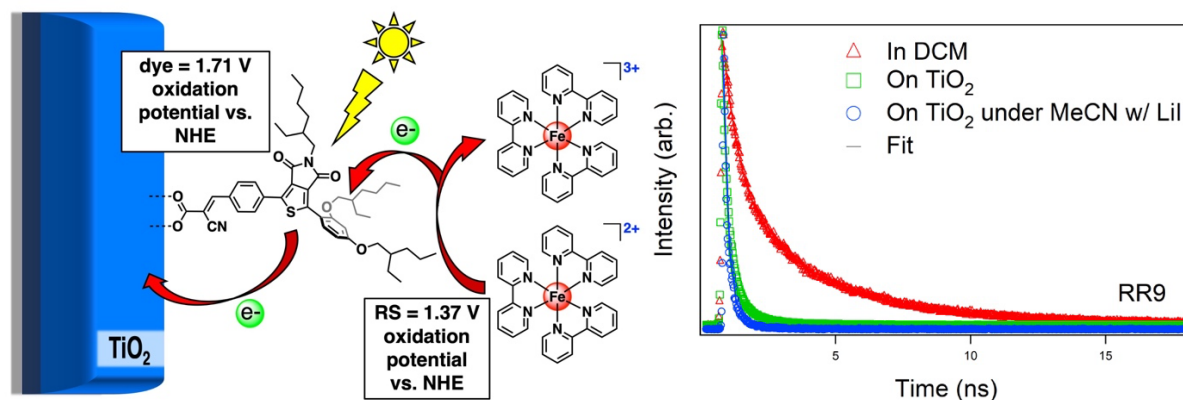


**Figure.** Left: Illustration of an amine-free aryl-ether based dye transferring electrons to  $\text{TiO}_2$  upon photoexcitation followed by electron transfer from  $\text{Fe}(\text{bpy})_3^{2+}$ . Right: Time-correlated single photon counting (TCSPC) studies of an amine-free aryl-ether based dye in solution and on  $\text{TiO}_2$ .

## Photoacid dye-sensitized solar energy conversion using water as a protonic semiconductor

Leanna Schulte,<sup>1</sup> Simon Luo,<sup>1</sup> Rylan Kautz,<sup>2</sup> Joseph Cardon,<sup>1</sup> William White,<sup>1</sup> and Shane Ardo  
Dept. of <sup>1</sup>Chemistry, <sup>2</sup>Materials Science & Engineering, <sup>3</sup>Chemical & Biomolecular Engineering  
University of California Irvine  
Irvine, CA 92697-2025

My group is pioneering the development of solar energy conversion processes that use the energy in light to directly drive ion transport, which is relevant to photoelectrochemical energy conversion and storage. Our initial focus uses water as the ionic charge-transport medium and photoacid dyes, such as that shown in **Figure 1**, to convert the energy in light into mobile charge carrier protons ( $H^+$ ) and/or hydroxides ( $OH^-$ ). We are designing materials systems infiltrated with water that rectify ionic current like a diode and have the smallest interference from ions besides  $H^+$  and  $OH^-$ . During my talk, I will share my group's methodical approach to fabricating effective ionic diodes in the dark by doping water with fixed charges, as well as efforts to understand mechanistic details of the photoacid sensitization cycle.

Our first materials system under study is based on the hydrated ion-exchange-membrane-liquid (hIEM|liq) junction as a direct analog of the electronic semiconductor-liquid junction. The built-in potential of the hIEM|liq is dictated by the difference in activity of protons inside and outside of the membrane. In addition, unique to ionic systems, the built-in (Donnan) potential can be measured directly, without interference from the chemical potential of  $H^+$  and  $OH^-$ , using two nominally identical reference electrodes whose redox reactions do not involve  $H^+$  and/or  $OH^-$ . Through significant efforts to minimize crossover of salt ions, which is inevitable in hIEM|liq electrolyte junctions, we recently measured net built-in potentials that were extremely stable on the timescale of hours to days using Nafion in contact with acidic aqueous electrolytes.

Our second and third materials systems under study are direct analogs of the electronic semiconductor pn/pin-junction. By laminating a cation-exchange membrane to an anion-exchange membrane to form a bipolar ion-exchange membrane (p(i)n-BPM), current rectification is observed. Different from all other uses of p(i)n-BPMs as passive ionic conductors in electrochemical solar energy conversion constructs, we do not intentionally add functional groups

at the interface of our p(i)n-BPMs and thus we observe small reverse saturation current densities and slow undesired electric-field-enhanced water dissociation.

Like hIEM|liq junctions, we can

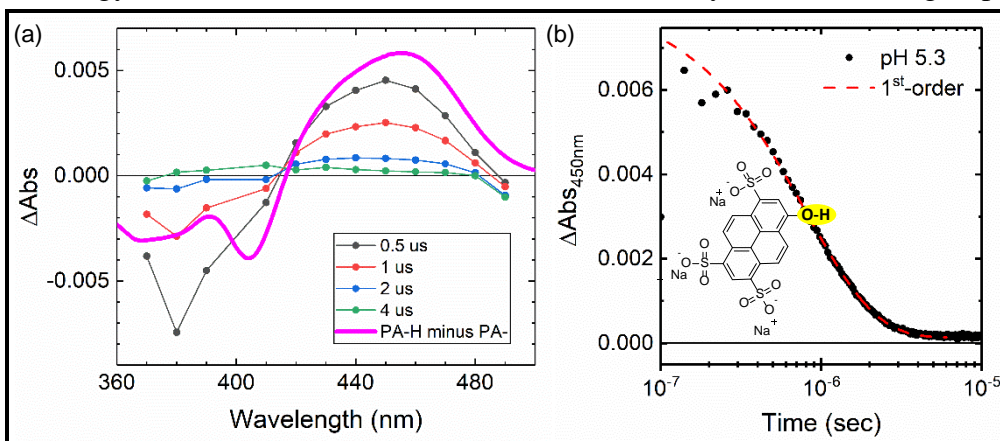


**Figure 1.** Transient absorption (a) spectra and (b) kinetics after pulsed 355 nm light excitation of an aqueous solution of 8-hydroxypyrene-1,3,6-trisulfonate salt (inset), resolving the process of ground-state dye regeneration via reprotonation.

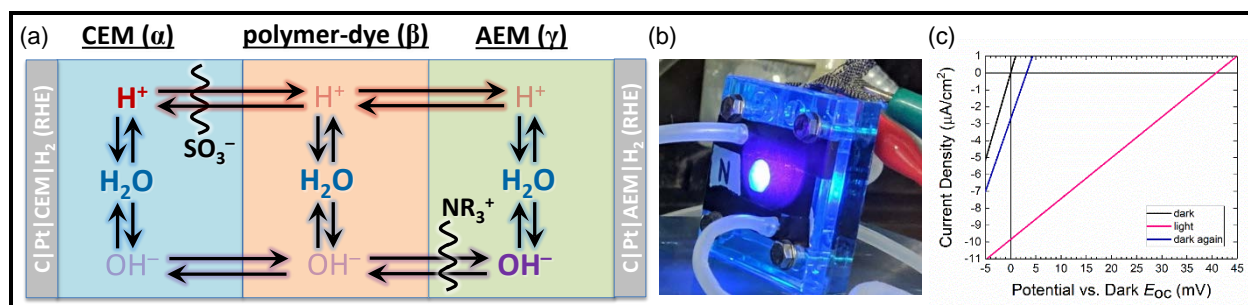


**Figure 2.** (a) Structure and reactivity in BPM MEA, (b) experiment, and (c) representative photovoltaic behavior.

directly measure the net built-in (Donnan) potential of our p(i)n-BPMs when the membrane separates acidic and alkaline aqueous liquid electrolytes; however, due to the unique nature of the p(i)n-BPM, we can also remove all inherent salt ions and characterize the materials in the presence of only high-purity water. This allows us to more cleanly isolate the properties of liquid water as a protonic semiconductor and is achieved by (i) fabricating membrane–electrode–assemblies (MEAs) out of our p(i)n-BPMs by interfacing them with two platinumized current collectors, (ii) replacing the acidic and alkaline aqueous liquid electrolytes with humidified forming gas (5% H<sub>2</sub> in N<sub>2</sub>), and (iii) performing solely two-electrode photo-iono-chemical measurements using the two Pt reversible hydrogen electrodes (**Figure 2**). While use of an MEA removes our ability to directly measure built-in potentials, it is more analogous to the traditional electronic semiconductor pn-junction therefore enabling the fundamental properties of liquid water as a protonic semiconductor to be quantified. Studies are underway to characterize these materials systems using electrochemical impedance spectroscopy, and for photoacid-dye-sensitized p(i)n-BPMs, spectral response and transient absorption spectroscopy. Notable recent results using photoacid-dye-sensitized pn-BPMs include quantification of quantum yields for photochemical processes.

Our final materials system under study is even more analogous to the electronic semiconductor pn-junction than a p(i)n-BPM. It entails doping water using simple acids like HCl and simple bases like KOH and then freezing the liquid water to immobilize the Cl<sup>-</sup> and K<sup>+</sup> counterions, thus forming doped amorphous solid protonic semiconductors. In this regard, we are making p(i)n-junction ice cube diodes (p(i)n-ice) and solar energy conversion constructs. While likely less practical from a technology standpoint, the simplicity in the design and ability to incorporate photoacid dye molecules that absorb throughout the thickness of the material make photoacid-dye-sensitized p(i)n-ice an excellent mimic of the traditional electronic semiconductor pn-junction. Through careful engineering of cell setups to reproducibly measure photo-iono-chemical behavior, we recently demonstrated excellent current rectification properties from pn-ice (**Figure 3**).

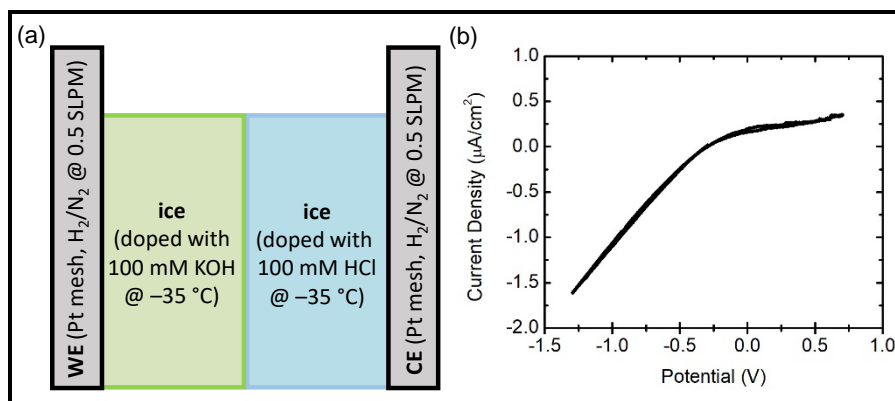


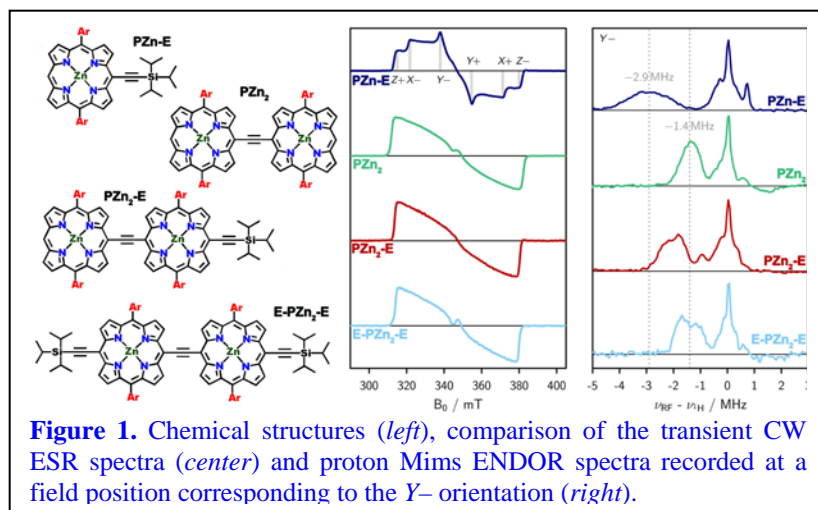
**Figure 3.** (a) Structure of ice cube diode MEA and (b) resulting rectifying current-density–potential behavior.

## Organic, Nanoscale, and Self-Assembled Structures Relevant to Solar Energy Conversion

Michael J. Therien  
Department of Chemistry  
French Family Science Center, 124 Science Drive  
Duke University  
Durham, NC 27708-0354

Understanding the molecular-level principles by which complex chemical systems carry out photochemical charge separation, transport, and storage will impact the design of practical solar energy conversion and storage devices. Towards this goal, this proposal focuses on several broad themes. We propose to: (i) delineate new compositions of matter relevant to solar energy conversion, (ii) understand the basic photophysical properties of next-generation conjugated materials for excitonic solar cells, (iii) elucidate rules and principles that govern charge transfer, charge migration, photoconductivity, the extent of charge and exciton delocalization, and exciton diffusion dynamics in structures and assemblies relevant to light-driven energy transduction, (iv) probe and modulate the extent of electronic coupling between conjugated organic materials and nanoscale structures in both ground and excited states, and (v) engineer high quantum yield electron-hole pair production from initially prepared excitonic states in organic materials and organic compositions that feature nanoscale, electrooptically active components. Accomplishments over the current funding period include:

*Probing the Role of Electronic Symmetry for Triplet State Electronic Delocalization.* We explored the influence of electronic symmetry on triplet state delocalization in linear zinc

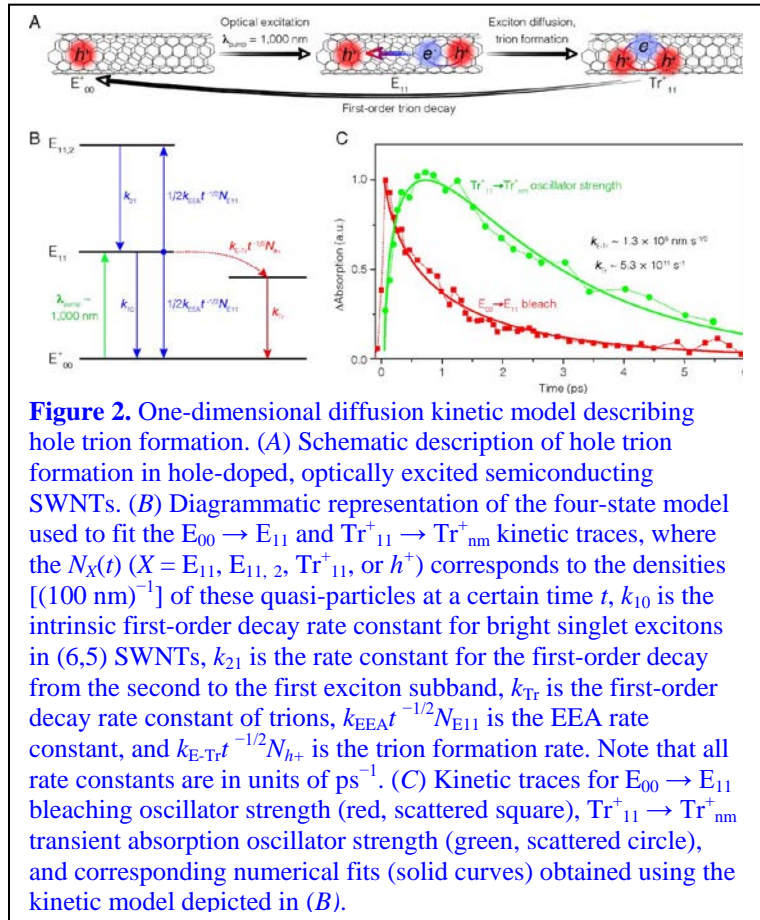


porphyrin oligomers using electron spin resonance (ESR) techniques. Exploiting a combination of transient continuous wave (CW) and pulse electron nuclear double resonance (ENDOR) spectroscopies, we demonstrated experimentally that complete triplet state delocalization requires the chemical equivalence of all porphyrin units (**Figure 1**). The experimental results are supported by DFT calculations; for example, when uneven delocalization in a porphyrin dimer is driven by the presence of a terminal ethynyl group on only one side of the porphyrin chain, the two (porphinato)metal units become inequivalent: this inequivalence is manifest in a diminution of the magnitude of triplet exciton delocalization relative to the symmetric PZn<sub>2</sub> structure. When the conjugation length of the molecule is further increased upon addition of a second terminal ethynyl group, which restores the symmetry of the system, the triplet state wavefunction again becomes completely delocalized. These observations suggest that electronic symmetry is of greater importance for triplet state delocalization than other frequently invoked factors such as conformational rigidity or fundamental length-scale limitations.

*Elucidation of Single Walled Carbon Nanotube (SWNT) Hole-Trion Absorptive and Dynamical Properties.* Trions (quasi-particles comprised of a charge and an exciton) have been extensively

studied in inorganic semiconductors, particularly quantum wells, under low-temperature conditions, as these species may provide new opportunities to manipulate charge, spin, and electronic excitation. Recently, it has been reported that optical photoexcitation of the SWNT charged ground state gives rise to trions even at room temperature. Reports to date that describe SWNT trion photophysics are ambiguous, particularly with respect to trion absorption signatures, as well as trion formation and decay dynamics, due in large part to the heterogeneous nature of carbon nanotube samples that have been thus far interrogated. A clear picture of trion photophysics can only emerge from pump-probe spectroscopic studies that correlate dynamical processes characteristic of singlet exciton and free carriers, in single chirality SWNT samples in which polaron concentrations and exciton densities are rigorously controlled.

We investigated the transient absorptive and dynamical properties of electron and hole trions in charge-doped polymer-wrapped semiconducting SWNTs. This work exploits redox titration experiments that fix electron or hole concentrations in the polymer-wrapped SWNT superstructures, and ultrafast pump-probe transient spectroscopic measurements that determine trion transient absorption signatures and dynamics as functions of absolute electron- or hole-doping levels. Ultrafast pump-probe transient absorption spectroscopic studies of heavily hole-doped (6,5) SWNTs (100 holes / 700 nm) indicate: (i) ultrafast decay of both the  $E_{11}$  exciton and hole-polaron bleaching signals, as well as the evolution of a new transient absorption band in 1180-1200 nm spectral domain that is absent in analogous experiments carried out with neutral, undoped SWNTs; (ii) dynamical correlation of the decay of the  $E_{11}$  exciton and hole-polaron bleach signals, and evolution of a nascent transient absorption ( $\tau_{\text{rise}} \sim 400\text{-}500$  fs), indicating that trions are produced via exciton migration to a stationary hole polaron site (**Figure 2**). (6,5) SWNTs featuring a wide range of fixed and quantified hole doping levels were investigated in order to ascertain how trion formation and decay dynamics are influenced by hole polaron density. These studies show that under appropriate carrier-doping densities, exciton-to-trion conversion in SWNTs can approach 100% at ambient temperature, and provides new insights into how trion states can be exploited in energy conversion processes.



## DOE Solar Photochemistry Sponsored Publications 2016-2019

- 1) Valence Band Dependent Charge Transport in Bulk Molecular Electronic Devices Incorporating Highly Conjugated Multi[(Porphinato)Metal] Oligomers, R. C. Bruce, R. Wang, J. Rawson, M. J. Therien, and W. You, *J. Am. Chem. Soc.* **2016**, *138*, 2078–2081. DOI: 10.1021/jacs.5b10772.
- 2) First-Order Hyperpolarizabilities of Chiral, Polymer-Wrapped Single-Walled Carbon Nanotubes, G. Depotter, J.-H. Olivier, M. G. Glesner, P. Deria, Y. Bai, G. Bullard, A. S. Kumbhar, M. J. Therien, and K. Clays, *Chem. Commun.* **2016**, *52*, 12206–12209. DOI: 10.1039/C6CC06190G.
- 3) On the Importance of Electronic Symmetry for Triplet State Delocalization, S. Richert, G. Bullard, J. Rawson, P. J. Angiolillo, M. J. Therien, and C. R. Timmel, *J. Am. Chem. Soc.* **2017**, *139*, 5301–5304. DOI: 10.1021/jacs.7b01204.
- 4) Controlling the Excited-State Dynamics of Low Band Gap, NIR Absorbers via Proquinoidal Unit Electronic Structural Modulation, Y. Bai, J. Rawson, S. A. Roget, J.-H. Olivier, J. Lin, P. Zhang, D. N. Beratan, and M. J. Therien, *Chem. Sci.* **2017**, *8*, 5889–5901. DOI: 10.1039/c7sc02150j.
- 5) Additive Engineering for High-Performance Room-Temperature-Processed Perovskite Absorbers with Micron-Size Grains and Microsecond-Range Carrier Lifetimes, Q. Han, Y. Bai, J. Liu, K. Du, D. Ji, Y. Zhou, C. Cao, D. Shin, A. D. Franklin, J. T. Glass, J. Hu, M. J. Therien, J. Liu, and D. B. Mitzi, *Energy Environ. Sci.* **2017**, *10*, 2365–2371. DOI: 10.1039/C7EE02272G.
- 6) Dynamics of Charged Excitons in Electronically and Morphologically Homogeneous Single-Walled Carbon Nanotubes, Y. Bai, J.-H. Olivier, G. Bullard, C. Liu, and M. J. Therien. *Proc. Natl. Acad. Sci. U.S.A.* **2018**, *115*, 674-679. DOI: 10.1073/pnas.1712971115.
- 7) Unusual Solvent Polarity Dependent Excitation Relaxation Dynamics of a Bis[*p*-ethynyldithiobenzoato]Pd-linked Bis[(porphinato)zinc] Complex, J. Park, T.-H. Park, L. E. Sinks, P. Deria, J. Park, M.-H. Baik, and M. J. Therien, *Mol. Syst. Des. Eng.* **2018**, *3*, 275–284. DOI: 10.1039/c8me00001h.
- 8) Carrier Dynamics Engineering for High-Performance Electron-Transport-Layer-Free Perovskite Photovoltaics, Q. Han, J. Ding, Y. Bai, T. Li, J. Ma, Y. Chen, Y. Zhou, J. Liu, Q. Ge, J. Chen, J. T. Glass, M. J. Therien, J. Liu, D. B. Mitzi, and J. Hu, *Chem.* **2018**, *4*, 2405–2417. DOI: 10.1016/j.chempr.2018.08.004.
- 9) Solvent and Wavelength-Dependent Photoluminescence Relaxation Dynamics of Carbon Nanotube  $sp^3$  Defect States, X. He, K. A. Velizhanin, G. Bullard, Y. Bai, J.-H. Olivier, N. F. Hartmann, B. J. Gifford, S. Kilina, S. Tretiak, H. Htoon, M. J. Therien, and S. K. Doorn, *ACS Nano* **2018**, *12*, 8060–8070. DOI: 10.1021/acsnano.8b02909.
- 10) Quantitative Evaluation of Optical Free Carrier Generation in Semiconducting Single-Walled Carbon Nanotubes, Y. Bai, G. Bullard, J.-H. Olivier, and M. J. Therien, *J. Am. Chem. Soc.* **2018**, *140*, 14619–14626. DOI: 10.1021/jacs.8b05598.

# Microsecond Charge Separation Lifetimes in Semiconducting Single-walled Carbon Nanotube Heterojunctions

Jeff Blackburn, Hyun Suk Kang, Dana Sulas, Andrew Ferguson, Justin Johnson, Garry Rumbles  
Chemistry and Nanoscience Center  
National Renewable Energy Laboratory  
Golden, CO 80401

Semiconducting single-walled carbon nanotubes (s-SWCNTs) are attractive absorbers for use in solar energy harvesting schemes because of their strong and energetically tunable optical absorption, and high charge 1D carrier/exciton mobilities due to the delocalized nature of the  $\pi$ -electron system. Monolayer two-dimensional (2D) transition metal dichalcogenides (TMDCs) are another attractive model system for studying photoinduced carrier generation mechanisms in low-dimensional excitonic materials, since they possess strong direct bandgap absorption, large exciton binding energies, and are only a few atoms thick. Additionally, the conduction and valence band energies of several of these monolayer TMDCs make them potentially useful in electro- and photocatalytic (e.g. solar-driven) fuel generation schemes. In both s-SWCNTs and TMDCs, strong quantum confinement and low dielectric screening produce exciton-binding energies substantially exceeding  $k_B T$  at room temperature. The crucial first step in using excitonic semiconductors for solar energy harvesting applications is to dissociate excitons, and much of our work within the Solar Photochemistry program is devoted to the rational development of donor/acceptor heterojunctions with properties that facilitate exciton dissociation to produce high yields of long-lived separated charges. As such, we are interested in understanding the impact of interfacial thermodynamics and entropic factors on the kinetics of critical excited-state events such as photoinduced charge transfer and carrier recombination.

In this presentation, I will discuss recent studies that probe the generation and recombination of long-lived charges in samples consisting of heterojunctions consisting of highly pure (6,5) s-SWCNTs and either organic (perylene diimide) or inorganic (monolayer of  $\text{MoS}_2$ ) electron acceptor layers. In previous studies, our results have suggested that the low charge transfer reorganization energies and high carrier mobilities in s-SWCNTs help to facilitate rapid photoinduced exciton dissociation and subsequent diffusion of charges away from the charge separation interface. The resulting charge-separated state tends to recombine quite slowly, on the order of nanoseconds or even microseconds. These recent studies confirm these findings, and additionally show that the charge-separation lifetime can be further prolonged in systems where aggregates within the acceptor phase also allow for diffusion or delocalization of electrons.

## The Role of Molecular Aggregates in Photoinduced Charge Separation Across SWCNT/Organic Interfaces

In this study, we investigate excited-state dynamics at the heterojunction between (6,5) s-SWCNTs and two perylene diimide (PDI)-based electron acceptors (**hPDI2-pyr-hPDI2** and **Trip-hPDI2**, Fig. 1). The two PDI-based acceptors were synthesized by Dr. Colin Nuckolls' group at U. Columbia, and were chosen to have distinct molecular geometries and frontier orbital energies that establish

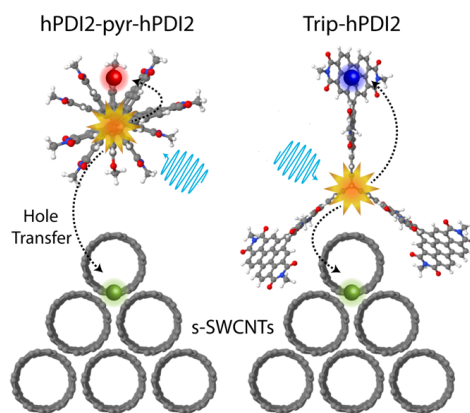
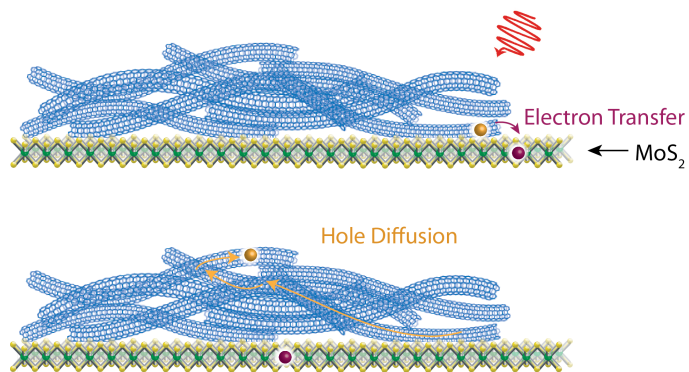


Figure 1. Ultrafast charge separation across PDI /s-SWCNT interfaces by picosecond hole transfer.

sufficient thermodynamic driving force for exciton dissociation at the heterojunction with (6,5) s-SWCNTs. Transient absorption (TA) measurements demonstrate that photoinduced charge transfer occurs on a time scale of  $< 2$  ps, producing long-lived separated charges with lifetimes exceeding  $1.0 \mu\text{s}$ . A second slower charge transfer step is observed for the **hPDI2-pyr-hPDI2** bilayer and charge recombination also occurs substantially more slowly in this bilayer than within the **Trip-hPDI2** bilayer. To explain such differences, we consider the potential roles of the thermodynamic charge transfer driving force available at each interface and the different molecular structure and inter-molecular interactions of PDI-based acceptors. Importantly, our results demonstrate that aggregates formed within the **hPDI2-pyr-hPDI2** film help in moving the transferred electron away from the dissociation site, reducing the rate of geminate recombination.

### Photoinduced Charge Separation Across a Mixed-Dimensionality SWCNT/MoS<sub>2</sub> Interface

In this study, we investigate photoinduced electron and hole transfer across interfaces between (6,5) s-SWCNTs and monolayer MoS<sub>2</sub>, where a Type II heterojunction is expected to provide a thermodynamic driving force for photoinduced electron and hole transfer. Deposition of a thin layer of (6,5) s-SWCNTs on CVD-grown MoS<sub>2</sub> strongly quenches MoS<sub>2</sub> photoluminescence, suggesting photoinduced electron (and/or) energy transfer, and TA measurements confirm the predominance of charge transfer. We observe sub-picosecond



**Figure 2.** Ultrafast charge separation across s-SWCNT/MoS<sub>2</sub> interfaces by sub-picosecond photoinduced electron transfer.

kinetics for both electron and hole transfer, and in both cases, the charge-separated state lasts for ca.  $1 \mu\text{s}$  ( $\tau \approx 150$  ns). The monolayer thickness of the MoS<sub>2</sub> layer used here provides an interesting counterpart to our previously studied SWCNT/organic heterojunctions. In these *organic* ‘bilayers’, neither donor or acceptor can be considered a true ‘monolayer’, making it difficult to distinguish the degree to which recombination is affected by (1) hole diffusion/delocalization in the SWCNT phase and/or (2) electron diffusion/delocalization in the acceptor phase. In the MoS<sub>2</sub> monolayer, the electron cannot diffuse away from the interface, strongly suggesting that diffusion and/or delocalization of holes within the s-SWCNT phase plays a critical role in producing the microsecond charge separation lifetimes observed in these systems. Interestingly, we can synthesize MoS<sub>2</sub> monolayers that contain very small amounts ( $<1\%$  of the total film area) of multi-layer sections. In striking analogy to the PDI studies, SWCNT/MoS<sub>2</sub> heterojunctions containing these minute amounts of MoS<sub>2</sub> ‘aggregates’ demonstrate recombination lifetimes that are slowed by an order of magnitude, compared to samples with no multi-layers.

Both studies discussed here support the notion that long-lived charge-separated states can be facilitated by designing interfaces where strong electronic coupling within each phase (donor and acceptor) enables charges to efficiently escape the interface. In our future studies, we will devote ongoing effort to disentangle the effects of interfacial thermodynamics (i.e. exciton dissociation driving force) and molecular structure considerations (i.e. steric effects, electronic coupling, reorganization energy) on photoinduced charge transfer at model interfaces between s-SWCNTs and a broad array of both organic and inorganic acceptors.

## DOE Sponsored Publications 2016-2019

1. Andrew J. Ferguson, Obadiah G. Reid, Sanjini U. Nanayakkara, Rachele Ihly, Jeffrey L. Blackburn.\* Efficiency of Charge-Transfer Doping in Organic Semiconductors Probed with Quantitative Microwave and Direct-Current Conductance. *Journal of Physical Chemistry Letters* **2018** *9*, 6864 – 6870. DOI: 10.1021/acs.jpcclett.8b03074
2. Tong Sun, Hanyu Zhang, Xiang Wang, Jun Liu, Chuanxiao Xiao, Sanjini Nanayakkara, Jeffrey L. Blackburn, Michael Mirkin, Elisa Miller. Nanoscale Mapping of Hydrogen Evolution on Metallic and Semiconducting MoS<sub>2</sub> Nanosheets. *Nanoscale Horizons* **2018** *Advance Article*. DOI: 10.1039/C8NH00346G
3. Lenore Kubie, Kevin Watkins, Rachele Ihly, Henry Wladkowski, Jeffrey Blackburn, William Rice, Bruce Parkinson. Optically Generated Free-carrier Collection From and All Single-walled Carbon Nanotube Active Layer. *J. Phys. Chem. Lett.* **2018**, *9*, 4841 - 4847. DOI: 10.1021/acs.jpcclett.8b01850
4. Kamran Shayan, Xiaowei He, Yue Luo, Claire Rabut, Xiangzhi Li, Nicolai F. Hartmann, Jeffrey L. Blackburn, Stephen K. Doorn, Han Htoon and Stefan Strauf. Suppression of Exciton Dephasing in Sidewall-functionalized Carbon Nanotubes Embedded into Metallo-dielectric Antennas. *Nanoscale* **2018**, *10*, 12631. DOI: 10.1039/C8NR03542C.
5. Jeffrey L. Blackburn,\* Obadiah G. Reid, Andrew J. Ferguson. Spectroscopy of Ground- and Excited-State Charge Carriers in Single-Walled Carbon Nanotubes. *Invited Book Chapter* in “Optical Properties of Carbon Nanotubes, Volume 9 - A Volume Dedicated to the Memory of Professor Mildred Dresselhaus.” **2018** (World Scientific).
6. Stein van Bezouw, Dylan H. Arias, Rachele Ihly, Sofie Cambré, Andrew J. Ferguson, Jochen Campo, Justin C. Johnson, Joeri Defiliet, Wim Wenseleers,\* and Jeffrey L. Blackburn.\* Diameter-dependent Absorption and Energy Transfer from Encapsulated Dye Molecules Towards Single-walled Carbon Nanotubes. *ACS Nano*. **2018**, *12*, 6881 – 6894. DOI: 10.1021/acsnano.8b02213
7. Long-lived Charge Separation at Heterojunctions Between Semiconducting Single-walled Carbon Nanotubes and Perylene Diimide Electron Acceptors. Hyun Suk Kang, Thomas J. Sisto, Samuel Peurifoy, Dylan H. Arias, Boyuan Zhang, Colin Nuckolls, Jeffrey L. Blackburn\* *J. Phys. Chem. C* **2018**, *122*, 14150. (Invited Article for Prashant Kamat Festschrift). DOI: 10.1021/acs.jpcc.8b01400.
8. Eric E. Benson, Hanyu Zhang, Samuel A. Schuman, Sanjini U. Nanayakkara, Noah D. Bronstein, Suzanne Ferrere, Jeffrey L. Blackburn, and Elisa M. Miller. Balancing the Hydrogen Evolution Reaction, Surface Energetics, and Stability of Metallic MoS<sub>2</sub> Nanosheets via Covalent Functionalization. *Journal of the American Chemical Society* **2018**, *140*, 441. DOI: 10.1021/jacs.7b11242
9. Kamran Shayan, Claire Rabut, Xiaoqing Kong, Xiangzhi Li, Yue Luo, Kevin S. Mistry, Jeffrey L. Blackburn, Stephanie S. Lee, Stefan Strauf. Broadband light collection efficiency enhancement of carbon nanotube excitons coupled to metallo-dielectric antenna arrays. *ACS Photonics* **2018**, *5*, 289. DOI: 10.1021/acsp Photonics.7b00786

10. Daniel M. Kroupa, Dylan H. Arias, Jeffrey L. Blackburn, Gerard M. Carroll, Devin B. Granger, John E. Anthony, Matthew C. Beard, Justin C. Johnson. Control of Energy Flow Dynamics between Tetracene Ligands and PbS Quantum Dots by Size Tuning and Ligand Coverage. *Nano Letters* **2017** *18*, 865-873. doi: 10.1021/acs.nanolett.7b04144
11. Lance M. Wheeler, Rachele Ihly, David T. Moore, Noah J. Stanton, Jeffrey L. Blackburn, Nathan R. Neale. Switchable Photovoltaic Windows Enabled by Reversible Photothermal Complex Dissociation from Metal Halide Perovskites. *Nature Communications* **2017**, *8*, 1722. DOI: 10.1038/s41467-017-01842-4
12. Xiaowe He, Brendan Gifford, N. F. Hartmann, Rachele Ihly, Xuedan Ma, Svetlana Kilina, Yue Luo, Kamran Shayan, Stefan Strauf, Jeffrey L. Blackburn, Sergei Tretiak, Stephen K. Doorn, and Han Htoon. Low Temperature Single Carbon Nanotube Spectroscopy of  $sp^3$  Quantum Defects. *ACS Nano* **2017**, *11*, 10785. DOI: 10.1021/acsnano.7b03022
13. Bradley A. MacLeod, Noah J. Stanton, Isaac E. Gould, Devin Wesenberg, Rachele Ihly, Zbyslaw R. Owczarczyk, Katherine E. Hurst, Christopher S. Fewox, Christopher N. Folmar, Katherine Holman Hughes, Barry L. Zink, Jeffrey L. Blackburn\* and Andrew J. Ferguson.\* Large  $n$ - and  $p$ -type thermoelectric power factors from doped semiconducting single-walled carbon nanotube thin films. *Energy & Environmental Science* **2017** *10*, 2168. DOI: 10.1039/C7EE01130J
14. He, X., Hartmann, N.F., Ma, X., Ihly, R., Blackburn, J.L., Gao, W., Kono, J., Yomogida, Y., Hirano, A., Tanaka, T., Kataura, H., Htoon, H., Doorn, S.K. Tunable Room-Temperature Single-Photon Emission at Telecom Wavelengths from Carbon Nanotube Quantum Defects. *Nature Photonics* **2017**, *11*, 577. DOI: 10.1038/NPHOTON.2017.119
15. Luo, Y., Ahmadi, E.D., Shayan, K., Ma, Y., Mistry, K.S., Zhang, C., Hone, J., Blackburn, J.L., Strauf, S. Purcell-enhanced quantum yield from carbon nanotube excitons coupled to plasmonic nanocavities. *Nature Communications* **2017**, *8*, 1413. doi:10.1038/s41467-017-01777-w.
16. Blackburn, J.L.\* Semiconducting Single-walled Carbon Nanotubes in Solar Energy Harvesting. *ACS Energy Letters* **2017**, *2*, 1598. DOI: 10.1021/acsenerylett.7b00228 (Invited Perspective)
17. Hartmann, N. F., Pramanik, R., Dowgiallo, A-M, Ihly, R., Blackburn, J.L., Doorn, S.K. Photoluminescence Imaging of Polyfluorene Surface Structures on Semiconducting Carbon Nanotubes: Implications for Thin Film Exciton Transport. *ACS Nano* **2016**, *10*, 11449. DOI: 10.1021/acsnano.6b07168
18. Mallojusyla, A. Gupta, G., Blackburn, J.L., Doorn, S., Mohite, A. Critical Role of the Sorting Polymer in Carbon Nanotube Based Minority Carrier Devices. *ACS Nano* **2016**, *10*, 10808. DOI: 10.1021/acsnano.6b04885
19. Kadria-Vili, Y. Bachilo, S., Blackburn, J.L., Weisman, B., Photoluminescence Side Band Spectroscopy of Individual Single-Walled Carbon Nanotubes. *J. Phys. Chem. C*, **2016**, *120*, 23898. DOI: 10.1021/acs.jpcc.6b08768
20. Norton-Baker, B., Ihly, R., Gould, I.E., Avery, A.D., Owczarczyk, Z., Ferguson, A.J., Blackburn, J.L.\* Polymer-free Carbon Nanotube Thermoelectrics with Improved Charge

- Carrier Transport and Power Factor. *ACS Energy Letters*, **2016**, *1*, 1212. DOI: 10.1021/acseenergylett.6b00417
21. M.C. Beard, J.L. Blackburn, J.C. Johnson, G. Rumbles, “Status and Prognosis of Future Generation Photoconversion to Photovoltaics and Solar Fuels”, *ACS Energy Lett.*, **2016**, *1*, 344. DOI: 10.1021/acseenergylett.6b00204
  22. Nenon, D.P., Christians, J.A., Wheeler, L.M., Blackburn, J.L., Sanehira, E.M., Dou, B., Olsen, M., Zhu, K., Berry, J.J., Luther, J.M. Structural and Chemical Evolution of Methylammonium Lead Halide Perovskites During Thermal Processing from Solution. *Energy & Environmental Science*, **2016**, *9*, 2072, DOI: 10.1039/C6EE01047D.
  23. Ihly, R., Mistry, K.S., Ferguson, A.J., Clikeman, T.T., Larson, B.W., Boltalina, O.V., Strauss, S.H., Rumbles, G., Blackburn, J.L.\* Tuning the Driving Force for Exciton Dissociation in Single-walled Carbon Nanotube Heterojunctions. *Nature Chemistry*, **2016**, *8*, 603. DOI: 10.1038/nchem.2496
  24. Dowgiallo, A-M, Mistry, K.S., Johnson, J.C., Ferguson, A.J., Reid, O.G., Blackburn, J.L. Probing Exciton Diffusion and Dissociation in Single-walled Carbon Nanotube-C<sub>60</sub> Heterojunctions.\* *J. Phys. Chem. Lett.*, **2016**, *7*, 1794. DOI: 10.1021/acs.jpcllett.6b00604
  25. Ihly, R., Dowgiallo, A-M, Yang, M., Schulz, P., Stanton, N.J., Reid, O.G., Ferguson, A.J., Zhu, K., Berry, J.J., Blackburn, J.L.\* Efficient Charge Extraction and Slow Recombination in Organic-Inorganic Perovskites Capped with Semiconducting Single-walled Carbon Nanotubes. *Energy & Environmental Science*, **2016**, *Advance Article*, DOI: 10.1039/C5EE03806E.
  26. Schulz, P., Dowgiallo, A-M, Yang, M., Zhu, K., Blackburn, J.L., Berry, J. Charge Transfer Dynamics between Carbon Nanotubes and Hybrid Organic Metal Halide Perovskite Films. *J. Phys. Chem. Lett.* **2016**, *7*, 418.
  27. Avery, A.D., Zhou, B.H., Lee, J.H., Lee, E-S, Miller, E.M., Ihly, R., Wesenberg, D., Mistry, K.S., Guillot, S.L., Zink, B.L., Kim, Y-H, Blackburn, J.L.,\* Ferguson, A.J.\* Tailored Semiconducting Carbon Nanotube Networks with Enhanced Thermoelectric Properties. *Nature Energy*, **2016**, *1*, 16033, DOI: 10.1038/nenergy.2016.33.

# Ultrafast Vibrational Nano-Thermometers to Probe Triplet Separation vs. Relaxation During Singlet Fission

Eric R. Kennehan, Grayson S. Doucette, and John B. Asbury  
 Department of Chemistry, The Pennsylvania State University  
 University Park, PA 16802

The objective of this research is to elucidate the dynamics of critical intermediates involved in solar energy transduction mechanisms in singlet fission sensitizers and colloidal quantum dots using ultrafast infrared spectroscopy. In both cases, broad electronic transitions specific to intermediate electronic states are probed in the mid-infrared while simultaneously examining the vibrational spectra of the molecular species. This combination is uniquely able to explore the dynamics of electronic states and the structural properties of the molecules that give rise to those states. The research program leverages the simultaneous measurement of electronic and vibrational processes to gain new insight about how molecular structure affects electronic and optical properties to inform the development of fundamental design principles for next generation solar energy transduction systems based on singlet fission and quantum dot sensitizers.

We used ultrafast vibrational spectroscopy in the mid-infrared spectral range to probe the dynamics of electronic states involved in all stages of the singlet fission reaction through their unique electronic and vibrational signatures. This capability was demonstrated using a model singlet fission chromophore, 6,13-bis(triisopropylsilylethynyl) pentacene (TIPS-Pn). We identified new electronic transitions in the mid-infrared spectral range (Figure 1a) that were distinct for both initially excited singlet states and correlated triplet pair intermediates  $^1(\text{TT})$ . We used these transitions to show that the dissociation dynamics of the intermediates could be measured directly – revealing that complete dissociation to form independent triplet excitons  $\text{T}$  occurred on time scales ranging from 100 ps to 1 ns. This finding indicates that relaxation processes competing with triplet harvesting or charge transfer should be controlled on time scales that are far longer than previously believed even when the primary singlet fission events occur on ultrafast time scales.

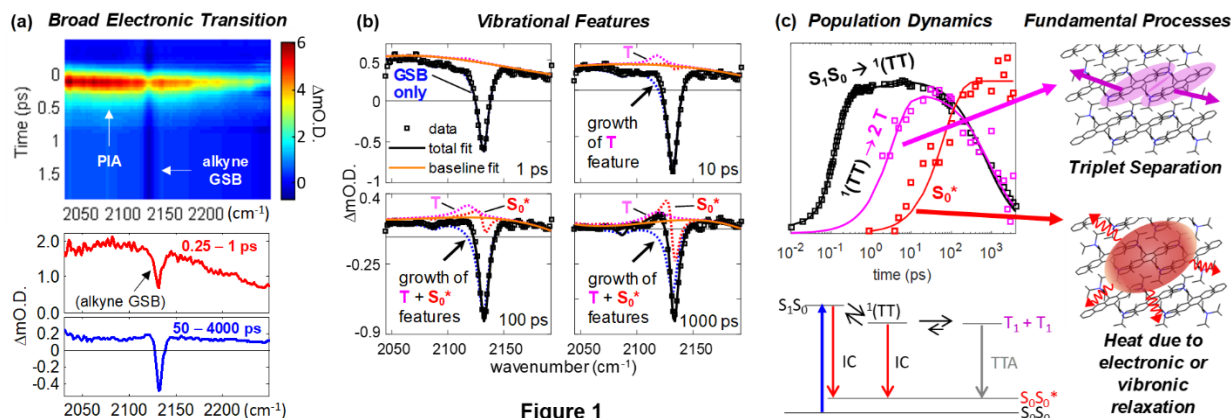
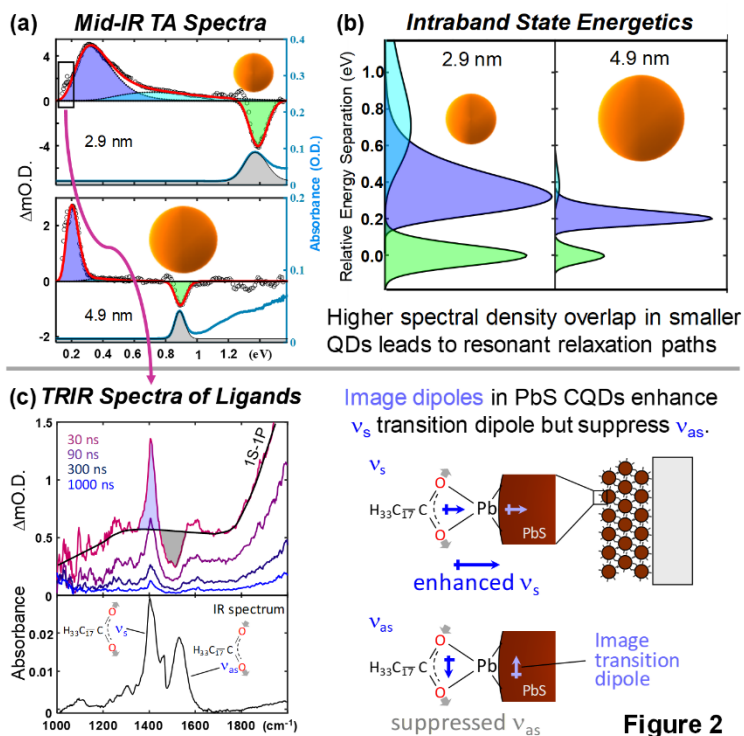


Figure 1

Furthermore, we used the alkyne groups of the TIPS side chains to examine the dynamics of triplet excitons that successfully separated from correlated triplet pair states in crystalline films of TIPS-Pn. This could be done because the alkyne groups were coupled to the conjugated framework of the pentacene cores and therefore exhibited distinct frequencies for singlet versus triplet excitons (Figure 1b). Relaxation processes during the separation of triplet excitons and triplet-triplet

annihilation after their separation resulted in the formation of hot ground state molecules  $S_0^*$  that also exhibited unique vibrational frequencies (Figure 1c). In future work, we will use the vibrational features to track the energies of electronic states during singlet fission to understand how structure and energetics influence the rate and yield of triplet exciton multiplication.

We also used the ability to measure electronic transitions and vibrational features in the mid-infrared to examine resonant relaxation channels that bypassed the predicted phonon-bottleneck in PbS quantum dots over a range of sizes and passivated with a variety of ligands. Direct measurements of higher energy 1P and 1D intraband states in the mid-infrared (Figure 2a) permitted detailed analysis of the electronic overlap of the quantum confined states that influenced their relaxation processes (Figure 2b). In smaller PbS nanocrystals, where the phonon bottleneck is expected to be most pronounced, relaxation of parity selection rules combined with stronger electron-phonon coupling led to greater overlap of the energetic distributions of quantum confined states. The effect was observed across a variety of ligands and likely reflected electron-phonon coupling of the nanocrystals and surfaces rather than their ligands. Larger but still quantum confined nanocrystals did not exhibit such relaxation of the parity selection rules and possessed narrower intraband states. These findings indicated that, at small radii, electron-phonon interactions overcome the advantageous increase in energetic separation of the electronic states for PbS quantum dots. Selection of appropriately sized quantum dots, which minimize spectral broadening due to electron-phonon interactions while maximizing electronic state separation, is necessary to observe the phonon bottleneck. In future work, we will explore how quantum dot composition and structure influence electron-phonon coupling and how these can be tuned to achieve efficient hot carrier collection and multiple exciton generation.



Furthermore, the generation of excitons in PbS quantum dots created highly polarizable states that modulated the vibrational spectra of the carboxylate groups of ligands attached to the nanocrystal surfaces through the formation of image dipoles (Figure 2c). The symmetric vibrational mode with a transition dipole moment normal to the quantum dot surfaces was enhanced by the image dipoles, while the antisymmetric vibrational mode with a transition moment parallel to the surfaces was suppressed. This selectivity toward the direction of the transition dipole moments was a result of the interference of the image dipoles with the vibrational motion of the ligands. Analysis of the size dependent variation of the vibrational spectra revealed different chelating versus bridging bonding geometries that varied according to the edge-to-facet ratio of the nanocrystals.

Furthermore, the generation of excitons in PbS quantum dots created highly polarizable states that modulated the vibrational spectra of the carboxylate groups of ligands attached to the nanocrystal surfaces through the formation of image dipoles (Figure 2c). The symmetric vibrational mode with a transition dipole moment normal to the quantum dot surfaces was enhanced by the image dipoles, while the antisymmetric vibrational mode with a transition moment parallel to the surfaces was suppressed. This selectivity toward the direction of the transition dipole moments was a result of the interference of the image dipoles with the vibrational motion of the ligands. Analysis of the size dependent variation of the vibrational spectra revealed different chelating versus bridging bonding geometries that varied according to the edge-to-facet ratio of the nanocrystals.

## DOE Solar Photochemistry Sponsored Publications 2016-2019

1. “Molecular Origins of Defects in Organo-Halide Perovskites and Their Influence on Charge Carrier Dynamics,” Robert J. Stewart, Christopher Grieco, Alec V. Larsen, Grayson S. Doucette and John B. Asbury, *J. Phys. Chem. C*, **120**, 12392-12402 (2016). DOI: 10.1021/acs.jpcc.6b03472
2. “Observation of Two Triplet-Pair Intermediates in Singlet Exciton Fission,” Ryan D. Penscak, Evgeny E. Ostroumov, Andrew J. Tilley, Samuel Mazza, Christopher Grieco, Karl J. Thorley, John B. Asbury, Dwight S. Seferos, John E. Anthony, Gregory D. Scholes, *J. Phys. Chem. Lett.*, **7**, 2370-2375 (2016). DOI: 10.1021/acs.jpcclett.6b00947
3. “Dynamic Exchange During Triplet Transport in Nanocrystalline TIPS-Pentacene Films,” Christopher Grieco, Grayson S. Doucette, Ryan D. Penscak, Marcia M. Payne, Adam Rimshaw, Gregory D. Scholes, John E. Anthony, and John B. Asbury, *J. Am. Chem. Soc.*, **138**, 16069-16080 (2016). DOI: 10.1021/jacs.6b10010
4. “Approaching Bulk Carrier Dynamics in Organo-Halide Perovskite Nanocrystalline Films by Surface Passivation,” Robert J. Stewart, Christopher Grieco, Alec V. Larsen, Joshua J. Maier and John B. Asbury, *J. Phys. Chem. Lett.*, **7**, 1148-1153 (2016). DOI: 10.1021/acs.jpcclett.6b00366
5. “Mechanisms of Energy Transfer and Enhanced Stability of Carbide Nitride Phosphors for Solid State Lighting,” Christopher Grieco, Kurt F. Hirsekorn, Andrew T. Heitsch, Alan C. Thomas, Mark H. McAdon, Britt A. Vanchura, Michael M. Romanelli, Lora L. Brehm, Anne Leugers, Anatoliy N. Sokolov, and John B. Asbury, *ACS Appl. Mater. Interfaces*, **9**, 12457-12455 (2017). DOI: 10.1021/acsami.6b15323
6. “Time-Resolved Infrared Spectroscopy Directly Probes Free and Trapped Carriers in Organo-Halide Perovskites,” Kyle T. Munson, Christopher Grieco, Eric R. Kennehan, Robert J. Stewart, and John B. Asbury, *ACS Energy Lett.*, **2**, 651-658 (2017). DOI: 10.1021/acsenerylett.7b00033
7. “Triplet Transfer Mediates Triplet Pair Separation During Singlet Fission in TIPS-Pentacene,” Christopher Grieco, Grayson S. Doucette, Jason M. Munro, Eric R. Kennehan, Youngmin Lee, Adam Rimshaw, Marcia M. Payne, Nichole Wonderling, John E. Anthony, Ismaila Dabo, Enrique D. Gomez and John B. Asbury, *Adv. Funct. Mater.*, **27**, 1703929 (2017). DOI: 10.1002/adfm.201703929
8. “Using Molecular Vibrations to Probe Exciton Delocalization in Films of Perylene Diimides with Ultrafast Mid-IR Spectroscopy,” Eric R. Kennehan, Christopher Grieco, Alyssa N. Brigeman, Grayson S. Doucette, Adam Rimshaw, Kayla Bisgaier, Noel C. Giebink, and John B. Asbury, *Phys. Chem. Chem. Phys.*, **19**, 24829-24839 (2017). DOI: 10.1039/c7cp04819j
9. “Solution-Processable, Crystalline Material for Quantitative Singlet Fission,” Ryan D. Penscak, Christopher Grieco, Geoffrey E. Purdum, Samuel M. Mazza, Andrew J. Tilley, Evgeny E. Ostroumov, Dwight S. Seferos, Yueh-Lin Loo, John B. Asbury, John E. Anthony and Gregory D. Scholes, *Materials Horizons*, **4**, 915-923 (2017). DOI: 10.1039/c7mh00303j
10. “Harnessing Molecular Vibrations to Probe Triplet Dynamics During Singlet Fission,” Christopher Grieco, Eric R. Kennehan, Adam Rimshaw, Marcia M. Payne, John E. Anthony, John B. Asbury, *J. Phys. Chem. Lett.*, **8**, 5700-5706 (2017). DOI: 10.1021/acs.jpcclett.7b02434
11. “Charged Polaron Polaritons in an Organic Semiconductor Microcavity,” Chiao-Yu Cheng, Rijul Dhanker, Christopher L. Gray, Sukrit Mukhopadhyay, Eric R. Kennehan, John B. Asbury, Anatoliy Sokolov, and Noel C. Giebink, *Phys. Rev. Lett.*, **120**, 017402 (2018). DOI: 10.1103/PhysRevLett.120.017402
12. “Direct Observation of Correlated Triplet Pair Dynamics during Singlet Fission Using Ultrafast Mid-IR Spectroscopy,” Christopher Grieco, Eric R. Kennehan, Hwon Kim, Ryan D. Penscak, Alyssa N.

Brigeman, Adam Rimshaw, Marcia M. Payne, John E. Anthony, Noel C. Giebink, Gregory D. Scholes, and John B. Asbury, *J. Phys. Chem. C*, **122**, 2012-2022 (2018). **DOI:** 10.1021/acs.jpcc.7b11228

13. “Striking the right balance of intermolecular coupling for high-efficiency singlet fission,” Ryan D. Pensack, Andrew J. Tilley, Christopher Grieco, Geoffrey E. Purdum, Evgeny E. Ostroumov, Devin B. Granger, Daniel G. Oblinsky, Jacob C. Dean, Grayson S. Doucette, John B. Asbury, Yueh-Lin Loo, Dwight S. Seferos, John E. Anthony, and Gregory D. Scholes, *Chem. Sci.*, **9**, 6240-6259 (2018). **DOI:** 10.1039/c8sc00293b

14. “Electron-Phonon Coupling and Resonant Relaxation from 1D and 1P States in PbS Quantum Dots,” Eric R. Kennehan, Grayson S. Doucette, Ashley R. Marshall, Christopher Grieco, Kyle T. Munson, Matthew C. Beard, John B. Asbury, *ACS Nano*, **12**, 6263-6272 (2018). **DOI:** 10.1021/acsnano.8b03216

15. “Structural Origins of the Electronic Properties of Materials via Time-Resolved Infrared Spectroscopy,” Kyle T. Munson, Eric R. Kennehan and John B. Asbury, *J. Mater. Chem. C*, **7**, 5889-5909 (2019). **DOI:** 10.1039/C9TC01348B

## Triplet Energy Transduction in Designed Chromophore Architectures

Melissa K. Gish,<sup>1</sup> Nadia V. Korovina,<sup>1</sup> Marissa Martinez,<sup>1,2</sup> Natalie A. Pace,<sup>1,2</sup> Nicholas Pompetti,<sup>1,2</sup> Matthew C. Beard,<sup>1</sup> Justin C. Johnson<sup>1</sup>

<sup>1</sup>Chemistry and Nanoscience Center  
National Renewable Energy Laboratory  
Golden, CO 80401

<sup>2</sup>Department of Chemistry, University of Colorado, Boulder

Design features that promote long excited state lifetimes and energy or charge transfer involving triplet excitons are required in order to take advantage of the multiple excitons generated from singlet fission in molecular chromophores. Recent advances in our understanding of the singlet fission mechanism have enriched the photophysical picture to include the role of exciton diffusion and/or triplet pair dephasing in the ultimate efficiency of converting each photon to two electron-hole pairs. We now strive to control not only the first step in the process, fast production of the correlated triplet pair, but also the subsequent evolution toward charge carriers.

There are three aspects of the work that are described here: (i) production of long-lived and high energy triplets through covalent oligomer design; (ii) promotion of triplet formation and dissociation at a nanostructure oxide interface, and (iii) singlet and triplet energy transfer between molecular ligands and quantum dots (QDs). Each of these topics encompasses a variety of unstudied or unanswered questions, the resolution of which could enlighten a particular pathway for enhanced solar energy utilization involving singlet fission.

In properly designed covalent dimer systems, singlet fission can be fast and efficient. For example, a diverse variety of pentacene dimers have produced triplet pairs quickly (100 fs to a few ps) with yields approaching 200%. However, in most cases the triplet pair lifetime is limited to  $\ll 1 \mu\text{s}$  due to strong interactions between the constituent triplets as they are confined in the molecular structure. Further, while the strong driving force for singlet fission enhances the rate, it wastes photon potential energy that could be applied toward photovoltaic or photoelectrochemical schemes. Our hypothesis, born from these shortcomings, is that slightly endothermic singlet fission to produce high energy triplets ( $E_T > 1.3 \text{ eV}$ ) would be more useful as an energy transfer partner for silicon and potentially in some photochemical reactions. To this end, we have designed and constructed perylene oligomers, Figure 1, that leverage multi-chromophore delocalization in the singlet excited state and localization in the triplet state to produce long-lived triplet pairs with relatively high efficiency. Spectroscopy and calculations have aided our understanding of the dynamics of this system, which has a variety of intriguing properties if further

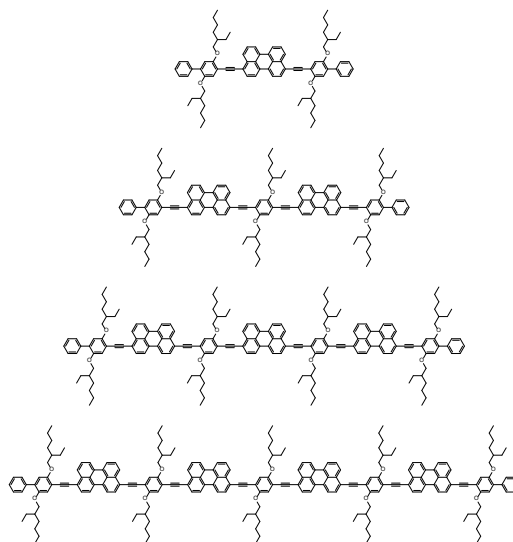


**Figure 1.** Substituted perylene monomer through tetramer (top to bottom).

improvements in triplet yield can be made.

The now archetypal dye-sensitized solar cell serves as the inspiration for the second topic. If a singlet fission chromophore replaces the conventional dye in a photoelectrode and performs charge transfer from the triplet state efficiently, the photocurrent at blue/green wavelengths could be doubled. We have recently substituted binding groups on polyacene derivatives for attachment to  $\text{TiO}_2$  and other mesoporous oxides in order to quantify the excited state dynamics of a photoexcited dye monolayer at the surface. The singlet fission dynamics themselves are modified due to the unique mode of intermolecular coupling found in a monolayer vs. a crystalline film. The intermolecular interactions are weakened but can be controlled with strategic substitution. In particular, we have tested the dependence of dynamics on the geometry of binding through carboxylic acid groups installed along either the long or short axis of a tetracene derivative. We also control the density of singlet fission dyes adsorbed and build multilayers of anthradithiophene dyes, (synthesized by collaborator Prof. John Anthony at Univ. Kentucky, Figure 2), to improve interchromophore coupling and increase the layer dimensionality such that photo-excitations can arise in a non-adjacent fashion to the charge separating interface and may have more facile pathways for triplet pair separation.

Lastly, we have chosen infrared emitting quantum dots as a potential platform for transducing triplet energy into a more useful form. We have demonstrated that triplet energy transfer at the interface between a surface bound ligand capable of singlet fission and a PbS QD can occur, but the details remain poorly understood. Energy transfer from the singlet state is fast

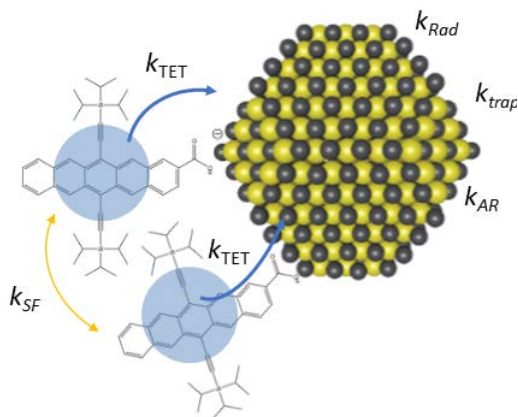


**Figure 3.** Illustration of various processes at photoexcited ligand-QD interface.

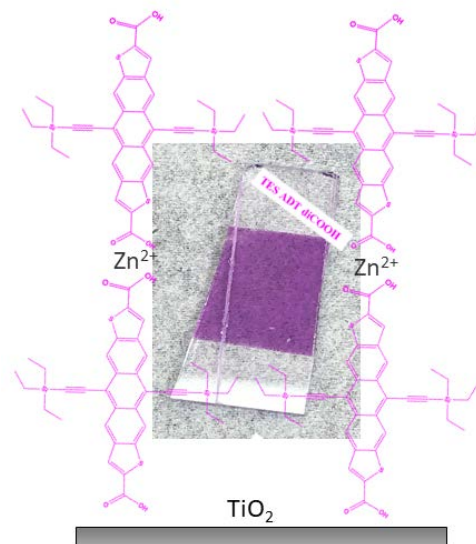


**Figure 2.** Strategy for bilayer formation of singlet fission dyes and photograph of sample (background).

(ps timescale) if the chromophore is proximal, but triplet energy transfer can also occur on a ns timescale in either direction (from QD to chromophore or vice versa), Figure 3. As with oxides, separating the chromophores from the QD could be useful, and we have taken steps toward fabricating and studying a guest:host matrix in which triplets formed in the host can migrate to the guest where triplet energy transfer and QD emission occurs. Careful spectroscopic analysis is key to evaluating the complex movement of excited species in these systems, and a suite of tools is used including transient absorption, transient grating, and photoluminescence excitation spectroscopy.

## DOE Solar Photochemistry Sponsored Publications 2016-2019

1. Pace, N.A.; Korovina, N.V.; Clikeman, T.T.; Strauss, S.H.; Boltalina, O.V.; Johnson, J.C.; Rumbles, G.; Reid, O.G. "Triplet States Generated Through Singlet Fission Exhibit a Marcus-like Optimum in Photoinduced Electron Transfer Yield." Under revision
2. Korovina, N.V.; Chang, C.; Johnson, J.C. "Spatial Separation of Triplet Excitons Drives Endothermic Singlet Fission." Under revision
3. Buchanan, E.A.; Kaleta, J.; Wen, J.; Lapidus, S.H.; Cisařova, I.; Havlas, Z.; Johnson, J.C.; and Michl, J. "Molecular Packing and Singlet Fission: Three Fluorinated 1,3-Diphenylisobenzofurans," *J. Phys. Chem. Lett.* **2019**, *10*, 1947.
4. Haipeng, Lu.; Chen, X.; Anthony, J.E.; Johnson, J.C.; Beard, M.C.; "Singlet Fission of Pentacene Molecules on Perovskite Nanocrystals." *J. Am. Chem. Soc.* **2019**, *141*, 4919.
5. Gish, M.; Pace, N.; Rumbles, G.; Johnson, J.C. "Emerging Design Principles for Enhanced Solar Energy Utilization with Singlet Fission." *J. Phys. Chem. C* **2019**, *123*, 3923.
6. Wan, Y.; Wiederrecht, G.; Schaller, R.D.; Johnson, J.C.; Huang, L. "Highly Mobile Triplet Pairs Prepared by Singlet Fission in Tetracene Single Crystals." *J. Phys. Chem. Lett.* **2018**, *9*, 6731.
7. Kroupa, D.M.; Pach, G.F.; Vörös, M.; Giberti, F.; Chernomordik, B.D.; Crisp, R.W.; Nozik, A.; Johnson, J.C.; Sing, R.; Klimov, V.; Galli, G.; Beard, M. "Enhanced Multiple Exciton Generation in PbS| CdS Janus-Like Heterostructured Nanocrystals." *ACS Nano*, **2018**, *12*, 10084.
8. Arias, D.; Moore, D.; van de Lagemaat, J.; Johnson, J.C. "Direct Measurements of Carrier Transport in Methylammonium Lead Halide Perovskites." *J. Phys. Chem. Lett.* **2018**, *9*, 5710.
9. Bezouw, S.; Arias, D.H.; Ihly, R.; Cambré, S.; Ferguson, A.J.; Campo, J.; Johnson, J.C.; Defiliet, J.; Wenseleers, W.; Blackburn, J.L. "Diameter-dependent Optical Absorption and Excitation Energy Transfer from Encapsulated Dye Molecules towards Single Wall cCarbon Nanotubes." *ACS Nano*, **2018**, *12*, 6881-6894.
10. Pace, N.A.; Arias, D.H.; Granger, D.B.; Christensen, S.; Anthony, J.E.; Johnson, J.C. "Dynamics of Singlet Fission and Electron Injection in Self-Assembled Acene Monolayers on Titanium Dioxide," *Chem. Sci.*, **2018**, *9*, 3004.
11. Kroupa, D.M.; Arias, D.H.; Blackburn, J.L.; Carroll, G.M.; Granger, D.B.; Anthony, J.E.; Beard, M.C.; Johnson, J.C. "Control of Energy Flow Dynamics between Tetracene Ligands and PbS Quantum Dots by Size Tuning and Ligand Coverage," *Nano Lett.*, **2018**, *18*, 865—873. 10.1021/acs.nanolett.7b04144.
12. Le, A.K.; Bender, J.A.; Arias, D.H.; Cotton, D.E.; Johnson, J.C.; Roberts, S.T. "Singlet Fission Involves an Interplay Between Energetic Driving Force and Electronic Coupling in Perylenediimide Films," *J. Am. Chem. Soc.*, **2018**, *140*, 814.
13. Pace, N.A.; Zhang, W.; Arias, D.H.; McCulloch, I.; Rumbles, G.; Johnson, J.C. "Controlling Long-Lived Triplet Generation from Intramolecular Singlet Fission in the Solid State," *J. Phys. Chem. Lett.* **2017**, *8*, 6086.

14. Cook, J.; Carey, T.; Arias, D.; Johnson, J.; Damrauer, N. "Solvent Controlled Branching of Localized versus Delocalized Singlet Exciton States and Equilibration with Charge Transfer in a Structurally Well-Defined Tetracene Dimer." *J. Phys. Chem. A*, **2017**, *121*, 9229.
15. Dron, P.I.; Michl, J.; Johnson, J.C. "Singlet Fission and Excimer Formation in Disordered Solids of Alkyl-Substituted 1,3-Diphenylisobenzofurans." *J. Phys. Chem. A* **2017**, *121*, 8596.
16. Johnson, J.C.; Michl, J.; "1,3-Diphenylisobenzofuran as a Model Singlet Fission Chromophore." *Top. Curr. Chem.*, **2017**, *357*, 80.
17. Beard, M.; Blackburn, J.; Johnson, J.C.; Rumbles, G.R.; "Status and Prognosis of Future Generation Photoconversion to Photovoltaics and Solar Fuels." *ACS Energy Lett.* **2016**, *1*, 344.
18. Yang, Y.; Yang, M.; Zhu, K.; Johnson, J.C.; van de Lagemaat, J.; Beard, M.C. "Large Polarization-Dependent Optical Stark Effect in Lead Iodide Perovskites." *Nature Comm.*, **2016**, 12613.
19. Johnson, J.C.; Li, Z.; Ndione, P. Zhu, K. "Large Third-Order Nonlinearity of Methylammonium Lead Bromide Perovskite Thin Films." *J. Mater. Chem. C*, **2016**, *4*, 4847.
20. Wan, Y.; Guo, Z.; Zhu, T.; Yan, S.; Johnson, J.C.; Huang, L. "Two Birds with One Stone: Tailoring Singlet Fission for Both Triplet Yield and Exciton Diffusion Length." *Adv. Mater.* **2016**, *28*, 3579.
21. Schrauben, J.N.; Akdag, A.; Wen, J.; Ryerson, J.L.; Havlas, Z.; Michl, J.; Johnson, J.C. "Triplet Formation in Strongly Coupled Dimers of 1,3-Diphenylisobenzofuran with Excitation Localization/Delocalization Isomerism." *J. Phys. Chem. A*, **2016**, *120*, 3473.
22. Dowgiallo, A.M.; Mistry, K.; Johnson, J.C.; Reid, O.G.; Blackburn, J.L. "Probing Exciton Diffusion and Dissociation in Single-Walled Carbon Nanotube-C60 Heterojunctions." *J. Phys. Chem. Lett.* **2016**, *7*, 1794.

## Singlet fission in nanocrystal-molecule hybrid structures

Zhiyuan Huang, Ming Lee Tang  
 Department of Chemistry  
 University of California, Riverside  
 Riverside, CA 92521

Hybrid organic-inorganic nanostructures capable of singlet fission and subsequent spin-triplet exciton transfer will be synthesized and characterized to address the problems of cost and efficiency of modern day photovoltaics and photocatalysts.

Here, organic singlet fission materials, diphenylhexatriene (DPH) and tetracene that absorb maximally in the ultra-violet and green will be bound to lead chalcogenide nanocrystals such that the spin-triplet excitons can be harvested. The parent molecules have well established high singlet fission quantum yields between 90-100%. Asymmetric derivatives will be designed and synthesized to investigate how the resultant molecular geometry on the nanocrystal surface affects the singlet fission quantum yield, and the efficiencies of singlet and triplet energy transfer. The electronic coupling between the molecular triplet exciton donor and nanocrystal acceptor will be tuned by varying the anchoring group binding the organic moiety to the inorganic surface. Fundamental insight will be obtained on the factors affecting these multi-excitonic processes that may provide a way to exceed the Shockley-Queisser limit using inexpensive, earth-abundant materials.

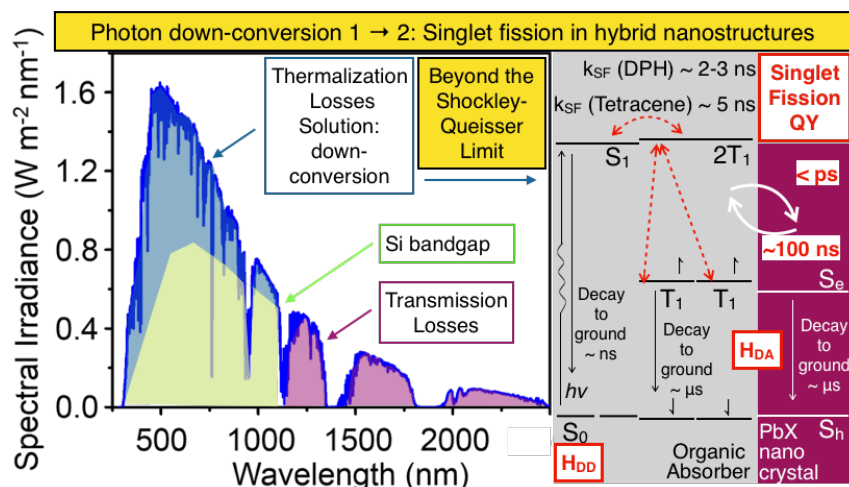


**Figure 1.** The ability to harvest triplets formed by singlet fission (SF) will address thermalization losses (blue) in photovoltaics and photocatalysts. The focus here (highlighted in the red boxes) is on a hybrid nanosystem, specifically on the singlet fission quantum yield, the resultant rates of triplet transfer to nanocrystal acceptors, and the intermolecular and organic-inorganic electronic coupling,  $H_{DD}$  and  $H_{DA}$  respectively.

The structure- efficiency relationships obtained here will answer three fundamental questions in the fields of artificial photosynthetic systems, colloidal nanocrystals, donor-acceptor interactions and singlet fission. Firstly, what is the origin of the marked asymmetry in rates of triplet energy transfer between nanocrystals and molecules? Secondly, how can electronic coupling between (a) molecules on nanocrystal surfaces be tuned to promote singlet fission, and (b) molecules

and nanocrystals be controlled to enhance triplet energy transfer? Finally, can triplet excitons, with their intrinsically long-lived microsecond lifetimes, be more efficiently extracted to do work in an external circuit than their singlet exciton counterparts with nanosecond lifetimes? The hybrid platform here makes synergistic use of unique features of each component: singlet fission

exclusive to molecules, and the microsecond exciton lifetimes of the lead chalcogenide nanocrystals as a possible pathway to next-generation photovoltaic cells or photocatalysts. The findings will be directly applicable to a potential tetracene-silicon platform that may increase the power conversion efficiency of silicon solar cells from the current 28% to 36%.

#### **DOE Solar Photochemistry Sponsored Publications 2019**

1. Z. Huang, Z. Xu, M. Mahboub, Z. Liang, P. Jaimes, K. Graham, M. L. Tang, T. Lian, " Enhanced near-infrared-to-visible upconversion by synthetic control of PbS nanocrystal triplet photosensitizers" *J. Am. Chem. Soc.* Submitted.

## Quantum Interferences Among Dexter Energy Transfer Pathways

Shuming Bai<sup>1</sup>, Peng Zhang<sup>1</sup>, Spiros S. Skourtis<sup>2</sup> and David N. Beratan<sup>1,3,4</sup>

<sup>1</sup>Department of Chemistry Duke University, Durham, NC 27708

<sup>2</sup>Departments of Physics, University of Cyprus, 1678 Nicosia, Cyprus

<sup>3</sup>Department of Physics Duke University, Durham, NC 27708

<sup>4</sup>Department of Biochemistry, Duke University, Durham, NC 27710

Dexter energy transfer moves an exciton (i.e., an electron – hole pair) between species with different spin multiplicities. In many cases, the interaction is mediated by a chemical bridge between chromophores. As well, Dexter couplings are closely related to interactions that underpin singlet fission and triplet fusion, and arise from a combination of one- and two-electron interactions. Assuming that there is no real intermediate state population of an electron, hole, or exciton on the bridge during Dexter transport, the reaction involves initial and final states that are coupled non-adiabatically. As such, coherent quantum interferences arise among the Dexter energy coupling pathways (see Figure 1), in stark contrast to the case of Förster energy transfer. These interferences are particularly rich because of the two particle nature of the Dexter process. Despite this complexity, simple rules can govern Dexter coupling pathway interferences in special cases. As in the case of single-electron transfer, parallel coupling pathways may interfere constructively or destructively, and these interferences help to determine the Dexter energy transfer kinetics. Because of the virtual particle combinatorics associated with two-particle and one-particle superexchange, parallel and chemically equivalent Dexter coupling routes may be expected to enhance the Dexter coupling. We explored Dexter coupling pathway interferences in non-covalent assemblies. We found that both one- and two-particle pathways contribute significantly. In a model noncovalent structure consisting of two parallel pathways, we find that the Dexter coupling is enhanced by about a factor of five compared to the single pathway system (see Figure 2). (Back of envelope single-particle coupling analysis predicts a factor of four enhancement, but mischaracterizes the coupling mechanism.)

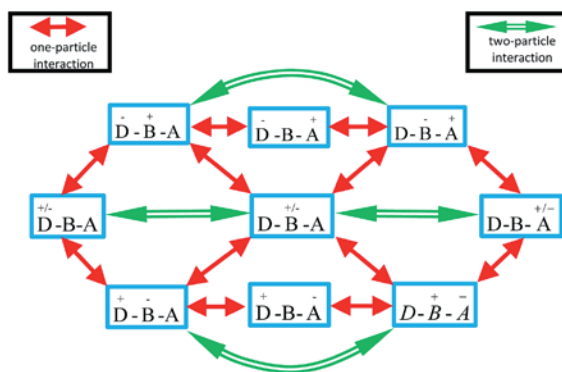


**Figure 1.** Schematic representation of one- and two-particle Dexter energy transfer coupling interactions that underpin the Dexter coupling pathways in a DBA systems. Electrons are represented by a – symbol, holes by a + symbol and excitons by a +/- symbol.

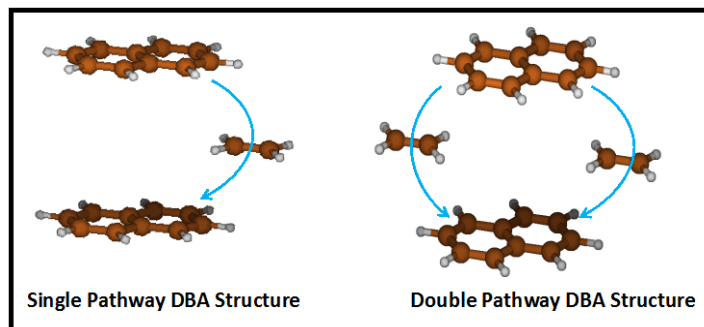


**Figure 2.** Naphthalene-ethylene-naphthalene DBA model structures used to examine bridge-mediated Dexter energy transfer mechanisms and pathways. We find that the Dexter coupling grows by a factor of five when the second bridging ethylene is added to create the double pathway structure.

Our analysis of Dexter couplings in these systems uses constrained density functional theory to compute diabatic states, energies, and couplings, and Green's function methods to dissect the contributions of specific coupling pathways. This approach is useful when the bridge-mediated coupling is weak. Despite the relative simplicity of the model systems, the Dexter pathways are rich and complex, compared to the case for single electron transfer in DBA systems. These studies are suggesting approaches to manipulate the Dexter coupling strengths, and hence the Dexter kinetics and efficiencies, by tailoring the chemical structure of the pathways. The studies also point to the possibility of creating luminescent probes that are sensitive to distance as well as medium structure. Our ongoing studies are targeting DBA systems that feature nanocrystal donor and/or acceptor components. We are particularly interested in families of structures that could provide access to photoinduced electron and Dexter energy transfer reactions in structurally similar constructs. The associated theoretical studies will likely require the use of tight-binding methods to describe the larger semiconducting nanoparticles of interest. As well, linkage to other bridge-mediated Dexter-like processes (exciton fission and fusion) may be explored in the language of one- and two-particle coupling pathways.

### DOE Solar Photochemistry Sponsored Publication

1. Bai, S.; Zhang P.; Antoniou P.; Skourtis S.; Beratan D. Quantum Interferences Among Dexter Energy Transfer Pathways. *Faraday Discuss.* **2019**, in press. DOI: 10.1039/c9fd00007k

## Modular Nanoscale and Biomimetic Assemblies for Photocatalytic Hydrogen Generation

Kara L. Bren, Todd D. Krauss, Ellen M. Matson

Department of Chemistry  
University of Rochester  
Rochester, NY and 14627

Hydrogen ( $H_2$ ) is an energy-dense fuel and an important feedstock in the chemical industry. Currently,  $H_2$  is primarily derived from natural gas, which itself is a valuable resource. In this collaborative project, we are developing new methods to prepare  $H_2$  from water in reactions driven by light. Our approach is to couple nanocrystalline quantum dot (QD) photosensitizers with biomolecular and inorganic base metal catalysts that facilitate the reduction of aqueous protons to  $H_2$ . The development and analysis of these assemblies provides fundamental insight into the physical and chemical properties of QDs, which have become widely used in photocatalysis but remain poorly characterized. Furthermore, successfully meeting our aims will yield new mechanistic insights into the activity of catalysts for  $H_2$  production from water that function in 100% water. Finally, analysis of integrated systems will inform us on factors impacting the efficiency of electron and hole transfers required for catalysis. This project draws broadly on materials chemistry, photophysics and physical chemistry, biochemistry, and synthetic chemistry to address challenging fundamental questions in the fields of photochemistry and catalysis.

One thrust focuses on developing and understanding the QD photosensitizers for  $H_2$  production. We studied the efficiency of photocatalytic  $H_2$  production for integrated systems of large diameter

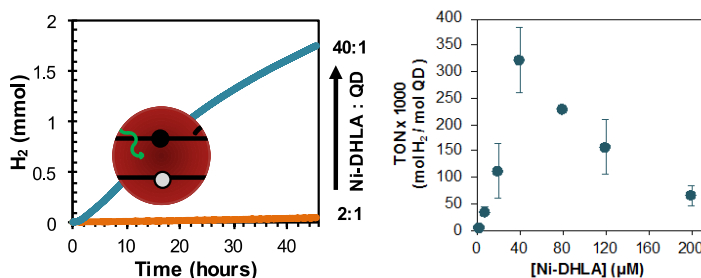


**Figure 1.** (Left) Total  $H_2$  produced showing a dramatic increase in activity as the Ni:QD ratio increases from 2:1 (orange trace) to 40:1 (blue trace). (Right) Turnover number (TON) for  $H_2$  production using 1  $\mu M$  CdSe MPA-QDs. At 40:1 Ni:QD, the TON for these larger QDs has completely recovered to the level of the smaller QDs.

increasing Ni-DHLA:QD molar ratios. Surprisingly, this high activity was only observed with the use of 3-mercaptopropionic acid (MPA) ligands, while CdSe QDs capped with dihydrolipoic acid (DHLA) exhibited poor performance in comparison, indicating that the QD capping ligand has a substantial impact on the catalytic performance. Ultrafast transient absorption spectroscopic measurements of the electron transfer (ET) dynamics show an increase in ET efficiency as the catalyst concentration is increased. Together, these results suggest that for these large QDs, tailoring the QD surface environment for facile ET and increasing catalyst concentrations increases the probability of ET from QDs to Ni-DHLA, overcoming the relatively small driving force for ET and decreased surface electron density for large diameter QDs.

Another approach to developing QD photosensitizers that absorb low-energy light is to use CdTe QDs rather than the more common CdSe. CdTe QDs are attractive because they may be used to harvest near-infrared solar photons. To that end, a series of photocatalysis experiments were conducted using CdTe QDs as a photosensitizer and Ni-DHLA as a catalyst. Interestingly, we found that 3.2-nm diameter CdTe QDs have the best photocatalytic performance (Figure 2), which contrasts with CdSe QDs for which the relative amount of H<sub>2</sub> produced increases steadily as the QD size is decreased. However, overall, CdTe QDs have a substantially reduced ability to act as a photosensitizer for H<sub>2</sub> production, having an order-of-magnitude lower efficiency than CdSe QDs under optimized conditions. Ultrafast transient absorption experiments suggest that this relatively poor performance compared to CdSe QDs is due to extremely fast (< 2 ps) trapping of the photogenerated electron, which contrasts with typical charge transfer times to the Ni-DHLA catalyst from CdSe QDs (~20 ps).

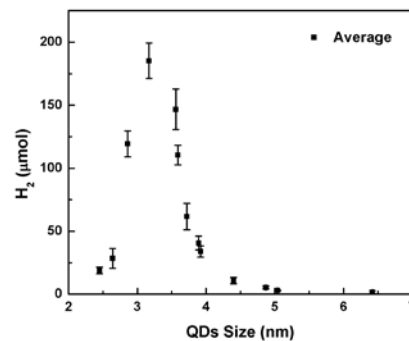


**Figure 2.** Size dependent hydrogen production measured over 48 hours, converted to μmoles of hydrogen. Conditions for these experiments were 1 μM CdTe-DHLA and 20 μM Ni-DHLA at pH=4.5 and EtOH/H<sub>2</sub>O=1:1.

In the area of catalyst development and analysis, we have been investigating both metal-ligand complexes prepared in situ from QD ligands and metal salts and engineered biomolecular catalysts. A new and promising system combines CdSe QDs modified with the biological thiol glutathione (GSH) as a capping ligand and Co(II) salts. Irradiation of this mixture yields 100,000 mol H<sub>2</sub> per mol Co(II) over two days. We propose that a Co-GSH complex formed in situ acts as the catalyst, which was confirmed through the observation of a catalytic wave for H<sub>2</sub> production at a half-peak potential of -0.91 V vs. Ag/AgCl (1 M KCl) for a Co(II)-GSH mixture. Furthermore, electrochemistry of complexes of cobalt and simplified ligands containing key functional groups found in GSH (thiol, amine, carboxylate) has provided insight into the cobalt coordination environment in the active catalyst species. Study of these derivatives reveals that the thiol moiety is essential to the formation of a catalytically active complex.

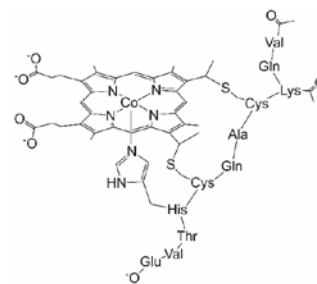


**Figure 3:** CoMP11-Ac

Other mechanistic studies on H<sub>2</sub> evolution catalysts in water have yielded further insight into factors that impact reactivity under aqueous conditions. Our biomolecular catalyst CoMP11-Ac (Figure 3) displays remarkable stability over a wide pH range (1-13), facilitating mechanistic study. Electrochemistry of this catalyst over a range of conditions reveals that its primary proton source (H<sub>3</sub>O<sup>+</sup>, H<sub>2</sub>O, or protonated buffer) depends on pH and buffer pK<sub>a</sub>.

Furthermore, the H<sub>2</sub> evolution mechanism is dependent upon these conditions. In particular, high-pK<sub>a</sub> buffers result in a rate-determining first chemical step, proposed to be cobalt-hydride (Co(III)-H) formation. In contrast, low-pK<sub>a</sub> buffers yield a rate-determining second chemical step, proposed to be hydride protonation to yield H<sub>2</sub>. Ongoing work reveals that the nature of the proton donor also impacts the performance of photocatalytic reactions. Thus, choice of buffer used in catalysis in water has implications for reactivity well beyond its role in regulating solution pH.

## DOE Solar Photochemistry Sponsored Publications 2016-2019

1. Kandemir, B.; Chakraborty, S.; Guo, Y.; Bren, K. L. Semisynthetic and Biomolecular Hydrogen Evolution Catalysts, *Inorg. Chem.* **2016**, *55*, 467-477. DOI: 10.1021/acs.inorgchem.5b02054
2. Bren, K. L. Go with the Electron Flow: Effects of Heme Electronic Structure on Electron Transfer, *Isr. J. Chem.* **2016**, *56*, 693-704. DOI: 10.1002/ijch.201600021.
3. Lv, H.; Ruberu, T. P. A.; Fleischauer, V. E.; Brennessel, W. W.; Neidig, M. L.; Eisenberg, R., Catalytic Light-Driven Generation of Hydrogen from Water by Iron Dithiolene Complexes. *J. Am. Chem. Soc.* **2016**, *138*, 11654-11663. DOI: 10.1021/jacs.6b05040
4. Krauss, T. D.; Lampa-Pastirk, S.; Liu, C.; Qiu, F., Photons to Fuels: Ultrafast Dynamics of Semiconductor Nanocrystals, *SPIE Newsroom* **2016**, DOI: 10.1117/2.1201605.006467
5. Qiu, F.; Han, Z.; Peterson, M.; Odoi, M. Y.; Sowers, K. L.; Krauss, T. D., Photocatalytic Hydrogen Generation by CdSe/CdS Nanoparticles, *Nano Lett.* **2016**, *16*, 5347-5352. DOI: 10.1021/acs.nanolett.6b01087
6. Pilgrim, G. A.; Amori, A. R.; Hou, Z.; Qiu, F.; Krauss, T. D. Carbon Nanotube Based Membrane for Light-Driven Simultaneous Proton and Electron Transport. *ACS Energy Lett.* **2017**, *2*, 129-133. DOI: DOI: 10.1021/acsenerylett.6b00578
7. Waldron, D.; Burke, R.; Preske, A.; Krauss, T. D.; Zawodny, J. M.; Gupta, M. C. Temperature Dependent Optical Properties of Lead Selenide Quantum Dot Polymer Nanocomposites. *Appl. Opt.* **2017**, *56*, 1982-1989. DOI: 10.1364/AO.56.001982
8. Kleingardner, E. C.; Asher, W. B.; Bren, K. L. Efficient and Flexible Preparation of Biosynthetic Microperoxidases, *Biochemistry*, **2017**, *56*, 143-148. DOI: 10.1021/acs.biochem.6b00915
9. Kubie, L.; Amori, A. R.; Chakraborty, S.; Bren, K. L.; Krauss, T. D., Photoinduced Charge Separation in Single-Walled Carbon Nanotube/Protein Integrated Systems, *Nanoscale Horiz.*, **2017**, *2*, 163-166. DOI: 10.1039/C6NH00172F
10. Lv, H.; Wang, C.; Li, G.; Burke, R.; Krauss, T. D.; Gao, Y.; Eisenberg, R., Semiconductor Quantum Dot-Sensitized Rainbow Photocathode for Effective Photoelectrochemical Hydrogen Generation. *Proc. Natl. Acad. Sci. U.S.A.* **2017**, *114*, 11297-11302. DOI: 10.1073/pnas.1712325114
11. Burke, R.; Cogan, N. M. B.; Oi, A.; Krauss, T. D. Recovery of Active and Efficient Photocatalytic H<sub>2</sub> production for CdSe Quantum Dots, *J. Phys. Chem. C*, **2018** *122*, 14099-14106. DOI: 10.1021/acs.jpcc.8b01237
12. Firpo, V.; Le, J. M.; Pavone, V.; Lombardi, A.; Bren, K. L., Hydrogen Evolution from Water Catalyzed by Cobalt-mimochrome VI\*a, a Synthetic Mini-protein. *Chem. Sci.* **2018**, *9*, 8582-8589.
13. Kleingardner, J. G.; Levin, B. D.; Zoppellaro, G.; Andersson, K. K.; Elliott, S. J.; Bren, K. L., Influence of heme *c* attachment on heme conformation and potential. *J. Biol. Inorg. Chem.* **2018**, *23*, 1073-1083.
14. Burke, R.; Chakraborty, S.; Jelusic, J.; Fertig, A.; Matson, E. M.; Bren, K. L.; Krauss, T. D. Photocatalytic H<sub>2</sub> Production with CdSe Quantum Dots and a Cobalt Glutathione Catalyst, **2019**, submitted.

## Photochemical N<sub>2</sub> Reduction by Nanoparticle-Nitrogenase Complexes

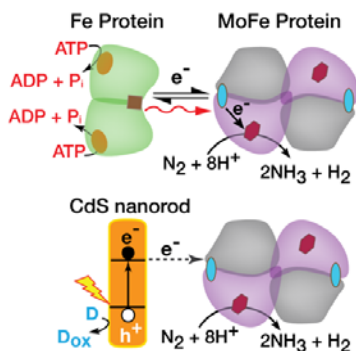
Katherine A. Brown<sup>1</sup>, Jesse Ruzicka, Hayden Kallas<sup>2</sup>, Bryant Chica<sup>1</sup>, David W. Mulder<sup>1</sup>, John W. Peters, Gordana Dukovic, Lance C. Seefeldt, and Paul W. King

<sup>1</sup>Biosciences Center  
NREL Golden, CO 80401

and

<sup>2</sup>Department of Chemistry and Biochemistry  
Utah State University, Logan, UT 84322

The activation and reduction of dinitrogen (N<sub>2</sub>) to ammonia (NH<sub>3</sub>) is one of the most energy demanding and difficult chemical reactions. Nitrogenase catalyzes this chemical transformation



**Scheme 1.** Biological (top) and photochemical (bottom) electron transfer into MoFe protein.

by coupling ATP hydrolysis by the Fe protein to drive the sequential delivery of electrons to the MoFe protein. We demonstrated that light-harvesting and photoexcited electron transfer by semiconducting nanocrystals can be coupled to nitrogenase to accomplish light-driven N<sub>2</sub> reduction. This molecular system has been enabling studies on the electron transfer mechanisms that support nitrogenase catalysis. In this work, nanocrystalline materials are being used to photochemically activate electron transfer into MoFe protein, in lieu of ATP-dependent electron transfer by the Fe protein (Scheme 1). The extraordinary light-harvesting properties and tunability of nanocrystal photochemistry is being used in combination with chemical and biophysical approaches to determine the requirements for injection of electrons into MoFe protein, transfer of electrons through the protein, and the substrate reduction chemistry at the catalytic site FeMo-cofactor. These approaches include light-driven, electron paramagnetic resonance (EPR) spectroscopy to address the site of electron injection into MoFe protein and subsequent electron transfer to the FeMo-cofactor for catalytic reduction of substrates and Transient Absorption (TA) spectroscopy study interfacial electron transfer rates.

(i) Photoexcited electron transfer. The assembly of nanocrystal-MoFe complexes is presumably an electrostatically driven process that may result in different arrangements of binding interactions for interfacial electron transfer. Transient Absorption (TA) spectroscopy and EPR were used to determine the kinetics and pathway of electron injection (Figure 1). Monitoring the changes in oxidation state of the MoFe protein P cluster and FeMo-co cofactors as a function of

chemical and biophysical approaches to determine the requirements for injection of electrons into MoFe protein, transfer of electrons through the protein, and the substrate reduction chemistry at the catalytic site FeMo-cofactor. These approaches include light-driven, electron paramagnetic resonance (EPR) spectroscopy to address the site of electron injection into MoFe protein and subsequent electron transfer to the FeMo-cofactor for catalytic reduction of substrates and Transient Absorption (TA) spectroscopy study interfacial electron transfer rates.

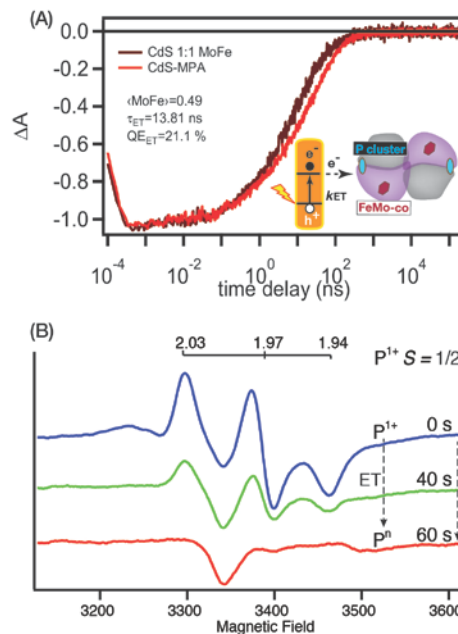


**Figure 1.** (a) TA spectra of photoexcited CdS with (black) and without (red) MoFe protein. (c) EPR spectra of the P cluster in photo-activated CdS-MoFe complexes.

time using EPR results reveals light-driven oxidation state changes in both clusters over time suggesting that the electron transfer into MoFe contributes to redox changes in both the P cluster and M cluster. We are in the process of significance of these observations on electron transfer within MoFe protein and how photochemical reduction supports catalytic N<sub>2</sub> reduction chemistry.

(ii). Effect of nanocrystal diameter on substrate reduction. The nanocrystal diameter can influence the photoexcited state lifetime, reduction potentials due to confinement effects. We have tested these effect on photochemical reduction of MoFe protein for catalyzing both N<sub>2</sub> reduction reaction, and the reduction of protons to H<sub>2</sub> (Figure 2). The initial results indicate the diameter of the nanocrystal has a strong influence on the rates of product formation, where there is a drop in rate as diameter increases.

(iii). Photochemistry by isolated FeMo-cofactor. In order to gain insights into the photo-driven reduction of substrates by nitrogenase, we have initiated a project to understand the mechanism of substrate reduction catalyzed by the active cofactor FeMo-co isolated in organic solvent when coupled to CdS-nano particles. To date, most work investigating isolated FeMo-co has either focused on the binding mode of various substrates and inhibitors or electron transfer to the cofactor. With the CdS-FeMo-co system, we benefit from being able to study electron transfer with the precise control that photoreduction allows as well as being able to turn-over enough substrate to study how the chemical environment of FeMo-co effects its product distributions. We have extracted FeMo-cofactor and found evidence that with the CdS:FeMo-co system, it is possible to reduce H<sup>+</sup> to H<sub>2</sub>, C<sub>2</sub>H<sub>2</sub> to C<sub>2</sub>H<sub>6</sub>, and CO to CH<sub>4</sub>. Optimization of the system via kinetic studies is currently underway. EPR and TA spectroscopic studies are being performed in parallel to establish the nature of trapped intermediates during catalysis.

### DOE Solar Photochemistry Sponsored Publications 2018-2019

1. Chica, B., Kallas, H., Ruzicka, J., Mulder, D.W., Brown, K., Peters, J.W., Seefeldt, L.C., Dukovic, G., and King, P.W. 2018. "Photochemical Electron Transfer in Nanocrystal-Nitrogenase Complexes." *In preparation*.
2. Kallas, H. Chica, B. / Ruzicka J., Brown, K., Peters, J.W., Dukovic, G., King, P.W., Seefeldt, L.C. 2019 "Photo-driven substrate reduction in a CdS:FeMo-cofactor hybrid system." *In preparation*.

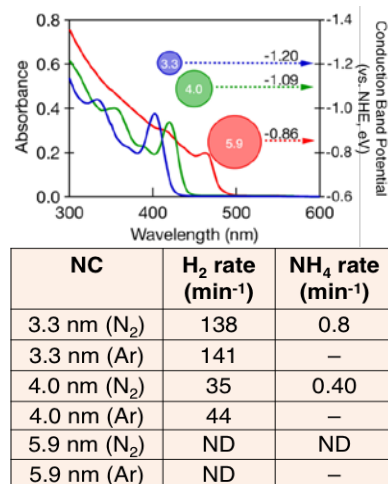


**Figure 2.** Effect of nanocrystal diameter on photochemical production of H<sub>2</sub> and NH<sub>3</sub> by nanocrystal-MoFe protein complexes.

# Controlling the Optical and Electrical Properties of QDs, QD assemblies, and QD films for Solar Energy Conversion

Daniel Kroupa, Haipeng Lu, Noah Bronstein, Yong Yan, Nathan Neale, Elisa Miller, Mike Carroll, Marissa Martinez, Arthur J. Nozik, Justin C. Johnson, Matthew C. Beard  
Chemistry and Nanoscience Center  
National Renewable Energy Laboratory  
Golden, CO 80007

Quantum dots and other colloidal nanocrystals have seen a tremendous amount of research over the last three decades. A large body of work has focused on synthesis with shape, size, and composition control of the inorganic core. Subsequent work has examined the surface chemistry and shown that the surface chemistry is itself responsible for much of the very same synthetic control. Often, important features of the nanocrystal shape can be traced to an impurity in the solvent, precursor, or preparation, which can result in various molecules binding preferentially to particular surface facets during NC synthesis. Beyond the preparation of nanocrystals, control of the ligand shell is a prerequisite for any application: the surface of the quantum dot is key to QD-QD electronic coupling to make conductive films; and ligand-shell vacancies can be the source of electronic defects that degrade performance. Controlling carrier dynamics so as to enhance beneficial processes such as Multiple exciton generation (MEG), light emission, charge transfer and/or energy transfer while at the same time decrease process that lead to degradation of these key characteristics is the goal of our program. Finally, we seek to learn how to controllably dope the nanocrystals and activate those dopants in nanocrystal arrays and films so as to modulate their conductivity while retaining beneficial quantum-confinement properties. The presentation will summarize our recent progress in increasing the MEG efficiency, producing *n* and *p*-type impurity doping and controlling and understanding ligand/QD interactions.

We demonstrated that MEG in PbS|CdS Janus-like hetero-nanostructures is enhanced over that of single-component and core/shell nanocrystal architectures, achieving 1.2 excitons per absorbed photon at 2.2 times the PbS band gap. We attribute the enhanced MEG to the asymmetric nature of the hetero-nanostructure. Heterostructuring is one way to achieve asymmetric structures and Janus-like particles are important because they cause a compositional asymmetry while maintaining structural symmetry similar to core/shell heterostructures. The compositional asymmetry also allows for the practical aspect of spatially separating the individual charges. Slowed cooling occurs through the interaction of hot-holes with a manifold of valence band interfacial states having

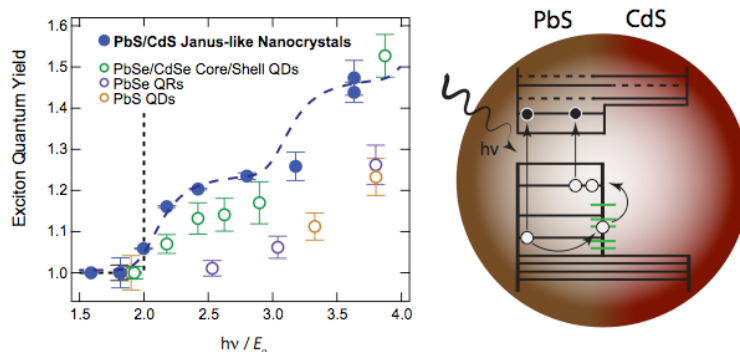


Figure 1. PbS|CdS Janus-heterostructures have a MEG onset at  $2E_g$  that reaches 1.2 excitons per photon at  $2.5 E_g$

character of both PbS and CdS, as evidenced by photoluminescence studies.

We developed a facile method to prepare *n* and *p*-doped PbSe QDs via a post-synthetic cation exchange technique. Quantitative XRD analysis suggests a substitutional doping mechanism, with the lattice parameters decreasing upon either Ag<sup>+</sup> or In<sup>3+</sup> incorporation. A significant bleach of the first excitonic transition is observed, which is coupled with the appearance of a size-dependent intraband absorption in NIR, indicating a successful introduction of electron/hole impurities dopants. We also observe a decrease of PLQY and a faster exciton decay with higher cation incorporation. Spectroelectrochemical measurements show a characteristic *n*-type behavior, which agrees with the substitutional doping mechanism of In<sup>3+</sup> in PbSe. We proposed a model whereby the majority of the added cations remains at the QD surface and do not interact with the PbSe QD core states. Small amounts of excess cations diffuse into the lattice and establish equilibrium between surface-bound and lattice-incorporated cation dopants.

Finally, we have studied the coupling and impact of ligands on the QD optical and electrical properties. We demonstrated that the bandedge energies can be shifted by over 2 eV for a QD absorber with 1 eV bandgap. We also demonstrated that the addition of ligands causes the optical absorption of the QD/ligand complex to increase due to electronic coupling between the QD and ligands. The coupling increases for smaller ligand optical gaps. We can utilize the enhanced absorbance of the QD/ligand to construct ligand adsorption isotherms. Despite their importance, ligand binding and exchange isotherms on nanocrystal surfaces remain underexplored. We model these isotherms with a 2-d square lattice model, which allows us to extract differences in trends of binding free energies and nearest neighbor coupling. As expected oleate binds more strongly than any of the functionalized cinnamates, but the binding preference is mitigated by the dipole interactions for both large positive and large negative dipoles. We explain this trend in binding free energy as a function of dipole moment *via* a collective electrostatic interaction with the lattice. For cinnamic acids with electron withdrawing molecular dipoles (negative dipoles), the isotherms show behavior associated with strong nearest neighbor association that causes the ligand exchange reaction to display a phase transition from all oleate coverage to all cinnamate coverage as more cinnamate is added, with a sharpness dictated by the ligand dipole moment: more negative dipole moments leads to sharper order-disorder phase transitions than those observed with positive dipole moments, as a function of ligand addition. Using these observations, we prepared PbS QD with Janus-shell ligands.

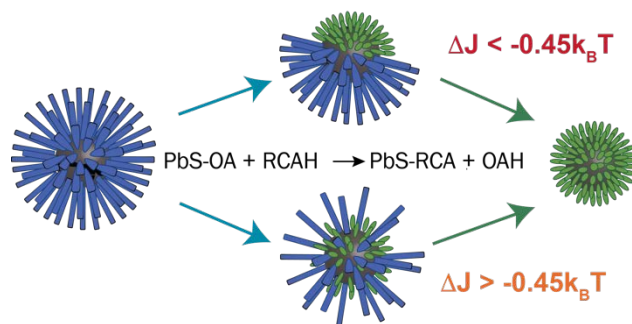


Figure 2. When the ligand-ligand coupling energy is less than  $0.45 k_B T$  patchy or Janus-ligand shells can be constructed. When the coupling energy is greater than the random ligand shells are constructed.

## DOE Solar Photochemistry Sponsored Publications 2016-2019

1. N. Bronstein, M. Martinez, D.M. Kroupa, M. Voros, H. Lu, N.P. Brawand, A.J. Nozik, A. Sellinger, G. Galli, M.C. Beard, “Designing Janus Ligand Shells on PbS Quantum Dots using Ligand-Ligand Cooperativity”, *ASAP, ACS Nano*, **2019**, [doi:10.1021/acsnano.9b00191](https://doi.org/10.1021/acsnano.9b00191)
2. H. Lu, X. Chen, J.E. Anthony, J.C. Johnson, M.C. Beard, “Sensitizing Singlet Fission with Perovskite Nanocrystals”, *JACS*, **2019**, 141, 12, 4919-4927 [doi:10.1021/jacs.8b13562](https://doi.org/10.1021/jacs.8b13562)
3. H. Lu, G. M. Carroll, N. R. Neale, M.C. Beard, “Infrared Quantum Dots: Progress, Challenges and Opportunities”, *ACS Nano*, **2019**, 13(2), pp. 939-953, [doi:10.1021/acsnano.8b09815](https://doi.org/10.1021/acsnano.8b09815)
4. H. Lu, G.M. Carroll, X. Chen, D. K. Amarasinghe, N.R. Neale, E.M. Miller, P. Sercel, F.A. Rauffetti, AL. Efros, M.C. Beard, “n-Type PbSe Quantum Dots via Post-Synthetic Indium Doping”, *JACS*, 140, 42, 13753-13763, **2018**, [doi:10.1021/jacs.8b07910](https://doi.org/10.1021/jacs.8b07910)
5. D. M. Kroupa, G. F. Pach, M. Vörös, F. Giberti, R. W. Crisp, B. D. Chernomordik, A. J. Nozik, J. C. Johnson, V. I. Klimov, G. Galli, and M. C. Beard, “Enhanced Multiple Exciton Generation in PbS/CdS Janus-like Heterostructure Nanocrystals”, *ACS Nano*, 12, 10, 10084-10094, **2018**, [doi:10.1021/acsnano.8b04850](https://doi.org/10.1021/acsnano.8b04850)
6. D.M. Kroupa, M. Voros, N.P. Brawand, B.W. McNichols, C.V. Castaneda, N. Bronstein, A.J. Nozik, A. Sellinger, G. Galli, M.C. Beard, “Optical absorbance enhancement in PbS QD/cinnamate ligand complexes”, *JPCL*, 9, 3425-3433, **2018**, [doi:10.1021/acs.jpcllett.8b01451](https://doi.org/10.1021/acs.jpcllett.8b01451)
7. E. R. Kennehan, G. S. Doucette, A. R. Marshall, C. Grieco, K. T. Munson, M. C. Beard, J. B. Asbury,” Origins of Fast Relaxation from High Energy Intraband States in PbS Quantum Dots”, *ACS Nano*, 12, 6, 6263-6272, **2018**, [doi:10.1021/acsnano.8b03216](https://doi.org/10.1021/acsnano.8b03216)
8. T. Liu, Y. Zhou, Z. Li, L. Zhang, M.G. Ju, D. Luo, Y. Yang, M. Yang, D. Kim, W. Yang, N.P. Padture, M.C. Beard, X. Cheng Zeng, K. Zhu, R. Zhu, Q. Gong, “Stable Formamidinium-Based Perovskite Solar Cells via in Situ Encapsulation”, *Adv. Energy Mater.*, 1800232, **2018**, [doi:10.1002/aenm.201800232](https://doi.org/10.1002/aenm.201800232)
9. X. Chen, H. Lu, Y. Yang, and M.C. Beard, “Excitonic Effect in Methylammonium Lead Halide Perovskites”, *JPCL*, 9, 2595-2603, **2018**, [doi:10.1021/acs.jpcllett.8b00526](https://doi.org/10.1021/acs.jpcllett.8b00526)
10. S. Dunfield, D. Moore, T. Klein, D. Fabian, J. Christians, A. Dixon, B. Dou, S. Ardo, M.C. Beard, S. Shaheen, J. Berry, M. van Hest, ”Curtailling Perovskite Processing Limitations via Lamination at the Perovskite/Perovskite Interface”, *ACS Energy Lett.*,3, 1192-1197, **2018**, [doi:10.1021/acsenergylett.8b00548](https://doi.org/10.1021/acsenergylett.8b00548)
11. D.M. Kroupa, D.H. Arias, J.L. Blackburn, D.B. Granger, J.E. Anthony, M.C. Beard, J.C. Johnson “Control of Energy Flow Dynamics between Tetracene Ligands and PbS Quantum Dots by Size Tuning and Ligand Coverage”, *Nano Lett.*, 18 (2), pp 865–873, **2018**, [doi:10.1021/acs.nanolett.7b04144](https://doi.org/10.1021/acs.nanolett.7b04144)

- 12.** D.M. Kroupa, B.K. Hughes, E.M. Miller, B.D. Chernomordik, A.J. Nozik, M.C. Beard, “Synthesis and Spectroscopy of Silver Doped PbSe Quantum Dots”, *JACS*, 139, 10382-10394, **2017**, [doi:10.1021/jacs.7b04551](https://doi.org/10.1021/jacs.7b04551)
- 13.** Z. Li, C. Xiao, Y. Yang, S. Harvey, D. Kim, J.A. Christians, M. Yang, P. Schulz, C-S. Jiang, J.M. Luther, J. Berry, M.C. Beard, M.M. Al-Jassim, K. Zhu, “Extrinsic ion migration in perovskite solar cells”, *EES*, 10, 1234, **2017**, [doi:10.1039/c7ee00358g](https://doi.org/10.1039/c7ee00358g)
- 14.** D.M. Kroupa, M. Voros, N. Brawand, B. McNichols, E.M. Miller, J. Gu, A.J. Nozik, A. Sellinger, G. Galli, M.C. Beard, “Tuning Colloidal Quantum Dot Band Edge Positions through Solution-Phase Surface Chemistry Modification”, *Nature Comm.*, 8, 15257, **2017** [doi:10.1038/ncomms15257](https://doi.org/10.1038/ncomms15257)
- 15.** Y. Yan, R. W. Crisp, J. Gu, B.D. Chernomordik, G.F. Pach, A.R. Marshall, J. A. Turner, M.C. Beard, “Multiple Exciton Generation for Photoelectrochemical Hydrogen Evolution Reactions with Quantum Yields Exceeding 100%”, 2, 17052, *Nature Energy*, **2017**, [doi:10.1038/nenergy.2017.52](https://doi.org/10.1038/nenergy.2017.52)
- 16.** Y. Yang, M. Yang, D.T. Moore, Y. Yan, E.M. Miller, K. Zhu, M.C. Beard, “Top and Bottom Surfaces Limit Carrier Lifetime in Lead Iodide Perovskite Films”, *Nature Energy*, 2, 16207, **2017**, [doi:10.1038/nenergy.2016.207](https://doi.org/10.1038/nenergy.2016.207)
- 17.** D.M. Kroupa, N.C. Anderson, C.V. Castaneda, A.J. Nozik, M.C. Beard, “In-situ Spectroscopic Characterization of an X-Type Solution-Phase Ligand Exchange at Colloidal Lead Sulphide Quantum Dot Surfaces”, *ChemComm.*, 52, 13893-13896, **2016**, [doi:10.1039/C6CC08114B](https://doi.org/10.1039/C6CC08114B)
- 18.** Y. Yang, M. Yang, K. Zhu, J.C. Johnson, J. J. Berry, J. van de Lagemaat, and M. C. Beard, “Large Polarization-Dependent Optical Stark Effect in Lead Iodide Perovskites”, *Nature Comm.*, 7, 12613, **2016**, [doi:10.1038/ncomms12613](https://doi.org/10.1038/ncomms12613)
- 19.** M.C. Beard, J.L. Blackburn, J.C. Johnson, G. Rumbles, “Status and Prognosis of Future Generation Photoconversion to Photovoltaics and Solar Fuels”, *ACS Energy Lett.*, 1, 344-347, **2016**, [doi:10.1021/acseenergylett.6b00204](https://doi.org/10.1021/acseenergylett.6b00204)
- 20.** Y. Yang, K. Wu, A. Shabaev, Al. L. Efros, T. Lian, M.C. Beard, “Direct Observation of Photo-Excited Hole Localization in CdSe Nanorods”, *ACS Energy Lett.*, 1, 76-81, **2016**, [doi:10.1021/acseenergylett.6b00036](https://doi.org/10.1021/acseenergylett.6b00036)
- 21.** B.G. Lee, L.W. Luo, N.R. Neale, M.C. Beard, D. Hiller, M. Zacharias, A. Zunger, P. Stradins, “Quasi-Direct Optical Transitions in Silicon Nanocrystals with intensity exceeding the bulk”, *Nano Letters*, 16, 1583, **2016**, [doi: 10.1021/acLians.nanolett.5b04256](https://doi.org/10.1021/acLians.nanolett.5b04256)
- 22.** E.M. Miller, D. M. Kroupa, J. Zhang, P. Schulz, A. Khan, J. M. Luther, M.C. Beard, C.L. Perkins, J. van de Lagemaat, “Revisiting the Size-dependent Valence and Conduction Bands of PbS QDs: Photoelectron and Inverse Photoelectron Spectroscopy”, *ACS Nano*, 10, 3302-3311, **2016**, [doi: 10.1021/acsnano.5b06833](https://doi.org/10.1021/acsnano.5b06833)

- 23.** M. R. Bergren, P.B. Palomaki, N.R. Neale, T.E. Furtak, M.C. Beard, “Size-Dependent Exciton Formation Dynamics in Colloidal Silicon Quantum Dots”, *ACS Nano*, 10, 2316-2323, **2016**, doi: [10.1021/acsnano.5b07073](https://doi.org/10.1021/acsnano.5b07073)
- 24.** L.M. Wheeler, A.W. Nichols, B.D. Chernomordik, N. C. Anderson, M. C. Beard, N.R. Neale, “All-Inorganic Germanium Nanocrystal Films by Cationic Ligand Exchange”, *Nano Letters*, 16(3), 1949-1954, **2016**, doi: [10.1021/acs.nanolett.5b05192](https://doi.org/10.1021/acs.nanolett.5b05192)
- 25.** S. Boriskina, M.A. Green, K. Catchpole, E. Yablonovitch, M. C. Beard, Y. Okada, S. Lany, T. Gershon, A. Zakutayev, M. Tahersima, V. J. Sorger, M. Naughton, K. Kempa, M. Dagenais, Y. Yao, L. Xu, X. Shing, N. D. Bronstein, J. A. Rogers, A. P. Alivisatos, R. G. Nuzzo, J. M. Gordon, D. M. Wu, M. D. Wisser, A. Salleo, J. Dionne, P. Bermel, J.J. Greffet, I. Celanovic, M. Soljacic, A. Manor, C. Rotschild, A. Raman, L. Shu, S. Fan, G. Chen “Roadmap for Optical Energy Conversion: Quantum-confined semiconductor nanostructures for enhanced solar energy photoconversion”, *J. of Optics*, 18, 073004, **2016**, doi: [10.1088/2040-8978/18/7/073004](https://doi.org/10.1088/2040-8978/18/7/073004)
- 26.** Y. Yang, D. Ostrowski, R. France, K. Zhu, J. van de Lagemaat, J.M. Luther, M.C. Beard, “Observation of a Hot-Phonon Bottleneck in Lead Iodide Perovskites”, *Nature Photonics*, 10, 53-59, **2016** doi: [10.1038/nphoton.2015.213](https://doi.org/10.1038/nphoton.2015.213)

## Hot-Carrier Dynamics in Quantum Dots Manipulated by Spin-Exchange Auger Interactions

Rohan Singh, Wenyong Liu, Jaehoon Lim, Istvan Robel, Victor I. Klimov  
C-PCS, Chemistry Division  
Los Alamos National Laboratory  
Los Alamos, New Mexico 87544

The ability to effectively manipulate nonequilibrium ‘hot’ carriers could enable novel schemes for highly efficient energy harvesting and interconversion. One approach to harness a kinetic energy of hot carriers is through exploiting Auger interactions. In particular, using inverse Auger recombination or impact ionization, one can generate additional electron-hole pairs, which could, in principle, enhance efficiencies of photoelectrical and photochemical transformations<sup>1</sup>. In this process, often referred to as carrier multiplication (CM), a high-energy ‘hot’ carrier relaxes to a lower-lying state within the same band by transferring its energy to a valence-band electron exciting it across the energy gap. The Auger interactions driving CM compete with carrier cooling due to processes such as phonon emission. In particular, electron-hole creation energy ( $\epsilon_{eh}$ ), an important CM characteristic, is directly controlled by this competition through the expression  $\epsilon_{eh} = r_c \tau_{im}$ , where  $r_c$  is an energy-loss rate and  $\tau_{im}$  is a characteristic time of impact ionization<sup>2</sup>. During impact ionization, an electron excited from the valence band gains energy  $E_g$ . The corresponding energy-gain rate ( $r_g$ ) can be linked to  $\tau_{im}$  by  $r_g = E_g/\tau_{im}$ , which yields  $\epsilon_{eh} = E_g(r_c/r_g)$ . In bulk semiconductors,  $\epsilon_{eh}$  is at least  $3E_g$  (ref<sup>3</sup>); hence,  $r_c/r_g \geq 3$ , which suggests that the energy-gain rate due to Auger-type energy transfer (ET) is always lower than that of intraband cooling. This, in particular, explains fairly low efficiencies of impact-ionization in bulk solids.

Due to relaxation of translational momentum conservation and reduced dielectric screening, Auger interactions are enhanced in quantum-confined semiconductor nanocrystals or quantum dots (QDs), which leads to the enhancement of the CM effect manifested most prominently in the reduction of its threshold down to the fundamental  $2E_g$  limit<sup>4,5</sup>. The effects of quantum confinement also reduce  $\epsilon_{eh}$ , however, to a lesser degree. The lowest reported values of  $\epsilon_{eh}$  are from  $\sim 2.3E_g$  to  $\sim 3.3E_g$ , suggesting that the rate of intraband carrier cooling still exceeds the energy-gain rate on average by a factor of  $\sim 2.8$ , which is just slightly less than the bulk-semiconductor limit of  $\sim 3$ .

Here we demonstrate that combining effects of three-dimensional confinement with strong spin-exchange interactions realized in magnetically doped QDs, we can boost the Auger energy-gain rate almost ten-fold to  $\sim 15$  eV ps<sup>-1</sup>. The corresponding ratio between the energy gain/loss rates becomes greater than 7, which represents a dramatic shift from the traditional situation where  $r_g/r_c$  is around or less than 0.3. The fact that Auger-type ET outcompetes intraband cooling is indicated by observations of highly efficient Auger processes involving unrelaxed, hot carriers. In particular, we observe very fast ( $\sim 140$  fs) excitation of a magnetic ion (Mn in our experiments) by spin-exchange ET from an exciton originally injected into a semiconductor host (a CdSe QD). Furthermore, we also resolve an upconversion-like process wherein a hot photoinjected electron is intercepted by the spin-exchange Auger process and instead of relaxing

to the band-edge is promoted to a higher energy state ‘vacuum’ state outside the dot (**Fig. 1**). Based on our transient absorption (TA) measurements, the timescale of this process is  $\sim 150$  fs, which is one-to-two orders of magnitude faster than the rate of standard impact-ionization collisions driving CM.

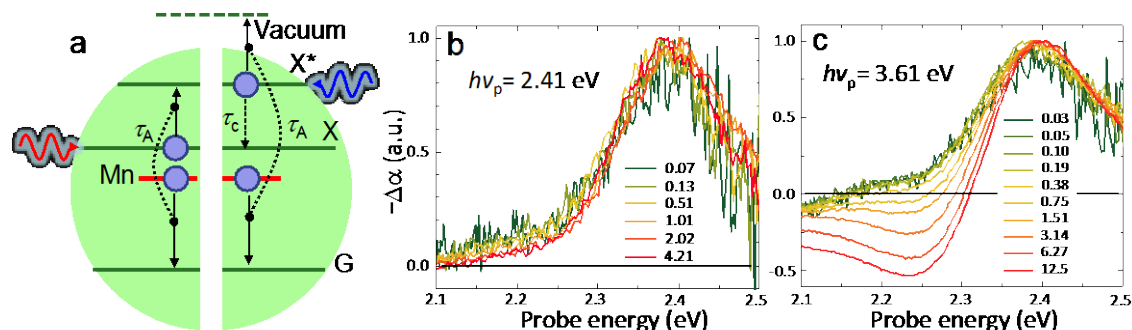


**Figure 1| Spin-exchange Auger ionization of Mn-doped CdSe/CdS QDs.** **a**, Schematic depiction of Auger interactions between an excited Mn ion and a ‘cold’ (left) and a ‘hot’ (right) QD electron generated using photon energies  $h\nu_p = 2.41$  and  $3.61$  eV, respectively. When  $h\nu_p = 2.41$  eV, the energy transferred from the Mn-ion to the band-edge electron is insufficient to promote it to a ‘vacuum’ state outside the dot. As a result, the TA spectra ( $\Delta t = 2$  ps) exhibit a usual band-edge bleach due to Pauli blocking (**b**). When  $h\nu_p = 3.61$  eV, the energy transferred from the Mn ion is combined with a kinetic energy of a hot electron, which leads to its ejection outside the dot. This is possible due to extremely fast Auger-type spin exchange characterized by time constant  $\tau_A = 150$  fs, which is a factor of  $\sim 7$  faster than the cooling rate ( $\tau_c = 1$  ps). The ejected electron is observed in TA as a Stark-effect-related photoinduced absorption feature at  $2.25$  eV (**c**). The TA spectra shown in **b** and **c** were measured as a function of average QD excitonic occupancy (indicated in the legends).

In our future work on this topic, we plan to elucidate the mechanism(s) underlying the observed hot-carrier Auger ionization *via* comprehensive TA studies that will take advantage of our newly developed system for ultrafast magnetic-field spectroscopy. Using these measurements, we intend to clarify the energetic threshold of spin-exchange Auger-ionization, its temperature dependence, and the influence of QD parameters such as the QD band-gap energy, doping levels, and the identity of surface ligands. Finally, we will attempt to capture an ejected electron in an adjacent high-mobility layer of a transition metal dichalcogenide and detect it using ultrafast photoconductive spectroscopy. This would demonstrate the utility of the discovered phenomenon in practical photoconversion, which could exploit processes such as spin-exchange-mediated CM and upconversion, hot-carrier extraction, and electron photoemission.

1. Werner, J. H., Kolodinski, S. & Queisser, H. J. *Phys Rev. Lett.* **72**, 3851-3854 (1994).
2. Stewart, J. T., *et al.* *J. Phys. Chem. Lett.* **4**, 2061-2068 (2013).
3. Alig, R. C. & Bloom, S. *Phys Rev. Lett.* **35**, 1522-1525 (1975).
4. Cirloganu, C. M., *et al.* *Nat. Comm.* **5**, 4148 (2014).
5. Kroupa, D. M., *et al.* *ACS Nano* **12**, 10084-10094 (2018).

### DOE Solar Photochemistry Sponsored Publications

1. R. Singh, W. Liu, J. Lim, I. Robel, V. I. Klimov, Hot-electron dynamics in quantum dots manipulated by spin-exchange Auger interactions, (under revision) *Nat. Nanotech.* (2019)
2. Y.-S. Park, J. Lim, V. I. Klimov, Asymmetrically strained quantum dots with non-fluctuating single-dot emission spectra and subthermal linewidths, *Nat. Mater.* **18**, 249 (2019)
3. H.J. Yun, J. Lim, A.S. Fuhr, N.S. Makarov, S. Keene, M. Law, J.M. Pietryga, V.I. Klimov, Charge-transport mechanisms in  $\text{CuInSe}_x\text{S}_{1-x}$  quantum-dot films, *ACS Nano* **12**, 12587 (2018)

# Time-Domain Atomistic Studies of Far-from-Equilibrium Dynamics in Nanoscale Materials for Solar Energy Harvesting

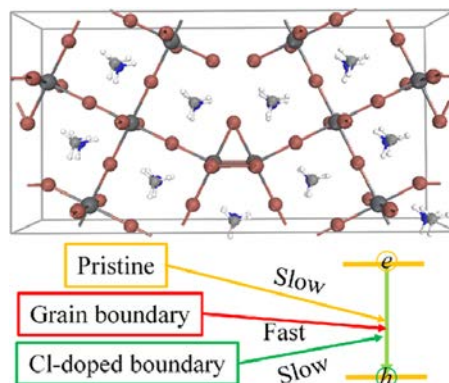
Oleg V. Prezhdo

Department of Chemistry  
University of Southern California  
Los Angeles, CA 90089

Absorption of a photon from the visible part of the solar spectrum puts a light-harvesting system in a highly non-equilibrium state. The ensuing ultrafast dynamics determines whether the sun energy will be converted to electricity or fuel, or lost to heat. Multiple experimental groups study such dynamics using time-resolved spectroscopies. In close collaboration with experiment, we develop state-of-the-art methodologies combining nonadiabatic molecular dynamics and time-dependent density functional theory, and apply them to study specific systems and processes. The talk will highlight our recent DOE funded efforts to model ultrafast far-from-equilibrium dynamics in several classes of nanoscale materials for energy harvesting, including

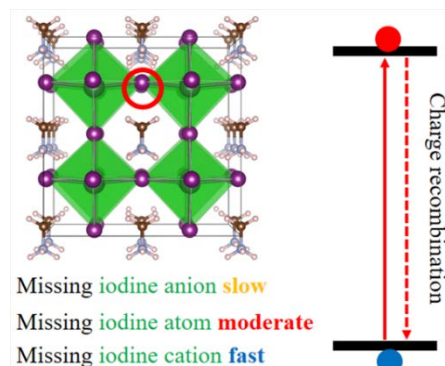
## Charge recombination at pristine and doped perovskite grain boundaries (GB).

Nonradiative relaxation is a major pathway of energy and charge losses. We showed that GBs, common in perovskite polycrystalline films, can notably accelerate charge recombination by decreasing bandgap, activating additional phonons, and enhancing nonadiabatic coupling. GB doping by chlorines reduces charge recombination, since the hole wavefunction is pushed away from the boundary. The work was featured in a *JACS spotlight*. More recently, we showed that charge separation and localization happening at GBs due to symmetry breaking can suppress the recombination. Even though GBs lower the bandgap and charge localization enhances interactions with phonons, electron-hole separation decreases the nonadiabatic coupling. Our studies rationalize how GBs can have both positive and negative influence on perovskite optoelectronic properties.



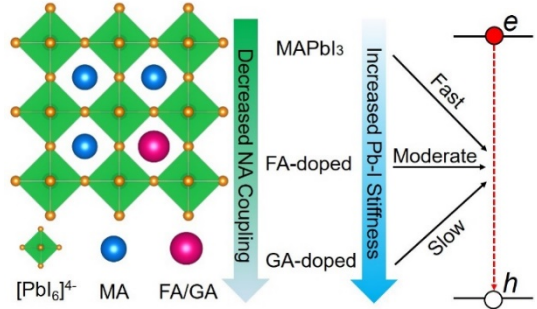
## Control of charge recombination by defect oxidation state.

We demonstrated that charge recombination in perovskites is extremely sensitive to oxidation state of the halogen vacancy. A missing iodide in MAPbI<sub>3</sub> has almost no effect on charge losses. However, when the vacancy is reduced, the recombination is accelerated by up to two orders of magnitude. The acceleration occurs due to formation of hole traps. The doubly reduced vacancy exhibits a significant rearrangement of the Pb-I lattice, leading to a new chemical species, a Pb-Pb dimer bound by the vacancy charge, and under-coordinated iodine bonds. Iodide vacancies can improve performance, since they cause minor changes to carrier lifetimes, while increasing carrier concentration. However, neutral iodine and iodine cation vacancies should be strongly avoided.



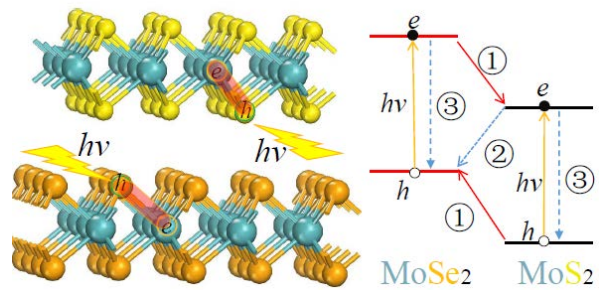
Increased lattice stiffness suppresses charge recombination in MAPbI<sub>3</sub> doped with larger cations.

Experiments report that halide perovskites containing several organic cations exhibit much longer charge carrier lifetimes than pristine MAPbI<sub>3</sub>. We showed that partial replacement of MA with formamidinium (FA) or guanidinium (GA) significantly reduces the electron-vibrational coupling. The effect arises due to stiffening of the inorganic Pb-I lattice, which fluctuates less, while maintaining its original structure and bandgap. The reduced lattice motions, and particularly of iodides, suggest decreased ion diffusion that is responsible for formation of defects, such as iodine interstitials and vacancies, and current-voltage hysteresis.



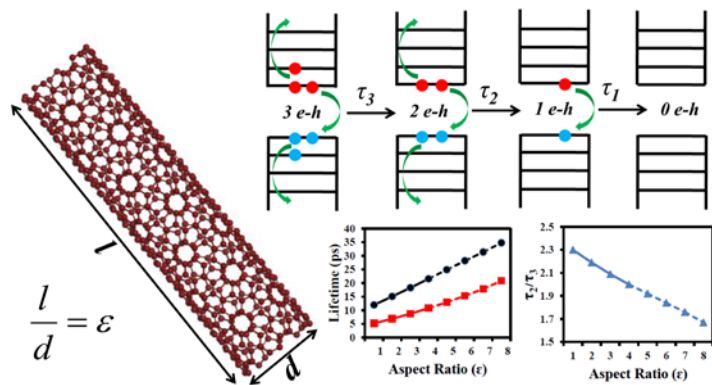
Efficient charge separation at the MoS<sub>2</sub>/MoSe<sub>2</sub> van der Waals junction.

Two-dimensional transition metal dichalcogenides hold great potential in optoelectronics and photovoltaics. To achieve efficient light-to-electricity conversion, excitons must dissociate into free charges. We showed that quantum coherence and donor-acceptor delocalization facilitate rapid charge transfer. The delocalization is larger for electron than hole, resulting in longer coherence and faster transfer. The transfers are promoted by the out-of-plane Mo-X modes of the acceptors. The relatively slow relaxation of the “hot” hole suggests long-distance band-like transport, observed in organic photovoltaics. Charge recombination is longer across the interface than in isolated MoS<sub>2</sub> and MoSe<sub>2</sub>, favoring long-lived charge separation.



Multiparticle Auger recombination in single-walled carbon nanotubes.

Many-particle Auger-type processes are common in nanoscale materials due to a combination of high densities of states that can support multiple excitations, and substantial Coulomb coupling between charges enhanced by quantum confinement. We simulated Auger decay dynamics in (10,5) semiconductor carbon nanotubes (CNT) with different aspect ratios and particle densities. Despite an increasing density of states, the multiparticle Auger recombination rate decreases in longer CNTs, due to decreased charge carrier interactions. The length dependence is stronger for three-exciton than two-exciton recombination, and the calculated timescale ratio approaches the experimental value measured for long CNTs. Phonon-assisted transitions play a particularly important role. Electron-phonon relaxation is faster than the recombination, and Auger transitions are assisted by phonons over a range of frequencies up to the G-mode. The involvement of phonons strongly enhances the probability of transitions involving asymmetric electron-hole pairs.



## DOE Solar Photochemistry Sponsored Publications 2016-2019

### Reviews

1. A. A. Chistyakov, M. A. Zvaigzne, V. R. Nikitenko, A. R. Tameev, I. L. Martynov, O. V. Prezhdo, "Optoelectronic properties of semiconductor quantum dot solids for photovoltaic applications", *J. Phys. Chem. Lett.*, **8**, 4129-4139 (2017)
2. J. Jankowska, R. Long, O. V. Prezhdo, "Quantum dynamics of photogenerated charge carriers in hybrid perovskites: dopants, grain boundaries, electric order, and other realistic aspects", *ACS Energ. Lett.*, **2**, 1588-1597 (2017)
3. R. Long, O. V. Prezhdo, W. H. Fang, "Nonadiabatic charge dynamics in novel solar cell materials", *Wiley Interdisciplinary Reviews-Computational Molecular Science*, **7**, e1305 (2017)
4. X. Zhou, J. Jankowska, H. Dong, O. V. Prezhdo, "Recent theoretical progress in the development of perovskite photovoltaic materials", *J. Energ. Chem.*, **27**, 637-649 (2018)
5. W. Li, R. Long, J. F. Tang, O. V. Prezhdo, "Influence of Defects on Excited State Dynamics in Lead Halide Perovskites: Time-Domain Ab Initio Studies", *J. Phys. Chem. Lett.*, submitted

### Regular Articles

6. R. Long, J. Liu, O. V. Prezhdo "Unravelling the effects of grain boundary and chemical doping on electron-hole recombination in  $\text{CH}_3\text{NH}_3\text{PbI}_3$  perovskite by time-domain atomistic simulation", *J. Am. Chem. Soc.*, **138**, 3884-3890 (2016)
7. V. V. Chaban, S. Pal, O. V. Prezhdo, "Laser-induced explosion of nitrated carbon nanotubes: nonadiabatic and reactive molecular dynamics simulations", *J. Am. Chem. Soc.*, **138**, 15927-15934 (2016)
8. V. V. Chaban, O. V. Prezhdo, "Pressure-driven opening of carbon nanotubes", *Nanoscale*, **8**, 6014-6020 (2016)
9. X. Chen, O. V. Prezhdo, Z. Y. Ma, T. J. Hou, Z. Y. Guo, Y. Y. Li, "Ab initio phonon-coupled nonadiabatic relaxation dynamics of  $[\text{Au}_{25}(\text{SH})_{18}]$  cluster", *Phys. Status Solidi B -Basic Solid State Phys.*, **253**, 458-462 (2016)
10. V. V. Chaban, O. V. Prezhdo, "Ab initio molecular dynamics of dimerization and clustering in alkali metal vapors", *J. Phys. Chem. A*, **120**, 4302-4306 (2016)
11. W. B. Chu, W. A. Saidi, Q. J. Zheng, Y. Xie, Z. G. Lan, O. V. Prezhdo, H. Petek, J. Zhao, "Ultrafast dynamics of photo-generated holes at a  $\text{CH}_3\text{OH}/\text{TiO}_2$  rutile interface", *J. Am. Chem. Soc.*, **138**, 13740-13749 (2016)
12. V. V. Chaban, O. V. Prezhdo, "Ionic vapor composition in critical and supercritical states of strongly interacting ionic compounds", *J. Phys. Chem. B*, **120**, 4302-4309 (2016)
13. O. Ranasingha, H. Wang, V. Zobac, P. Jelinek, G. Panapitiya, A. J. Neukirch, O. V. Prezhdo, J. P. Lewis, "Slow relaxation of surface plasmon excitations in  $\text{Au}_{55}$ : the key to efficient plasmonic heating in  $\text{Au}/\text{TiO}_2$ ", *J. Phys. Chem. Lett.*, **7**, 1563-1569 (2016).
14. V. V. Chaban, O. V. Prezhdo, "Electron solvation in liquid ammonia: lithium, sodium, magnesium and calcium as electron sources", *J. Phys. Chem. C*, **120**, 2500-2506 (2016)
15. R. Long, O. V. Prezhdo "Quantum coherence facilitates efficient charge separation at a  $\text{MoS}_2/\text{MoSe}_2$  van der Waals junction", *Nano Lett.*, **16**, 1996-2003 (2016)
16. O. M. Korsun, O. N. Kalugin, A. S. Vasenko, O. V. Prezhdo, "Electronic properties of carbon nanotubes intercalated with  $\text{Li}^+$  and  $\text{Mg}^{2+}$ : effects of ion charge and ion solvation", *J. Phys. Chem. C*, **120**, 26514-26521 (2016)

17. Z. H. Zhou, F. S. Han, L. J. Guo, O. V. Prezhdo, "Understanding divergent behaviors in the photocatalytic hydrogen evolution reaction on CdS and ZnS: a DFT based study", *Phys. Chem. Chem. Phys.*, **18**, 16862-16869 (2016)
18. O. M. Korsun, O. N. Kalugin, I. O. Fritsky, O. V. Prezhdo, "Ion association in aprotic solvents for lithium ion batteries requires discrete-continuum approach: lithium bis(oxalato)borate in ethylene carbonate based mixtures", *J. Phys. Chem. C*, **120**, 16545-16552 (2016)
19. A. E. Sifain, J. A. Bjorgaard, T. W. Myers, J. M. Veauthier, D. E. Chavez, O. V. Prezhdo, R. J. Scharff, S. Tretiak, "Photoactive excited states in explosive Fe(II) tetrazine complexes: a time-dependent density functional theory study", *J. Phys. Chem. C*, **120**, 28762-28773 (2016)
20. L. Q. Li, R. Long, O. V. Prezhdo, "Charge separation and recombination in two-dimensional MoS<sub>2</sub>/WS<sub>2</sub>: time-domain ab initio modeling", *Chem. Mat.*, **29**, 2466-2473 (2017)
21. A. E. Sifain, L. F. Tadesse, J. A. Bjorgaard, D. E. Chavez, O. V. Prezhdo, R. J. Scharff, S. Tretiak, "Cooperative enhancement of the nonlinear optical response in conjugated energetic materials: A TD-DFT study", *J. Chem. Phys.*, **146**, 114308 (2017)
22. W. Li, Y.-Y. Su, L. Q. Li, Z. H. Zhou, J. F. Tang, O. V. Prezhdo, "Control of charge recombination in perovskites by oxidation state of halide vacancy", *J. Am. Chem. Soc.*, **140**, 15753-15763 (2018)
23. Y. Nam, L. Li, J. Y. Lee, O. V. Prezhdo, "Size and shape effects on charge recombination dynamics of TiO<sub>2</sub> nanoclusters", *J. Phys. Chem. C*, **122**, 5201-5208 (2018)
24. S. Pal, D. Casanova, O. V. Prezhdo, "Effect of aspect ratio on multiparticle Auger recombination in single-walled carbon nanotubes: time domain atomistic simulation", *Nano Lett.*, **18**, 58-63 (2018)
25. R. D. Senanayake, E. B. Guidez, A. J. Neukirch, O. V. Prezhdo, C. M. Aikens, "Theoretical investigation of relaxation dynamics in Au<sub>38</sub>(SH)<sub>24</sub> thiolate-protected gold nanoclusters", *J. Phys. Chem. C.*, **122**, 16380-16388 (2018)
26. A. E. Sifain, J. A. Bjorgaard, T. R. Nelson, B. T. Nebgen, A. J. White, B. J. Gifford, D. W. Gao, O. V. Prezhdo, S. Fernandez-Alberti, A. E. Roitberg, S. Tretiak, "Photoexcited nonadiabatic dynamics of solvated push-pull pi-conjugated oligomers with the NEXMD software", *J. Chem. Theor. Comp.*, **14**, 3955-3966 (2018)
27. J. L. He, W. H. Fang, R. Long, O. V. Prezhdo, "Increased lattice stiffness suppresses nonradiative charge recombination in MAPbI<sub>3</sub> doped with larger cations: time domain ab initio analysis", *ACS Energ. Lett.*, **3**, 2070-2076 (2018)
28. A. E. Sifain, B. J. Gifford, D. W. Gao, L. Lystrom, T. R. Nelson, S. Tretiak, "NEXMD modeling of photoisomerization dynamics of 4-styrylquinoline", *J. Phys. Chem. A*, **122**, 9403-9411 (2018)
29. L. H. Liu, W. H. Fang, R. Long, O. V. Prezhdo, "Lewis base passivation of hybrid halide perovskites slows electron-hole recombination: time-domain ab initio analysis", *J. Phys. Chem. Lett.*, **9**, 1164-1171 (2018)
30. A. E. Sifain, N. Lubbers, B. T. Nebgen, S. Smith, A. Y. Lokhov, O. Isayev, A. E. Roitberg, K. Barros, S. Tretiak, "Discovering a transferable charge assignment model using machine learning", *J. Phys. Chem. Lett.*, **9**, 4495-4501 (2018).
31. W. H. Zhong, Y. X. Liu, M. S. Deng, Y. C. Zhang, C. Y. Jia, O. V. Prezhdo, J. Y. Yuan, J. Jiang, "C<sub>2</sub>N-supported single metal ion catalysts for HCOOH dehydrogenation", *J. Mat. Chem. A*, **24**, 11105-11112 (2018)

32. R. Sarkar, M. Habib, S. Pal, O. V. Prezhdo, “Ultrafast, asymmetric charge transfer and slow charge recombination in porphyrin/CNT composites demonstrated by time-domain atomistic simulation”, *Nanoscale*, **10**, 12683-12694 (2018)
33. W. Li, J. F. Tang, D. Casanova, O. V. Prezhdo, “Time-domain ab initio analysis rationalizes the unusual temperature dependence of charge carrier relaxation in lead halide perovskite”, *ACS Energ. Lett.*, **3**, 2713–2720 (2018)
34. Y. Wang, W. H. Fang, R. Long, O. V. Prezhdo, “Symmetry breaking at MAPbI<sub>3</sub> perovskite grain boundaries suppresses charge recombination: time-domain ab initio analysis”, submitted.

# Metal-Tipped and Electrochemically Wired Semiconductor Nanocrystals: Modular Constructs for Directed Charge Transfer

Jeffrey Pyun, S. Scott Saavedra, Neal R. Armstrong  
 Departments of Chemistry/Biochemistry/Optical Sciences  
 University of Arizona  
 Tucson, Arizona 85721

[nra@email.arizona.edu](mailto:nra@email.arizona.edu), [jpyun@email.arizona.edu](mailto:jpyun@email.arizona.edu), [saavedra@email.arizona.edu](mailto:saavedra@email.arizona.edu)

Current DOE supported research efforts, which build on previous DOE support,<sup>1-6</sup> are focused on: i) creation and characterization of new asymmetric photoactive nanomaterial constructs, including monodisperse CdSe@CdS nanorods (NRs) and tetrapods (TPs), with an without single metal catalyst tips (Au,Pt) – Fig. 1; ii) new approaches to the characterization of band edge offset energies in these prototypical nanomaterials using combinations of *in vacuo* photoemission (XPS/UPS) of tethered monolayers and multilayer films (Figure 2). These band edge offsets control efficiencies for photogeneration of charges and ultimately photoelectrochemical efficiencies for creation of fuels (e.g. HER). Our approaches are intended to provide guidelines for creation and characterization of a wider variety of isolated nanomaterial photocatalysts, and for surface-supported complex thin film nanomaterials.

New routes to monodisperse CdSe@CdS NRs and TPs appear to provide precise control over energetics (Type I versus quasi-Type II heterojunctions) via control of CdSe seed size. Creation of these new nanostructured materials has enabled experiments which probe dynamics of charge formation, charge harvesting and recombination (collaborations Lian et al.) all of which point to the important role that defect sites along the NR or TP arm play in limiting energy conversion efficiencies. Spectroelectrochemical characterization of the band edge energies of these new TPs, which build upon our previous studies of both simple Qds and CdSe@CdS NRs, show that we are able to estimate ECB as a function of CdSe seed size, and that the as-constructed TPs contain a distribution of mid-gap trap states that can be passivated by electron-injection in the first voltammetric scan, or by addition of monolayers of ZnS via a SILAR process. For optimized TPs exhibiting quasi-Type II heterojunctions a photoelectrochemical process has been developed to selectively add Au nanocatalysts to just one tip of the TP via excitation with light above the CdS or CdSe bandedge, demonstrating efficient charge separation and the intrinsic asymmetry of these nanomaterials, even though in electron microscopy they appear to be uniform compositionally and crystallographically for each arm in the TP.

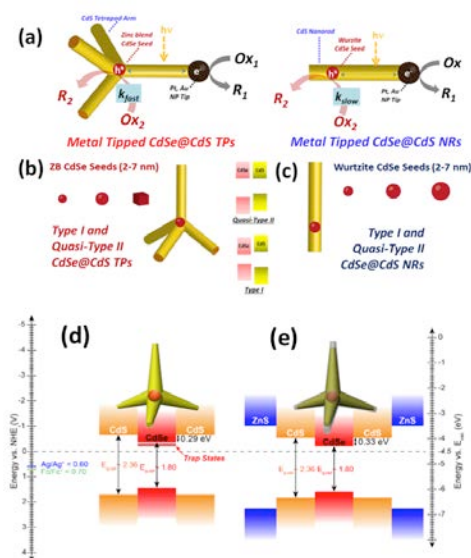


**Fig. 1** – CdSe@CdS tetrapods (a) and nanorod (b) constructs with control over Type I versus quasi-Type II band edge offsets afforded by type and size of the CdSe seed; mid-gap states arise in these nanomaterials, which limit photo-conversion efficiencies. Thin ZnS added via SILAR processes mitigate those defects and improve photoactivity.

We have returned to characterization of those factors which control  $E_{VB}$ ,  $E_{CB}$  and local  $E_{vac}$  in simple QDs and CdSe@CdS core-shell QD constructs using combinations of XPS and UPS photoemission of tethered monolayers, with special attention paid to processing in oxygen-free versus ambient environments (Fig. 2). The combined characterization of core-level and valence band spectral shifts and relative atomic ratios in these tethered QDs shows that the surface chalcogen atoms are replaced by a “ligand-like” oxygen species (not CdO), previously demonstrated for CdSe single crystal materials. For QDs processed in inert environments vacuum level shifts, and the transition from “n-type” to “p-type” with decreasing QD diameter are impacted, as are changes in  $E_{VB}$  and  $E_{CB}$ , i.e. the effective mass approximation is not strictly obeyed, and is found to be strongly dependent upon the dipolar character for the nanomaterial, imparted by the composition of the surface region. These findings, and our approach to their characterization, are predicted to have significant impact on the design of a wide variety of photoactive catalytic nanomaterials.

### DOE Solar Photochemistry Sponsored Publications Related to This Effort:

- (1) Shallcross, C. R.; Karayilan, M.; Pavlopolous, N. G.; Pyun, J.; Saavedra, S. S.; Armstrong, N. R. Size-Dependent Composition and Electronic Structure of Monolayer-Tethered CdSe Quantum Dots Revealed Using Photoemission Spectroscopies (XPS & UPS). *ACD Applied Mater. Int.* **submitted**.
- (2) Ehamparam, R.; Pavlopoulos, N. G.; Liao, M. W.; Hill, L. J.; Armstrong, N. R.; Pyun, J.; Saavedra, S. S. Band Edge Energetics of Heterostructured Nanorods: Photoemission Spectroscopy and Waveguide Spectroelectrochemistry of Au-Tipped CdSe Nanorod Monolayers. *Acs Nano* **2015**, *9*, 8786-8800.
- (3) Pavlopoulos, N. G.; Dubose, J. T.; Liu, Y.; Huang, X.; Pinna, N.; Willinger, M.-G.; Lian, T.; Char, K.; Pyun, J. Type I vs. quasi-type II modulation in CdSe@CdS tetrapods: ramifications for noble metal tipping. *Crystengcomm* **2017**, *19*, 6443-6453.
- (4) Wu, K.; Hill, L. J.; Chen, J.; McBride, J. R.; Pavlopolous, N. G.; Richey, N. E.; Pyun, J.; Lian, T. Universal Length Dependence of Rod-to-Seed Exciton Localization Efficiency in Type I and Quasi-Type II CdSe@CdS Nanorods. *Acs Nano* **2015**, *9*, 4591-4599.
- (5) Shallcross, R. C.; D'Ambruoso, G. D.; Pyun, J.; Armstrong, N. R. Photoelectrochemical Processes in Polymer-Tethered CdSe Nanocrystals. *Journal of the American Chemical Society* **2010**, *132*, 2622-2632.
- (6) Araci, Z. O.; Shallcross, C. R.; Armstrong, N. R.; Saavedra, S. S. Potential-Modulated Attenuated Total Reflectance Characterization of Charge Injection Processes in Monolayer-Tethered CdSe Nanocrystals. *Journal of Physical Chemistry Letters* **2010**, *1*, 1900-1905.

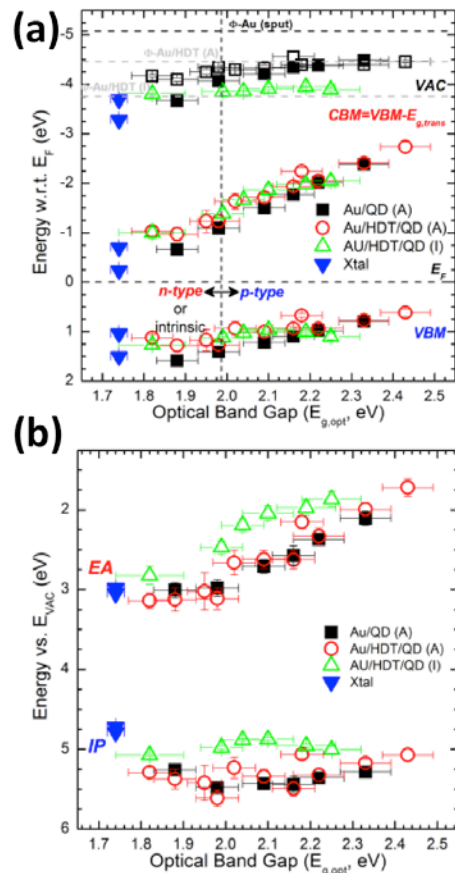


**Fig. 2 – XPS/UPS-derived energetics ( $E_{VB}$ ,  $E_{CB}$ ,  $E_{vac}$  – IP/EA) of monolayer-tethered CdSe QDs as a function of size (optical gap), and as a function of processing conditions. Combinations of XPS and UPS of these nanomaterials can uniquely determine whether these materials are p-type (larger QDs) or n-type (smaller QDs), controlled by the surface Cd/Se ratio (and surface-to-volume ratio) and whether processing in air or inert environments. Atmospheric oxygen displaces the chalcogen, creating a “ligand-like” surface oxygen species which plays a significant role in determining energetic and electrical properties, and ultimately the energetic displacement and photoactivity of core-shell NRs and TPs.**

## Modulation of Photoinduced Charge Transfer at the Semiconductor Interface

Rebecca Scheidt, Elizabeth Kerns, Greg Samu and Prashant V. Kamat  
Radiation laboratory and Department of Chemistry & Biochemistry  
University of Notre Dame, Notre Dame, Indiana 46556

Ternary semiconductors quantum dots such as  $\text{CuInS}_2$  and  $\text{CsPbBr}_3$  are gaining attention because of their ability to serve as light harvesters in solar cells and optoelectronic applications. Fundamental understanding of excited state dynamics and interfacial charge transfer processes are important for stable performance of such devices. In a quantum dot and perovskite solar cell, mesoscopic  $\text{TiO}_2$  film serves as an electron transport layer (ETL). Despite the extensive use of metal halide perovskites in solar cells for example, their interaction with ETL such as  $\text{TiO}_2$  is yet to be explored fully. The semiconducting metal oxides such as  $\text{TiO}_2$ ,  $\text{SnO}_2$ , and  $\text{ZnO}$  are well known photocatalysts and they can initiate degradation of adsorbed sensitizers following photoexcitation. So the question is whether these metal oxides are mere facilitators or participants in the photosensitization process.

We first employed ultra-fast transient absorbance spectroscopy to elucidate the excited

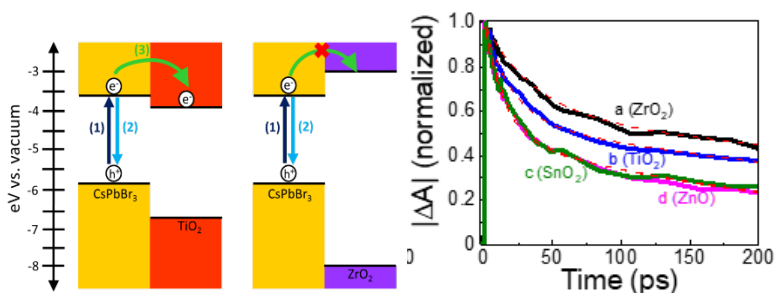


Figure 1: Left: Energy level diagram illustrating excited state pathways of the photogenerated charge carriers in  $\text{CsPbBr}_3$  nanocrystals adsorbed on  $\text{TiO}_2$  and  $\text{ZrO}_2$  films. Right: The transient bleach recovery recorded at the bleach maximum ( $\sim 500$  nm) for samples of  $\text{CsPbBr}_3$  NCs adsorbed on (a,)  $\text{ZrO}_2$ , (b)  $\text{TiO}_2$ , (c)  $\text{SnO}_2$ , and (d)  $\text{ZnO}$ .

state dynamics of  $\text{CsPbBr}_3$  nanocrystals (NCs) adsorbed on metal oxide films. The support material makes an important contribution to the deactivation of excited  $\text{CsPbBr}_3$  NCs (Figure 1). Semiconductor oxides such as  $\text{TiO}_2$ ,  $\text{ZnO}$ , and  $\text{SnO}_2$  are good electron acceptors as their conduction band edge thermodynamically favors electron transfer from excited  $\text{CsPbBr}_3$  NCs. Comparison of the excited state dynamics of the electron transporting metal oxides to insulating  $\text{ZrO}_2$  allows us to estimate the electron transfer rate constant from  $\text{CsPbBr}_3$  to metal oxide. The estimated electron transfer rate constants were  $2.28 \times 10^{10} \text{ s}^{-1}$ ,  $3.44 \times 10^{10} \text{ s}^{-1}$ , and  $4.25 \times 10^{10} \text{ s}^{-1}$  for  $\text{CsPbBr}_3/\text{TiO}_2$ ,  $\text{CsPbBr}_3/\text{ZnO}$ , and  $\text{CsPbBr}_3/\text{SnO}_2$  respectively.

$\text{CsPbBr}_3/\text{TiO}_2$  and  $\text{CsPbBr}_3/\text{ZrO}_2$  samples were irradiated with visible light in both ambient and  $\text{N}_2$  atmospheres to investigate the role of semiconducting oxide and the ultimate fate of the photoexcited  $\text{CsPbBr}_3$  NCs in the absence of a hole scavenger. The films were stable when irradiated in the  $\text{N}_2$  atmosphere. However, when  $\text{CsPbBr}_3/\text{TiO}_2$  is irradiated under ambient conditions (*i.e.* exposed to air), photogenerated electrons are scavenged by  $\text{O}_2$  and holes get accumulated within NCs. This accumulation of holes within  $\text{CsPbBr}_3$  NCs initiates oxidation into constituent products (*e.g.*, lead (II) oxide). These findings show the importance of careful selection of hole transport layer (HTL) for minimizing hole accumulation and thus achieving greater stability of quantum dot solar cells and light emitting devices.

In order to establish the fate of charge carriers under solar cell operation conditions it is

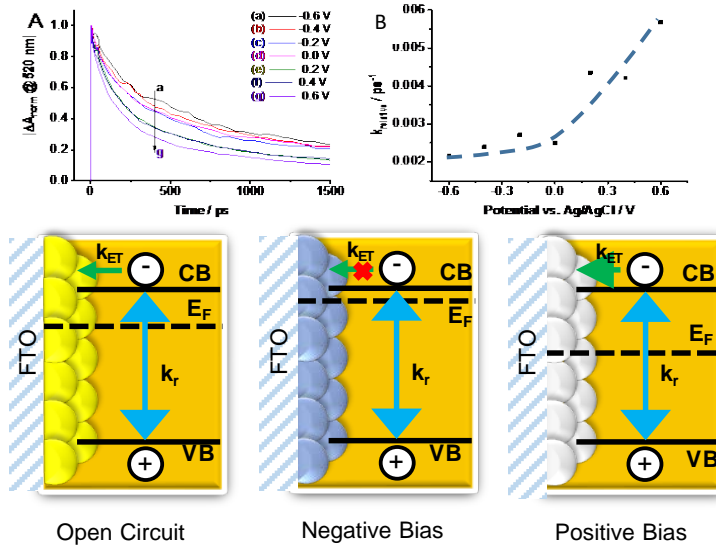


Figure 2. . **A.** Bleaching recovery profiles, and **B.** Relative rate constants of of FTO/TiO<sub>2</sub>/CsPbBr<sub>3</sub> electrode in a spectroelectrochemical cell with deaerated dichloromethane containing 0.1 M Bu<sub>4</sub>NPF<sub>6</sub> electrolyte. Time-resolved transient absorption spectra were recorded at different applied potentials in the range between -0.6 to +0.6 V vs. Ag/AgCl. The schematic diagram at the bottom shows the effect of electron accumulation in ETL on the electron injection and charge carrier recombination.

V to +0.6 V in steps (Figure 2). At 0.0 V potential and more negative potentials the rate constant of charge carrier recombination showed little variation. On the other hand, at anodic bias (more positive than 0.0 V vs. Ag/AgCl) we observed a faster decay kinetics. An increase by a factor of three in the bleaching recovery rate constant is seen as we increased the applied bias to +0.6 V. Since electrons are depleted from the TiO<sub>2</sub> layer under anodic bias, one can expect an additional pathway for photogenerated electrons to participate in the charge injection into TiO<sub>2</sub> film (k<sub>ET</sub>). The competing charge injection process thus renders faster bleaching recovery at anodic bias. Thus the role of TiO<sub>2</sub> as an ETL that captures electrons from excited CsPbBr<sub>3</sub> seems to play an important role in delivering superior device performance. The influence of electron accumulation on the charge recombination rate is a good indication why higher efficiencies are observed in photovoltaic devices containing mesoscopic TiO<sub>2</sub> films.

The spectroelectrochemical measurements in the present study show our ability to selectively inject electrons and holes in a semiconductor film and simultaneously probe the excited state dynamics of semiconductor nanostructures. Future studies will involve elucidation of interaction of CsPbBr<sub>3</sub> and other ternary semiconductors with hole transport materials at different applied electrochemical bias. In addition we will also probe the excited state processes leading to the photoinduced phase segregation in mixed halide perovskite films. A better understanding of ion mobility will help us to overcome the issues related to long term stable performance of perovskite and quantum dot solar cells.

necessary to understand how the electron storage in the ETL influences the charge carrier recombination in the semiconductor films. Such effects can be well studied by utilizing the principles of semiconductor photoelectrochemistry. The influence of charging of TiO<sub>2</sub> layer on the excited state behavior of CsPbBr<sub>3</sub> NCs was elucidated by probing the charge carrier recombination of CsPbBr<sub>3</sub>/TiO<sub>2</sub> films at different electrochemical biases and under laser pulse excitation.

By employing a narrow electrochemical window between -0.8 to +0.6 V vs. Ag/AgCl we carried out spectroelectrochemical experiments with good reversibility. The relative rate constants measured at different applied potentials showed an interesting trend as we increased the applied bias from -0.6

## DOE Solar Photochemistry Sponsored Publications 2017-2019

1. Hoffman, J. B.; Alam, R.; Kamat, P. V. Why Surface Chemistry Matters for QD–QD Resonance Energy Transfer, *ACS Energy Letters* **2017**, 391-396.
2. Kobosko, S. M.; Jara, D. H.; Kamat, P. V. AgInS<sub>2</sub>–ZnS Quantum Dots: Excited State Interactions with TiO<sub>2</sub> and Photovoltaic Performance, *ACS Applied Materials & Interfaces* **2017**, 9, 33379–33388.
3. Kamat, P. V. Semiconductor Surface Chemistry as Holy Grail in Photocatalysis and Photovoltaics, *Accounts of Chemical Research* **2017**, 50, 527-531.
4. Grigioni, I.; Stampelcoskie, K. G.; Jara, D. H.; Dozzi, M. V.; Oriana, A.; Cerullo, G.; Kamat, P. V.; Selli, E. Wavelength-Dependent Ultrafast Charge Carrier Separation in the WO<sub>3</sub>/BiVO<sub>4</sub> Coupled System, *ACS Energy Letters* **2017**, 1362-1367.
5. Yoon, S. J.; Kuno, M.; Kamat, P. V. Shift Happens. How Halide Ion Defects Influence Photoinduced Segregation in Mixed Halide Perovskites, *ACS Energy Letters* **2017**, 2, 1507–1514.
6. Samu, G. F.; Janáky, C.; Kamat, P. V. A Victim of Halide Ion Segregation. How Light Soaking Affects Solar Cell Performance of Mixed Halide Lead Perovskites, *ACS Energy Letters* **2017**, 2, 1860-1861.
7. Abbas, M. A.; Basit, M. A.; Yoon, S. J.; Lee, G. J.; Lee, M. D.; Park, T. J.; Kamat, P. V.; Bang, J. H. Revival of Solar Paint Concept: Air-Processable Solar Paints for the Fabrication of Quantum Dot-Sensitized Solar Cells, *The Journal of Physical Chemistry C* **2017**, 121, 17658–17670.
8. Draguta, S.; Sharia, O.; Yoon, S. J.; Brennan, M. C.; Morozov, Y. V.; Manser, J. M.; Kamat, P. V.; Schneider, W. F.; Kuno, M. Rationalizing the Light-Induced Phase Separation of Mixed Halide Organic-Inorganic Perovskites, *Nature Communications* **2018**, 8, Article No. 200 (DOI: 10.1038/s41467-017-00284-2).
9. Hoffman, J. B.; Zaiats, G.; Wappes, I.; Kamat, P. V. CsPbBr<sub>3</sub> Solar Cells: Controlled Film Growth through Layer-by-Layer Quantum Dot Deposition, *Chemistry of Materials* **2017**, 29, 9767–9774.
10. Brennan, M. C.; Draguta, S.; Kamat, P. V.; Kuno, M. Light-Induced Anion Phase Segregation in Mixed Halide Perovskites, *ACS Energy Letters* **2018**, 3, 204-213.
11. Scheidt, R. A.; Samu, G. F.; Janáky, C.; Kamat, P. V. Modulation of Charge Recombination in CsPbBr<sub>3</sub> Perovskite Films with Electrochemical Bias, *Journal of the American Chemical Society* **2018**, 140, 86-89.
12. Samu, G. F.; Scheidt, R. A.; Kamat, P. V.; Janáky, C. Electrochemistry and Spectroelectrochemistry of Lead Halide Perovskite Films: Materials Science Aspects and Boundary Conditions, *Chemistry of Materials* **2018**, 30, 561-569.
13. Ravi, V. K.; Scheidt, R. A.; Nag, A.; Kuno, M.; Kamat, P. V. To Exchange or Not to Exchange. Suppressing Anion Exchange in Cesium Lead Halide Perovskites with PbSO<sub>4</sub>–Oleate Capping, *ACS Energy Letters* **2018**, 3, 1049-1055.
14. Abbas, M. A.; Kamat, P. V.; Bang, J. H. Thiolated Gold Nanoclusters for Light Energy Conversion, *ACS Energy Letters* **2018**, 3, 840-854.

15. Samu, G. F.; Scheidt, R. A.; Zaiats, G.; Kamat, P. V.; Janáky, C. Electrodeposition of Hole-Transport Layer on Methylammonium Lead Iodide Film: A Strategy To Assemble Perovskite Solar Cells, *Chemistry of Materials* **2018**, 30, 4202–4206.
16. Kobosko, S. M.; Kamat, P. V. Indium-Rich AgInS<sub>2</sub>–ZnS Quantum Dots—Ag-/Zn-Dependent Photophysics and Photovoltaics, *The Journal of Physical Chemistry C* **2018**, 122, 14336–14344.
17. Ravi, V. K.; Scheidt, R. A.; DuBose, J.; Kamat, P. V. Hierarchical Arrays of Cesium Lead Halide Perovskite Nanocrystals through Electrophoretic Deposition, *Journal of the American Chemical Society* **2018**, 140, 8887–8894.
18. Zhang, X.; Chen, Y.-S.; Kamat, P. V.; Ptasinska, S. Probing Interfacial Electrochemistry on a Co<sub>3</sub>O<sub>4</sub> Water Oxidation Catalyst Using Lab-Based Ambient Pressure X-ray Photoelectron Spectroscopy, *The Journal of Physical Chemistry C* **2018**, 122, 13894–13901.
19. Balakrishna, R. G.; Kobosko, S. M.; Kamat, P. V. Mixed Halide Perovskite Solar Cells. Consequence of Iodide Treatment on Phase Segregation Recovery, *ACS Energy Letters* **2018**, 3, 2267–2272.
20. Scheidt, R. A.; Kerns, E.; Kamat, P. V. Interfacial Charge Transfer between Excited CsPbBr<sub>3</sub> Nanocrystals and TiO<sub>2</sub>: Charge Injection versus Photodegradation, *The Journal of Physical Chemistry Letters* **2018**, 9, 5962–5969.
21. Talavera, C.; Kamat, P. V. Glutathione-capped gold nanoclusters: photoinduced energy transfer and singlet oxygen generation, *Journal of Chemical Sciences* **2018**, 130, 130–143.
22. Samu, G. F.; Scheidt, R. A.; Balog, Á.; Janáky, C.; Kamat, P. V. Tuning the Excited-State Dynamics of CuI Films with Electrochemical Bias, *ACS Energy Letters* **2019**, 702–708.
23. Balog, Á.; Samu, G. F.; Kamat, P. V.; Janáky, C. Optoelectronic Properties of CuI Photoelectrodes, *The Journal of Physical Chemistry Letters* **2019**, 10, 259–264.
24. Muthu, S.; Zaiats, G.; Sridharan, M. B.; Kamat, P. V. Influence of Plasmonic Cu<sub>x</sub>S Interfacing Layer on Photovoltaic Performance of CIZS Quantum Dot Sensitized Solar Cells, *Journal of The Electrochemical Society* **2019**, 166, H3133–H3137.
25. Scheidt, R. A.; Atwell, C.; Kamat, P. V. Tracking Transformative Transitions: From CsPbBr<sub>3</sub> Nanocrystals to Bulk Perovskite Films, *ACS Materials Letters* **2019**, 1, 8–13.
26. Abbas, M. A.; Yoon, S. J.; Kim, H.; Lee, J.; Kamat, P. V.; Bang, J. H. Ag(I)-Thiolate-Protected Silver Nanoclusters for Solar Cells: Electrochemical and Spectroscopic Look into the Photoelectrode/Electrolyte Interface, *ACS Applied Materials & Interfaces* **2019**, 11, 12492–12503.

# Molecular Level Functionalization, Atomically Thin Photoelectrodes, and Protective Coatings Based on Two-Dimensional Materials

Ellen X. Yan, Annelise C. Thompson, Burton H. Simpson, Miguel A. Cabán-Acevedo, Kimberly M. Papadantonakis, Bruce S. Brunshwig, and Nathan S. Lewis  
Division of Chemistry and Chemical Engineering  
California Institute of Technology  
Pasadena, CA 91125

The objective of our work is to understand and control the electrochemistry of two-dimensional (2-D) materials and of interfaces between 2-D materials and photoelectrodes.

## Reductant Activated Functionalization of 1T'-MoS<sub>2</sub>

We have developed reductant activated functionalization of 1T'-MoS<sub>2</sub>.<sup>1</sup> The first steps of the process follow an existing route to functionalization based on exfoliation of MoS<sub>2</sub> via lithium intercalation and reaction with an alkyl halide. We then introduce a one-electron reductant to drive the reaction with the alkyl halide further than achievable by the initial step. The reductant activated functionalization increases the achievable coverage of covalently bound functional groups on MoS<sub>2</sub> relative to other synthetic routes (<25-30% per MoS<sub>2</sub> unit) and enables functionalization by weak electrophiles that are otherwise unreactive with 1T'-MoS<sub>2</sub>.

Figure 1 summarizes our experimental results for functionalization with primary alkyl halides with varied leaving groups (I<sup>-</sup>, Br<sup>-</sup>, or Cl<sup>-</sup>). The functional group coverage increased according to the trend expected for the halide leaving groups, and for each primary halide, the coverage increased as the strength of the

reducing agent was increased. These results (up to 70% coverage per MoS<sub>2</sub> unit) demonstrate a significant increase in coverage compared to functionalization without reductants.

## Photoelectrochemistry of p-Si Coated with 2-D Materials

We have probed the effects of 2-D materials on photoelectrochemical performance by comparing the behavior of H-terminated p-Si(111) with that for p-Si(111) photoelectrodes covered with 2-D materials with significantly different densities of states, graphene (Gr) and hexagonal boron nitride (h-BN).<sup>2</sup> We have also compared macroscale measurements with nanoscale

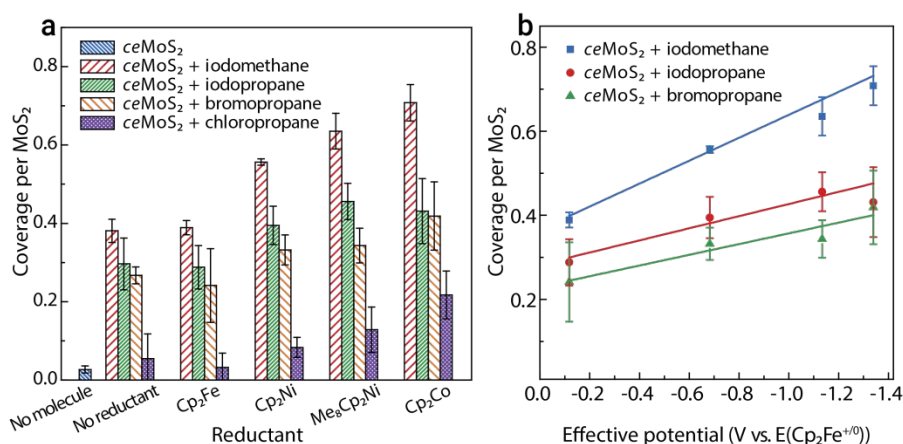


Figure 1. (a) Coverage per MoS<sub>2</sub> for synthesis using varied reductants. (b) Coverage per MoS<sub>2</sub> unit as a function of effective potential for the reductants ferrocene, nickelocene, octamethylnickelocene, and cobaltocene.

measurements performed using scanning electrochemical cell microscopy (SECCM).

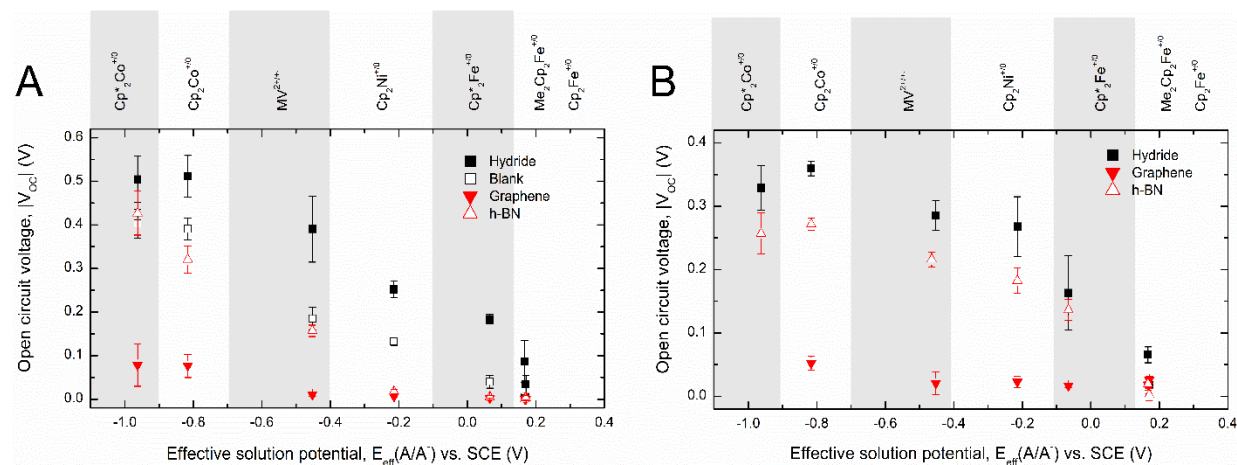


Figure 2. Comparison of  $V_{OC}$  for p-Si, p-Si/Gr, and p-Si/h-BN electrodes versus the effective potential of the contacting solution: (a) bulk measurements, (b) SECCM measurements.

Figure 2a shows how the open-circuit potentials ( $V_{OC}$ ) for p-Si, p-Si/Gr, and p-Si/h-BN contacts change with the effective potential of the contacting electrolyte. Figure 2b shows similar measurements obtained using SECCM. Since the electrodes are made identically, the large difference between the values of  $V_{OC}$  of p-Si/Gr and p-Si/h-BN is attributed to the difference in the density of states of the overlying 2-D material. The limited density of states introduced within the bandgap of silicon by Gr leads to a much more limited range of accessible  $V_{OC}$  values for the p-Si/Gr than the h-BN. The bulk measurements and SECCM measurements demonstrate similar behavior, indicating the SECCM can be used to probe the energetics of these interfaces on the nanoscale.

### DOE Solar Photochemistry Sponsored Publications 2016-2019

1. Yan, E. X.; Cabán-Acevedo, M. A.; Papadantonakis, K. M.; Brunshwig, B. S.; Lewis, N. S., Reductant-Activated High-Coverage Functionalization of 1T'-MoS<sub>2</sub>. *Submitted for publication*.
2. Thompson, A. C.; Simpson, B. H.; Lewis, N. S., Effects of graphene and hexagonal boron nitride coatings on p-Si photoelectrodes. *In preparation*.
3. Wiensch, J. D.; John, J.; Velazquez, J. M.; Torelli, D. A.; Pieterick, A. P.; McDowell, M. T.; Sun, K.; Zhao, X.; Brunshwig, B. S.; Lewis, N. S., Comparative Study in Acidic and Alkaline Media of the Effects of pH and Crystallinity on the Hydrogen-Evolution Reaction on MoS<sub>2</sub> and MoSe<sub>2</sub>. *ACS Energy Letters* **2017**, 2 (10), 2234-2238.
4. Yang, F.; Nielander, A. C.; Grimm, R. L.; Lewis, N. S., Photoelectrochemical Behavior of n-Type GaAs(100) Electrodes Coated by a Single Layer of Graphene. *J. Phys. Chem. C* **2016**, 120 (13), 6989-6995.
5. Velazquez, J. M.; John, J.; Esposito, D. V.; Pieterick, A.; Pala, R.; Sun, G.; Zhou, X.; Huang, Z.; Ardo, S.; Soriaga, M. P.; Brunshwig, B. S.; Lewis, N. S., A scanning probe investigation of the role of surface motifs in the behavior of p-WSe<sub>2</sub> photocathodes. *Energy Environ. Sci.* **2016**, 9, 164-175.
6. Lewis, N. S., Research opportunities to advance solar energy utilization. *Science* **2016**, 351, doi: 10.1126/science.aad1920.

## Photoexcited Charge Carrier Dynamics at Photocatalytic Semiconductor/liquid Interfaces

Zed Xu<sup>d</sup>, Haotian Shi<sup>c</sup>, Bingya Hou<sup>a</sup>, Fengyi Zhao<sup>d</sup>, Tim Lian<sup>d</sup>, and Stephen B. Cronin<sup>a,b,c</sup>

Departments of Electrical Engineering<sup>a</sup>, Physics<sup>b</sup>, and Chemistry<sup>c</sup>  
University of Southern California  
Los Angeles, CA 90089

Department of Chemistry<sup>d</sup>  
Emory University  
Atlanta, GA 30322

Photocatalysis at semiconductor-liquid interfaces represents a complex process, which includes band bending, built-in electric fields, surface recombination of photoexcited carriers, and ultimately charge transfer to the ions in solution, in which the electrostatic fields within the double layer plays an important role. There are loss mechanisms associated with each of these key components in the overall photoconversion efficiency. However, this complex process is often oversimplified in order to provide a basic interpretation of experimental data, largely because simple methods for separating these key components do not yet exist. The objective of this project is to apply spectroscopic tools to study and separate the key components of the photocatalytic process, and to systematically vary precisely-defined photocatalytic structures in order to improve our understanding of energy loss in this important energy conversion system. Specifically, we explore both charge carrier dynamics (CCD) and local electrostatic fields at photocatalytic interfaces using transient reflectance spectroscopy (TRS) and Stark-shift spectroscopy. These techniques probe the CCDs within the semiconductor and the electrostatic fields in the electrolyte double layer, both of which have been elusive experimentally. If successful, these measurements will enable us to divide the solid-state system from the interfacial chemistry.

During the past ten years, photocatalysis on TiO<sub>2</sub>-passivated III-V compounds has demonstrated promising photoconversion efficiencies as high as 14.2%. In this presentation, we report transient reflectance spectroscopy (TRS) of TiO<sub>2</sub>-passivated GaP, which enables us to monitor the free carrier dynamics and interfacial electric fields associated with photoexcitation. By varying the TiO<sub>2</sub> thickness, we observe a drastic increase in the charge carrier kinetics from 200psec in bare GaP to 25psec in TiO<sub>2</sub>-passivated GaP due to a modulation of the built-in electrical fields. The interfacial electric strength at the surface of the GaP is extracted from Franz-Keldysh oscillations observed at the band edge. Performing TRS *in situ* under electrochemical working conditions shows that we can further modulate these free carrier and interfacial field dynamics via the externally applied electrochemical potential. These dynamics are then correlated with the internal photoconversion efficiency (IPCE) of these photoelectrodes over a wide range of potentials, which provides direct evidence that the IPCE is heavily determined by the transiently separated charge carrier dynamics. This study also provides an applicable and powerful method to study similar HER and OER semiconductor electrode photogenerated charge carrier dynamics at ultrafast time scale.

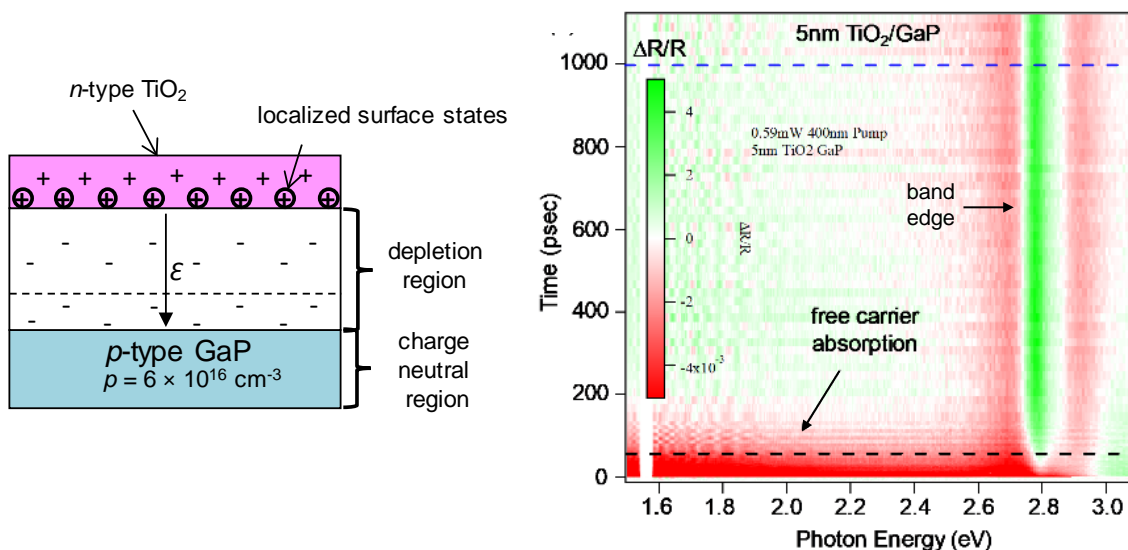


**Figure 1.** (a) Schematic diagram illustrating the TiO<sub>2</sub>/GaP photocatalytic heterostructure and its associated built-in electric field ( $\epsilon$ ) and depletion region. (b) Transient reflectance spectroscopy (TRS) of GaP passivated with 5nm thick TiO<sub>2</sub>.

### DOE Solar Photochemistry Sponsored Publications

1. Hou, B., L. Shen, H. Shi, J. Chen, B. Zhao, K. Li, Y. Wang, G. Shen, M.-A. Ha, F. Liu, A.N. Alexandrova, W.H. Hung, J. Dawlaty, P. Christopher, and S.B. Cronin, *Resonant and Selective Excitation of Photocatalytically Active Defect Sites in TiO<sub>2</sub>*. ACS Applied Materials & Interfaces, **11**, 10351 (2019).
2. Wang, Y., L. Shen, Y. Wang, B. Hou, G.N. Gibson, N. Poudel, J. Chen, H. Shi, E. Guignon, N.C.C.W.D. Page, A. Pilar, J. Dawlaty, and S.B. Cronina, *Hot Electron-driven Photocatalysis and Transient Absorption Spectroscopy in Plasmon Resonant Grating Structures*. Faraday Discussions, DOI:10.1039/C8FD00141C (2018).

# Investigating Ultrafast Dynamics in Solid-State Photocatalytic and Photovoltaic Materials Using Time-Resolved Mössbauer Spectroscopy

Cali Antolini, Melissa A. Smith, Jacqueline Escolastico, Nathan Girard, Xiaoyi Zhang, E. Ercan Alp, Benjamin T. Young, and Dugan Hayes

Physical Sciences Department  
Rhode Island College  
Providence, RI 02908

Department of Chemistry  
University of Rhode Island  
Kingston, RI 02881

Ultrafast optical and X-ray transient absorption experiments have become indispensable techniques for characterizing photophysical and photochemical dynamics of small molecules in solution, but applications of these methods to photocatalytic and photovoltaic thin films are often complicated by artifacts of laser-induced heating that obscure signals from the transient species of interest. To address this pervasive problem, we are developing a novel technique for investigating ultrafast dynamics in the solid state, time-resolved synchrotron radiation Mössbauer (TRSRM) spectroscopy. Like X-ray absorption, Mössbauer spectroscopy is an element-specific probe of oxidation and spin state, covalency, and local geometry, but it also boasts exceptionally narrow (neV) linewidths and only a very weak dependence on temperature. And while Mössbauer spectroscopy has traditionally been limited to only a handful of elements for which a radioisotope source is available, through the use of tunable synchrotron radiation lifts this restriction entirely.

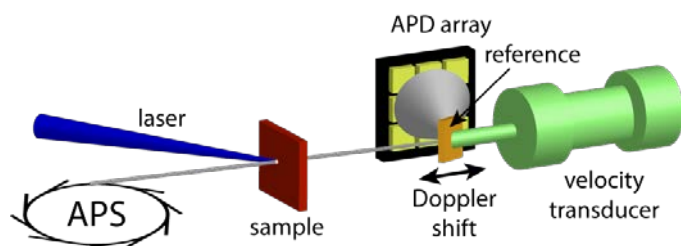


*Fig. 1. Schematic of frequency-domain TRSRM spectrometer.*

Because this technique has never been demonstrated, we prepared samples of three potential materials for our first attempt at the Advanced Photon Source later this year to improve our chance of success. Thin films of photovoltaic  $^{119}\text{Sn}$ -enriched perovskites and photocatalytic  $^{57}\text{Fe}$ -enriched iron titanate and hematite were prepared by oxidation of the isotopically enriched metals to the appropriate precursors followed by solution casting, spin coating, and electrodeposition, respectively. The films were then characterized by steady-state and femtosecond optical absorption and steady-state  $^{57}\text{Fe}$  Mössbauer spectroscopy.

First, we will measure the transient Mössbauer spectrum of lead-free Dion-Jacobson phase two-dimensional and pseudo-two-dimensional  $(4\text{AMP})(\text{FA})_{n-1}\text{Sn}_n\text{I}_{3n+1}$  perovskite thin films ( $n$  is the number of unit cell stacks in each 2D layer). These materials exhibit greatly improved thermal and optical stability and low toxicity relative to the celebrated  $\text{MAPbI}_3$  3D material, remaining undamaged for up to a day under intense ultrafast optical excitation. The low power conversion efficiency ( $\sim 4\%$ ) of devices employing these materials as active layers, however, must be substantially improved to achieve commercial viability. We aim to investigate the photocarrier dynamics in these materials as a first step toward this goal. Despite a lack of resolvable splitting in  $^{119}\text{Sn}$  Mössbauer spectra of inorganic tin halide perovskites, In 2016, Dalpian *et al.* showed that the isomer shift can report on the occupation of both the Sn 5s and 5p orbitals. Thus, we expect to observe a further shift of the nuclear resonance following generation of conduction band electrons, and the magnitude and behavior of this shift in comparison to kinetics observed in optical and

terahertz transient absorption experiments will provide crucial information on both the electronic structure of the material and the carrier migration and relaxation dynamics. By varying the value of  $n$ , we may then determine to what extent these properties are affected by the 2D confinement.

We will first measure the transient Mössbauer spectrum of the photoexcited 2D perovskite films using a time-domain approach, in which the nuclear forward scattering from the optically excited sample is measured as a function of time. While the 23.88 keV  $^{119}\text{Sn}$  nuclear transition has a lifetime 26 ns, the long-lived component of the optical transient absorption spectra of these

materials persists beyond 50 ns. Thus, we expect to obtain the time-averaged picture of the photoexcited material across a 5-75 ns window. If signal to noise is adequate, we will also attempt a frequency-domain experiment that is limited in resolution only by the  $\sim 100$  ps duration of the X-ray pulse. In this scheme, the Mössbauer probe is transmitted through the sample and the absorption spectrum is obtained by integrating the nuclear forward scattering from a reference material as the Doppler velocity is scanned. Optical transient absorption traces for the  $n = 1$  material exhibit a fascinating slow modulation throughout the first 1.5 ns that could be due to 4AMP rotational motion, precession of the octahedral units, or even the propagation and reversal of a thermally induced phase change, and frequency-domain Mössbauer measurements may provide additional information to assist the assignment of this complex behavior.

After concluding our perovskite measurements, we will attempt to measure the transient Mössbauer spectra of  $^{57}\text{Fe}_2\text{Ti}_2\text{O}_7$  (iron titanate) and  $\alpha\text{-}^{57}\text{Fe}_2\text{O}_3$  (hematite) thin films. In the 2000s, Kisch and coworkers showed that iron titanate thin films are capable of reducing  $\text{N}_2$  upon near-UV excitation in the presence of ethanol, but the mechanism of this reaction remains unclear. Hematite, meanwhile is a remarkably stable and inexpensive heterogeneous photocatalyst for water oxidation with absorption extending to the near-IR, but its performance is limited by poor carrier mobility and a quantum efficiency of zero for photon energies below 2 eV. Because both the isomer shift and quadrupole splitting in  $^{57}\text{Fe}$  Mössbauer spectra are usually quite distinct for tri- and divalent iron species,  $^{57}\text{Fe}$  TRSRM will first allow us to determine the nature of the optical transitions in both of these materials *ex situ* and follow the evolution of the (presumably) LMCT states following excitation. While the  $\sim 75$  ps excited state lifetime of hematite will only permit frequency-domain measurements, we will attempt to observe the proposed interfacial photocurrent doubling process in ethanol-immersed iron titanate films via time-domain TRSRM. This will provide the first step toward a complete picture of how solar energy can be used to drive one of the most challenging and important chemical transformations.

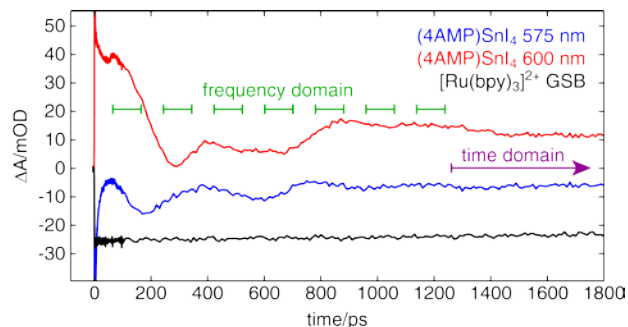


**Fig. 2.** Optical transient absorption spectra of (4AMP)SnI<sub>4</sub> 2D perovskite thin film. The absorption (red) and bleach (blue) features show a strong, slow modulation out to 1.5 ns that does not appear in the [Ru(bpy)<sub>3</sub>]<sup>2+</sup> control (black). Frequency domain TRSRM spectra may be acquired at several delay times in the first few ns, while a time-domain spectrum provides a time-averaged picture over  $\sim 75$  ns.

# Tracking Structures in Solar Fuels Catalysis: In-situ X-ray Characterization of Interfacial Water-Splitting Molecular and Thin-Film Catalysts

David M. Tiede<sup>1</sup>, Gihan Kwon<sup>2</sup>, Alex B. F. Martinson<sup>2</sup>, Tae Wu Kim<sup>1</sup>, Emily Sprague-Klein<sup>1</sup>, Karen L. Mulfort<sup>1</sup>, Oleg G. Poluektov<sup>1</sup>, Lin X. Chen<sup>1</sup>

<sup>1</sup>Chemical Sciences and Engineering and <sup>2</sup>Materials Sciences Divisions  
Argonne National Laboratory, Argonne, IL, 60439

The program in solar photochemistry at the Argonne National Laboratory investigates fundamental mechanisms for coupling light-generated excited-states to multiple-electron, proton-coupled water-splitting and fuels catalysis. The program combines modular synthesis and biomimetic designs with a suite of advanced ultrafast optical, electron paramagnetic resonance, and X-ray analyses that probe structure and function with atomic scale resolution. This presentation will discuss our development of X-ray techniques aimed at the resolution of atomic scale structures that underlie interfacial charge transfer and photo-driven water-splitting catalysis under conditions relevant to photoelectrochemical function. We have developed high surface area TiO<sub>2</sub> semiconductor and ITO and IZO conducting oxide porous assemblies that duplicate oxide-supported dye and catalyst architectures widely used in dye sensitized solar cells (DSSC) and photoelectrochemical (PEC) electrodes, but have been tailored to allow for interfacial X-ray structure characterization.

**1. Thin-Film Metal-Oxide Water Oxidation Catalysts.** Non-noble-metal, thin film oxides are widely investigated as promising catalysts for oxygen evolution reactions (OER). Amorphous cobalt oxide films electrochemically formed in the presence of borate (CoBi) and phosphate (CoPi) share a common cobaltate domain building block, but differ significantly in OER performance that derives from different electron-proton charge transport properties. Here, we use a combination of L-edge synchrotron X-ray absorption (XAS), resonant X-ray emission (RXES), resonant inelastic X-ray scattering (RIXS), resonant Raman (RR) scattering, and high-energy X-ray pair distribution function (PDF) analyses that identify electronic and structural factors correlated to the charge transport differences for CoPi and CoBi. The analyses show that CoBi is composed primarily of cobalt in octahedral coordination, while CoPi contains approximately 17% tetrahedral Co(II), with the remainder in octahedral coordination. Oxygen-mediated  $4p$ - $3d$  hybridization through Co-O-Co bonding was detected by RXES and the inter-site  $dd$  excitation was observed by RIXS

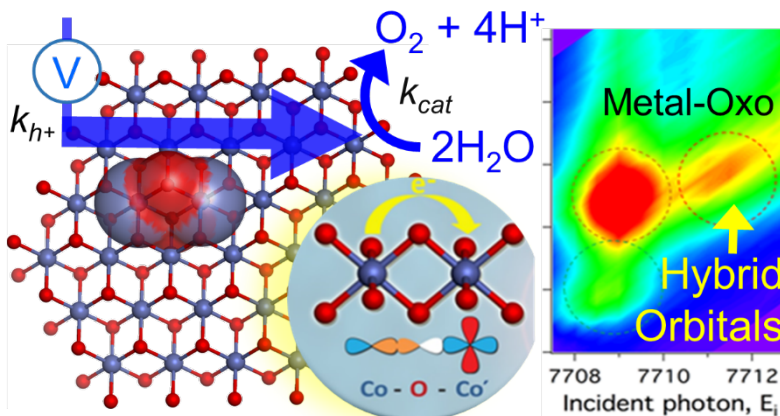


**Figure 1.** Summary of the atomic and electronic structures for the amorphous cobalt oxide formed with a sodium borate electrolyte, CoBi. Catalytic currents are a product of electron, proton transfers and water-splitting rates,  $(k_{cat}k_{h,e})^{1/2}$ . The domain structure shown on the left determined by PDF. The  $d$ - $d$  electronic transitions measured by RIXS on the right, present in CoBi but absent in the analogous CoPi, was identified as an oxygen-mediated metal-to-metal charge transfer band, and was found to correlate with enhanced catalytic reactivity of the films.

in CoBi, but not in CoPi. RR shows that CoBi resembles a disordered layered  $\text{LiCoO}_2$ -like structure while CoPi is amorphous. Distinct domain models in the nanometer range for CoBi and CoPi have been proposed on the basis of the PDF analysis coupled to XAS data. The observed differences provide information on electronic and structural factors that enhance OEC performance. The combined electronic and structural analyses, Figure 1, demonstrate that hole transfer to catalytic sites in amorphous cobalt oxide thin films is the rate-limiting step for electrochemical water-splitting rather than the multi-step catalytic events themselves. The macroscopic catalytic properties of the thin films were found to be correlated to the electronic structures measured at the atomic scale for the metal-oxo cluster domains. These results show the interplay between intrinsic catalytic activity and charge transport properties of semiconductor thin-film catalysts.

**2. In-situ Structure-Function Analysis of Molecular Water Oxidation Catalysts.** Building from the microporous electrodes for *in-situ* X-ray analyses of amorphous oxide thin-film OECs, we

have extended this approach by the development of nano-porous electrode architectures which enable the use of combined PDF and X-ray spectroscopy analyses of coordination structures for molecular photosensitizers and catalysts in solution and when bound to semiconductor oxide surfaces. PDF measurements require PEC oxide supports with sufficiently low background scattering to permit detection of the surface bound complexes. We have found that atomic layer deposition of semiconductor oxides on anodic aluminium oxide templates, AAO, provides a suitable layered, high-surface area architecture. Figure 2 shows

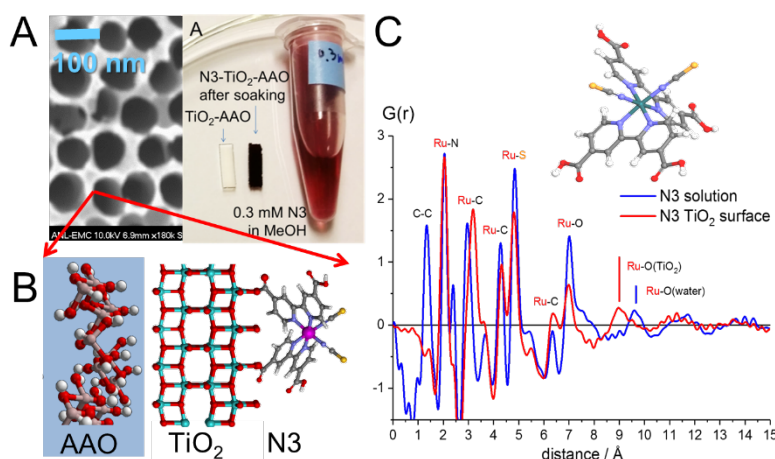


Figure 2 shows resolution of PDF patterns for the N3 dye, cis-bis(isothiocyanato) bis(2,2'-bipyridyl-4,4'-dicarboxylato) ruthenium(II), bound to an amorphous  $\text{TiO}_2$  surface. PDF measurements reveal details on outer sphere ligand structures. Each of the PDF peaks can be assigned to the atom pair distances calculated from crystal and DFT structures. Measurements on ruthenium photosensitizer complexes bound to the  $\text{TiO}_2$  surface resolve distortions in the surface-coordinating ligand structures. On-going work is investigating the correlation between ligand structural distortion and the metal-to-ligand charge-transfer (MLCT) states with interfacial charge injection function.

## DOE Solar Photochemistry Sponsored Publications 2016-2019

1. Microfluidic Electrochemical Cell for in-situ Structural Characterization of Amorphous Thin-Film Catalysts using High-Energy X-ray Scattering. Gihan Kwon, Yeong-Ho Cho, Ki-Bum Kim, Jonathan D. Emery, In Soo Kim, Xiaoyi Zhang, Alex B.F. Martinson, and David M. Tiede, *J. of Synchrotron Radiation* (2019) Accepted.
2. Design Concept for the In Situ Nanoprobe Beamline for the APS Upgrade. Maser, J., Lai, B., De Andrade, V., Bare, S., Bertoni, M., Buonassisi, T., Evans, P., Fenning, D. P., Heald, S., Johnson, C., Lanzirotti, T., Murray, C., Rajh, T., Rose, V., Reininger, R., Shi, X., Stuckelberger, M., Tiede, D., Vogt, S., and Winans, R. (2018) *Microscopy and Microanalysis*, 24(S2), 194-195. doi:10.1017/S1431927618013314.
3. Resolution of Electronic and Structural Factors Underlying Oxygen-Evolving Performance in Amorphous Cobalt Oxide Catalysts, G. Kwon, H. Yang, J.-S. Lee, A. Mane, S. Soltau, L. M. Utschig, A. B. F. Martinson, D. M. Tiede, H. Kim, J. Kim, *J. Amer. Chem. Soc.* (2018) DOI 10.1021/jacs.8b02719.
4. Excitations partition into two distinct populations in bulk Single-Domain-Single-Crystal  $\text{CH}_3\text{NH}_3\text{PbBr}_3$  Perovskites due to polaron formation. Lili Wang, Nicholas P. Brawand, Márton Vörös, Peter D. Dahlberg, John P. Otto, Nicholas E. Williams, David M. Tiede, and Giulia Galli, Gregory S. Engel, (2018) *Adv. Opt. Mater.* **6**, 1700975. <http://dx.doi.org/10.1002/adom.201700975>
5. Domain Structures of Ni and NiFe (Oxy)Hydroxide Oxygen-Evolution Catalysts from X-ray Pair Distribution Function Analysis. Adam S. Batchellor, Gihan Kwon, David M. Tiede, and Shannon W. Boettcher, (2017) *J. Phys Chem. C*, 121, 25421-25429. <http://dx.doi.org/10.1021/acs.jpcc.7b10306>
6. Search for Water-Splitting Catalysts for Global Usage (2017) Fellet, M., and Tiede, D. M. *MRS Bulletin*, 42(3), 190-194. <http://dx.doi.org/10.1557/mrs.2017.35>
7. Butterfly Deformation Modes in a Photoexcited Pyrazolate-Bridged Pt Complex Measured by Time-Resolved X-Ray Scattering in Solution. Haldrup, Kristoffer, Dohn, Asmus O., Shelby, Megan L, Mara, Michael W., Stickrath, Andrew B., Harpham, Michael R., Huang, Jier, Zhang, Xiaoyi, Møller, Klaus B., Chakraborty, Arnab, Castellano, Felix N., Tiede, David M., Chen, Lin X. *The Journal of Physical Chemistry A*, (2016). 120(38): p. 7475-7483.
8. Solution Structures of Highly Active Ir Water Oxidation Catalysts from Density Functional Theory Combined with High-Energy X-Ray Scattering and EXAFS Spectroscopy. Ke R. Yang, Adam J. Matula, Gihan Kwon, Jiyun Hong, Julianne Thomsen, Gary W. Brudvig, Robert H. Crabtree, David M. Tiede, Lin X. Chen, and Victor S. Batista, (2016) *J. Amer. Chem. Soc.*, 138, 5511-5514.

## Nanoscale Probing of Carrier-Selective Catalyst-Semiconductor Contacts in Water-Splitting Photoelectrodes

**Shannon W. Boettcher**, Forrest Laskowski, Michael Nellist, Jingjing Qui, Sebastian Oener, Adrian Gordon

Department of Chemistry and Biochemistry  
University of Oregon  
Eugene, Oregon, 97403

Heterogeneous electrochemical processes, including photoelectrochemical water splitting to evolve hydrogen using electrocatalyst-coated semiconductors, are driven by the accumulation of charge carriers and thus the interfacial electrochemical potential gradients that promote charge transfer. Conventional electrochemical techniques measure/control potentials at the conductive substrate or semiconductor ohmic contact, but are unable to isolate processes and electrochemical potentials at the surface during operation.

This presentation will focus on our recent work demonstrating that the nanoelectrode tip of an atomic-force-microscope (AFM) cantilever can effectively sense the surface electrochemical potential of electrocatalysts *in operando*. Fundamental aspects and capabilities of the probes used, which we originally obtained through collaboration with Bruker (Fig. 1a), will be introduced.

The potential-sensing electrochemical AFM (PS-EC-AFM) technique allows for measurement of the surface potential and thickness-dependent electronic properties of cobalt (oxy)hydroxide phosphate (CoPi) deposited on illuminated photoanodes such as hematite ( $\alpha\text{-Fe}_2\text{O}_3$ ) and bismuth vanadate ( $\text{BiVO}_4$ ). By comparing the electrochemical potential that the catalyst reaches under illumination on a semiconductor with the potential the catalyst reaches on a metallic substrate passing the same current density, we directly show that metal (oxy)hydroxide layers act as both hole collectors and an oxygen-evolution catalysts (Fig. 1b). These results clarify recent conflicting literature results where the (oxy)hydroxide layers were claimed to play a non-catalytic role in enhancing photoelectrochemical performance.

PS-EC-AFM can also be used to spatially resolve

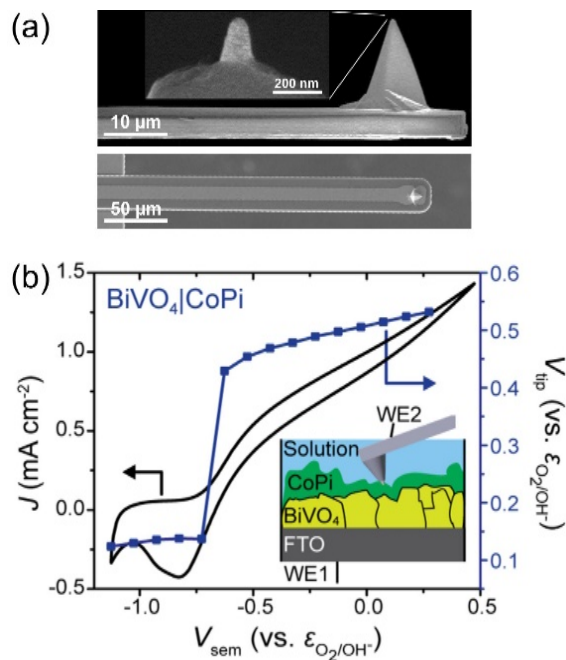


**Fig. 1.** (a) Electron microscope images of EC-AFM tips used in this study. Only the Pt tip of the conductive probe is exposed. (b) Data collected using PS-EC-AFM that shows the catalyst potent ( $V_{\text{tip}}$ ) as a function of the photocurrent flowing through the structure. The photoelectrode is illuminated from the bottom. The data directly shows that, as the photocurrent onset potential is reached in the current-voltage response, the catalyst is rapidly charged with holes. The potential to which the catalyst is charged is exactly that needed to catalytically drive the oxygen evolution photocurrent.

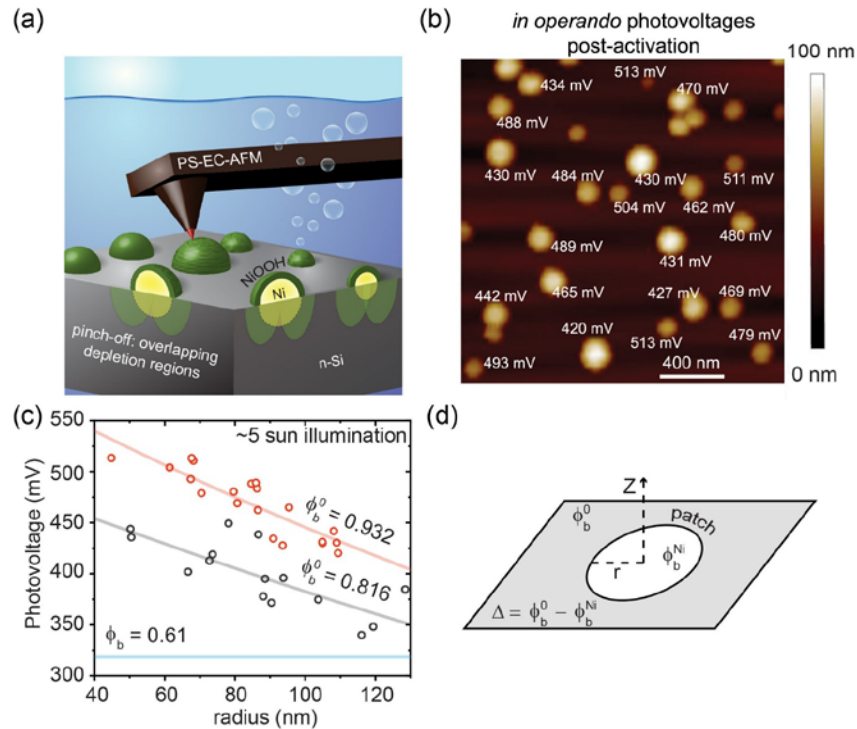


**Fig. 2.** (a) Schematic showing how the AFM tip measures the photovoltage generated at a single nanoparticle/semiconductor photoelectrochemical junction. (b) Spatially resolved photovoltages at each Ni/n-Si interface. (c) Size dependence of measured photovoltage fit to pinch-off model for nanoscale interfaces. (d) Schematic of major variables in the pinch-off model.

charge-separation processes on the nanoscale – critical for understanding how photoelectrochemical assemblies function. Our initial results have focused on a model system consisting of Ni nanoparticles deposited on n-type Si. This system has been studied extensively as a quasi-stable photoanode for water oxidation under neutral to basic conditions. Previous studies have found that the manner in which the Ni is deposited on the Si and how it is electrochemically conditioned dramatically affect the resulting photovoltage output of the electrode. We first measure the Ni nanoparticle / Si interface ex-situ under dry conditions and find that the Ni/n-Si Schottky barrier height ( $\sim 0.6$  eV) and photovoltage ( $\sim 0.3$  V) are low and independent of particle size, consistent with traditional bulk measurements. We then measure the nanoparticle/semiconductor junction under photoelectrochemical conditions (Fig. 2a-2c). Remarkably, we find a significantly increased Ni-nanoparticle/n-Si photovoltage ( $> 500$  mV in some cases) and a strong dependence of that photovoltage on the Ni nanoparticle size. The observed size dependence can be analytically described by the so-called “pinch-off” effect (Fig. 2c and 2d). In this model, a small-barrier-height nanoscale patch (e.g. the Ni-nanoparticle/Si junction) is surrounded by a larger background barrier height. We discover, through a series of careful control measurements, that the background barrier height is set by the oxidized NiOOH that forms in-situ on the Ni nanoparticle surface (Fig. 2a).

These results not only demonstrate the practical utility of PS-EC-AFM to uncover dynamic nanoscale interfacial properties in situ, but also, fundamentally, provide the first direct experimental observation of the pinch-off effect occurring at the single-nanoparticle level. The results are thus broadly important in understanding and designing nanoscale semiconductor contacts.

**DOE Solar Photochemistry Sponsored Publications 2018-2019 (current grant started in 2018)**

1. Qiu, J.; Hajibabaei, H.; Nellist, M. R.; Laskowski, F. A. L.; Oener, S. Z.; Hamann, T. W.; Boettcher, S. W., Catalyst Deposition on Photoanodes: The Roles of Intrinsic Catalytic Activity, Catalyst Electrical Conductivity, and Semiconductor Morphology. *ACS Energy Lett.* **2018**, *3* (4), 961-969.
2. Nellist, M. R.; Qiu, J.; Laskowski, F. A. L.; Toma, F. M.; Boettcher, S. W., Potential-Sensing Electrochemical AFM Shows CoPi as a Hole Collector and Oxygen Evolution Catalyst on BiVO<sub>4</sub> Water-Splitting Photoanodes. *ACS Energy Lett.* **2018**, 2286-2291.
3. Nellist, M. R.; Laskowski, F. A. L.; Qiu, J.; Hajibabaei, H.; Sivula, K.; Hamann, T. W.; Boettcher, S. W., Potential-sensing electrochemical atomic force microscopy for in operando analysis of water-splitting catalysts and interfaces. *Nature Energy* **2018**, *3* (1), 46-52.
4. Laskowski, F. A. L.; Qiu, J.; Nellist, M. R.; Oener, S. Z.; Gordon, A. M.; Boettcher, S. W., Transient photocurrents on catalyst-modified n-Si photoelectrodes: insight from dual-working electrode photoelectrochemistry. *Sustainable Energy & Fuels* **2018**, *2* (9), 1995-2005.
5. Laskowski, F. A. L.; Nellist, M. R.; Qiu, J.; Boettcher, S. W., Metal Oxide/(oxy)hydroxide Overlayers as Hole Collectors and Oxygen-Evolution Catalysts on Water-Splitting Photoanodes. *J. Am. Chem. Soc.* **2019**, *141* (4), 1394-1405.

# Proton-Coupled Electron Transfer Studies of Homogeneous and Heterogeneous Energy Conversion Catalysts

Daniel G. Nocera  
Department of Chemistry and Chemical Biology  
Harvard University  
Cambridge, MA 02138

The activation of small molecules of energy consequence requires the coupling of electrons and protons. Whereas great strides have been made in defining proton-coupled electron transfer (PCET) at molecular centers, an atomistic level of detail for PCET reactions of heterogeneous catalysts is under-developed. Using the knowledge gained from molecular studies as a guidepost, we seek to shed insight on the PCET mechanism of heterogeneous catalysts coupled to light absorbers.

Our efforts have focused on the kinetically challenging activations of water and carbon dioxide. For the latter, we have begun studies to define comprehensively the kinetic and chemical impediments to the CO<sub>2</sub> reduction reaction (CO<sub>2</sub>RR), for which catalyst efficacy is generally characterized by faradaic efficiency, FE(CO). We have examined CO<sub>2</sub>RR on flat and nanostructured gold catalyst surfaces (Fig 1) and provided a general model for potential-selectivity

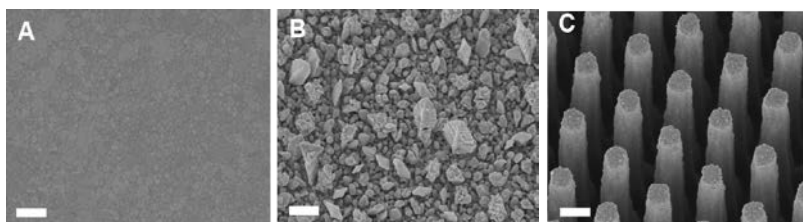


**Fig 1** | SEM image of (A) evaporated gold film (B) electrodeposited gold leaf and (C) electrodeposited gold nanowire array catalysts used for the study of CO<sub>2</sub>RR. Scale bar is 500 nm.

and potential-current relationships for CO<sub>2</sub>RR. From this work, we find that an important yet underappreciated consideration for CO<sub>2</sub>RR is the homogeneous reaction chemistry between CO<sub>2</sub> and water and hydroxide (OH<sup>-</sup>) and the impact of these reactions beyond FE(CO). These homogeneous reactions are not manifested in FE(CO) loss as there is no current associated with them; thus the conversion efficiency of CO<sub>2</sub> may be low despite high FE(CO). This issue is especially relevant for studies seeking to achieve high current densities for CO<sub>2</sub>RR with gas-diffusion electrodes in basic solutions. We find that while a high FE(CO) is obtained, there is poor mass balance as most of the CO<sub>2</sub> is converted to carbonate.

To define the kinetics of the challenging water splitting reaction, we have developed methods to interface oxidic metallates such as CoP<sub>1</sub> with photoabsorbers. We have developed a versatile electrochemical technique that engenders periodically spaced sub-micron catalyst nanostructures on photovoltaic materials over large areas (Fig 2) under a minute with no need for lithography, engendering the technique useful

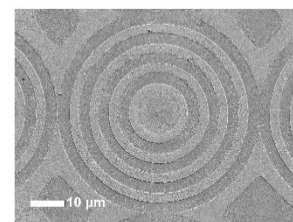


**Fig 2** | Oxidic metallate catalysts formed from a newly developed electrochemical patterning technique.

for high throughput manufacturing of integrated catalysts/photovoltaic materials. Extending methods for catalyst-photoabsorber interfaces, we have modified mesoporous TiO<sub>2</sub>/carbon nitride with CoP<sub>1</sub>. As shown in Fig 3 (left), the system is a competent photoanode for water splitting. Spectroelectrochemistry (Fig 3, right) shows a pronounced feature for the Co(IV) LMCT transition. This transition may be exploited (i) to isolate the key PCET bond-making steps of photodriven water splitting and (ii) to define the kinetics of O–O bond formation by transient absorption studies. To this end, we have designed an electrochemical flow cell to enable ultrafast spectroelectrochemical transient absorption measurements to be undertaken. We are expanding this work to include other oxygen evolution catalysts and to employ additional spectroscopic techniques including impulsive Raman spectroscopy to observe O–O bond formation in real time.

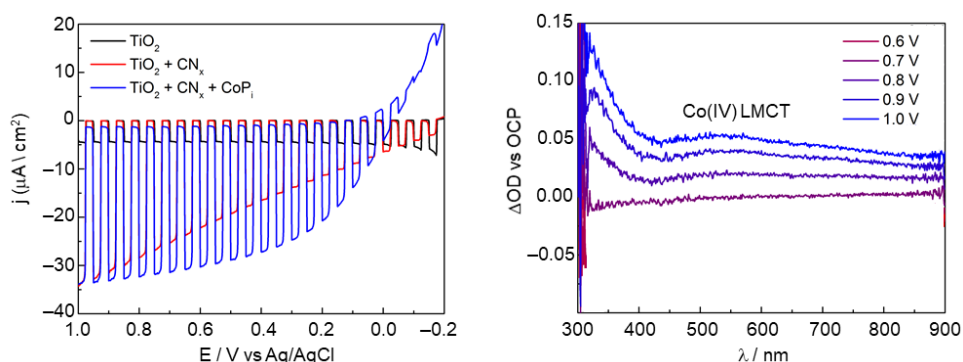


Fig 3 | (left) Mesoporous TiO<sub>2</sub>/carbon nitride/CoP<sub>1</sub> photoanode; irradiation with ~450 nm light drives oxygen evolution. Spectroelectrochemistry of photoanode thin film, showing the Co(IV) LMCT which may be used in transient absorption laser studies to monitor the kinetics of O–O bond formation.

### DOE Solar Photochemistry Sponsored Publications 2016-2019

1. On the Conversion Efficiency of CO<sub>2</sub> Electroreduction on Gold. Benjamin A. Zhang, Cyrille Costentin and Daniel G. Nocera, *Joule*, **2019**, in press.
2. Interplay of Homogeneous Reactions, Mass Transport and Kinetics in Determining Selectivity of the Reduction of CO<sub>2</sub> on Gold Electrodes. Benjamin A. Zhang, Tuncay Ozel, Joseph S. Elias, Cyrille Costentin and Daniel G. Nocera, *ACS Cent. Sci.* **2019**, in press.
3. Ligand Non-innocence in Nickel Porphyrins: Nickel Isobacteriochlorin Formation under Hydrogen Evolution Conditions. Andrew G. Maher, Mengran Liu and Daniel G. Nocera, *Inorg. Chem.* **2019**, in press.
4. Carbon Dioxide Reduction by Iron Hangman Porphyrins. Charles G. Margarit, Christoph Schnedermann, Naomi G. Asimow and Daniel G. Nocera, *Organometallics* **2019**, *38*, 1219-1223.
5. Dual-Phase Molecular-Like Charge Transport in Nanoporous Transition Metal Oxides. Cyrille Costentin and Daniel G. Nocera, *J. Phys. Chem. C* **2019**, *123*, 1966-1973.
6. Oxidative Degradation of Multi-Carbon Substrates by an Oxidic Cobalt Phosphate Catalyst. Thomas P. Keane, Casey N. Brodsky and Daniel G. Nocera, *Organometallics* **2019**, *38*, 1200-1203.

7. Proton-Electron Conductivity in Thin Films of a Cobalt-Oxygen Evolving Catalyst. Casey N. Brodsky, D. Kwabena Bediako, Chenyang Shi, Thomas P. Keane, Cyrille Costentin, Simon J. L. Billinge and Daniel G. Nocera, *ACS Appl. Energy Mater.* **2019**, *2*, 3-12.
8. Lithography-Free Electrochemical Patterning of Conductive Substrates with Metal Oxides. Evan C. Jones and Daniel G. Nocera, *Small* **2018**, *14*, 1801134.
9. Oxygen Activation at a Dicobalt Centre of a Dipyridylethane Naphthyridine Complex. Casey N. Brodsky, Guillaume Passard, Andrew M. Ullman, David E. Jaramillo, Eric D. Bloch, Michael Huynh, David Gygi, Cyrille Costentin and Daniel G. Nocera, *Dalton Trans.* **2018**, *47*, 11903-11907.
10. Oxygen Reduction Reaction Promoted by Manganese Porphyrins. Guillaume Passard, Dilek K. Dogutan, Mengting Qiu, Cyrille Costentin and Daniel G. Nocera, *ACS. Catal.* **2018**, *8*, 8671-8679.
11. Solar-Powered CO<sub>2</sub> Reduction by a Hybrid Biological | Inorganic System. Chong Liu, Brandon E. Colon, Pamela A. Silver and Daniel G. Nocera, *J. Photochem. Photobiol. A Chem.* **2018**, *358*, 411-415.
12. Design of Template-Stabilized Active and Earth-Abundant Oxygen Evolution Catalysts in Acid, Michael Huynh, Tuncay Ozel, Chong Liu, Eric C. Lau and Daniel G. Nocera. *Chem. Sci.* **2017**, *8*, 4779-47794.
13. Hydrogen Evolution Catalysis by a Sparsely Substituted Cobalt Chlorin. Andrew G. Maher, Guillaume Passard, Dilek K. Dogutan, Robert L. Halbach, Bryce L. Anderson, Christopher J. Gagliardi, Masahiko Taniguchi, Jonathan S. Lindsey and Daniel G. Nocera. *ACS Catal.* **2017**, *7*, 3597-3606.
14. In Situ Characterization of Cofacial Co(IV) Centers in Co<sub>4</sub>O<sub>4</sub> Cubane: Modeling the High-Valent Active Site in Oxygen-Evolving Catalyst. Casey N. Brodsky, Ryan G. Hadt, Dugan Hayes, Benjamin J. Reinhart, Nancy Li, Lin X. Chen and Daniel G. Nocera, *Proc. Natl. Acad. Sci. U.S.A.* **2017**, *114*, 3885-3860.
15. Influence of Iron Doping on Tetravalent Nickel Content in Catalytic Oxygen Evolving Films. Nancy Li, D. Kwabena Bediako, Ryan G. Hadt, Dugan Hayes, Thomas J. Kempa, Felix von Cube, David C. Bell, Lin X. Chen and Daniel G. Nocera, *Proc. Natl. Acad. Sci. U.S.A.* **2017**, *114*, 1486-1491.
16. Multielectron, Multisubstrate Molecular Catalysis of Electrochemical Reactions: Formal Kinetic Analysis in the Total Catalysis Regime. Cyrille Costentin, Daniel G. Nocera and Casey N. Brodsky, *Proc. Natl. Acad. Sci. U.S.A.* **2017**, *114*, 11303-11308.
17. Self-Healing Catalysis in Water. Cyrille Costentin and Daniel G. Nocera, *Proc. Natl. Acad. Sci. U.S.A.* **2017**, *114*, 13380-13384.
18. Activation of Electron-Deficient Quinones through Hydrogen-Bond-Donor-Coupled Electron Transfer. Amanda K. Turek, David J. Hardee, Andrew M. Ullman, Daniel G. Nocera and Eric N. Jacobsen, *Angew. Chem. Int. Ed.* **2016**, *55*, 539-544.

19. Nickel Phlorin Intermediate Formed by Proton-Coupled Electron Transfer in Hydrogen Evolution Mechanism. Brian H. Solis, Andrew G. Maher, Dilek K. Dogutan, Daniel G. Nocera and Sharon Hammes-Schiffer, *Proc. Natl. Acad. Sci. U.S.A.* **2016**, *113*, 485–492.
20. X-ray Spectroscopic Characterization of Co(IV) and Metal-Metal Interactions in Co<sub>4</sub>O<sub>4</sub>: Electronic Structure Contributions to the Formation of High-Valent States Relevant to the Oxygen Evolution Reaction. Ryan G. Hadt, Dugan Hayes, Casey N. Brodsky, Andrew M. Ullman, Diego M. Casa, Mary H. Upton Daniel G. Nocera and Lin X. Chen, *J. Am. Chem. Soc.* **2016**, *138*, 11017–11030.
21. Catalytic Oxygen Evolution by Cobalt Oxide Thin Films. D. Kwabena Bediako, Andrew M. Ullman and Daniel G. Nocera, *Top. Curr. Chem.* **2016**, 173-213.
22. Probing Edge Site Reactivity of Oxidic Cobalt Water Oxidation Catalyst. Andrew M. Ullman, Casey N. Brodsky, Nancy Li, Shao-Liang Zheng and Daniel G. Nocera, *J. Am. Chem. Soc.* **2016**, *138*, 4229-4236.
23. Room Temperature Stable CO<sub>x</sub>-free H<sub>2</sub> Production from Methanol with Magnesium Oxide Nanophotocatalysts. Zhengqing Liu, Zongyou Yin, Casandra Cox, Michel Bosman, Xiaofeng Qian, Na Li, Hongyang Zhao, Yaping Du, Ju Li and Daniel G. Nocera, *Sci. Adv.* **2016**, *2*, e1501425/1-8.
24. Oxygen Reduction Catalysis at a Dicobalt Center: The Relationship of Faradaic Efficiency to Overpotential. Guillaume Passard, Andrew M. Ullman, Casey N. Brodsky and Daniel G. Nocera, *J. Am. Chem. Soc.* **2016**, *138*, 2925–2928.

## Exploring the Synergy between Semiconductor Surfaces and Molecular Catalysts for Efficient Solar CO<sub>2</sub> Reduction

Peipei Huang, Sebastian Pantovich, Ethan Jarvis, Christine A. Caputo, and Gonghu Li

Department of Chemistry  
University of New Hampshire  
Durham, NH 03824

A variety of hybrid photocatalysts have been reported using highly active molecular catalysts and robust surfaces. These hybrid systems demonstrated excellent properties in solar fuel production via water splitting and CO<sub>2</sub> reduction. Our project is focused on solar CO<sub>2</sub> reduction using macrocyclic complexes grafted on light-harvesting semiconductor surfaces. We collaborate with Dr. Tijana Rajh of Argonne National Lab to investigate structural features of such hybrid systems that are key to achieving efficient photocatalysis. We hypothesize that covalent linkages with appropriate bend angles and flexibility promote optimized interfacial electron transfer for fuel-producing reactions.

In our research, TiO<sub>2</sub> (bandgap 3.2 eV for anatase) and N-doped Ta<sub>2</sub>O<sub>5</sub> (bandgap 2.4 eV) have been employed as model support for macrocyclic Co(III) catalysts for use in solar CO<sub>2</sub> reduction in the presence of a sacrificial electron donor. A new modular synthetic strategy has been designed to obtain C-functionalized cyclam complexes with the ability to easily modify the flexibility and nature of the anchoring group. Several surface molecular catalysts have been synthesized (**Figure 1**) and are currently being investigated to establish correlation between linkage structure and their photocatalytic performance.

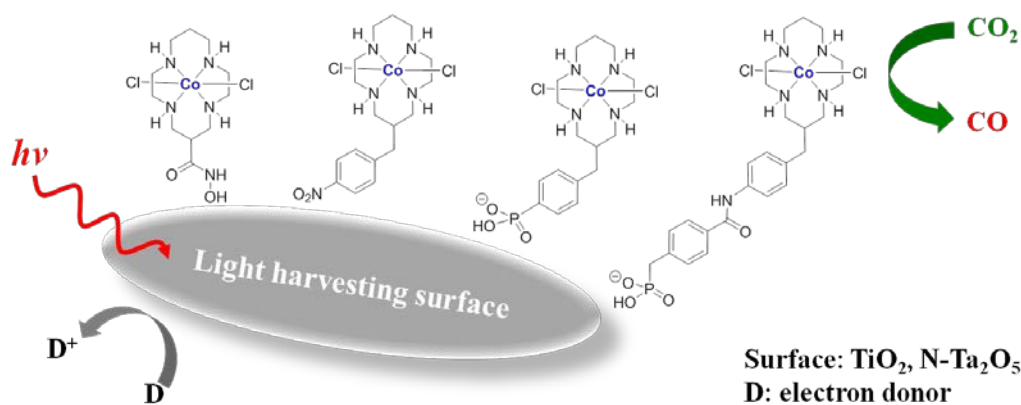


**Figure 1.** Grafting Co(III) cyclam catalysts on semiconductor surfaces for solar fuels.

We also investigated a metal-free semiconductor, graphitic carbon nitride (C<sub>3</sub>N<sub>4</sub>, bandgap 2.7 eV), which demonstrated excellent properties as support for the Co(III) cyclam complexes in visible-light photocatalysis. In a serendipitous discovery, C<sub>3</sub>N<sub>4</sub> was found to be able to activate Co<sup>2+</sup>, without the use of additional ligands, in visible-light CO<sub>2</sub> reduction (**Figure 2**). At relatively low cobalt loadings, single Co<sup>2+</sup> sites on C<sub>3</sub>N<sub>4</sub> demonstrated excellent activity and product selectivity toward CO formation. Inactive cobalt oxides formed at relatively high cobalt loadings but did not alter product selectivity. Further studies with X-ray absorption spectroscopy confirmed the presence of four-coordinated Co<sup>2+</sup> sites on C<sub>3</sub>N<sub>4</sub> and their important role in achieving selective CO<sub>2</sub> reduction (**Figure 3**).

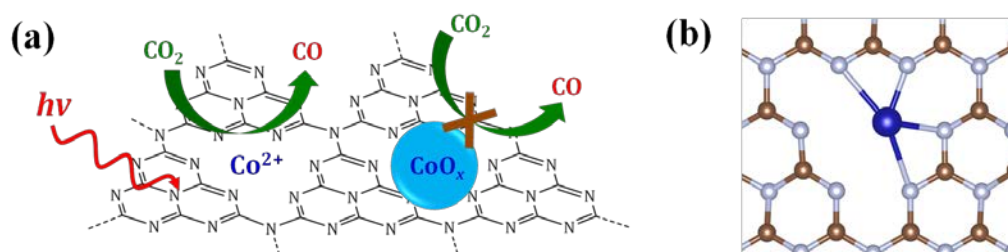


**Figure 2.** (a) Solar CO<sub>2</sub> reduction mediated by single Co<sup>2+</sup> sites on C<sub>3</sub>N<sub>4</sub> in the presence of an electron donor; (b) optimized geometry of a Co<sup>2+</sup> site on C<sub>3</sub>N<sub>4</sub> (courtesy of N. Aaron Deskins).

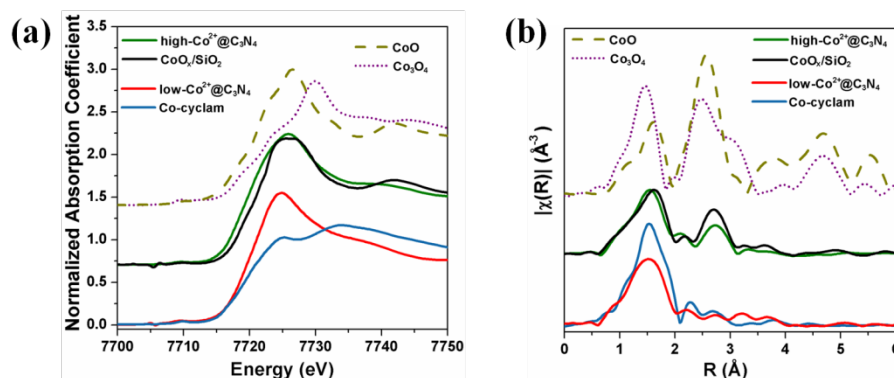


**Figure 3.** (a) Normalized Co K-edge XANES spectra and (b) Fourier transform magnitude of k<sub>2</sub>-weighted Co K-edge EXAFS spectra of different samples: Co(III) cyclam, high-Co<sup>2+</sup>@C<sub>3</sub>N<sub>4</sub>, low-Co<sup>2+</sup>@C<sub>3</sub>N<sub>4</sub>, CoOx/SiO<sub>2</sub>, and two standard cobalt compounds.

Our future work includes investigation of light-induced interfacial electron transfer in the surface molecular catalysts using electron paramagnetic resonance spectroscopy. In addition, we will study molecular functionalities on C<sub>3</sub>N<sub>4</sub> and explore their role in promoting photocatalysis.

This project is co-sponsored by the DOE EPSCoR Program.

### DOE Solar Photochemistry Sponsored Publications 2016-2019

- Huang, P.; Huang, J.; Pantovich, S.; Carl, A.; Fenton, T.; Caputo, C.A.; Grimm, R.; Frenkel, A.; Li, G. "Selective CO<sub>2</sub> Reduction Catalyzed by Single Cobalt Sites on Carbon Nitride under Visible-light Irradiation," *J. Am. Chem. Soc.* **2018**, *140*, 16042-16047.
- Stewart, B.; Huang, P.; He, H.; Fenton, T.; Li, G. "Visible-light Degradation of Orange II using an Fe(II)-terpyridine Complex Grafted onto TiO<sub>2</sub> Surface," *Can. J. Chem.* **2018**, *96*, 890-895.
- Huang, P.; Pantovich, S.; Deskins, N.; Li, G. "Solar CO<sub>2</sub> Reduction using Macrocyclic Co(III) Complexes Directly Deposited on Different Semiconductors," *Appl. Catal. B* (to be submitted).
- Huang, P.; Rajh, T.; Caputo, C.A.; Li, G. "Hybrid Systems for Solar CO<sub>2</sub> Reduction: Combining Molecular Catalysts with Semiconductor Surfaces," *ACS Appl. Energy Mater.* (to be submitted).
- Jarvis, E.; Pantovich, S.; Xu, S.; Li, G.; Caputo, C.A. "Synthetic Approaches to Surface Anchored C-functionalized Co-cyclams," (in preparation).

## Nanostructured Solar Fuel Systems

Pengtao Xu, Yugang C. Li, Zhifei Yan, Jeremy L. Hitt, Tian Huang, John R. Swierk, Nicholas S. McCool, Christopher L. Gray, and Thomas E. Mallouk

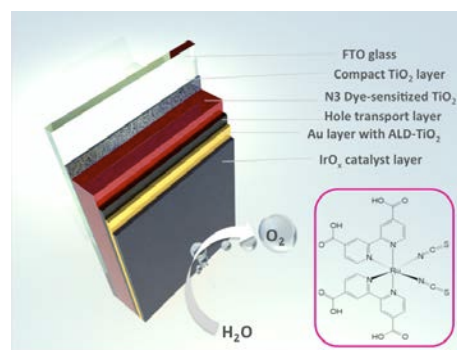
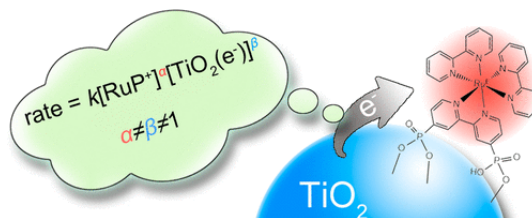
Department of Chemistry, Pennsylvania State University, University Park, PA 16802

This project seeks to achieve a better understanding of photoinduced electron transfer, proton transfer, and electrocatalytic processes that are at the heart of artificial photosynthesis. Our research efforts focus primarily on dye-sensitized water-splitting solar cells, using transient photoelectrochemical techniques to investigate the kinetic origin of the low quantum yield and the transient photocurrent behavior that has been observed in almost all of these cells. Our current work on this problem seeks to “evolve” the structure of the dye-sensitized photoanode and to create new photocathode assemblies for the water-splitting dye cell. A second goal is to address system-level problems in photoelectrochemistry, including proton balance and product crossover, which are relevant both to water-splitting dye cells and to a broader range of solar fuel problems such as CO<sub>2</sub> (photo)electrolysis. A third goal, which is connected to the first two, is to develop new ways to assemble molecules and other nanoscale components into functioning photosystems.

### Kinetics of electron transfer in water-splitting dye cells.

We have carried out a detailed kinetic study of light-induced electron transfer and charge recombination at the anode of the dye-sensitized water splitting cell. This study involved a combination of techniques (electrochemical impedance spectroscopy, intensity-modulated photovoltage spectroscopy, and transient absorbance spectroscopy) with the initial goal of understanding why transient electrochemical and photochemical techniques have reported very different timescales for charge recombination. While the reason for this turned out to be somewhat trivial (the photochemical techniques have involved high fluence, creating higher concentrations of oxidized donors and reduced acceptors that therefore recombine rapidly), a full kinetic analysis at low fluence revealed important findings. First, the rate law describing charge recombination contains fraction reaction orders, and second, when measured by transient techniques such as photovoltage decay, the rate is limited by an RC time constant at the electrode-solution interface. By obtaining the complete rate law we are now able to simulate the performance of the electrode under steady-state current conditions as a function of light intensity and other kinetic variables.

**Solid-state water-splitting dye cells.** We have also explored a new anode architecture for water-splitting dye cells, in which a solid-state hole conductor infiltrates the porous dye-sensitized electrode. In these cells a thin oxide tunneling barrier separates the hole conductor from the water oxidation catalyst, which is exposed to the aqueous electrolyte. This architecture dramatically improves the

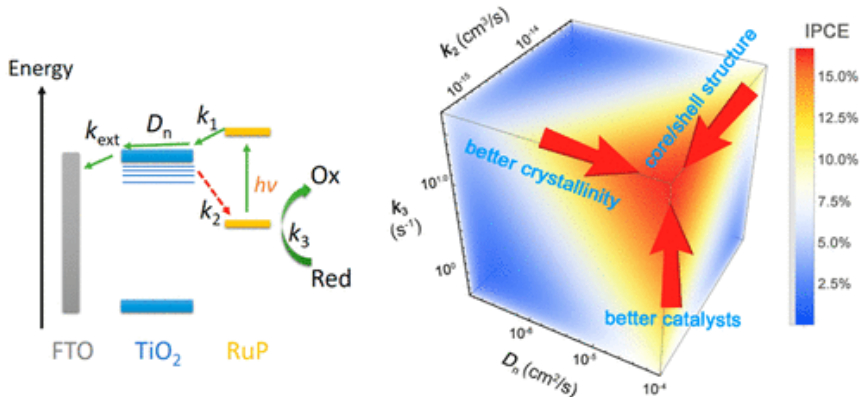


stability of the cell and enables the use of spectrally optimized dyes. We showed experimentally that the oxide tunneling barrier creates a buried junction rather than an adaptive junction. We are now experimenting with other kinds of barrier layers that may create adaptive junctions and may lower the series resistance of the electrode, increasing its efficiency.

### Probing the limits of efficiency in water-splitting dye cells.

We have recently combined intensity-modulated photocurrent spectroscopy (IMPS) with computational modeling to develop a full kinetic model of the aqueous dye-sensitized photoanode, including the transport of electrons in the semiconductor film.

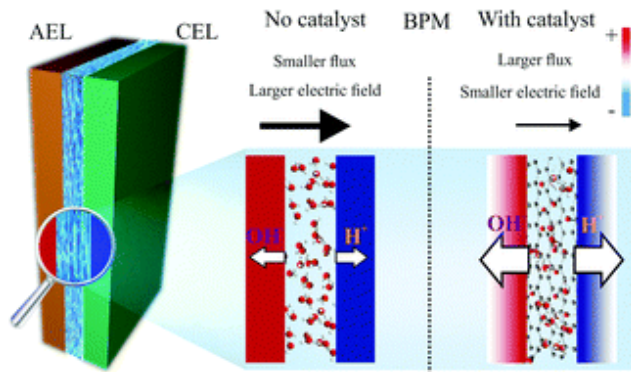
This study enabled us to estimate the incident photocurrent efficiency (IPCE) for water-splitting anodes as a function of charge diffusion, charge recombination, and catalytic water oxidation rates. The results provide guidance as to which parameters are most important for improving photoanode efficiency. Interestingly, there are relatively modest gains to be had by improving the catalyst or electrode structure beyond the best reported literature values. The largest gains will be obtained by improving the photoinjection yield and the spectral response of dyes used in the water-splitting cell.



### CO<sub>2</sub> electrolysis and bipolar membranes.

We have continued our fundamental studies of bipolar membranes that can enable light-driven electrolysis of water and CO<sub>2</sub> using dye-sensitized photoanodes. In one study we measured product crossover rates and verified that the bipolar membrane significantly impedes the crossover of neutral (e.g., methanol) and anionic (e.g., formate) CO<sub>2</sub> reduction products relative to simple anion- or cation-exchange membranes. We also

carried out a study of bipolar membranes containing 2-D and 3-D junctions, using electrochemical impedance spectroscopy to understand the roles of applied voltage and catalysis in accelerating water autodissociation at the cation/anion exchanger interface. This study has provided a prescription for optimizing the structure of bipolar membranes for photoelectrolysis applications. We are now investigating bipolar membranes that contain polymeric weak acids as cation exchange layers (CELs). These membrane structures, which are made by layer-by-layer assembly, are of potential interest for photoelectrolysis cells in which the cathode operates at weakly acidic or neutral pH, where catalytic CO<sub>2</sub> reduction is favorable relative to hydrogen evolution. Membranes that contain gradients of weak acid CELs are also interesting in the context of photochemical proton pumping.



## DOE Solar Photochemistry Sponsored Publications 2016-2019

1. J. R. Swierk, N. S. McCool, C. T. Nemes, T. E. Mallouk, and C. A. Schmittenmaer, "Ultrafast electron injection dynamics of photoanodes for water-splitting dye-sensitized photoelectrochemical cells," *J. Phys. Chem. C*, 120, 5940-5948 (2016).
2. C. Canales, F. Varas-Concha, T. E. Mallouk, and G. Ramirez, "Enhanced electrocatalytic hydrogen evolution reaction: supramolecular assemblies of metalloporphyrins on glassy carbon electrodes," *Appl. Catal. B: Environmental*, 188, 169-176 (2016).
3. Xu, T. J. Milstein, and T. E. Mallouk, "Flat-band potentials of molecularly thin metal oxide nanosheets," *ACS Appl. Mater. Interf.*, 8, 11539-11547 (2016).
4. N. S. McCool, J. R. Swierk, C. T. Nemes, T. P. Saunders, C. A. Schmittenmaer, and T. E. Mallouk, "Proton-induced trap states, injection and recombination dynamics in water-splitting dye-sensitized photoelectrochemical cells," *ACS App. Mater. Interf.*, 8, 16727-16735 (2016).
5. N. S. McCool, J. R. Swierk, C. T. Nemes, C. A. Schmittenmaer, and T. E. Mallouk, "Dynamics of electron injection in SnO<sub>2</sub>/TiO<sub>2</sub> core/shell electrodes for water-splitting dye-sensitized photoelectrochemical cells," *J. Phys. Chem. Lett.*, 7, 2930-2934 (2016).
6. Y. C. Li, D. Zhou, Z. Yan, R. H. Goncalves, D. A. Salvatore, C. P. Berlinguette, and T. E. Mallouk, "Electrolysis of CO<sub>2</sub> to syngas in bipolar membrane-based electrochemical cells," *ACS Energy Lett.* 1, 1149-1153 (2016).
7. P. Xu, N. S. McCool, and T. E. Mallouk, "Water splitting dye-sensitized solar cells," *Nano Today*, 14, 42-58 (2017).
8. J. R. Swierk, N. S. McCool, Jason A. Rohr, S. Hedstrom, S. J. Konezny, C. T. Nemes, P. Xu, V. S. Batista, T. E. Mallouk, and C. A. Schmittenmaer, "Ultrafast proton-assisted tunneling through ZrO<sub>2</sub> in dye-sensitized SnO<sub>2</sub>-core/ZrO<sub>2</sub>-shell films," *Chem. Comm.*, 54, 7971-7974 (2018).
9. D. A. Salvatore, D. M. Weekes, J. He, K. E. Dettelbach, Y. C. Li, T. E. Mallouk, and C. P. Berlinguette, "Gas phase electrolysis of CO<sub>2</sub> to CO in a flow cell," *ACS Energy Lett.*, 3, 149-154 (2017).
10. Z. Yan, L. Zhu, Y. C. Li, R. Wycisk, P. N. Pintauro, M. A. Hickner, and T. E. Mallouk, "The balance of electric field and interfacial catalysis in promoting water dissociation in bipolar membranes," *Energy Environ. Sci.*, 11, 2235-2245 (2018).
11. Y. C. Li, Z. Yan, J. L. Hitt, R. J. Wycisk, P. N. Pintauro, and T. E. Mallouk, "Bipolar membranes inhibit product crossover in CO<sub>2</sub> electrolysis cells," *Adv. Sus. Sys.*, 2, 1700187 (2018).
12. P. Xu, T. Huang, J. Huang, Y. Yan, and T. E. Mallouk, "Dye-sensitized photoelectrochemical water oxidation through a buried junction," *PNAS*, 115 6946-6951 (2018).
13. P. Xu, C. L. Gray, and T. E. Mallouk, "Charge recombination with fractional reaction Orders in water-splitting dye-sensitized photoelectrochemical cells," *J. Am. Chem. Soc.*, 2018, 140, 11647-11654.
14. K. Maeda and T. E. Mallouk, "Two-dimensional metal oxide nanosheets as building blocks for artificial photosynthetic assemblies," *Bull. Chem. Soc. Japan*, 92, 38-54 (2019).
15. P. Xu and T. E. Mallouk, "Charge transfer dynamics in aqueous dye-sensitized photoelectrochemical cells: implications for water splitting efficiency," *J. Phys. Chem. C*, 123, 299-305 (2019).

# Charge Transport and Catalytic Mechanisms for Coupling Visible Light Driven CO<sub>2</sub> Reduction and H<sub>2</sub>O Oxidation across Ultrathin Oxide Membrane

Heinz Frei

Molecular Biophysics and Integrated Bioimaging Division  
Lawrence Berkeley National Laboratory  
Berkeley, CA 9720

Artificial photosystems that accomplish the complete cycle of converting CO<sub>2</sub> and H<sub>2</sub>O to fuel on the shortest possible length scale – nanometers – avoid efficiency degrading ion transport resistance losses and unwanted side reactions while opening up an immense design space for scale-up. We are developing a Co oxide-silica core-shell nanotube array in which each core-shell tube operates as a complete, independent photosynthetic unit.<sup>2,11</sup> The ultrathin silica membrane separates the Co oxide H<sub>2</sub>O oxidation catalyst from light absorber and CO<sub>2</sub> reduction sites, transmits protons, and blocks O<sub>2</sub>. Precise control of electron transport across the insulating silica membrane is accomplished by embedded molecular wires with properly chosen orbital energetics. The goal of our research is to develop synthetic approaches for addressing efficiency challenges of light absorption, charge transfer and catalytic CO<sub>2</sub> reduction by H<sub>2</sub>O on the nanoscale under membrane separation, and elucidate mechanisms of these processes.

*Visible light driven charge separation and transport to catalytic sites across ultrathin oxide nanowall:* Using oxo-bridged heterobinuclear light absorbers such as TiOCo<sup>II</sup> to separate charges by Ti<sup>IV</sup>OCo<sup>II</sup> → Ti<sup>III</sup>OCo<sup>III</sup> metal-to-metal charge-transfer excitation (MMCT), or by analogous ZrOCo units, charge transfer to Co<sub>3</sub>O<sub>4</sub> catalyst across 2.5 nm SiO<sub>2</sub> membrane via embedded molecular wires was explored by transient optical absorption spectroscopy. Hole transfer from transient Co<sup>III</sup> to embedded *oligo p*-(phenylene vinylene) (3 aryl units) is observed within the 8 ns width of the 430 nm photolysis pulse by the 500–620 nm absorption of the radical cation (Figure 1). By selecting wire HOMO and LUMO to impose rectifying electronic property on the TiOCo-wire assembly, charge transfer between the light absorber and wire molecule was achieved without the need for molecularly defined linkage.<sup>13</sup> Combined with our previously observed 250 ps hole transfer from embedded wire to Co<sub>3</sub>O<sub>4</sub> catalyst,<sup>8</sup> the result implies visible light-induced hole transfer from binuclear light absorber to water oxidation catalyst across the silica separation membrane in a few ns or faster. When using ZrOCo light absorber, electron transfer from transient Zr<sup>III</sup> to weakly coordinated pyridine molecule is observed within ns as detected by the transient optical and time-resolved FT-IR spectra of pyridine radical anion

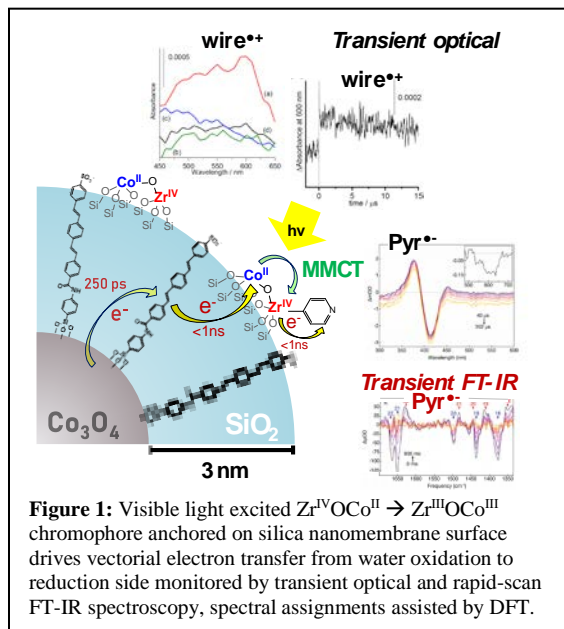
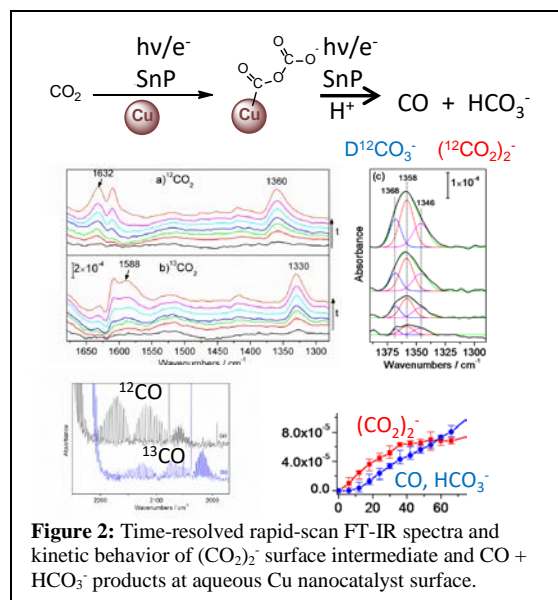


(Figure 1). The unusually long lifetime of 220 ms (room temperature, no sacrificial reagents present) is attributed to spin flip of the excited ZrOCo unit.<sup>14,18</sup>

Orientation and integrity of the silica embedded wires were monitored by polarized FT-IRRAS using planar  $\text{Co}_3\text{O}_4/\text{wire}/\text{SiO}_2$  constructs deposited on Pt nanolayer. Comparison with non-polarized GATR FT-IR spectra of the same sample confirmed perpendicular wire orientation and complete structural integrity after casting into 2.5 nm  $\text{SiO}_2$  by plasma enhanced ALD.

*Developing 2-photon tandem light absorber system incorporated into oxide nanowall:* For incorporating a viable solar light absorption system into the silica membrane, we are utilizing the hierarchical property of the core-shell nanotube geometry by coupling the  $\text{TiOCo}^{\text{II}}$  light absorber ( $\text{H}_2\text{O}$  oxidation side, Figure 1) to a  $\text{ZrOCu}^{\text{I}}$  chromophore with complementary optical absorption anchored on the outside of a second silica nanolayer ( $\text{CO}_2$  reduction side). The LUMO of the  $\text{SiO}_2$ -embedded wire molecules which electronically couple the two tandem light absorbers is energetically positioned between the potential of transient  $\text{Ti}^{\text{III}}$  acceptor and  $\text{Cu}^{\text{II}}$  donor. To this end, *oligo* p-(phenylene vinylene) wire with strongly electron withdrawing nitro and cyano substituents were synthesized based on Knoevenagel condensation approach and electrochemically characterized. The structural integrity and orientation of the new wires upon anchoring and casting into silica were monitored by FT-IRRAS and XPS. Optimization of the electron transport efficiency of the new wires using short circuit photocurrent measurements is in progress.



electrons into Cu nanoparticles in aqueous solution, carbon dioxide dimer radical anion ( $(\text{CO}_2)_2^-$ ) was detected and identified ( $^{12}\text{C}$ : 1632, 1358, 1346  $\text{cm}^{-1}$ ;  $^{13}\text{C}$ : 1588, 1326, 1316  $\text{cm}^{-1}$ ) (Figure 2). A key observation was spontaneous decrease of the intermediate after termination of photosensitized electron injection into Cu accompanied by growth of  $\text{HCO}_3^-$  and  $\text{CO}$ . The spectroscopic observations and kinetic link between  $(\text{CO}_2)_2^-$  intermediate and  $\text{CO}$  product were confirmed by analogous experiments with CdSe nanoparticle photocatalyst that features the same intermediate. The first observation of  $(\text{CO}_2)_2^-$  intermediate points to approaches for rate enhancement of heterogeneous  $\text{CO}_2$  reduction by creating environments that favor this low energy intermediate ( $< 0.3$  V) and offers insights for paths to more deeply reduced products.

*Future work:* Focus will be on the efficiency of electron transfer of the oxide nanowall-embedded 2-photon tandem light absorber system and coupling to the catalysts. Search of catalysts for energy dense products from  $\text{CO}_2$  photoreduction is pursued by exploring bimetallic nanocatalysts and identifying transient reaction intermediates to guide catalyst modifications.

## DOE Solar Photochemistry Sponsored Publications 2016-2019

1. W. Kim, B.A. McClure, E. Edri, and H. Frei. Coupling of Carbon Dioxide Reduction with Water Oxidation in Nanoscale Photocatalytic Assemblies. *Chem. Soc. Rev.* **45**, 3221-3243 (2016).
2. W. Kim, E. Edri, and H. Frei. Hierarchical Inorganic Assemblies for Artificial Photosynthesis. *Acc. Chem. Res.* **49**, 1634-1645 (2016).
3. C.F. Kisielowski, H. Frei, P. Specht, I.D. Sharp, J.A. Haber, and S. Helveg. Revisiting the Structure of Spinel  $\text{Co}_3\text{O}_4$  Catalysts by Controlling Beam-Induced Sample Alterations in the Vacuum of a Transmission Electron Microscope, *Adv. Struct. Chem. Imag.* **2**, 13 (2016).
4. H. Frei. Water Oxidation Investigated by Rapid-Scan FT-IR Spectroscopy. *Curr. Opin. Chem. Eng.* **12**, 91-97 (2016).
5. H.H. Pham, M.J. Cheng, H. Frei, and L.W. Wang. Surface Proton Hopping and Fast-Kinetics Pathway of Water Oxidation on  $\text{Co}_3\text{O}_4(001)$  Surface. *ACS Catal.* **6**, 5610-5617 (2016).
6. R. Alonso-Mori *et al.* Towards Characterization of Photo-Excited Electron Transfer and Catalysis in Natural and Artificial Systems Using XFELs. *Faraday Discuss.* **194**, 621-638 (2016).
7. M. Zhang and H. Frei. Water Oxidation Mechanisms of Metal Oxide Catalysts by Vibrational Spectroscopy of Transient Intermediates. *Annu. Rev. Phys. Chem.* **68**, 209-231 (2017).
8. E. Edri, J.K. Cooper, I.D. Sharp, D. Guldi, and H. Frei. Ultrafast Charge Transfer between Light Absorber and  $\text{Co}_3\text{O}_4$  Water Oxidation Catalyst across Molecular Wires Embedded in Silica Membrane. *J. Am. Chem. Soc.* **139**, 5458-5466 (2017).
9. H. Frei. Coupling of Metal Oxide Nanoparticle Catalysts for Water Oxidation to Molecular Light Absorbers. *J. Energy Chem.* **26**, 241-249 (2017).
10. H. Frei. Photocatalytic Fuel Production. *Curr. Opin. Electrochem.* **2**, 128-135 (2017).
11. E. Edri, S. Aloni and H. Frei. Fabrication of Core-Shell Nanotube Array for Artificial Photosynthesis Featuring Ultrathin Composite Separation Membrane. *ACS Nano* **12**, 533-541 (2018).
12. H. Sheng, M.H. Oh, W.T. Osowiecki, W. Kim, A.P. Alivisatos, and H. Frei. Carbon Dioxide Dimer Radical Anion as Surface Intermediate of Photo-Induced  $\text{CO}_2$  Reduction at Cu and CdSe Nanoparticle Catalysts by Rapid-Scan FT-IR Spectroscopy. *J. Am. Chem. Soc.* **140**, 4363-4371 (2018). Highlighted in *Nature Catal.* **1**, 234 (2018).
13. G. Katsoukis and H. Frei. Heterobinuclear Light Absorber Coupled to Molecular Wire for Charge Transport across Ultrathin Silica Membrane for Artificial Photosynthesis. *ACS Appl. Mater. Interfaces* **10**, 31422-31432 (2018).
14. A.D. Hill, G. Katsoukis, and H. Frei. Photon Induced Electron Transfer from  $\text{ZrOCo}$  Light Absorber to Pyridine Elucidated by Transient Optical and Infrared Spectroscopy. *J. Phys. Chem. C* **122**, 20176-20185 (2018).

15. A. Litke, H. Frei, E.J.M. Hensen, and J.P. Hofmann. Interfacial Charge Transfer in Pt-loaded TiO<sub>2</sub> P25 Photocatalysts Studied by In-Situ Diffuse Reflectance FT-IR Spectroscopy of Adsorbed CO. *J. Photochem. Photobiol. A* **370**, 84-88 (2019).
16. A.P. Palermo, C. Schoettle, S. Zhang, N. Grosso-Giordano, A. Okrut, D.A. Dixon, H. Frei, B.C. Gates, and A. Katz. Dioxygen Reacts on a Silica-Supported Tetrairidium Cluster to Form  $\mu$ - $\eta^1$ : $\eta^1$ -Peroxo Ligands. *J. Am. Chem. Soc.*, submitted
17. H. Liu and H. Frei. Observation of O-O Bond Forming Step of Molecular Co<sub>4</sub>O<sub>4</sub> Cubane Catalyst by Rapid-Scan FT-IR Spectroscopy. *ACS Catal.*, submitted.
18. G. Katsoukis and H. Frei. Ultrathin Oxide Layers for Nanoscale Integration of Light Absorbers, Catalysts and Complete Artificial Photosystems. *J. Chem. Phys.* **150**, 041501 (2019).

## Crystal Packing and Singlet Fission Rates

Paul I. Dron, Dean Antic, Christopher M. Pochas, Eric A. Buchanan, Andrew J. Chomas, Zdenek Havlas, Alexandr Zaykov, Josef Michl  
Department of Chemistry  
University of Colorado  
Boulder, Colorado 80309

Results of a theoretical examination of the effect of crystal packing on singlet fission rate are presented. For a model system (pair of ethylenes) and several known or suspected singlet fission materials (tetracene, cibalackrot, 1,3-diphenylisobenzofuran) we predict molecular pair arrangements that are especially favorable for the rate of singlet fission. The predictions are obtained from an approximate evaluation of squares of singlet fission matrix elements, based on a complete search of all possible pair packing geometries. This is refined by an evaluation of intermolecular contributions to the energy balance of the singlet fission process, used to reoptimize the best geometries, and by an evaluation of biexciton binding energies. Although a consideration of molecular pairs appears to be a useful first step and may be sufficient in some cases, experimental evidence is presented that shows convincingly a need to consider at least three molecules at a time in the future. Evaluation of triplet yields will require an additional evaluation of rates of competing processes, especially charge separation and excimer formation.

## Size Dependent Plasmon Induced Hot Electron Transfer in CdS-Au Nanorods

Tianquan (Tim) Lian  
Department of Chemistry  
Emory University  
Atlanta, Georgia 30022

Plasmonic hot carrier photocatalysis utilizes hot electrons and/or holes generated by plasmon decay to drive catalytic chemical transformations and may offer multiple potential advantages: Plasmonic nanomaterials are outstanding light absorbers; The energetics of hot carriers can be tuned through the choice of metal and morphology; and Plasmonic particles can be coupled with catalytically materials to form antenna-reactor systems. Despite this immense potential, the reported quantum efficiencies of plasmonic photocatalysts are often low and their reaction mechanisms are not well understood. The overall plasmon induced hot electron transfer (ET) processes is composed of sequential steps of hot carrier generation (by plasmon decay) and hot carrier transfer. The plasmon can decay by either intra- or inter- band pathways within the metal, depending on the band structure and size of the particle. For large Au particles, interband pathway dominates the plasmon and generates mostly hot holes in the d band with little energy for the hot electrons in the sp band. Furthermore, the transfer of hot electrons competes with ultrafast electron cooling ( $< 1$  ps). Thus, for the sequential plasmon induced hot ET, both the small initial distribution of hot electrons and competition of hot ET and electron relaxation lead to low hot ET quantum efficiency. In a previous study, we reported that hot ET efficiencies can be improved by plasmon induced interfacial charge transfer transition in Au particles that are coupled strongly with CdSe Nanorods. In this work, we report an alternative approach of improving hot ET efficiency by controlling the size of plasmonic particles.

We investigated how the efficiency of plasmon induced hot electron transfer depends on the size of Au particles in Au-tipped CdS nanorods (Figure 1 inset). As shown in Figure 1, the observed hot ET quantum efficiency increases at smaller particle size. We attribute the size dependence to two factors. First, smaller Au particle sizes relax momentum conservation requirements, increases the contribution of intraband plasmon decay pathway and leads to higher probability of hot electrons above the conduction band edge of CdS. Second, smaller Au particle size also increases the coupling strength with the CdS NR, resulting in faster electron transfer. These factors combined to increase hot ET efficiency at smaller Au particle sizes.

Our finding has identified a promising approach to increase the efficiency of plasmon induced hot electron transfer in CdS/Au heterostructures. Ongoing studies are examining the size dependence of plasmon induced hot electron transfer efficiency in a series of metal/semiconductor heterojunctions in an effort to examine whether this approach is generally applicable and how the efficiency depends on other materials and morphological parameters.

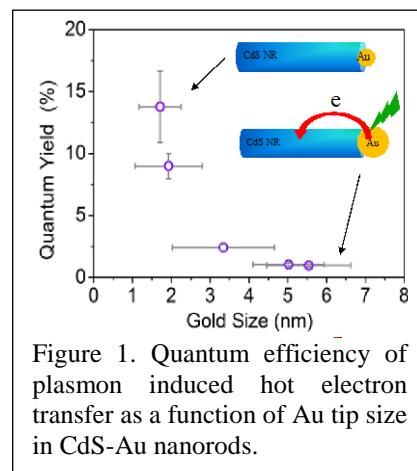


Figure 1. Quantum efficiency of plasmon induced hot electron transfer as a function of Au tip size in CdS-Au nanorods.

## Toward more stable water oxidation catalysts: progress in measurement and synthesis

Aaron G. Nash, Colton Breyer, Brett D. Vincenzini, Thomas Chi Cao, Dale Chatfield, Diane K. Smith, Douglas B. Grotjahn  
Department of Chemistry and Biochemistry  
San Diego State University  
San Diego, CA 92182-1030

We will report on our multipronged approach to measuring and increasing molecular WOC stability: (1) development of a novel electrochemical cell coupled with commercial gas analyzer, (2) use of  $(^{18}\text{O})_2$ -carboxylate WOC as highly sensitive probes of carboxylate decomposition, (3) use of phosphonates and sulfonates as alternatives to carboxylates in WOC.

(1) For electrochemical testing of catalyst efficiency and durability a standard “H”-type electrochemical cell has been constructed using a nafion membrane to separate the two compartments. A large area Pt gauze electrode is used on the  $\text{H}_2$  side and either a large area Pt flag electrode (for calibration) or a RVC electrode (for catalyst testing) is used on the  $\text{O}_2$  side. In addition, a Ag wire pseudo reference electrode and a C fiber microelectrode (for analytical measurement of dissolved  $\text{O}_2$  and catalyst concentration) are located in the anode compartment. Cell caps for both compartments and all electrodes are secured using threaded, gas-tight connections. Detection and quantification of  $\text{O}_2$  and possibly  $\text{CO}_2$  and CO (from electrode oxidation and/or catalyst decomposition) produced from electrolysis is done using a GC specifically designed for trace gas analysis. The instrument contains both TCD and FID detectors along with a methanizer for low level CO and  $\text{CO}_2$  measurement by FID. The details of our new cell will be presented. Gas management is a central challenge. For catalyst testing, initial Faradaic efficiency will be determined after headspace analysis following a short period of electrolysis. Electrolysis will then be resumed and the current monitored. At set periods, the electrolysis will be stopped and the concentration of remaining catalyst determined using the microelectrode followed by measurement of Faradaic efficiency.

(2)  $(^{18}\text{O})_2$ -carboxylate WOCs have been synthesized (e.g. analog of Sun bda catalyst) and apparatus for measuring trace levels of  $\text{C}(^{18}\text{O})_2$  by GC-MS is being developed. Controls show that we can quantitate as little as  $3.0\text{E}-13$  mol of  $\text{C}(^{18}\text{O})_2$  and that injecting air containing 1000 times more  $\text{C}(^{16}\text{O})_2$  and  $8.5\text{E}-6$  mol  $\text{O}_2$  gives no detectable  $\text{C}(^{18}\text{O})_2$  without interference from  $\text{O}_2$ . Because typical WOC amounts in test reactions are on the order of  $5\text{E}-06$  to  $5\text{E}-08$  mol, we expect that our method will be highly sensitive for any loss of  $\text{CO}_2$  from the catalyst. By the time of the meeting we expect to have preliminary results with WOCs.

(3) Previous work has shown that incorporation of a carboxylate on the  $[(\text{terpy})(\text{bipy})\text{Ru}(\text{OH}_2)]$  platform significantly improved catalyst performance. We incorporated a phosphonate monoester in place of the carboxylate. The solid-state structure revealed a water molecule hydrogen bonded to the oxygen bound to the ruthenium, illustrating the potential of the phosphonate to activate incoming water molecules. We are in the process of making a sulfonate ligand and complex for comparison.

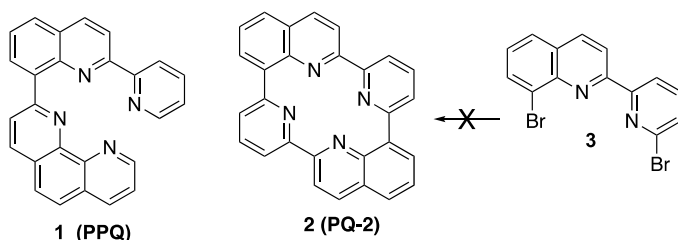
# Photoredox Catalysts Involving Square Planar Cyclotetrapyridyl-type Ligands and their Synthesis Using Metal Template Methodology

Lanka Wickramasinghe, Liubov Lifshits,

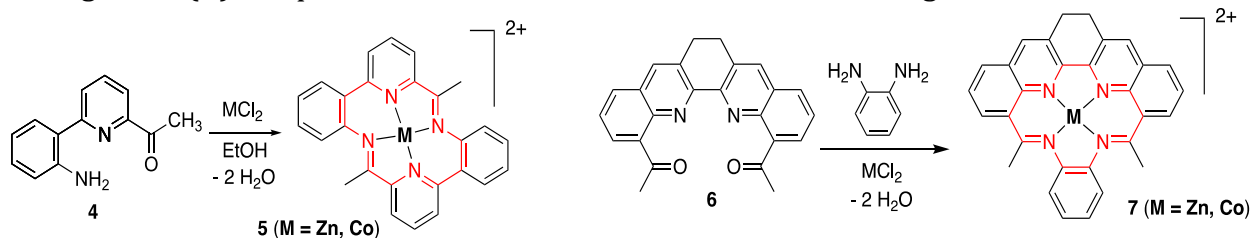
Elamparuthi Ramasamy, Ramesh Deshmukh and Randolph P. Thummel

Department of Chemistry, University of Houston, Houston, TX 77204-54003

Over the past 20 years considerable advances have been made in the development of catalysts for the photochemical decomposition of water into its elements. The most extensively explored homogeneous catalysts involve Ru(II) complexes of polypyridyl ligands. Substituting quinoline for pyridine in many of these ligands led to less strained six-membered chelate rings. An excellent example of this effect is found in 2-(pyridin-2'-yl)-8-(1'',10''-phenanthrolin-2''-yl)-quinoline (**1**, ppq) where the smaller binding cavity accommodates first row transition metals such as Co(II) and Fe(III), providing potent catalysts for the reduction (Co) and oxidation (Fe) of water.



We reasoned that the conversion of **1** into a cyclic tetra-pyridyl-type system such as **2** might improve catalyst performance. Numerous attempts to prepare **2** from **3** by a variety of coupling reactions proved unsuccessful. We then prepared the aminoketone **4** in four steps from readily available 2,6-dibromopyridine. In the presence of either acid or base we did not observe the desired cyclized product, most likely due to nitrogen lone pair repulsion. We used this Lewis base behavior to advantage by invoking the template effect of Zn(II). The resulting diamagnetic complex was readily identified by NMR and the analogous Co(II) complex could be formed in a similar manner using CoCl<sub>2</sub>.



Using the template effect to encourage the double Schiff base condensation, we carried out a similar reaction between the diacetyl 2,2'-biquinoline **6** and *ortho*-phenylene diamine to provide **7** both as its Zn(II) and Co(II) complex. The Co(II) complex of **5** showed catalytic behavior very similar to the Co(II) complex of **1**. The *in situ* generation of these novel tetraaza-macrocycles as their complexes with first row transition metals promises to lead to a wealth of interesting new catalytic chemistry.

## Nanoelectrode as a light guide for photoelectrochemical imaging and collision experiments

Je Hyun Bae, Alexander Nepomnyashchii, Qian Wang, Xiang Wang, and Michael V. Mirkin  
Department of Chemistry and Biochemistry  
Queens College-CUNY  
Flushing, NY 11367

This project is focused on developing high-resolution nanoelectrochemical techniques for probing heterogeneous reactions at single nanoparticles (NP). The scanning electrochemical microscope (SECM) is used as a tool for nanoscale mapping of charge-transfer reactions in the dark and under illumination. We developed an experimental setup for photo-SECM measurements on the nanoscale in which a glass-sealed tip simultaneously serves as a nanoelectrode and a light guide to carry out electrochemical experiments within a microscopic light spot produced on the sample surface.

In Fig. 1, SECM substrate transients (A) and current vs. distance curves (B, C) were obtained using through-tip illumination. High photocurrent density in Fig. 1A and a good agreement between the experimental approach curve and the theory of diffusion-controlled positive feedback in Fig. 1C suggest that the micrometer (or submicrometer) sized spot of light on the substrate surface facing the tip is sufficiently bright. We employed this approach for high-resolution photo-SECM imaging. A similar through-tip illumination setup was also used to prepare *in situ* platinized TiO<sub>2</sub> nanoparticles and measure oxygen evolution current transients produced by single particle collisions with the surface of the conductive SECM substrate.

In the future, the developed technique will be used to map local rates of water splitting on atomic steps and terraces of rutile TiO<sub>2</sub> single crystals and measure the kinetics of hydrogen evolution reaction at individual co-catalyst NPs electrodeposited on the semiconductor photocathode. This approach will be combined with the complimentary feedback-mode SECM imaging to enable size and shape characterization of a NP prior to photo-electrochemical activity measurement.

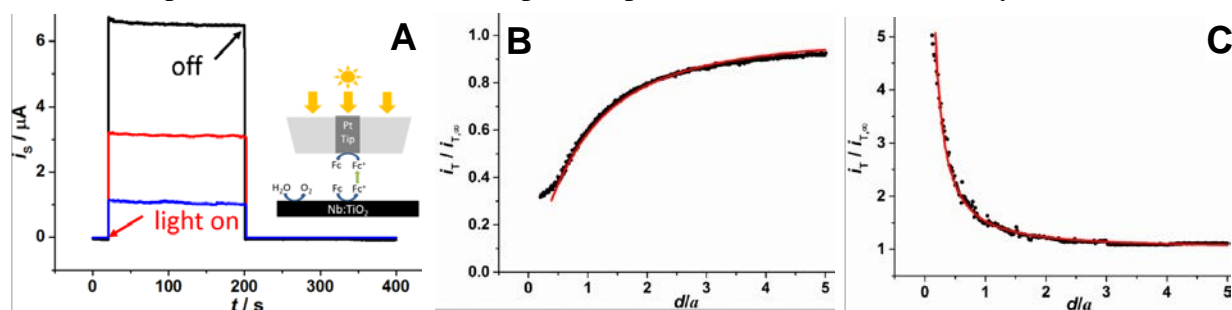


**Fig. 1.** Through-tip illumination in photo-SECM experiments. (A) Photo-transients of ferrocenemethanol and water oxidation at the 0.5% doped Nb:TiO<sub>2</sub> (110) rutile single crystal SECM substrate induced by UV illumination through the 40-nm-radius Pt nanotip as a function of light intensity. Substrate potential was 0 V vs Hg/HgSO<sub>4</sub>. Power density (mW/cm<sup>2</sup>) from top to bottom: 450, 180, and 80. Current-distance curves obtained with a 430-nm Pt tip approaching the same substrate (B) in the dark and (C) under illumination. Experimental data (symbols) was fitted to the theory (solid lines) for (B) negative and (C) positive feedback. The tip potential was -0.5 V, and the substrate potential was 0.2 V vs Hg/HgSO<sub>4</sub>. Solution contained 1 mM ferrocenemethanol (A) or 0.5 mM Fe(CN)<sub>6</sub><sup>3-</sup> in 0.1 M phosphate buffer (pH 7).

## Revealing oxidation mechanisms onto semiconductor surfaces

Xueqiang Zhang,<sup>1,2</sup> Tadashi Ogitsu,<sup>3</sup> Brandon C. Wood,<sup>3</sup> Tuan Anh Pham,<sup>3</sup> Sylwia Ptasinska<sup>1,4</sup>

<sup>1</sup>Radiation Laboratory, University of Notre Dame, Notre Dame, IN 46556, USA

<sup>2</sup>Department of Chemistry and Biochemistry, University of Notre Dame, IN 46556, USA

<sup>3</sup>Quantum Simulations Group, Lawrence Livermore National Laboratory, Livermore, CA 94550, USA

<sup>4</sup>Department of Physics, University of Notre Dame, Notre Dame, IN 46556, USA

A detailed mechanism of oxidation processes on the InP surface, which can reveal a clear correlation between electronic properties, oxide morphology and local chemical oxygen environment is necessary for tuning optoelectronic properties of InP-based photoelectrodes via surface oxidation. Our approach is to take advantage of recent advances in surface-sensitive techniques, i.e., ambient pressure X-ray photoelectron spectroscopy (AP-XPS) to track the dynamic electronic, morphological and chemical structures of the O<sub>2</sub>/InP interface that allows one to access surface reaction processes under ambient conditions. We also integrate our XPS study with DFT calculations and direct spectroscopic simulations [1] which allow to obtain explicit mechanistic understandings of the O<sub>2</sub>/InP(001) interface and the evolution of InP(001) oxidation under different O<sub>2</sub> pressures and temperatures. Our very preliminary results showed that introduction of O<sub>2</sub> onto InP(001) surface at a low temperature regime leads to the exclusive formation of a mixture of In and crosslinked PO<sub>4</sub> via bridging oxygen that aggregates on the surface of InP(001) with monolayer thickness. At higher temperatures, these InPO<sub>x</sub> sub-units begin to be linked amorphously across the surface forming 2-dimensional structure via bridging oxygen atoms. We also observed that different oxidation processes are activated at different O<sub>2</sub> pressures and temperatures (Figure 1), thus they give rise to different types of oxides and we are continuing to investigate them. Therefore, the surface oxide composition may effectively be controlled by leveraging thermodynamics against kinetic considerations.

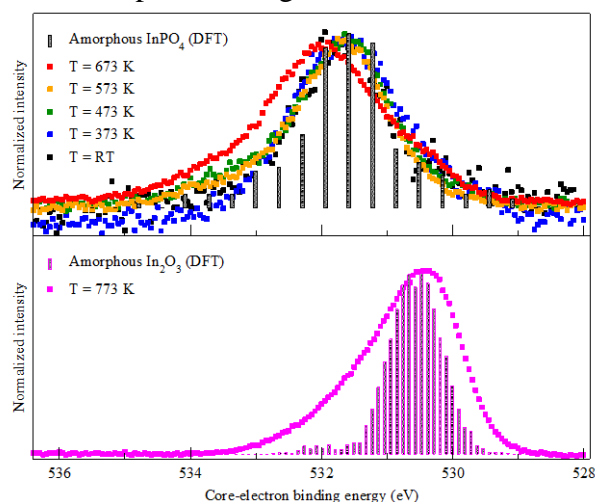


Figure 1. Calculated O 1s BE histogram (bars) and experimental data (symbol envelope). The experimental data is for isobaric measurements as indicated in the figure. The peak heights were normalized to the same between calculation and experiment.

[1] Pham, T. A.; Zhang, X.; Wood, B. C.; Prendergast, D.; Ptasinska, S.; Ogitsu, T. Integrating Ab Initio Simulations and X-ray Photoelectron Spectroscopy: Toward a Realistic Description of Oxidized Solid/Liquid Interfaces. *J. Phys. Chem. Lett.* **2018**, 9, 194-203

# Tuning 2D MoS<sub>2</sub> and WS<sub>2</sub> Catalytic Activity and Optoelectronic Properties

Hanyu Zhang,<sup>1</sup> Jeremy R. Dunklin,<sup>1</sup> Obadiah G. Reid,<sup>1</sup> Sanjini U. Nanayakkara,<sup>1</sup> Seok Joon Yun,<sup>2</sup> Young Hee Lee,<sup>2</sup> Tong Sun,<sup>3</sup> Xiang Wang,<sup>3</sup> Jun Liu,<sup>1</sup> Chuanxiao Xiao,<sup>1</sup> Michael V. Mirkin,<sup>3</sup> Jeffrey L. Blackburn,<sup>1</sup> and Elisa M. Miller<sup>1</sup>

<sup>1</sup>Materials and Chemical Science and Technology, National Renewable Energy Laboratory, Golden, CO 80401

<sup>2</sup>Center for Integrated Nanostructure Physics (CINAP), Institute for Basic Science (IBS) and Department of Energy Science, Sungkyunkwan University, Suwon, 16419 Republic of Korea

<sup>3</sup>Department of Chemistry and Biochemistry, Queens College–CUNY, Flushing, NY 11367 and Graduate Center of CUNY, New York, NY 10016

We aim to control the surface energetics and optoelectronic properties of 2D transition metal dichalcogenides (TMDCs) by tuning the phase, functionalizing the surface, and adjusting defects within the TMDCs. The 2D TMDCs are prepared via a top down (chemical exfoliation) and a bottom up approach (chemical vapor deposition), where the focus is on 2D MoS<sub>2</sub> and WS<sub>2</sub>. For 2D MoS<sub>2</sub>, it is well established that the metallic (1T) phase is better for H<sub>2</sub> generation than the thermodynamically stable semiconducting (2H) phase. To gain additional insight, we employ scanning electrochemical microscopy for high-resolution mapping of surface reactivity for mixed-phase (1T/2H) and pure 2H-only MoS<sub>2</sub> nanosheets. (DOI: 10.1039/c8nh00346g). For mixed-phase MoS<sub>2</sub> nanosheets, we find major differences in reactivity of the two phases, allowing us to locate 1T and 2H regions and directly map the corresponding HER activity. The correlations between the topography/phase and surface reactivity for H<sub>2</sub> generation were further elucidated by additional microscopies, where the lower energy, local workfunction measured on the mixed-phase nanosheets should provide a greater driving force to generate H<sub>2</sub>. Moreover, we find that the stability of the unfunctionalized metallic sheet is highly dependent on the type of 2D layer (chemical exfoliation vs chemical vapor deposition).

While preparing the surfaces of these 2D TMDCs, it is important to consider effects from the atmosphere. The 2D WS<sub>2</sub> layers are highly defective and have emission from defect-bound excitons when exposed to N<sub>2</sub> or O<sub>2</sub> only; however, these defect states are no longer emissive when exposed to H<sub>2</sub>O vapor (Figure 1). We also observe a significant PL increase when the 2D WS<sub>2</sub> is exposed to additional illumination in O<sub>2</sub> or H<sub>2</sub>O vapor environment, which we attribute to reversible, surface reactions.

These drastic changes in PL are anticorrelated with corresponding changes in photoconductivity. We observe that excitation of the defect states leads to greater photoconductivity than exciton excitation. This understanding is critical for interfacing these 2D TMDCs and controlling catalytic reactions.

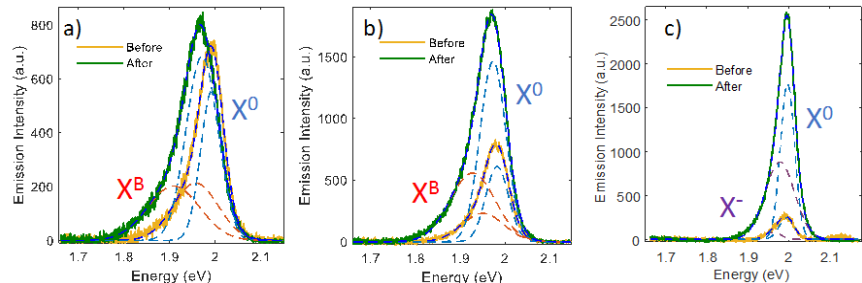


**Figure 1.** WS<sub>2</sub> PL changes under (a) N<sub>2</sub>, (b) O<sub>2</sub>, or (c) H<sub>2</sub>O conditions and 532-nm laser irradiation. PL intensity of monolayer WS<sub>2</sub> before (orange) and after (green) ~1000 s of continuous 532-nm laser illumination on one edge in N<sub>2</sub>, O<sub>2</sub>, and H<sub>2</sub>O, respectively. The dashed traces are Gaussian fits, which are assigned as excitons (X<sup>0</sup>, blue), bound excitons (X<sup>B</sup>, red), or negative trions (X<sup>-</sup>, purple).

## Collaboration between Experiment and Theory for Design of Panchromatic Dyes

Shin Hee Lee, Adam J. Matula, Gongfang Hu, Jennifer L. Troiano, Christopher J. Karpovich, Victor S. Batista, Gary W. Brudvig, Robert H. Crabtree and Charles A. Schmuttenmaer

Department of Chemistry and Energy Sciences Institute  
Yale University, New Haven, CT 06520

The goals of this collaborative research project are the development of high-potential photoanodes for oxidation chemistry and the characterization of interfacial processes for accumulation of multiple oxidizing equivalents on catalytic complexes. We focus on molecular assemblies that are robust under oxidative conditions.

The development of light-harvesting architectures with broad absorption coverage in the visible region continues to be an important research area in the field of artificial photosynthesis. Here, we introduce a new class of ethynyl-linked panchromatic dyads composed of dibenzophenazines coupled *ortho* and *meta* to tetrapyrroles with an anchoring group that can be grafted onto metal oxide surfaces (1). By using theory for the design, the Zn-porphyrin and phenazine units were chosen based on energy alignment of their respective frontier orbitals and an ethynyl group was chosen as the linker to maximize the coupling between the two monomers. Quantum chemical calculations and photophysical measurements of the synthesized materials reveal that the dyads absorb broadly from 300 to 650 nm and exhibit absorption bands different from those of the constituent chromophore units. The phenazine has a low molar absorption coefficient and absorbs to the blue side of the porphyrin's Soret band, but perturbs the porphyrin's electronic structure to create all new bands in the red region of the visible spectrum. The differing regiochemistry of the connection makes a big spectral difference that theory reveals is mainly the result of differences in the degree of dyad planarity that modulates the coupling between the two chromophore units. This strategy to combine theory and experiment (2) may prove useful for the rational design of improved panchromatic dyads. Our future aim is the utilize these and related panchromatic dyes as photosensitizers for water-splitting dye-sensitized photoelectrochemical cells.

1. "Strongly Coupled Phenazine-Porphyrin Dyads: Light-Harvesting Molecular Assemblies with Broad Absorption Coverage", Shin Hee Lee, Adam J. Matula, Gongfang Hu, Jennifer L. Troiano, Christopher J. Karpovich, Robert H. Crabtree, Victor S. Batista and Gary W. Brudvig (2019) *ACS Appl. Mater. Interfaces* **11**, 8000-8008.
2. "Collaboration between Experiment and Theory in Solar Fuels Research", Jacob A. Spies, Ethan A. Perets, Katherine J. Fisher, Benjamin Rudsteyn, Victor S. Batista, Gary W. Brudvig and Charles A. Schmuttenmaer (2019) *Chem. Soc. Rev.* **48**, 1865-1873.

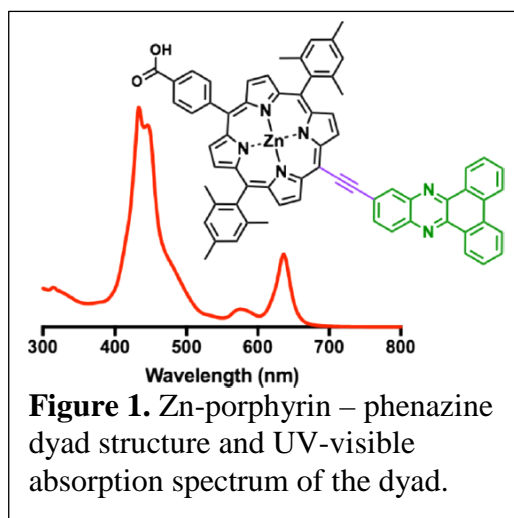


**Figure 1.** Zn-porphyrin – phenazine dyad structure and UV-visible absorption spectrum of the dyad.

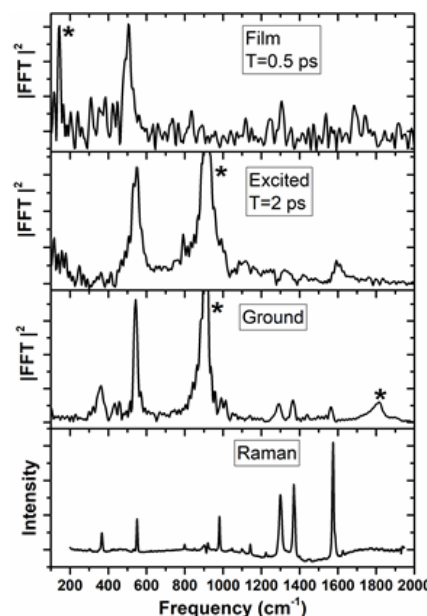
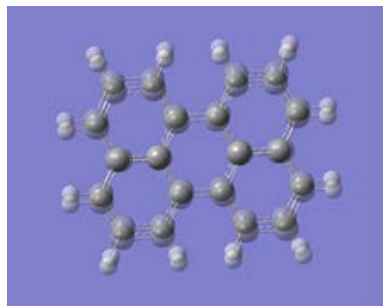
## Electronic and Vibrational Coherence in Heterogeneous Electron Transfer

Lars Gundlach<sup>#+</sup>, Elena Galoppini<sup>‡</sup>, Baxter Abraham<sup>+</sup>, Zhengxin Li<sup>+</sup>, Hao Fan<sup>†</sup>, Ryan Harmer<sup>†</sup>

<sup>†</sup>Chemistry Department, Rutgers University-Newark, Newark, NJ; <sup>‡</sup> Physics Department, Rutgers University-New Brunswick, Piscataway, NJ; Department of <sup>+</sup>Chemistry and <sup>#</sup>Physics, University of Delaware, Newark, DE.

The goal of this project is to measure and distinguish vibrational excitation, vibrational coherence and electronic coherence in heterogeneous electron transfer (HET) by combining appropriate methods and model systems.

Pump-DFWM measurements on the model dye perylene show three major vibrational modes coupled to electronic excitation. The actinic pump was resonant with the absorption maximum of the ground state and the probe was tuned to both the excited state and cation absorption regions. The figure (right) displays vibrational spectra of perylene in THF solution and bound to a colloidal TiO<sub>2</sub> film. The steady-state Raman spectrum is used for comparison with the DFWM measurements. The ground state DFWM spectrum in solution features multiple prominent peaks in the recorded frequency window, in good agreement with the Raman spectrum. The solvent peaks are not subtracted from the DFWM spectra. The excited state was probed at 2 ps, at which point the S<sub>1</sub> state is vibrationally stabilized. Peaks at 550, 800, and 1600 cm<sup>-1</sup> are observed, demonstrating that these vibrations are triggered by photo excitation and persist from the Franck-Condon state. Notably, the 1600 cm<sup>-1</sup> peak is blue shifted from its location at 1570 cm<sup>-1</sup> in the ground state. This vibrational mode is assigned to scissoring at the ring exterior by DFT calculation (figure left), and could indicate a different solvation environment in the pi\* state. The major vibrational mode at 550 cm<sup>-1</sup> is assigned to large scale ring breathing and is not displaced from the ground state. The feature at 880 cm<sup>-1</sup> is enhanced relative to its ground state amplitude. The spectrum was recorded after HET to a TiO<sub>2</sub> surface, at 0.5 ps. The 550 cm<sup>-1</sup> ring breathing mode (left) is evident, even after the oxidation has taken place.



**References (DOE):** (1) B. Abraham, L.G.C. Gego, L. Gundlach, *J. Phys. Chem. C*, **2019**, invited, *submitted*. (2) R.S. Oliboni, H. Yan, H. Fan, B. Abraham, J.P. Avenoso, E. Galoppini, V.S. Batista, L. Gundlach, L.G.C. Rego, *J. Phys. Chem. C*, **2019**, *revision submitted*. (3) M. Konh, C. He, Z. Li, Shi Bai, E. Galoppini, L. Gundlach, A. V. Teplyakova, *Journal of Vacuum Science* **36** **2018** 041404.

## Symmetry Breaking Charge Transfer for Rapid, Long-Lived Charge Separation

Mark Thompson, Stephen Bradforth, Mike Kellogg, Ali Akil, Laura Estergreen  
Department of Chemistry, University of Southern California  
Los Angeles, CA 90089

In this poster we will focus on strategies for achieving ultrafast and long lived photoinduced charge separation. Our approach is to couple strongly absorbing chromophores into orthogonal dimers to drive Symmetry Breaking Charge Transfer (SBCT) and form charge-separated excited states from the initially localized excited (LE) state. The SBCT transition takes place in picoseconds, outcompeting LE state emission and nonradiative decay.

A key design criterion for our SBCT dye studies is that they are capable of chelating to a metal center or being fused into a dimer by linking two dyes at their *meso*-carbons. We have found that for both Zn(dipyrrin)<sub>2</sub> and *meso*-bridged BODIPY and DIPYR compounds (Figure a-c) excitation initially give inter-dye charge separated state on the ps time scale, and that charge separated state lives for 0.5-2 ns. Both BODIPY and DIPYR dimers involve an intermediate partial charge transfer state (PCT) where charge density is pushed onto the *meso*-bridge of the dimer complex as observed in 9,9'-bianthryl.<sup>1</sup> The partial charge transfer state is facilitated by the positive overlap of the LUMO and HOMO orbitals, respectively, at the meso carbons. The HOMO orbital of the BODIPY dimer has a node at the meso carbon, so no such interaction exists, thus the BODIPY dimer is expected to transfer an electron to form the SBCT; for the DIPYR dimers it is the LUMO that has a node and therefore a hole should be transferred to form the SBCT state in this case. Polarization anisotropy measurements are being used investigate the nature of the electron transfer reactions in the three types of dimer studied here.

By adjusting the solvent polarity using different solvents and mixtures the equilibrium between the LE and SBCT states can be shifted to favor either state. Ultrafast transient absorption spectroscopy (TA) was used to probe the kinetics of the charge transfer for Zn(dipyrrin)<sub>2</sub> in solvents where the electron transfer is endergonic, exergonic and has a  $\Delta G$  close to zero (see Figure). It is interesting that even in cases where the CT is endergonic the charge transfer is rapid and the SBCT state plays a significant role in the excited state dynamics. Modeling studies predict a marked structural change in in the SBCT state. Time resolved EXAFS studies are underway (with Prof. Lin Chen at Northwestern) and will be discussed as well.

1. (a) Takaya, T.; Hamaguchi, H.; Iwata, K., *J. Chem. Phys.* **2009**, *130*, 014501 ; (b) Hashimoto, S.; Yabushita, A.; Kobayashi, T.; Okamura, K.; Iwakura, I., *Chem. Phys.* **2018**, *512*, 128-134.

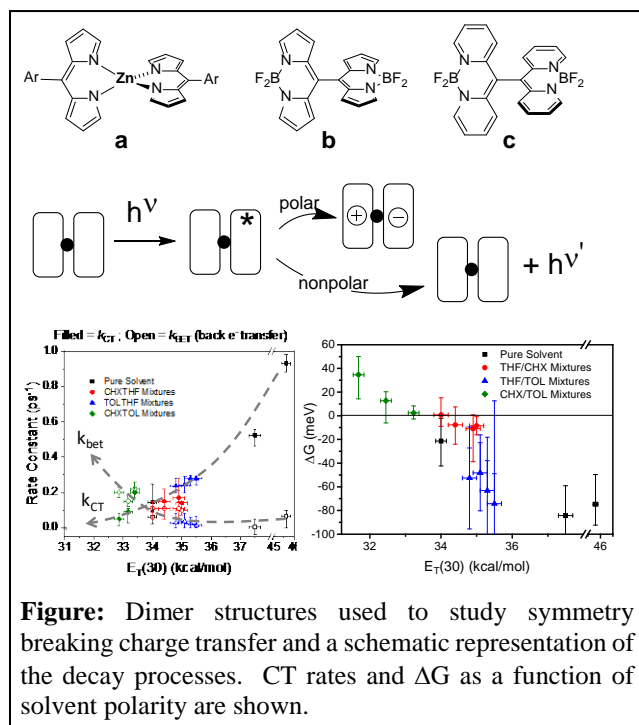


**Figure:** Dimer structures used to study symmetry breaking charge transfer and a schematic representation of the decay processes. CT rates and  $\Delta G$  as a function of solvent polarity are shown.

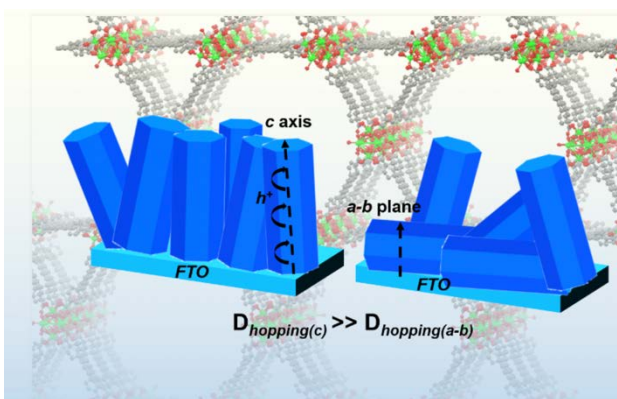
## MOFs as scaffolds for light-harvesting and solar energy conversion: Fundamental studies of energy and charge transport

Joseph T. Hupp  
Department of Chemistry  
Northwestern University  
Evanston, IL 60208

Electrode-integrated metal-organic frameworks (MOFs) are attractive as light-absorbing structures for powering photoelectrochemical cells. MOFs can be constructed in highly chromophoric form by using, for example, porphyrins as linkers between redox-inert, metal-ion-containing nodes. MOFs can also function as periodically structured supports for presenting at high density, catalysts for solar fuels formation. While solar-fuels catalysis itself is outside the scope of this project, the use of MOFs for this purpose and others entailed in photoelectrochemical energy conversion requires that the frameworks transport energy (molecular excitons) as well as charge (electrons, holes, ions) rapidly enough, and over suitably long distances, to match the requirements of other components of energy-converting cells.

This poster will highlight our recent work on extending exciton transport and making the transport highly directional. For these purposes, we make use of automated layer-by-layer (LbL) assembly of MOFs. The LbL approach allows for precise control over MOF film thickness and also allows for controlled, *i.e.* spatially defined, modulation of MOF composition.

The poster also will highlight our recent work on understanding and controlling the factors that define rates of charge-transport, via redox-hopping, within electrode-supported MOFs. As an illustrative example, the poster will describe the basis for highly anisotropic redox-hopping within the platform-MOF, NU-1000. In accord with computational predictions, we find that experimentally determined rates of charge-transport along the *c*-axis of NU-1000 are roughly 100-fold greater than through *a,b*-plane of NU-1000. To measure these rates we devised complementary methods for selectively orienting MOF crystallites on electrodes such that either the *c*-axis or the *a,b*-plane is directed toward the underlying electrode. Notably, the rates of charge-transport along the *c*-axis are more than sufficient to support current or photocurrent densities encountered in photoelectrochemical solar cells, but are less than sufficient when transport is through the *a,b*-plane.



## C-H Bond Formation with CO<sub>2</sub>: Toward Carbon Neutral Fuel Production

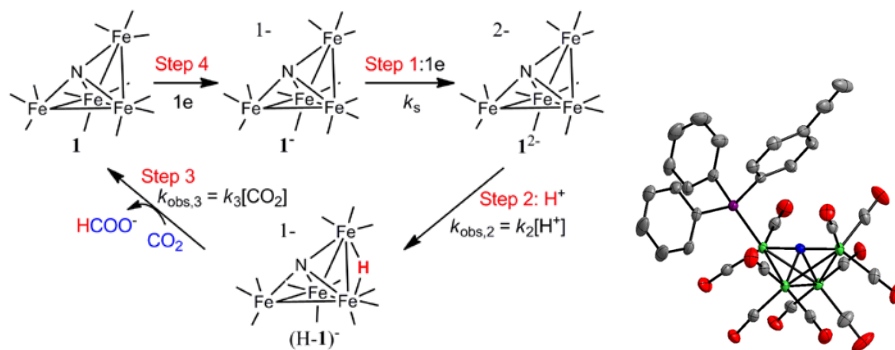
Louise A. Berben, Natalia D. Loewen, Cody R. Carr  
Department of Chemistry  
University of California  
Davis, CA 95616

Selective formate formation from CO<sub>2</sub> using [Fe<sub>4</sub>N(CO)<sub>12</sub>]<sup>-</sup> occurs at -1.2 V vs. SCE in pH 7 buffered water where the catalyst is stable for multiple days. Mechanistic studies of this catalyst have yielded insights into solvent effects on the free energy of the reaction and its relationship to solvent-dependent product selectivity, and also on the solvent dependence of the transition state kinetics where the activation energy is 3 kcalmol<sup>-1</sup> lower in water than in MeCN/H<sub>2</sub>O (95:5).

Our mechanistic studies initially focused on understanding the thermochemical factors that govern product selectivity using correlations between product selectivity and catalyst redox potential, and product selectivity with the hydride donor ability of the intermediate. We determined that (H-1)<sup>-</sup> is the likely hydride intermediate. Based on the correlations between hydride donor ability and redox potential of clusters, along with their known reaction selectivity we have defined potential ranges where catalysts will be most selective for C-H bond formation with CO<sub>2</sub> over H<sub>2</sub> evolution.

Efforts to selectively produce C-H bond-containing products from CO<sub>2</sub> electro-reduction have seen a significant emphasis on understanding the thermodynamics of the catalyst-hydride intermediate relative to those of the desired substrate and optimizing catalysts so that reactions with CO<sub>2</sub> can be favored over those with protons to give H<sub>2</sub>. Those studies, including our own as described in the previous paragraph, have shown that optimal thermochemistry is a necessary but not sufficient criteria

to access fast rates of selective C-H bond formation with CO<sub>2</sub>. The kinetic aspects of reactivity must be better understood. Our recent work particularly highlighted the importance of increasing local [CO<sub>2</sub>] at the active site of a catalyst when working in aqueous solution.



(left) Electrochemical methods probe elementary reaction steps to establish transition state parameters for CO<sub>2</sub> to formate conversion in pH 7 buffer and MeCN/H<sub>2</sub>O (95:5). (right) 1<sup>-</sup> functionalized with alkyne to enable attachment to glassy carbon.

We have also shown that the activity of 1<sup>-</sup> toward formate formation from CO<sub>2</sub> is maintained when it is covalently attached to a glassy carbon electrode.

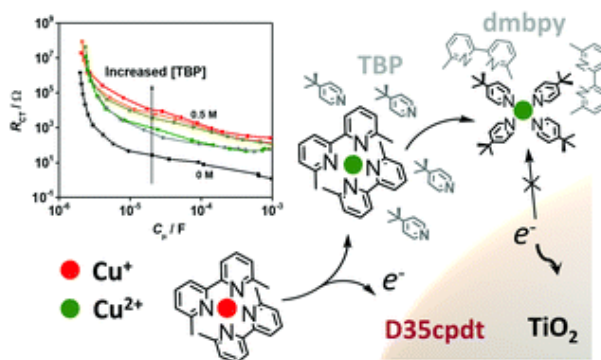
Our ongoing work targets photochemical CO<sub>2</sub> reduction with 1<sup>-</sup>, fast hydride formation using larger cobalt clusters, that have delocalized bonding like heterogeneous materials, and kinetic control of substrate transport to increase the rate limiting chemical steps in fuel formation.

## Dynamics of Liquid and Solid-State Copper Complex Electron Transfer and Transport

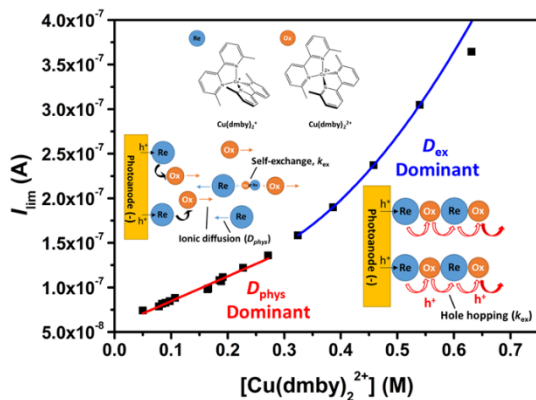
Tea-Yon Kim, Austin L. Raithel, Yujue Wang and Thomas W. Hamann  
 Department of Chemistry  
 Michigan State University  
 East Lansing, MI 48824-1322

The overarching goal of this project is to understand the mechanistic underpinnings of various charge-transfer reactions that control the performance of dye-sensitized solar cells. This poster will describe our recent efforts to understand the behavior of copper-based redox shuttles. One particularly interesting aspect of these copper-based redox shuttles is that they are not only good redox mediators when employed in conventional liquid electrolytes, but have also been shown to operate efficiently in the solid state. We therefore describe both the solution chemistry that results in high performance liquid electrolytes as well as the effect of transitioning from liquid to solid state system on the hole transport mechanism.

The behavior of  $[\text{Cu}(\text{dmbpy})_2]^{2+/+}$  (dmbpy = 6,6'-dimethyl-2,2'-bipyridine) liquid electrolytes are highly dependent on the solvent and additives. Specifically, using a combination of optical spectroscopy, electrochemistry and NMR measurements, we show that the presence of 4-tert-butylpyridine (TBP) in  $[\text{Cu}(\text{dmbpy})_2]^{2+/+}$  electrolytes results in a rapid ligand substitution reaction with the Cu(II) complex to form the  $[\text{Cu}(\text{TBP})_x]^{2+}/[\text{Cu}(\text{dmbpy})_2]^+$  redox species in solution. This ligand exchange results in a negative shift of the redox potential as well as a reduction in the recombination kinetics, reflected in an increase charge transfer resistance,  $R_{ct}$ . This motif will be expanded through investigation of alternative bases as additives in DSSC electrolyte in order to fully exploit the ligand substitution reaction as a means to control the resultant charge-transfer reactions.



When the solvent is removed from the  $[\text{Cu}(\text{dmbpy})_2]^{2+/+}$  liquid electrolytes, there is a conversion to a solid-state hole transport material (HTM). We have used *in-situ* electrochemical analysis to observe a change in the diffusion mechanism of  $[\text{Cu}(\text{dmbpy})_2]^{2+/+}$  that occurs during solidification. As the solidification progresses, the hole transport mechanism of  $[\text{Cu}(\text{dmbpy})_2]^{2+/+}$  changes from ionic ( $D_{\text{phys}}$ ) to electrical ( $D_{\text{ex}}$ ) diffusion, which leads to an increase in the apparent diffusion coefficient. The final high conductivity indicates a large self-exchange rate constant of ca.  $8.7 \times 10^8 \text{ M}^{-1}\text{s}^{-1}$  in the HTM. This in turn could also affect the heterogeneous charge transfer reaction with the electrode, which may control the performance in the cells, which is the subject of ongoing investigations.



## Electron/hole selectivity in organic semiconductor contacts for solar energy conversion

Kira Egelhofer, Ellis Roe, and Mark C. Lonergan  
 Department of Chemistry and Biochemistry  
 University of Oregon  
 Eugene, OR 97403

Solar energy conversion based on charge transfer processes typically involves an absorber that can transfer an electron at one contact and a hole at another either to a chemical species or an electrode. Neither contact is perfect and so the transfer of one type of charge is accompanied by some transfer of the other. Four charge-transfer processes need to be considered. Classic models focus on only one of these as a rate-determining process. When described in terms of an exchange current density ( $J_0$ ), this leads to various forms of the ideal diode equation with a single  $J_0$  describing the current density-voltage,  $J(V)$ , and hence energy conversion properties of the system. We have derived an analytical expression for the current-voltage of a charge transfer based energy conversion system in terms of all four of the relevant interfacial charge transfer processes, in other words, a four  $J_0$  diode equation:

$$J(V) = -\left(J_L + j_{on}^\alpha + j_{op}^\beta\right) + \frac{J_L + j_{on}^\alpha + J_{on}^\beta}{1 + \frac{J_{on}^\beta}{j_{on}^\alpha} e^{-\frac{qV}{kT}}} + \frac{J_L + j_{op}^\beta + J_{op}^\alpha}{1 + \frac{J_{op}^\alpha}{j_{op}^\beta} e^{-\frac{qV}{kT}}}$$

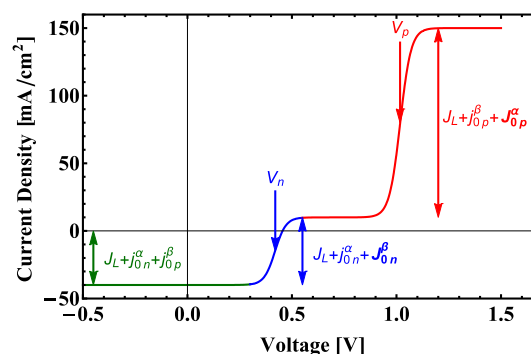


Figure 1: Four  $J_0$  diode equation.

The electron and hole  $J_0$ 's are labelled with  $n$  and  $p$ ; the  $\alpha$  and  $\beta$  mark the two different contacts. The  $J_L$  is the light current. This equation provides a unified picture of how electron/hole selectivity and recombination determine energy conversion properties and how limitations due to carrier collection leads to so-called  $S$ -shaped  $J(V)$  curves and the cross-over of light and dark curves.

In a second branch of our work, we have developed a quantitative approach to measuring contact selectivity and recombination including *in operando*.

The approach is based on making a third contact to an interdigitated back contact solar cell. The impact of this third contact on the short-circuit current ( $I_{sc}$ ) of the cell is a measure of recombination and the relative open-circuit voltage it develops between the other electron and hole selective contacts ( $V_N - V_P$ ) is a measure of selectivity. We have used this platform to demonstrate how the selectivity and recombination of interfacial layer modified contacts changes during operation.

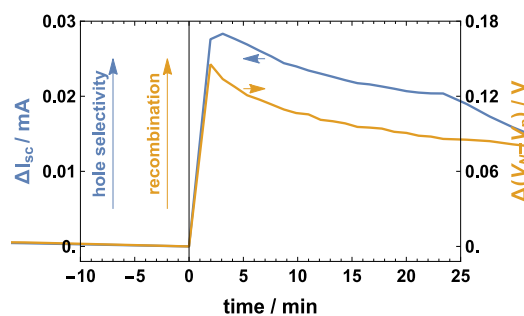


Figure 2. Transient change in selectivity and recombination of an interfacial layer modified contact in response to a potential step.

# Electrochemically and Plasmonically Modifying the Interfacial Thermodynamics, Excitonic and Charge Transfer Kinetics of 2D Transition Metal Dichalcogenides for (Photo)electrochemical Catalysis

G. Michael Carroll, Jeremy Dunklin, Aaron Rose, Hanyu Zhang, Elisa M. Miller, Nathan R. Neale and Jao van de Lagemaat  
 Chemistry and Nanoscience Center  
 National Renewable Energy Laboratory  
 Golden, Colorado 80401

In this study, we investigate the control of (photo)catalytic fuel forming reactions in two-dimensional transition metal dichalcogenide (TMDC) systems using electrical, optical, and plasmonic modulation of excitonic and electronic states using spectroelectrochemistry in-situ Raman spectroscopy, and ultrafast spectroscopy. Few-layer MoS<sub>2</sub> and WS<sub>2</sub> were studied in conditions relevant to their use in (photo)electrochemical water splitting and the exciton and charge carrier populations and energy shifts were studied. The applied electric field under these conditions causes uniaxial tensile strain indicating strong structural changes of the (photo)electrocatalyst. We also show that electron injection into the conduction band is coupled with a red-shift of the exciton resonance and that band gap reduction and modification of electron injection rates occur under photoelectrochemical hydrogen evolution conditions (Fig. 1). These observations do not follow the classical description of the free-energy of charge transfer ( $\Delta G_{CT}$ ) controlling the transfer rate and have strong implications for the scientific understanding of (photo)catalytic fuel forming reactions using two-dimensional.

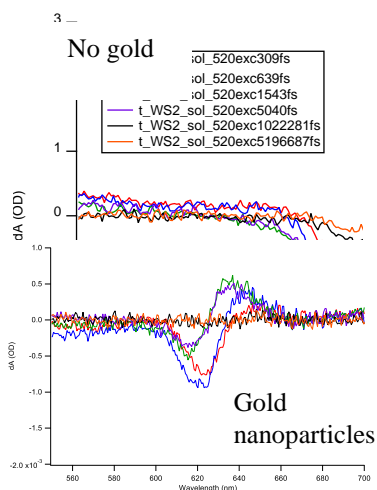


Fig. 2 Transient absorbance of WS<sub>2</sub> decorated with gold nanoparticles in water excited at the B-exciton shows strong change in dynamics from a 100ps to a 1ps lifetime indicating possible hot carrier transfer. Excitation at the A exciton does not show a change in kinetics.

enabled both from directly growing plasmonic nanoparticles on the TMDCs or by depositing TMDCs directly on metal substrates that are engineered to generate plasmon polaritons. We show this coupling permits both manipulation of the energy levels and dynamic changes related to hot carrier generation and transfer. Use of these effects in water splitting systems is investigated.

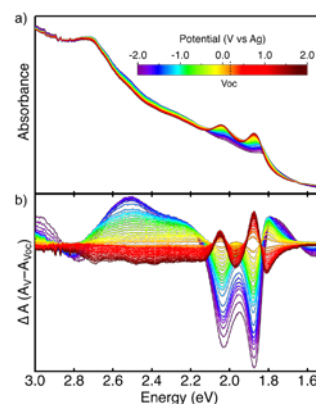


Fig. 1. Spectroelectrochemistry spectra of  $\langle N \rangle = 3$  ML MoS<sub>2</sub> on FTO in 0.1 M [Bu<sub>4</sub>N][PF<sub>6</sub>] acetonitrile electrolyte. a) linear absorbance, b) difference spectra wrt to open circuit at 0.1 V vs Ag/AgCl)

We also study the photoexcited dynamics of TMDCs coupled to plasmonic systems that can generate active polariton states that modify the energetics and dynamics of photo(electro)chemical reactions on the TMDCs (see Fig. 2). Such systems are shown to enable overall photo driven water splitting from TMDC systems that normally can't energetically. The coupling to plasmons is

We also study the photoexcited dynamics of TMDCs coupled to plasmonic systems that can generate active polariton states that modify the energetics and dynamics of photo(electro)chemical reactions on the TMDCs (see Fig. 2). Such systems are shown to enable overall photo driven water splitting from TMDC systems that normally can't energetically. The coupling to plasmons is

## Escape and Recombination of Delocalized Charge in Nonpolar Media

Jack Burke, Madison Jilek, Jake Keiper, Matthew Bird  
Chemistry Division  
Brookhaven National Laboratory  
Upton, NY 11973

Donor (D) – Acceptor (A) interfaces in molecular films enable tightly bound excitons to be separated into charge pairs, but they also introduce new energy loss pathways back to the ground state. We use a combination of pulse radiolysis, microwave conductivity and DC conductivity to investigate the fundamental steps of charge recombination and escape involving highly conjugated molecules in nonpolar media with a focus on the role of delocalization and the spin of CT states.

To investigate the role of *interchain* delocalization on the energetics of charge transfer and escape we studied ground state doping of a model system of aggregated poly(3-hexylthiophene) (nw-P3HT) in toluene. In this medium ( $\epsilon_r = 2.38$ ), the electron acceptor F<sub>4</sub>TCNQ only p-dopes the aggregated chains but does not dope single chains due to a lower oxidation potential from increased delocalization. The standard free energy change for the charge transfer to form an ion pair involving the aggregate was found to be  $\Delta G_{et}^\circ = -0.21$  eV. Using DC conductivity, the escape of ion pairs to free ions was characterized and the dissociation constant was found to be  $K_d^\circ = 1 \times 10^{-8} \pm 50\%$  ( $\Delta G_d^\circ = 0.48 \pm 0.05$  eV). For small molecular ions we would expect  $K_d^\circ \ll 1 \times 10^{-12}$ . Such a large  $K_d^\circ$ , for ions in such a low polarity medium is surprising and could reflect the interchain delocalization of the hole. The energetics of this particular system in toluene enables determination of both  $\Delta G_{et}^\circ$  and  $\Delta G_d^\circ$ , giving the overall free energy change from the two neutral species to completely separated ions in nonpolar media. This is not possible with CV. It is endergonic by  $+0.27 \pm 0.05$  eV in contrast to  $-0.6$  eV estimated from reported HOMO LUMO differences, illustrating the challenges that persist in determining such energetics in the relevant environments.

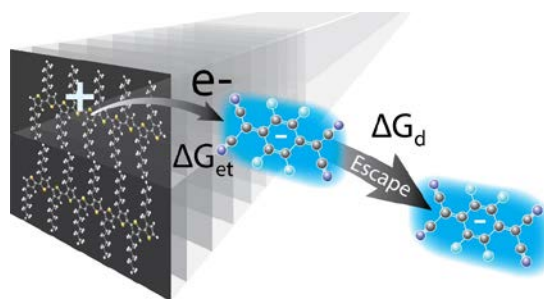


**Figure 1.** Escape of opposite charges helped by interchain delocalization of positive charge (+) in bundled aggregate of conjugated polymers.

In the current paradigm for organic solar cells, interfaces are required to split tightly bound excitons. While we might hope that the only possible, and unavoidable, loss from charge recombination is to reform the initial exciton, the DA interface introduces new energy-wasting decay pathways back to the ground state. The best we could hope for is that the fastest decay process, most likely being the spin allowed  $^1\text{CT} \rightarrow \text{S}_0$  electron transfer, is heavily in the inverted region. In nonpolar media with delocalized charge, we stand the best chance of seeing the inverted region due to low reorganization energy and potentially weak electronic coupling. However, the formation of triplet CT states,  $^3\text{CT}$ , enable a faster, spin-allowed path for electron transfer, resulting in local triplet excited states which can be a terminal loss pathway for charge separation. We investigate recombination in nonpolar media with new methods involving pulse radiolysis where we can control the spin of the initial CT state. Preliminary results paint a complex picture of recombination, but show some CT states living for microseconds.

# State Mixing Determines the Fate of the Multiexciton State in Singlet Fission

Michael R. Wasielewski

Department of Chemistry and Institute for Sustainability and Energy at Northwestern  
Northwestern University, Evanston, IL 60208

Singlet fission (SF) is the spin-allowed process in which a singlet exciton,  $^1(S_1S_0)$ , within an assembly of two or more chromophores spontaneously down-converts into two triplet excitons via a multiexciton correlated triplet pair state,  $^1(T_1T_1)$ . To elucidate the involvement of charge transfer (CT) states and vibronic coupling in SF, we performed 2D electronic spectroscopy (2DES) on dilute solutions of a covalently linked, slip-stacked terrylene-3,4:11,12-bis(dicarboximide) dimer (*ss*-TDI<sub>2</sub>). This dimer undergoes efficient SF in non-polar 1,4-dioxane and symmetry-breaking charge separation in polar CH<sub>2</sub>Cl<sub>2</sub>. The various 2DES spectral features in 1,4-dioxane show different pump wavelength dependencies, supporting the presence of mixed states with variable  $^1(S_1S_0)$ ,  $^1(T_1T_1)$ , and CT contributions that evolve with time. Analysis of the 2DES spectra in CH<sub>2</sub>Cl<sub>2</sub> reveals the presence of a state having largely  $^1(T_1T_1)$  character during charge separation. Therefore, the  $^1(T_1T_1)$  multiexciton state plays a role in the *ss*-TDI<sub>2</sub> photophysics irrespective of solvent polarity.

Femtosecond transient visible and NIR absorption spectroscopy of a linear TDI dimer (*lin*-TDI<sub>2</sub>) in which the two TDI molecules are directly linked at one of their imide positions also reveals ultrafast formation of the  $(T_1T_1)$  state. The spin dynamics of the  $(T_1T_1)$  state and the processes leading to uncoupled triplets were studied at room temperature for TDI<sub>2</sub> aligned in 4-cyano-4'-pentylbiphenyl (5CB), a nematic liquid crystal. Time-resolved electron paramagnetic resonance spectroscopy shows that the  $(T_1T_1)$  state has mixed  $^5(T_1T_1)$  and  $^3(T_1T_1)$  character at room temperature. This mixing is magnetic field dependent, resulting in a maximum triplet yield at ~200 mT. The accessibility of the  $^3(T_1T_1)$  state opens a pathway for triplet-triplet annihilation that produces a single uncorrelated T<sub>1</sub> state. The presence of the  $^5(T_1T_1)$  state at room temperature and its mixing with the  $^3(T_1T_1)$  state emphasize that understanding the relationship among different  $(T_1T_1)$  spin states is critical for ensuring high-yield singlet fission relevant to solar energy conversion.

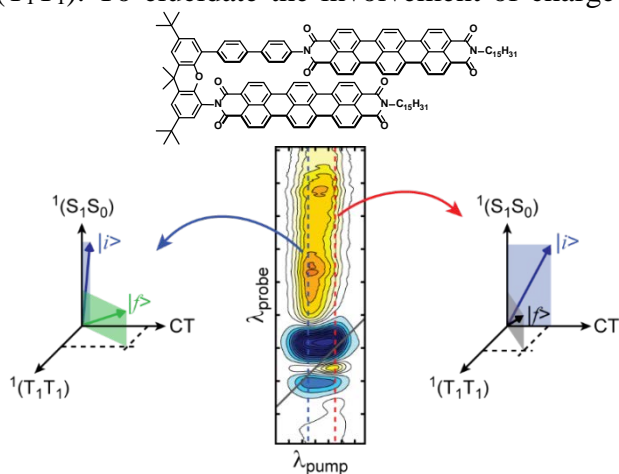


**Fig. 1** 2DES shows that the multi-exciton state of *ss*-TDI<sub>2</sub> is mixed state having singlet, CT, and triplet character.

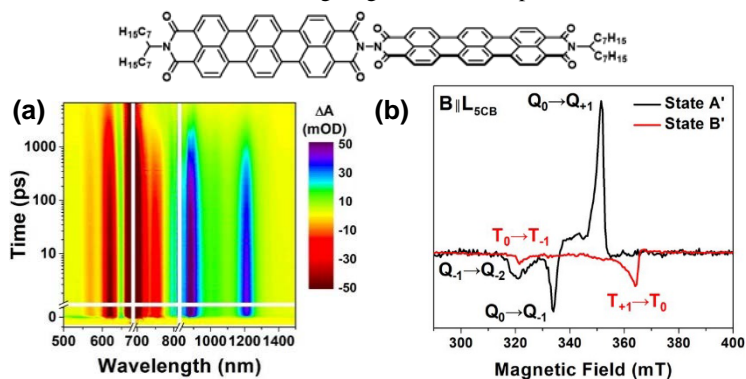


**Fig. 2** (a) Singlet fission occurs within ~300 fs in *lin*-TDI<sub>2</sub> and (b) TREPR spectroscopy shows  $^5(T_1T_1)$  to  $^3(T_1T_1)$  spin state evolution.

# Integrated Synthetic, Computational, Spectroelectrochemical Study of Polyoxometalate Water Oxidation Catalyst-Based Photoanodes

Craig L. Hill, Tianquan Lian, Djamaladdin G. Musaev

Department of Chemistry, Emory University, Atlanta, GA 30322

This ongoing multidisciplinary research program is focused on preparation of metal-oxide-cluster anions (polyoxometalates or “POMs”) water oxidation catalysts (POM-WOCs), their immobilization on photoelectrode surfaces for direct spectroscopic probing of charge transfer rates and water oxidation mechanisms, and development of new experimental and computational methods for interfacial charge transfer dynamics at the photoelectrode/catalyst interface. In this poster, we present progress in 3 key interlinked areas:

*Acid-compatible, earth-abundant-element catalysts for light-driven water oxidation.*

Water oxidation in strong acid remains a grand challenge in solar fuel work, thus, we continued our associated multi-disciplinary efforts and recently successfully prepared and characterized the first homogeneous catalyst **Co<sub>9</sub>P<sub>5</sub>**, (Figure 1) that contains only earth-abundant elements, is carbon-free and is stable for extended periods in strong acid. We have prepared the Cs<sup>+</sup>, Ba<sup>2+</sup>, La<sup>3+</sup> and Y<sup>3+</sup> salts of **Co<sub>9</sub>P<sub>5</sub>**, and developed methods to crystallize these species on FTO electrode surfaces. We demonstrated that all 4 salts of **Co<sub>9</sub>P<sub>5</sub>** are highly active WOCs in acidic media with the activity being highly dependent on the cation in the order Cs<sup>+</sup> < Ba<sup>2+</sup> < La<sup>3+</sup> < Y<sup>3+</sup>. Our computational analyses have established

key roles of weak interactions in these systems. Preliminary photocurrent and *in situ* transient absorption spectroscopic studies reveal that the **Co<sub>9</sub>P<sub>5</sub>**-modified BiVO<sub>4</sub> show enhanced photocurrent and lifetime of photogenerated holes. We have also prepared the *first mixed-transition-metal, molecular WOCs*, including the POM, [(Co<sup>II</sup>)<sub>2</sub>(Ni<sup>II</sup>)<sub>2</sub>(H<sub>2</sub>O)<sub>2</sub>(PW<sub>9</sub>O<sub>34</sub>)<sub>2</sub>]<sup>10-</sup>, **Ni<sub>2</sub>Co<sub>2</sub>P<sub>2</sub>**.

*Development of new experimental and computational methods probing the photoelectrode/catalyst interface.* The team is developing *in situ* spectroscopic methods for studying carrier dynamics and reaction in catalyst-functionalized planar photoelectrodes. We showed that *transient reflectance change* can be used to follow interfacial charge carrier dynamics and amplitude can be directly correlated to IPCE for water reduction on TiO<sub>2</sub>-protected GaP single crystals. This method is being extended to the study of POM WOC-modified photoanodes. More recently, we showed that *in situ* electric field induced second harmonic generation (*EFISH*) provides a direct method of probing the extent of band bending, charge separation and reaction order in catalyst-modified oxide electrodes. We also have developed an atomistic, Bulk-Adjusted LCAO (BA-LCAO) approach that facilitates an accurate generation of both periodic and non-periodic finite-sized nanocluster (NC) orbitals. This computational method combined with other electronic structure methods allows us to study charge carrier dynamics in NC/molecule dyads, and design better dyadic and triadic systems containing both periodic and non-periodic finite-sized NCs and WOCs.

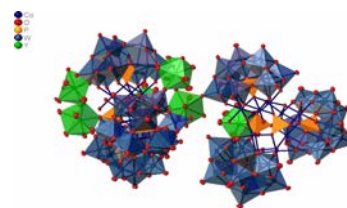


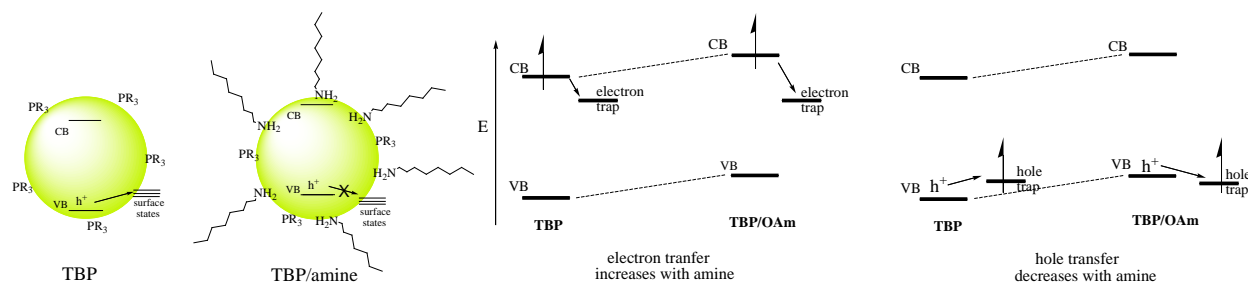
**Figure 1.** X-ray structure of Y<sup>III</sup><sub>5</sub>K [Co<sub>9</sub>(H<sub>2</sub>O)<sub>6</sub>(OH)<sub>3</sub>(HPO<sub>4</sub>)<sub>2</sub>(PW<sub>9</sub>O<sub>34</sub>)<sub>3</sub>], (Y-Co<sub>9</sub>P<sub>5</sub>), an acid compatible water oxidation catalyst. Two Co<sub>9</sub>P<sub>5</sub> units are shown linked by YO<sub>8</sub> polyhedra. Atom color code: Co atoms, dark blue; WO<sub>6</sub> units, blue; PO<sub>4</sub> units, orange; YO<sub>8</sub> polyhedra, green.

## Ligand Control of Nanocrystal Band Energetics

David P. Morgan and David F. Kelley  
Chemistry and Chemical Biology  
University of California Merced  
Merced, CA 95343

These studies examine the effects of surface dipoles on the interfacial charge transfer dynamics of semiconductor nanocrystals. The surface dipoles are associated with adsorbed polar ligands and can have large effects on the valence and conduction band energetics. These energetics can therefore be easily changed synthetically, i.e., by ligand exchange reactions.

In these initial studies, we use transient absorption and time-resolved photoluminescence spectroscopy to examine the charge separation and charge trapping dynamics of CdSe nanocrystals ligated with either tributyl phosphine (TBP) or a combination of TBP and an alkyl amine. We find that in the absence of adsorbed electron donors or acceptors, the main effect of the amine is to reduce the extent of surface hole trapping. This cannot be rationalized in terms of the traditional model in which the amine directly binds to and thereby passivates a surface trap site. An alternative mechanism is proposed wherein the absolute energies of the valence and conduction band edges shift to more negative redox potentials upon binding of the amine, decreasing the thermodynamic driving force for hole trapping, see Scheme 1. The energetic changes have the same effect on hole transfer to an adsorbed acceptor, 4-methylbenzenethiol. Amine binding increases the thermodynamic driving force for electron transfer to an adsorbed acceptor, methyl viologen, and dramatically increases the rate of interfacial electron transfer, as detailed in the reference.



Scheme 1. Changes in the thermodynamic driving force for electron and hole transfer to adsorbed acceptors upon ligation with amines. The effect on hole trapping is the same for hole transfer to an adsorbed acceptor.

Future studies will examine the dynamical effects of ligands having surface dipoles directed either toward or away from the nanocrystal and will also directly measure the changes in band energetics.

Reference. Morgan, D. P.; Kelley, D. F., Mechanism of Hole Trap Passivation in CdSe Quantum Dots by Alkylamines. *J. Phys. Chem. C* **2018**, *122*, 25661-25667.

## Spatial and Temporal Imaging of Energy Transport in Two-Dimensional Heterostructures

Long Yuan, Daria D. Blach, Shibin Deng, and Libai Huang  
Department of Chemistry, Purdue University, West Lafayette, IN 47907

*Scope of the Project:* Exciton transfer, transport, and dissociation at hetero-interfaces play a critical role in light to electricity conversion using organic and nanostructured materials. However, how excitons and charges migrate at these interfaces is poorly understood. Two-dimensional (2D) nanostructures provide a new platform to create architectures for directing interfacial energy transport. *The overarching goal of this program is to build the fundamental knowledge base for energy and charge transport at 2D interfaces, utilizing ultrafast microscopy tools with nanoscale spatial resolution and femtosecond temporal resolution.*[1-4]

*Transport of Interlayer Excitons in Moiré Potentials:* Interlayer charge-transfer (CT) excitons in van der Waals (vdW) type II vertical heterostructures of semiconducting transition metal dichalcogenides (TMDCs) provide a new approach toward engineering artificial exciton lattices. Moiré patterns with potential minima can be formed due to the mismatch in lattice constants, leading to a nanoscale periodic energy landscape (**Figure 1a**). How interlayer excitons migrate in such an energy landscape is an open question. The electron-hole separation in interlayer CT excitons results in a permanent electric dipole moment, which creates repulsive dipole-dipole interactions that screen the moiré potentials. We have employed transient absorption microscopy (TAM) to image exciton density and temperature dependent transport of interlayer excitons to measure the moiré potential in WS<sub>2</sub>-WSe<sub>2</sub> heterostructures. These results directly visualize the twist-angle dependent localization-delocalization transition of the interlayer excitons.[1]

*Energy Transport across 2D Lateral CdS/CdSe Heterostructures:* We have also investigated energy transport at the interfaces of type I CdSe/CdS lateral heterostructures with TAM, demonstrating efficient energy flow from CdS to CdSe (**Figure 1b**).[2] These measurements indicate energy transfer dominating at the interface and long-range transport at the  $\mu\text{m}$  length scale has been observed. We have developed a kinetic model to describe the spatial and temporal dependence of exciton population and transfer.

### References:

[1]. Long Yuan et al., in prep, 2019; [2]. Daria Blach et al., in prep, 2019; [3]. Tong Zhu et al., *Science Advances*, 4, eaao3104 (2018); [4]. Long Yuan et al., *Science Advances*, 4, e1700324, (2018).

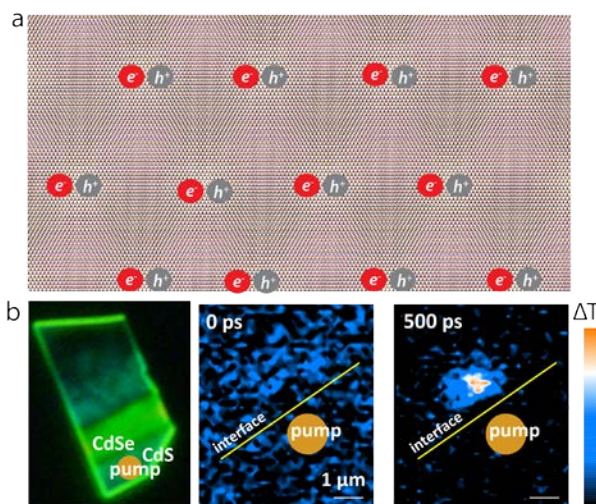


**Figure 1.** Exciton transport at 2D interfaces. (a) Interlayer exciton transport in moiré potential in WS<sub>2</sub>-WSe<sub>2</sub> heterostructures. (b) Energy transport across the interfaces of type I CdSe/CdS lateral heterostructures imaged by TAM.

# Advances in Controlling and Studying Semiconductor/Electrolyte Interfaces: Electrodeposition of Protective Layers on p-InGaP<sub>2</sub> and Operation of Semiconductor Ultramicroelectrodes under Accumulation Conditions

Mitchell Lancaster and Stephen Maldonado

Department of Chemistry

University of Michigan

Ann Arbor, MI 48109-1055

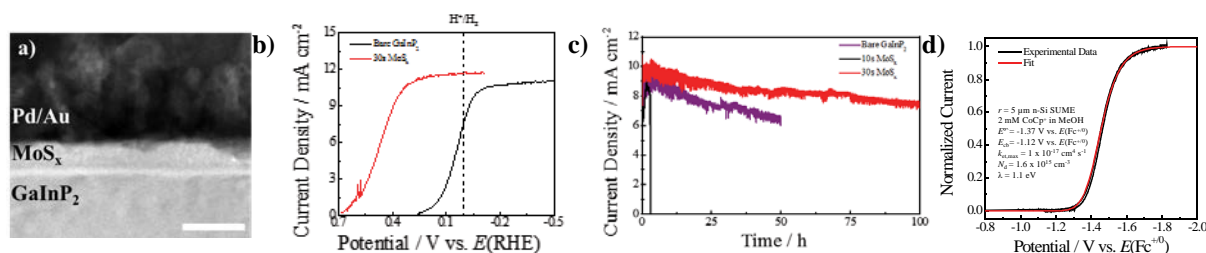


**Figure 1.** a) Bright-field STEM image of an as-deposited MoS<sub>x</sub> thin film and GaInP<sub>2</sub> interface. b) Voltammetric responses of MoS<sub>x</sub>/p-GaInP<sub>2</sub> and bare p-GaInP<sub>2</sub> photocathodes in 0.5 M H<sub>2</sub>SO<sub>4</sub> + 0.001 M Triton X-100 under AM 1.5G illumination. Scan rate: 50 mV s<sup>-1</sup>. The dashed line indicates the standard potential for the hydrogen evolution reaction on this scale. c) Durability measurements for bare p-GaInP<sub>2</sub>, 10s deposited MoS<sub>x</sub>/p-GaInP<sub>2</sub>, and 30s deposited MoS<sub>x</sub>/p-GaInP<sub>2</sub> photocathodes in 0.5 M H<sub>2</sub>SO<sub>4</sub> under AM 1.5G illumination. Applied bias: 0 V vs. E(RHE). d) Raw and fit voltammetric responses for a 5 μm n-Si SUME in CH<sub>3</sub>OH containing cobaltocenium.

This presentation will highlight two advances in our studies of semiconductor/electrolyte interfaces for the purpose of developing superior photoelectrochemical systems. First, data will be presented that shows that direct photo-electrodeposition of MoS<sub>x</sub> thin films on p-GaInP<sub>2</sub> epilayers provides excellent catalytic activity and enhanced durability for photoelectrochemical hydrogen evolution (Figure 1a-c). The key advancement presented here is the ability to fabricate thin metal sulfide films on high efficiency III-V substrates with good electrocatalytic performance and negligible photocurrent loss via a simple benchtop electrodeposition process. A notable conclusion is that these films can stabilize otherwise corrosion-prone materials, setting the basis for future studies aimed at depositing other catalytically active, yet stable materials on photoelectrodes. From a practical standpoint, the fact this stability enhancement was achieved without any other additional protection layer greatly simplifies interface design. Nevertheless, controlling the interfacial chemistry of the GaInP<sub>2</sub> electrode before photoelectrodeposition may also prove useful in manipulating the film morphology for adjusting the deposit's optical properties or altering the system energetics for enhanced overall performance.

The second topic covered is the analysis of semiconductor ultramicroelectrodes (SUMEs) operating under accumulation conditions (Figure 1d). In this regime, these semiconductor electrodes yield steady-state current-potential responses fully in line with expectations from Marcus theory. That is, the form and position of the redox response can be fit fully with only knowledge of the reorganization, the standard potential of the redox couple, and the band edge potential at the semiconductor/solution interface. Knowing only two of these parameters allows determination of the third by a least-squares fitting approach of experimentally obtained voltammetric responses. Accordingly, analysis of the voltammetric responses of SUMEs is an alternative and viable method for determining band edge potentials.



## Slow Charge Transfer from Pentacene Triplet States to Molecular Acceptors at the Optimal Driving Force

Natalie Pace<sup>1,2</sup>, Justin Johnson<sup>1</sup>, Garry Rumbles<sup>1,2,3</sup> and Obadiah Reid<sup>1,3</sup>

<sup>1</sup>Chemistry and Nanoscience Center, NREL, Golden, Colorado 80401

<sup>2</sup>Department of Chemistry, University of Colorado, Boulder, Colorado 80309

<sup>3</sup>Renewable and Sustainable Energy Institute, University of Colorado, Boulder, Colorado 80309

Singlet fission (SF) has the potential to significantly enhance solar cell performance if charges can be efficiently generated from the resulting triplet states. Here, we describe a study charge of separation from triplet excitons in polycrystalline pentacene using an electrochemical series of twelve different guest electron-acceptor molecules with varying reduction potentials, and we follow the SF and charge transfer dynamics using a combination of transient absorption spectroscopy and time-resolved microwave conductivity. We observe separate optima (Figure 1) in the charge yield as a function of driving force for singlet and triplet excitons, including inverted regimes for the dissociation of both states. Molecular acceptors can thus provide a strategic advantage to SF solar cells by suppressing singlet dissociation at optimal driving forces for triplet dissociation. However, even at the optimal driving force, the rate constant for charge transfer from the triplet state is surprisingly small,  $\leq 10^9$  s<sup>-1</sup>, presenting a previously unidentified obstacle to the design of efficient SF solar cells.

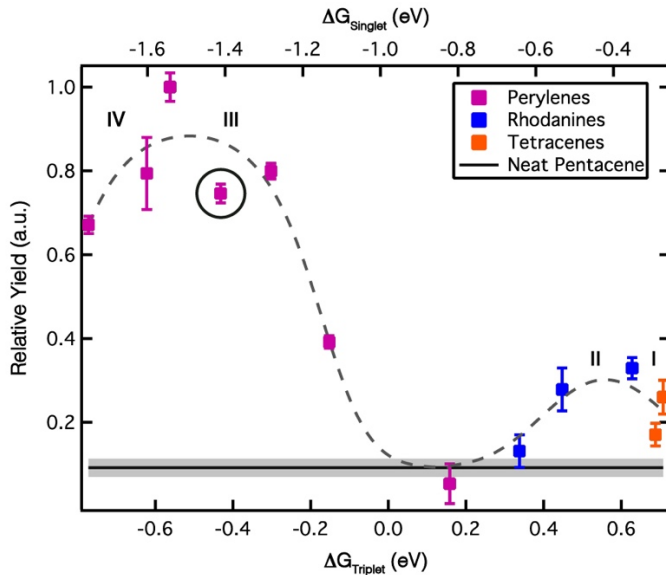


Figure 1: Trends in charge yield as a function of driving force. Relative charge yield reaches separate optimum values for singlet injection (negative  $\Delta G_{singlet}$  and positive  $\Delta G_{triplet}$ ) and triplet injection (negative  $\Delta G_{triplet}$  and large negative  $\Delta G_{singlet}$ ). The gray dashed curves are fits using equation 1.

$$\text{Equation 1} \quad \phi_r (\text{relative yield}) = \frac{\phi_n + \frac{\phi_n - \phi_r^{max}}{\phi_r^{max} - 1} e^{-\frac{-(\lambda + \Delta G_{PET})^2}{4\lambda k_B T}}}{1 + \frac{\phi_n - \phi_r^{max}}{\phi_r^{max} - 1} e^{-\frac{-(\lambda + \Delta G_{PET})^2}{4\lambda k_B T}}}$$

Here,  $\phi_n$  is the relative charge yield in neat pentacene,  $\phi_r^{max}$  is the peak relative charge yield between pentacene and an acceptor molecule, and  $\lambda$  is the reorganization energy.

# Sensitized Photocurrents on Single Crystal Semiconductors from Quantum Confined Semiconducting Carbon Nanotubes and Perovskite Quantum Dots: Hot Injection and Possible Multiple Excitons from Sub-bandgap Illumination

Kevin Watkins, Lenore Kubie, Yuqi Shi and Bruce Parkinson  
 Department of Chemistry and School of Energy Resources  
 University of Wyoming  
 Laramie, Wyoming 82071

The spectral sensitization of single crystal p-GaP by semiconducting single-walled carbon nanotubes (s-SWCNT) via hole injection into the p-GaP valence band is reported. The results are compared to SWNCT sensitized n-type single crystal substrates: TiO<sub>2</sub>, SnO<sub>2</sub>, and n-GaP. It was found that the sensitized photocurrents from CoMoCAT and HiPco s-SWCNTs were from a hole injection mechanism on all substrates, even when electron injection into the conduction band should be energetically favored. The results suggest an intrinsic p-type character of the s-SWCNTs surface films. In addition, it was observed that electron injection from the second excitonic states shows higher incident photon current efficiencies that from the lower energy first excitonic state suggesting the hotter carriers are more able to escape surface recombination.

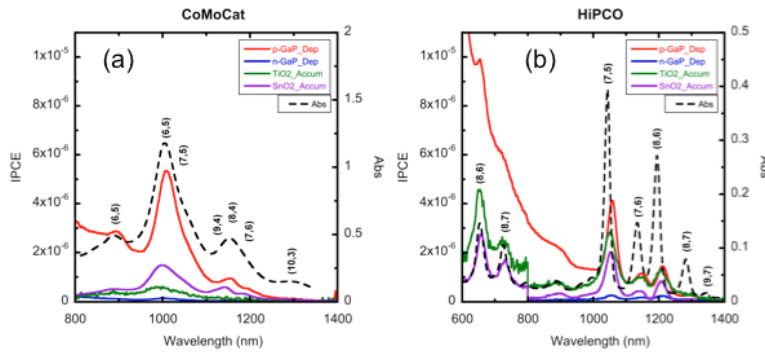


**Figure 1.** IPCE spectra (top) and normalized IPCE spectra (bottom) for CoMoCAT (left) and HiPco (right) s-SWCNTs deposited on various substrates. On all plots the absorption spectra of the s-SWCNT in solution are plotted on the right axis (dashed black) and the chiralities for each absorption feature is labeled above the peaks in a and b.

In addition we are investigating the *collection of multiple excitons from multiphoton sub-bandgap excitation* of perovskite quantum dots, a processes reported in a recent Nature Communication<sup>1</sup>.

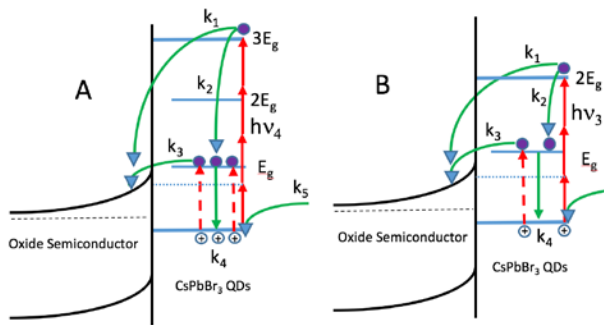


**Figure 2** Schematic showing the multiphoton processes for the 4 photon/3 exciton process (A) and the 3 photon/2 exciton process (B).  $h\nu_3$  and  $h\nu_4$  represent photon energies of  $1/3$  and  $1/4$  the energy of the third exciton level ( $3E_g$ ) and second exciton level ( $2E_g$ ) in the CsPbBr<sub>3</sub> QDs respectively. A competition between multiple exciton ( $k_3$ ) and hot injection ( $k_1$ ) will be measured.

## Transport and excitations in the photoanode of a dye-sensitized solar cell

Frances Houle and Thomas Cheshire  
Chemical Sciences Division  
Lawrence Berkeley National Laboratory  
Berkeley, CA 94720

We have focused this year on construction and characterization of two key components of a computational reaction-diffusion framework for solar-driven transformations in a dye-sensitized solar cell (DSSC). In this class of systems, molecular chromophores attached to internal surfaces of a porous anode convert sunlight to electricity via an  $I^-/I_3^-$  redox electrolyte. DSSCs operate through multiscale, multiphase couplings of excitation, charge flow and chemical reactions, which together govern their efficiency. A stochastic algorithm<sup>1</sup> is used to solve the master equation for the reaction-diffusion system. When the system's spatial and compositional characteristics and validated elementary reaction steps are used, the simulations have an absolute time base that enables computed and experimental data to be directly compared.

The first component is a detailed description of the kinetics of a typical ruthenium polypyridyl chromophore's excitation and relaxation processes. In collaboration with several groups from U. North Carolina,<sup>2</sup> we have compiled spectroscopic data from multiple studies and use simulations of transient absorption and photoluminescence measurements in solution to determine fundamental rate coefficients for ultrafast excitation, vibrational relaxation, intersystem crossing and nonradiative relaxation processes. The reaction scheme we have developed elucidates basic processes occurring on the sub-picosecond timescale and provides new information on the singlet-triplet conversion efficiency. In future, this basic scheme will be extended to include interfacial damping and charge injection kinetics.

The second component examines how the architecture of the porous anode housing the chromophores influences overall current generation efficiency.<sup>3</sup> It is often assumed that reactant transport through nanostructured solids limits the overall kinetics; in this case chromophore redox chemistry would be controlled by movement of electrolyte components in and out of the anode. Simulations show that intrapore transport does not limit current generation in typical DSSC structures: the current is determined by the specific pore structure, the chromophore coverage inside of the pores, and by the rate of diffusion of  $I_3^-$  from the anode to the cathode through bulk electrolyte solution. With this understanding of anode function, future work will focus on extensions to a range of dye excitation frequencies, and on identifying electron loss processes at the anode-electrolyte interior interfaces. The full chromophore photophysics scheme will be merged with this more detailed system model.

<sup>1</sup> W. D. Hinsberg and F. A. Houle, Kinetiscope, 2018. Available in open access at [www.hinsberg.net/kinetiscope](http://www.hinsberg.net/kinetiscope).

<sup>2</sup> M. K. Brennaman, P. G. Giokas, D. F. Zigler, A. M. Moran, J. M. Papanikolas, G. J. Meyer, T. J. Meyer

<sup>3</sup> F. A. Houle, 2019, submitted for publication.

# Probing Excited State Pathways by Coherent Vibrational Motions in Light Conversion Model Pt Dimer Complexes Using Femtosecond Optical Spectroscopy and X-ray Scattering

Pyosang Kim,<sup>1,2</sup> Denis Leshchev,<sup>2</sup> Subhangi Roy,<sup>3</sup> Andrew Valentine,<sup>4</sup> Antonio A. Lopez,<sup>3</sup>  
Felix N. Castellano,<sup>3</sup> Xiaosong Li,<sup>4</sup> Lin X. Chen<sup>1,2</sup>

<sup>1</sup>Chemical Sciences and Engineering Division, Argonne National Laboratory

<sup>2</sup>Department of Chemistry, Northwestern University

<sup>3</sup>Department of Chemistry, North Carolina State University

<sup>4</sup>Department of Chemistry, University of Washington

Many photochemical events, such as bond breaking, intersystem crossing and electron/energy transfer, can occur well before excited state vibrational relaxation. Using fs broadband transient spectroscopy and fs X-ray solution scattering, events of light-matter interactions in molecular systems, such as coherent vibrational wavepacket motions can be examined. From the time evolution of key vibrational modes, particularly the Pt-Pt stretching mode, we mapped out excited state trajectories on potential energy surfaces of model Pt-dimer complexes for light conversion, including coherent nuclear motions (**Figure 1**). These studies were carried out in a series of model platinum dimer complexes in solution featuring rich photochemistry and a set of intricate excited state potential energy surfaces on time scale previously unattainable. The combined molecular design, experimental and theoretical approaches enabled quantitative evaluation of the excited state trajectories of a series of Pt-dimer complexes in terms of actual nuclear motions via the Pt-Pt stretch as well as the energetic variations associated with these motions. This study was also extended to supramolecular systems featuring both Pt-dimer electron donor and NDI acceptors. Extensive studies have been carried out to map out how electronic coupling and coherent vibrational wavepacket motions are used to probe the excited state dynamics including intersystem crossing, internal conversion and electron transfer photochemistry with a time resolution <50 fs. The studies also suggest specific nuclear motions are critical for steering light induced electron transfer, ultimately controlling reaction directionality.

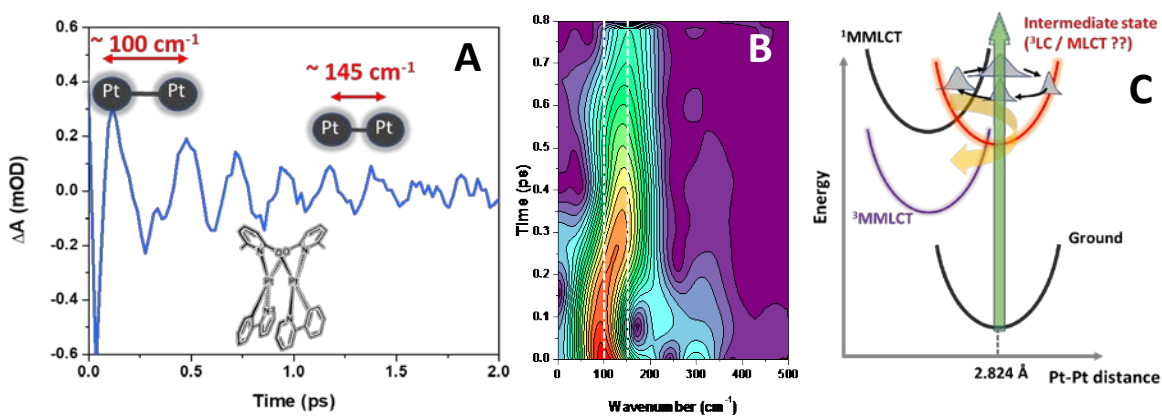
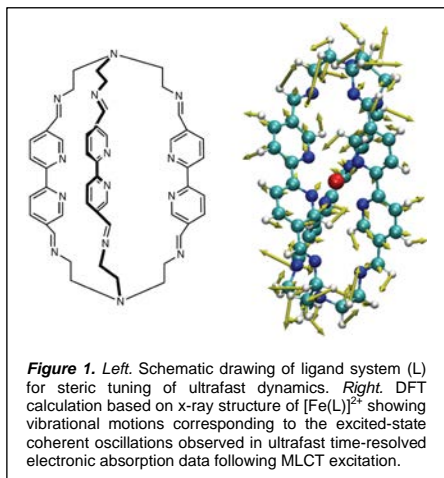


**Figure 1.** A) Excited state absorption signals featured with Pt-Pt stretching frequency evolution with the probe delay time; B) FT contour of the transient absorption spectra showing the frequency shift from 100  $\text{cm}^{-1}$  to 145  $\text{cm}^{-1}$ ; C) Excited state dynamics extracted from the Pt-Pt stretching frequency evolution.

## Insights into the Reaction Coordinate for MLCT-state Deactivation: Using Vibronic Coherence to Inform Synthetic Design

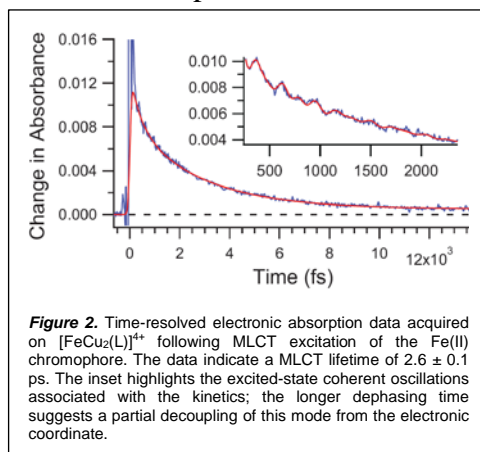
Bryan C. Paulus, Sara L. Adelman, Lindsey L. Jamula, and James K. McCusker\*  
Department of Chemistry, Michigan State University, East Lansing, MI 48824

Fundamental research on solar energy conversion – which will ultimately lead to the next generation of solar energy technologies – has sought to replicate Nature’s solution through the creation of artificial constructs that mimic various aspects of photosynthesis. Transition metal-based chromophores are particularly well-suited for use in such schemes by virtue of the charge-transfer excited-states that a majority of them possess. When dealing with earth-abundant transition elements (i.e., the first transition series), however,



the presence of low-lying ligand-field excited-states typically undermines their use in virtually *any* application that relies on charge separation following photon capture.<sup>1</sup> The focus of our research program is to understand the factors that determine the thermodynamics and kinetics that serve to define this situation, with the ultimate goal of circumventing and/or redefining their intrinsic photophysics in order to make feasible their use as light-harvesting components in solar energy conversion strategies.

We have developed a molecular platform that allows for systematic steric control of certain degrees of freedom of a polypyridyl-based ligand system in an effort to leverage information about electronic-vibrational coupling afforded by excited-state coherence. Time-resolved electronic absorption data on an Fe(II)-based version of this compound reveal a MLCT-state lifetime of  $110 \pm 30$  fs, which is typical for this class of chromophores. Analysis of the oscillatory features superimposed on the kinetics indicate large-amplitude motion associated with the capping portion of the ligand framework (Figure 1); dephasing times of ca. 300 fs, which are intermediate between pure electronic ( $< 10$  fs) and pure vibrational (1-10 ps) coherences, suggest a vibronic origin for these modes. Incorporation of Cu(I) ions at the apical 4-coordinate sites of the supramolecular framework results in a MLCT excited-state lifetime for the Fe(II) moiety of  $2.6 \pm 0.1$  ps: this corresponds to a  $> 10$ -fold increase in the charge transfer-state lifetime and represents the longest-lived MLCT species ever reported for a Fe(II)-polypyridyl complex (Figure 2). The  $> 2$ -fold increase in dephasing time for the coherent oscillations suggests a partial decoupling of the degree of freedom shown in Figure 1 from the electronic evolution of the compound, implying that we have successfully identified at least one significant contribution to the reaction coordinate that defines MLCT-to-LF conversion in this class of compounds.<sup>2</sup>



<sup>1</sup> McCusker, J.K. *Science* **2019**, *363*, 484-488.

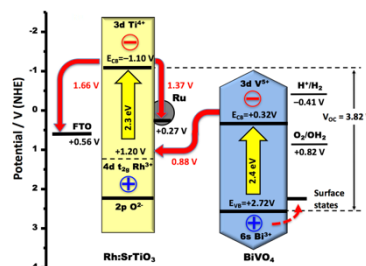
<sup>2</sup> Paulus, B.C.; Adelman, S.L.; Jamula, L.L.; McCusker, J.K. *Nat. Chem.*, submitted for publication.

# Surface Photovoltage Studies on Inorganic Tandem Photocatalysts for Overall Water Splitting, 03/01/2018 - 02/28/2021

Frank E. Osterloh  
Department of Chemistry  
University of California  
Davis, CA 95616

**Project Scope:** Surface Photovoltage Spectroscopy (SPS) was introduced in the 50's for the measurement of light induced charge transfer processes at semiconductor interfaces (Brattain and Bardeen in Bell Labs). The technique observes the intrinsic charge transfer properties of materials without any applied electrochemical bias or liquid electrolytes. Here, we use SPS to study photochemical charge separation and trapping at solid-solid and solid-liquid interfaces of micrometer sized particles of  $\text{BiVO}_4$ ,  $\text{Cu}_2\text{O}$ , and  $\text{Rh}:\text{SrTiO}_3$ . Such particles are of interest as light absorbers for next generation solar energy conversion systems, incl. tandem water splitting photocatalysts.

**Results:**  $\text{Cu}_2\text{O}$  particle layers on fluorine doped tin oxide (FTO) substrates show p-type behavior and  $\text{BiVO}_4$  particles show n-type behavior. In a  $\text{FTO}/\text{Cu}_2\text{O}/\text{BiVO}_4$  particle stack, both light absorbers act in tandem, producing up to 2.1 V photovoltage under 2.5 eV excitation, which corresponds to 90% of the ideal limit. The spectra reveal the effects of shading at high excitation energy and the effects of low absorber strength at low excitation energy. This suggests that photochemical charge separation at irregular particle contacts can approach the thermodynamic limit and that tandem photoelectrodes for water splitting can be constructed by layering the two materials. [1] In the second example, SPS measures the photopotential across a  $\text{Ru}-\text{SrTiO}_3:\text{Rh}/\text{BiVO}_4$  particle tandem overall water splitting photocatalyst for the first time. A photovoltage develops above 2.20 eV, the effective band gap of the tandem, and reaches its maximal value of  $-2.45$  V at 435 nm ( $2.44 \text{ mW cm}^{-2}$ ), which corresponds to 96% of the theoretical limit of the photocatalyst film on the fluorine-doped tin-oxide-coated glass (FTO) substrate. Photovoltage generation occurs on the 800 s time scale, showing that electron transport in the particle film occurs by diffusion. Charge separation is 82% reversible with 18% of charge carriers being trapped in defect states. The unusually strong light intensity dependence of the photovoltage (1.16 V per decade) is attributed to depletion layer changes inside of the  $\text{BiVO}_4$  microcrystals.[2] Future plans are to use SPS to observe depletion layer effects in  $\text{Cu}_2\text{O}$  particles and to correlate the photovoltage in the tandem to its photocatalytic water splitting properties.



## References

1. Wu, Z., G. Cheung, J. Wang, Z. Zhao, and F.E. Osterloh, *Wavelength dependent photochemical charge transfer at the  $\text{Cu}_2\text{O}-\text{BiVO}_4$  particle interface – evidence for tandem excitation*. *Chemical Communications*, **2018**, 54 (65), 9023-9026. <https://doi.org/10.1039/C8CC04123G>
2. Melo, M.A., Z. Wu, B.A. Nail, A.T. De Denko, A.F. Nogueira, and F.E. Osterloh, *Surface Photovoltage Measurements on a Particle Tandem Photocatalyst for Overall Water Splitting*. *Nano Letters*, **2018**, 18 (2), 805-810. <https://doi.org/10.1021/acs.nanolett.7b04020>

## New Chromophores for Bookending the Near Ultraviolet and Near Infrared Regions: “Blue” BODIPYs and Annulated Bacteriochlorins

David F. Bocian,<sup>a</sup> Dewey Holten<sup>b</sup> Christine Kirmaier,<sup>b</sup> and Jonathan S. Lindsey<sup>c</sup>

Departments of Chemistry

<sup>a</sup>University of California, Riverside CA 92521-0403

<sup>b</sup>Washington University, St. Louis, MO 63130-4889

<sup>c</sup>North Carolina State University, Raleigh, CA 27695-8204

The long-term objective of our research program is to design, synthesize, and characterize tetrapyrrole-based molecular architectures that absorb sunlight, funnel energy, and separate charge with high efficiency in a manner compatible with current and future solar-energy conversion schemes. This presentation reports recent studies aimed at developing new chromophores for light-harvesting in the near-ultraviolet (NUV) and near-infrared (NIR) spectral regions.

Dihydrodipyrins are precursors in the *de novo* synthesis of bacteriochlorins. They can be boronated to afford dihydrodipyrinatoboron complexes that have quite interesting properties (Figure 1). The complexes with  $-\text{BF}_2$  or  $-\text{BBu}_2$  absorb in the NUV region ( $\lambda_{\text{abs}} \sim 400$  nm) and fluoresce ( $\lambda_{\text{em}} \sim 500$  nm) with large Stokes shift ( $\sim 100$ – $150$  nm), almost no absorption-fluorescence spectral overlap, high fluorescence quantum yield ( $\Phi_f \sim 0.4$ – $0.9$ ), and long singlet excited-state lifetimes ( $\sim 5$ – $9$  ns). These “blue” BODIPYs may be useful as broadband photosensitizers upon NUV/violet-laser excitation.

Molecules with strong absorption in the NIR spectral region are of interest for a variety of applications in the photosciences. Annulation of a bacteriochlorin at the  $\beta$ ,meso-sites with either phenaleno (**Phen-BC**) or benzo (**Benz-BC**) groups results in strong NIR absorption at 913 or 1033 nm, with singlet excited-state lifetimes of 150 ps or 7 ps and commensurably low fluorescence quantum yields ( $\Phi_f$ ) of  $\sim 4 \times 10^{-3}$  or  $\sim 3 \times 10^{-5}$ , respectively. The substantially diminished NUV Soret band of **Phen-BC** is unusual. The quite strong  $Q_y(1,0)$  band (913 nm) of **Benz-BC** is also noteworthy and indicates strong vibronic coupling. Such strong vibrational-electronic coupling may contribute to the short excited-state lifetime of **Benz-BC**. The short lifetime is not simply a consequence of the energy-gap law for non-radiative decay derived from our studies of diverse porphyrins, chlorins and bacteriochlorins.

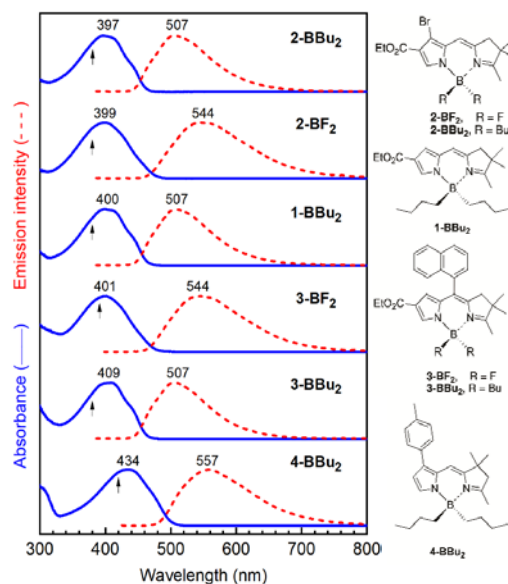


**Figure 1.** Spectra and structures of BODIPYs.

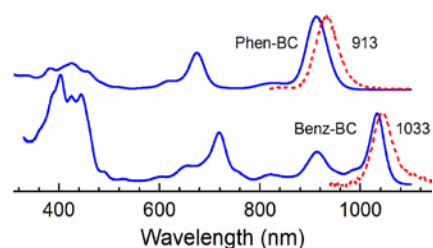


**Figure 2.** Spectra and structures of annulated bacteriochlorins.

# Controlling Singlet Fission by Molecular Contortion (DE-SC0014563)

X.-Y. Zhu & C. Nuckolls

Department of Chemistry  
Columbia University  
New York, NY 10027

Singlet fission, the generation of two triplet excited states from the absorption of a single photon, may potentially increase solar energy conversion efficiency. A major roadblock in realizing this potential is the limited number of molecules available with high singlet fission yields and sufficient chemical stability. Here, we demonstrate a strategy for developing singlet fission materials in which we start with a stable molecular platform and use strain to tune the singlet and triplet energies. Using perylene diimide (PDI) as a model system, we tune the singlet fission energetics from endoergic to iso-energetic by straining the molecular backbone.

The result is an increase in the singlet fission rate by two orders of magnitude. Fig. 1a displays the contorted PDI-B molecule we designed, with crystal packing structure in Fig. 1b. In this system there is only pi-pi interaction along the b-axis, and due to the curvature, these close contacts only occur between dimer pairs. The calculated first singlet and triplet excited state energies of PDI and PDI-B are shown in Fig. 1c. The energetic changes for singlet fission is  $\Delta E_{SF} = 2E_{T1} - E_{S1} \sim 0.3$  eV in PDI and  $\Delta E_{SF} \sim 0.0$  eV in PDI-B. Transient absorption spectra excited at 515 nm shown in Fig. 1d reveals fast singlet fission with a time constant of 2.5 ps, which is two-orders of magnitude faster than those in PDI films.

This demonstration opens a door to greatly expanding the molecular toolbox for singlet fission. Based on this success, we plan on extending the molecular contortion idea to a class of perylene-based chromophores. We are also exploring dimers and oligomers of PDI-B for solution phase singlet fission and for molecular photocatalysis.

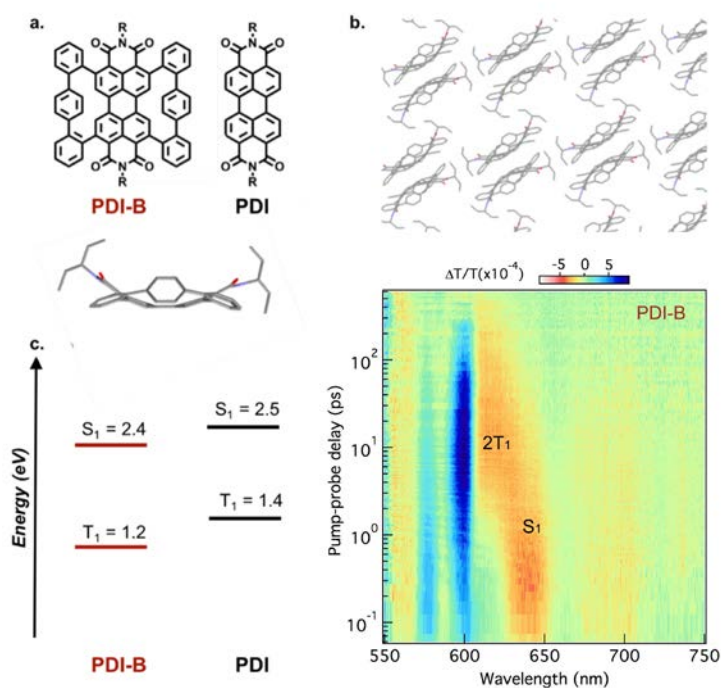


**Fig. 1 Structure, excited state energies, and singlet fission in contorted PDI.** a) Chemical structure of PDI-B derivative versus PDI, and curvature of PDI-B; b) Crystal packing structure along a- and b- axes of PDI-B, c) DFT calculations of singlet and triplet energy levels of both PDI-B and PDI, d) 2D pseudo-color ( $\Delta T/T$ ) plot of transient absorption spectra for a PDI-B film excited at 515 nm at 77K in vacuum.

## Toward Photo-induced Water Oxidation by Dual-Function Metal Organic Frameworks

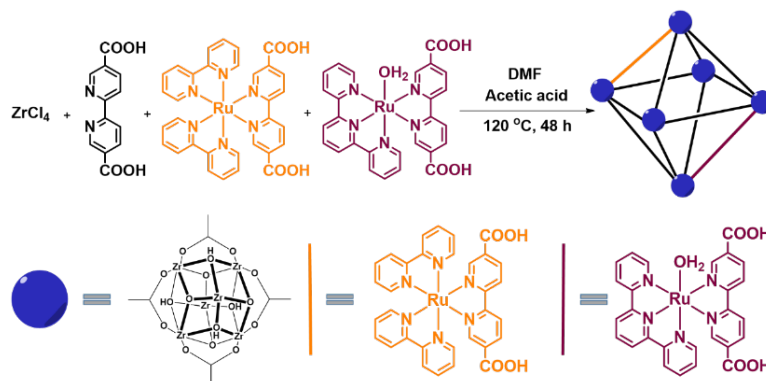
Shaoyang Lin, Arnab Chakraborty, Shaunak Shaikh, Bradley Gibbons, and Amanda Morris\*

Department of Chemistry

Virginia Tech

Blacksburg, VA 24060

The Morris research group has explored in detail energy transfer and water oxidation catalysis in metal organic frameworks (MOFs). With the design rules we have uncovered, we are now making strides toward combining these two components – light harvesting and water oxidation catalysis – into one MOF scaffold. As a first step, we have investigated a dual-



functionalized MOFs that has both chromophores ( $[Ru(dcbpy)(bpy)_2]^{2+}$ , where bpy = bpy = bipyridine, dcbpy = 5,5'-dicarboxy-2,2'-bipyridine) and catalysts ( $[Ru(tpy)(dcbpy)OH_2]^{2+}$ , where tpy = 2,2':6',2''-terpyridine) into a UiO-67 framework. We have explored the ability for this architecture to photoelectrochemically oxidize alcohols. We, specifically, chose a photoelectrochemical arrangement to avoid the use of sacrificial agents. The potentials applied at the electrode are not necessary to drive the reaction and simply remove electrons from the photoanode to drive proton reduction at a dark cathode. The construct is capable of photo-induced benzyl alcohol oxidation with a Faradaic efficiency of near 40% - without structural optimization. Additionally, transient spectroscopic studies support a mechanism by which the  $[Ru(dcbpy)(bpy)_2]^{2+}$  absorb photons to generate an excited state that injects into a  $TiO_2$  substrate with near unity efficiency. The oxidized sensitizer then oxidizes the  $[Ru(tpy)(dcbpy)OH_2]^{2+}$  catalysts on a nanosecond time scale, which in turn oxidizes the benzyl alcohol.

In addition to these dual component systems, we continue to investigate energy transfer in MOFs constructs to optimize light harvesting and energy transport. One of the major goals that directly impacts our dual-component MOFs is the investigation of the role of spin-orbit coupling in energy transfer in  $Ru(bpy)_3$  doped MOFs. Namely, the spacing between the chromophores in these structures necessitates the invoking of a Förster energy transfer mechanism. From a pragmatic point of view, Förster energy transfer between triplets is not observed due to the poor overlap between essentially non-existent  $^3MLCT$  absorption and the observed  $^3MLCT$  emission. Therefore, we have embarked on a systematic study of Förster energy transfer in MOFs doped with chromophores that exhibit different spin-orbit couplings –  $Ru(bpy)_3$ ,  $Os(bpy)_3$ , and  $Ir(ppy)_3$ . Remarkably, in photophysical studies we have determined that homo-RET in  $Os(bpy)_3$  is over 4 times more efficient in  $Os(bpy)_3$ -doped frameworks than  $Ru(bpy)_3$ -based frameworks ( $R_0 = 90$  and  $20 \text{ \AA}$ , respectively). We have also explored the role of dipole orientation in porphyrinic frameworks on the rate of energy transfer. Through the synthesis of a new MOF, VPI-110, we have demonstrated field-leading energy transfer distances.

# Combined Theoretical and Experimental Investigations of Atomic Doping to Enhance Photon Absorption and Carrier Transport of LaFeO<sub>3</sub> Photocathodes

Garrett P. Wheeler,<sup>1</sup> Valentin Baltazar,<sup>2</sup> Tyler Smart,<sup>2</sup> Andjela Radmilovic,<sup>1</sup> Yuan Ping<sup>2</sup> and Kyoung-Shin Choi<sup>1</sup>

<sup>1</sup>Department of Chemistry, University of Wisconsin-Madison, Madison, WI 53706

<sup>2</sup>Department of Chemistry and Biochemistry, University of California, Santa Cruz, CA 95064

The overall objective of our project is to bring about marked advancements in the construction, understanding, and available variety of high-quality, polycrystalline, oxide-based semiconductor electrodes for use in solar hydrogen production. We achieve this goal through the development of inexpensive and practical solution-based electrochemical synthesis methods that can produce semiconductors and other critical components (i.e. catalyst and protection layers) of the photoelectrodes of interest with systematically varied compositions and morphologies. By investigating the resulting photoelectrodes, we elucidate composition-morphology-property relationships and establish effective strategies to address the critical limitations of each system and improve desired photoelectrochemical properties and stabilities.

In this presentation, we will discuss our recent efforts in developing LaFeO<sub>3</sub> photocathodes. Perovskite-type lanthanum iron oxide, LaFeO<sub>3</sub>, is a p-type semiconductor that can achieve overall water splitting using visible light; its bandgap energy is 2.1-2.2 eV, and its conduction band minimum and valence band maximum straddle the water reduction and oxidation potentials, respectively. Furthermore, LaFeO<sub>3</sub> is stable against photocorrosion. The major limitation of a LaFeO<sub>3</sub> photocathode is known to be considerable bulk electron-hole recombination. In order to address this issue, we conducted computational and experimental studies to investigate atomic doping at the La site of LaFeO<sub>3</sub>, which resulted in an increase not only in electron-hole separation but also in photon absorption. In this presentation, we will discuss how substitutionally replacing La<sup>3+</sup> with K<sup>+</sup> can affect the electronic and atomic structures, majority carrier density, hole-polaron formation, and optical properties of LaFeO<sub>3</sub> to enhance its photoelectrochemical properties (Fig. 1).

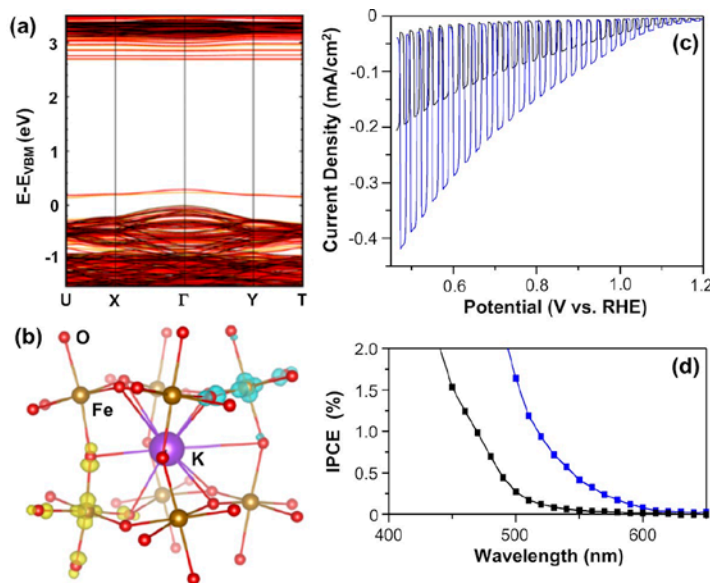
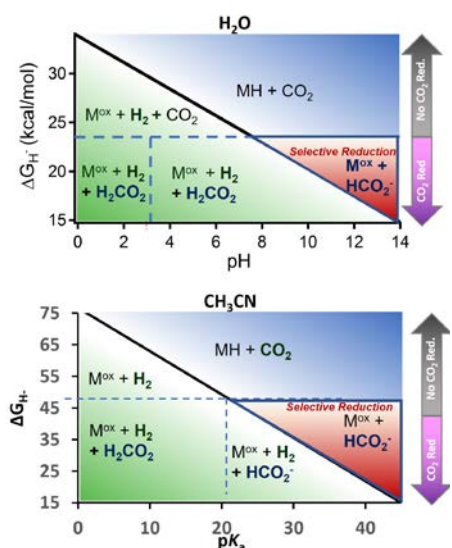


**Fig. 1.** (a) The electronic band structure of pristine LaFeO<sub>3</sub> (black) and K-doped LaFeO<sub>3</sub> (red = spin up and orange = spin down); (b) Hole polaron wavefunction modulus showing two hole-polarons formed on Fe atoms (one shown in yellow and the other shown in light blue) around the K<sup>+</sup> dopant occupying the La<sup>3+</sup> site; (c) J-V plots and (d) IPCE measurements obtained using LaFeO<sub>3</sub> (black) and K-doped LaFeO<sub>3</sub> (blue) for O<sub>2</sub> reduction in pH 13 NaOH solution under AM 1.5G illumination.

# Thermochemical Guidelines for Designing Efficient H<sub>2</sub> Evolution or Selective CO<sub>2</sub> Reduction Catalysts & First Stable and Selective Synthetic Electrocatalyst for Reversible CO<sub>2</sub>/HCO<sub>2</sub><sup>-</sup> Conversion

Bianca Ceballos, Drew Cunningham, Caitlin Hanna, Zachary Thammavongsy, Reyna Velasquez, Andrew Luu, Jenny Y. Yang  
 Department of Chemistry  
 University of California, Irvine  
 Irvine, CA 92617

Scheme 1



Our primary goals are to 1) develop a thermochemical framework to guide the design of efficient molecular catalysts for aqueous H<sup>+</sup> to H<sub>2</sub> at various pH conditions or selective CO<sub>2</sub> reduction to HCO<sub>2</sub><sup>-</sup>. Selectivity is a challenge because metal hydrides are a common intermediate in both reaction pathways; understanding the reactivity of CO<sub>2</sub> and H<sup>+</sup> with metal hydrides is key to controlling the bifurcating reaction pathways that ultimately determine selectivity. Our diagrams (Scheme 1) describes the thermodynamic products as a function of hydricity and delineating a region where combinations of hydricity and pK<sub>a</sub> lead to thermodynamic favorability for selective CO<sub>2</sub> reduction over H<sub>2</sub> evolution. We establish the utility of our diagram by selecting a known metal hydride [HPt(dmpe)<sub>2</sub>]<sup>+</sup> with an appropriate hydricity and demonstrate exclusive CO<sub>2</sub> reduction with high Faradaic efficiency and low

overpotential.

Reversible catalysis is a hallmark of energy efficient chemical transformations and can only be achieved if the changes in free energy of intermediate steps are minimized and the catalytic pathway is devoid of high transition state barriers. Utilizing thermodynamic considerations, we describe the first example of stable and highly selective catalyst for reversible CO<sub>2</sub>/HCO<sub>2</sub><sup>-</sup> conversion, [Pt(depe)<sub>2</sub>]<sup>2+</sup>. Direct measurement of the free energies associated with each step in the catalytic cycle correctly predicts a slight bias towards CO<sub>2</sub> reduction. The energy

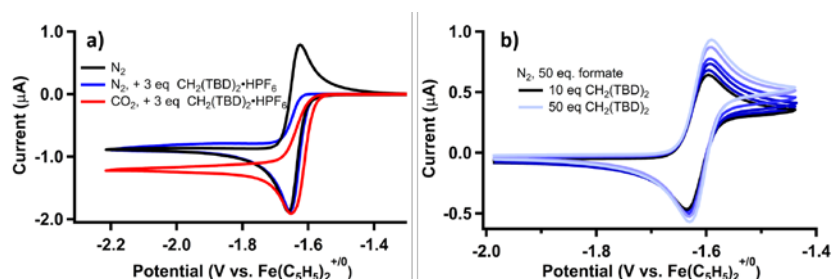


**Figure 1.** a) CVs of [Pt(depe)<sub>2</sub>][PF<sub>6</sub>]<sub>2</sub> (1.0 mM) under N<sub>2</sub> (—) and in the presence of 3 equivalents of CH<sub>2</sub>(TBD)<sub>2</sub>·HPF<sub>6</sub> under dinitrogen (—) and under CO<sub>2</sub> (—). b) CVs of [HPt(depe)<sub>2</sub>][PF<sub>6</sub>] (1.0 mM) under N<sub>2</sub> in the presence of [n-Bu<sub>4</sub>N][HCO<sub>2</sub>] (50 mM) with concentrations of CH<sub>2</sub>(TBD)<sub>2</sub> ranging between 10 mM (—) and 50 mM (—). 0.2 M TBAPF<sub>6</sub> in acetonitrile at a scan rate of 5 mV/s.

landscape for the catalytic cycle illustrates how the free energy of each step contributes to the overpotential. Under optimized conditions for reversible CO<sub>2</sub>/HCO<sub>2</sub><sup>-</sup> conversion, parasitic H<sub>2</sub> evolution is negligible and the Faradaic efficiency for HCO<sub>2</sub><sup>-</sup> production is nearly quantitative.

# Theoretical Limits of Multiple Exciton Generation and Singlet Fission Tandem Devices for Solar Water Splitting

Marissa Martinez<sup>1,2</sup>, Arthur J. Nozik<sup>1,2</sup>, and Matthew C. Beard<sup>2</sup>

<sup>1</sup>Department of Chemistry and RASEI

University of Colorado

Boulder, CO 80309

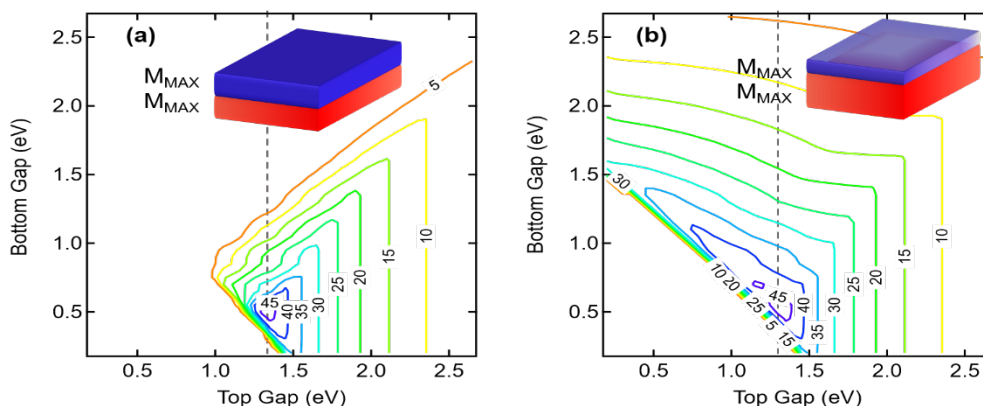
and

<sup>2</sup>Materials and Chemical Sciences & Technology Directorate

National Renewable Energy Laboratory

Golden, CO 80409

As solar water splitting research intensifies, it is important to examine the ultimate limiting efficiencies of this approach. In this study, we determine the maximum thermodynamic power conversion efficiencies (PCE) of photoelectrochemical (PEC) water splitting two-bandgap tandem devices of various architectures that produce multiple carriers per absorbed photon via multiple exciton generation (MEG) or Singlet Fission (SF) and in the presence of solar concentration. Here we employ a Shockley-Queisser type detailed balance thermodynamic analysis to determine the effects of top cell thickness, solar concentration, carrier multiplication, electrode overvoltage ( $V_{op}$ ), and water absorption on PEC power conversion efficiency. We have found a maximum PEC power conversion efficiency of 62.9% in cells using two ideal tandem MEG absorbers with bandgaps of 0.3 and 1.2 eV at 1000-suns solar concentration and 0.0 overvoltage; the maximum PCE for two tandem SF absorbers under the same conditions is nearly the same at 59% with the same values for the absorption thresholds. At 1 sun concentration both of these tandem cells have PCEs of about 47% at 0.0 overvoltage; at a more realistic overvoltage of 0.4 V they maintain approximately the same 47% PCE but at a solar concentration of 1000X. For comparison, a single absorber producing a single exciton per absorbed photon only reaches 30% PCE for H<sub>2</sub>O splitting at 1 sun and 0.0 V overvoltage. A very interesting and important result is that upon thinning the top cell to allow some supra-bandgap photons to pass through into the bottom cell to create multiple carriers per absorbed photon, the range of viable bandgaps for both the top and bottom cells are extended by as much as 0.5 to 1 eV, while still maintaining relatively high maximum power conversion efficiency (40-45%). The effects of having different tandem configurations of singlet fission and multiple exciton generation absorber layers were also studied and are reported here.



## Polarizability and low-frequency vibrations in electron-transfer reactions

D. V. Matyushov<sup>1</sup> and M. D. Newton<sup>2</sup>

<sup>1</sup>School of Molecular Sciences, Arizona State University, Tempe, AZ 85287

<sup>2</sup>Brookhaven National Laboratory, Chemistry Department, Upton, NY 11973-5000

We report here the results [1-5] published in the first year of the project initiated in June 2018. We studied the following problems related to the kinetics of electronic transitions in molecules and at electrodes: (i) electrochemistry of polarizable molecules [1,2], (ii) theory of electrode reactions altering force constants of intramolecular vibrations [3], (iii) entropy and enthalpy surfaces along the reaction coordinate in electron transfer [4], and (iv) nonequilibrium population of internal vibrations in electron-transfer reactions [5].

The issue of electron transfer in polarizable molecules is of general interest for solar photochemistry since many successful charge-transfer molecules are highly polarizable. Polarizability strongly shifts the maximum of the inverted Marcus parabola allowing activationless reactions at lower driving force. As an observable consequence of the effect of molecular polarizability on redox reactions, the theory predicts different activation barriers in a sequence of electron reduction reactions at the electrode [2]. A similar scenario is realized when the force constants of intramolecular vibrations change in the redox reaction. The Butler-Volmer plot of electrode electron transfer becomes asymmetric between anodic and cathodic currents [3], producing non-equal transfer coefficients. An exactly solvable model was formulated in terms of two separate intramolecular reorganization energies for two redox states of the molecule.

Nonequilibrium population of intramolecular vibrations offers a new tool to control rates of electron transfer. While first experimental evidence of this effect was published, no established mechanism has been proposed of how pulses of infra-red (IR) radiation can affect the rate constant. A general theory of radiationless transitions with nonequilibrium populations of vibrations was developed [5]. It shows that IR pulsing can substantially influence the rate when excess vibrational population is created in the vibrational modes altering the donor-acceptor distance.

[1] D. V. Matyushov, "Electrode reactions with polarizable molecules", *J. Chem. Phys.* 148 154501 (2018).

[2] S. M. Sarhangi, et al "Half reactions with multiple redox states do not follow the standard theory: A computational study of electrochemistry of C60", *J. Phys. Chem. C* 122, 17080-17087 (2018).

[3] D. V. Matyushov and M. D. Newton, "Q-model of electrode reactions: altering force constants of intramolecular vibrations", *Phys.Chem.Chem.Phys.* 20, 24176-24185 (2018).

[4] D. V. Matyushov and M. D. Newton, "Thermodynamics of reactions affecting by medium reorganization", *J. Phys. Chem. B* 122, 12302-12311 (2018).

[5] D. V. Matyushov, "Nonequilibrium vibrational population and donor-acceptor vibrations affecting rates of radiationless transitions", *J. Chem. Phys.* 150, 074504 (2019).

## Two Dimensional Electronic Vibrational (2DEV) Spectroscopy and Quantum Light Spectroscopy

G.R. Fleming, Eric Wu, Eric Arsenault, Pallavi Bhattacharyya and Kaydren Orcutt

Molecular Biophysics and Integrated Bioimaging Division  
Lawrence Berkeley National Laboratory  
and  
Department of Chemistry  
University of California Berkeley  
Berkeley CA 94720

In the past year we have developed our own understanding of 2DEV spectroscopy in several directions. We have developed a nearly analytical theory to describe 2DEV spectra of strongly coupled vibronic dimers, in which the mixing allows IR transitions that would be forbidden in un- or weakly-coupled systems. We find that the initial amplitude of vibronic coherences can be similar to peaks arising from population terms although the former decay on the few 100 fs timescale, giving rise to a spectrum dominated by population peaks.

We have demonstrated that the centerline slope (CLS), which describes the correlation between electronic and vibrational frequencies, can be used to label donor/acceptor partners even in highly complex and congested spectra such as the 2DEV spectrum of LHCII. The CLS provides information that appears to be unique to the 2DEV method and our models of heterodimers reveal the extremely rich behavior of the CLS even in a comparatively simple model.

The focus of 2DEV spectroscopy on both the electronic and vibrational degrees of freedom makes it well-suited to explore proton-coupled electron transfer (PCET) and we have begun a collaboration with T. Moore, A. Moore, D. Gust and coworkers on this topic. In a system designed to mimic the tyrosine-histidine couple of photosystem II we find both proton and electron move within 100fs, however an analysis of the detailed kinetics has been hindered by an extraordinary series of equipment failures.

Turning to the development of a quantum light spectrometer based on entangled pairs of photons we have focused on optimizing the source and coincidence detection system.

### Publications since July 2018

1. Two-Dimensional Electronic-Vibrational Spectroscopy and Ultrafast Excitonic and Vibronic Photosynthetic Energy Transfer. E.C.Wu, E. Arsenault, P. Bhattacharyya, N.H.C.Lewis and G.R. Fleming. Faraday Discussion. (In Press)
2. Two-Dimensional Electronic-Vibrational Spectroscopy of Coupled Molecular Complexes: A Near Analytical Approach. G.R. Fleming and P. Bhattacharyya. J. Phys. Chem Lett. (In Press) DOI: 10.1021/acs.jpcllett.9b00588
3. Two-Dimensional Electronic Vibrational Spectroscopy in Coherent Multidimensional Spectroscopy. Graham R. Fleming, Nicholas H.C. Lewis, E.A. Arsenault, Eric C. Wu, Sabine Oldemeyer. Ed. M.Cho. Springer. (In Press)

## Z-Scheme Solar Water Splitting via Self-Assembly of Photosystem I-Catalyst Hybrids in Thylakoid Membranes

Lisa M. Utschig, Sarah R. Soltau, Karen L. Mulfort, Jens Niklas, and Oleg G. Poluektov  
Chemical Sciences and Engineering Division  
Argonne National Laboratory  
Lemont, IL 60439

Sunlight is an abundant and environmentally clean source of energy. Current solar energy research involves developing practical schemes for capturing, converting, and storing the sun's energy in the form of high-energy molecular bonds as a reduced fuel, or "solar fuel". The direct production of the solar fuel hydrogen using sunlight and water is a particularly attractive approach to sustainable energy production. Our research program has been developing systems that link Nature's solar energy converters, photosynthetic reaction center proteins, to abiotic inorganic catalysts for light-driven hydrogen production.

The reaction centers Photosystem I and Photosystem II efficiently manage photon capture and conversion processes in plants, algae, and cyanobacteria to drive oxygenic water splitting and carbon fixation. In recent work, we utilize the native photosynthetic Z-scheme electron transport chain to drive hydrogen production from thylakoid membranes by directional electron transport to abiotic catalysts bound at the stromal end of Photosystem I. Pt-nanoparticle and first-row transition metal molecular catalysts readily self-assemble with Photosystem I in spinach and cyanobacterial membranes. We show that, by self-assembling catalysts within the photosynthetic membrane, the system is self-sustaining as electrons that originate from the light-driven oxidation of water are transferred through Nature's inherent, highly tuned electron transport chain to the abiotic sites for hydrogen generation. This work provides the basis for future studies implementing *in vivo* approaches to generate living photosynthetic systems as a sustainable energy solution and benchmarks a significant advance toward improving photosynthetic efficiency for solar fuel production.

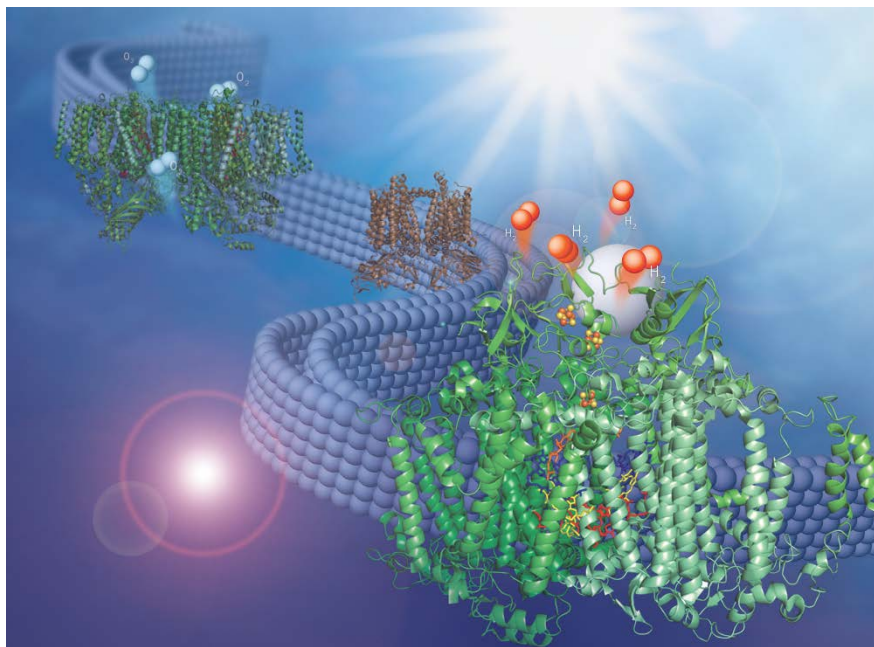


**Figure 1.** Illustration of a photosynthetic thylakoid membrane including the membrane bound proteins Photosystem II, Cyt *b<sub>6</sub>f*, and Photosystem I. Electrons originating from the light-driven oxidation of water by Photosystem II are transferred through Nature's inherent finely tuned electron transport chain to Photosystem I bound catalyst sites for the light-driven generation of hydrogen.

## Determination of vibrational motions driving photoinduced electron transfer reactions in molecular crystals and organic thin films

Christopher C. Rich, Kajari Bera, Alyssa A. Cassabaum, and Renee R. Frontiera

Department of Chemistry  
University of Minnesota  
Minneapolis, MN 55455

The goal of our research program is to quantify the contribution of coherent nuclear motion to light-driven charge and energy transport in molecular crystals. Using femtosecond stimulated Raman spectroscopy (FSRS) and microscopy approaches, we measure the structural evolution of molecular vibrations and crystal phonon modes following photoexcitation. The high temporal, structural, and spatial resolution permits us to probe ultrafast charge transfer dynamics as well as resolve coupling between vibrational coherences which can drive phenomena such as singlet fission and photocatalysis. By understanding the nuclear coordinates which promote and suppress favorable electronic processes, we can guide rational design of molecular systems for low cost, high performing photocatalysts and photovoltaics.

Our recent results examined the role of coherent phonon excitation in driving photoinduced phase transitions (Fig. 1). Coherent excitation of multiple or single phonon modes can drive or suppress the reaction, isolating the critical contribution of these nuclear coordinates to the charge transfer reaction. Ongoing research includes investigation of the mechanism of singlet fission in TIPS-pentacene thin films, applying spatially-offset FSRS for measuring charge transport and polaron diffusion, and implementing coherent control experiments to determine how photocatalysis and charge transfer processes are driven by vibrational coherences.

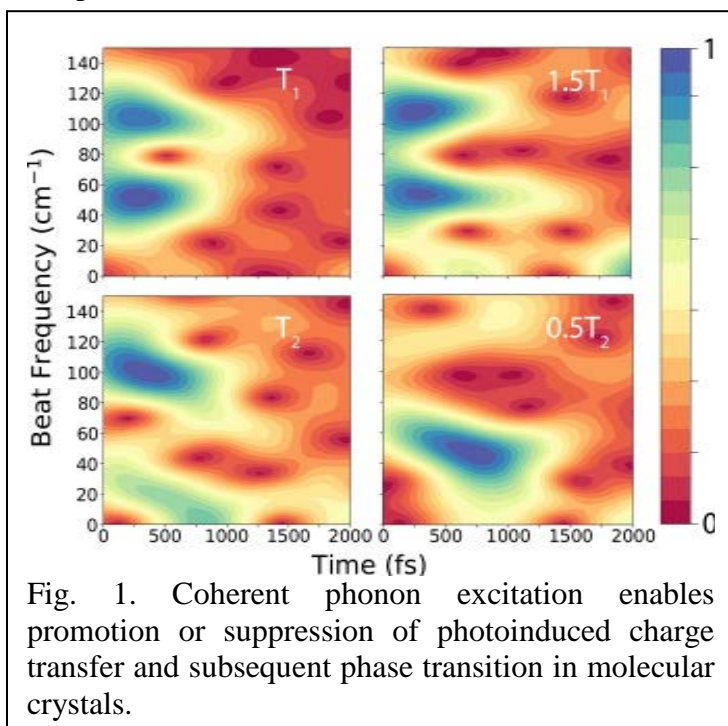


Fig. 1. Coherent phonon excitation enables promotion or suppression of photoinduced charge transfer and subsequent phase transition in molecular crystals.

### DOE Sponsored Publications

1. Bera, K., Kwang, S. Y., Cassabaum, A. A., Rich, C. C., Frontiera, R. R., “Effective background removal in femtosecond stimulated Raman spectroscopy using a dual frequency Raman pump technique”, *J. Phys. Chem. A.*, **2019**, *in review*.
2. Cassabaum, A. A., Silva, W. R., Frontiera, R. R., “Orientation and polarization dependence of ground and excited state FSRS in crystalline betaine-30”, *J. Phys. Chem. C*, **2019**, *in review*.
3. Hart, S. M., Silva, W. R., Frontiera, R. R., “Femtosecond stimulated Raman evidence for charge-transfer character in pentacene singlet fission”, *Chemical Science*, **2018**, *9*, 1242.

## Charge Separation and Triplet Exciton Formation Pathways in Small-Molecule Bulk Heterojunction Blends as Studied by Time-Resolved EPR Spectroscopy

Oleg G. Poluektov, Jens Niklas, Karen L. Mulfort, Lin X. Chen, David M. Tiede  
Chemical Sciences and Engineering Division, Argonne National Laboratory

Lemont, IL 60439

Kristy L. Mardis

Department of Chemistry and Physics, Chicago State University  
Chicago, IL 60628

The ultimate goal of our solar energy conversion research is to resolve fundamental mechanisms of photochemical energy conversion and, particularly, investigate use of bulk heterojunctions, BHJ, for photovoltaic charge collection, and go beyond by investigating possibilities to extent this to use BHJ as organic semiconductor photoanodes/cathodes for solar fuels catalysis.

Photovoltaic system based on donor-acceptor BHJ are attracting renewed interest because of remarkable gains that have been achieved in the efficiency of charge separation and collection. Initially BHJ were made from semiconductor polymer donors and fullerene-derivative acceptors. However, low efficiency, *ca.* 10%, in combination with costly fullerene derivatives made these material not applicable for industrial production. Recently, breakthrough in efficiency of OPVs, *ca.* 16%, were reported for cells based on organic small molecules BHJ. Important question which is awaiting its resolution is what are the crucial factors which determines the higher solar energy conversion efficiency in small molecules OPV? As a first step to address this question we use advanced light-induced EPR spectroscopy in combination with DFT modeling to study the electronic excited states, charge transfer dynamics, and triplet exciton formation pathways across five representative of a widely studied dithienosilole, DTS, family of small-molecule electron donors with fullerene derivative PC<sub>61</sub>BM as aa acceptor. High-frequency EPR results have been compared with DFT calculations which revealed that the spin density of the positive polaron is distributed over a dimer or trimer of DTS molecules. Time-resolved EPR spectra attributed to singlet charge separation states were identified and analyzed. This analysis allowed identify the difference in charge separation dynamics between five donors under study. Using TR-EPR the triplet exciton formation pathways were investigated. The polarization patterns provide the direct evidence that the excitons originate from both intersystem crossing and back electron transfer processes (see Figure). The higher BET triplet exciton population is directly related to the slower charge separation dynamics observed in this blend. These data are compared with a previously obtained data on semiconductor polymers-fullerenes BHJ blends. In the future we will focus on BHJ with non-fullerene small molecule acceptors.

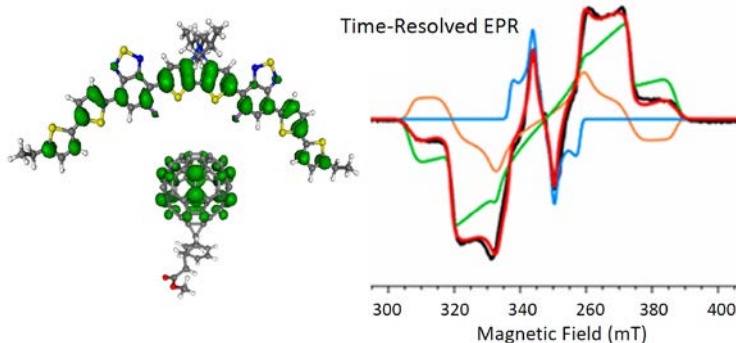
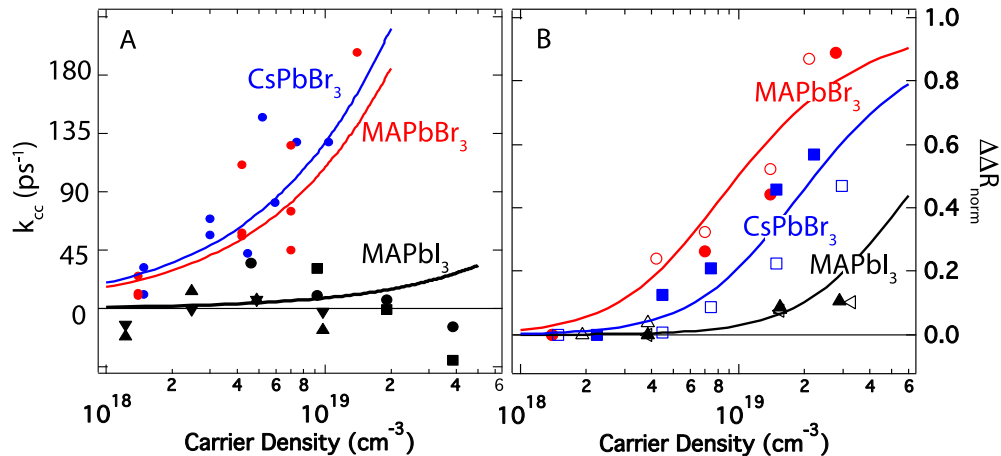


**Figure.** Small molecule BHJ consist of dithienosilole, TDS, based donor and PC<sub>61</sub>BM acceptor (left). Decomposition of the TR-EPR spectra (black-experimental, red-simulation)) for ISC triplet exciton (green), BET triplet exciton (orange), and ISC triplet exciton residing on PC<sub>61</sub>BM (blue).

## Halide Substitution Modulates Screening in Lead Halide Perovskites

Casey L. Kennedy, Andrew H. Hill, Erik M. Grumstrup  
Department of Chemistry and Biochemistry  
Montana State University  
Bozeman, MT 59717

We have examined the effects of halide substitution on charge transport and recombination in individual LHP domains using transient absorption microscopy. We find that, in contrast to methylammonium lead triiodide (MAPbI<sub>3</sub>), the diffusion coefficient of MAPbBr<sub>3</sub> is reduced significantly at high excitation densities due to carrier-carrier scattering (Panel A). Measurements performed on CsPbBr<sub>3</sub>, in which the A-site cation had been substituted, show similar behavior as MAPbBr<sub>3</sub>. Fits to the density-dependent diffusion data suggests that the effective dielectric, which screens Coulomb interactions for the mobile charge carriers, is smaller in the bromide perovskites ( $\epsilon \sim 12$ ) by a factor of 2-3 than in the iodide perovskites ( $\epsilon \sim 30$ ). The effective dielectric in MAPbBr<sub>3</sub> and CsPbBr<sub>3</sub> is also a factor of 3-5 lower than previously measured values of the static dielectric, suggesting that mobile carriers are descreened relative to the static limit at room temperature. Behavior consistent with these results is apparent in the recombination dynamics as well. Because nonlinear recombination mechanisms (Auger, radiative) proceed via pairwise interaction of charge carriers in the lattice, it would be expected that such mechanisms would play a larger role for bromide perovskites (with a lower effective dielectric) than for iodide perovskites (with a larger dielectric). Transient absorption kinetics collected on individual perovskite domains confirm this expectation. In (Cs or MA)PbBr<sub>3</sub>, a larger fraction of the excited state population decays via nonlinear recombination than in MaPbI<sub>3</sub> as carrier density is increased (Panel B).



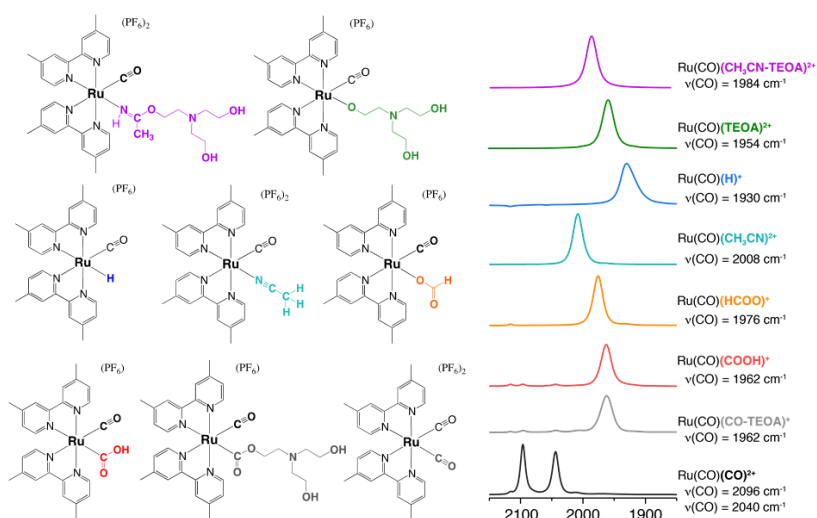
## Roles of Triethanolamine in Photochemical CO<sub>2</sub> Reduction with [Ru(dmb)<sub>2</sub>(CO)<sub>2</sub>]<sup>2+</sup> and Ru(II)-Ru(II) Supramolecular Systems

R. N. Sampaio, D. C. Grills, D. E. Polyansky, and E. Fujita

Chemistry Division, Brookhaven National Laboratory, Upton, NY 11973-5000, USA

A supramolecular assembly in which Ru(II) photosensitizer and Ru(II) catalyst units are connected by an ethylene linker is among the most effective and robust photocatalysts for CO<sub>2</sub> reduction to produce formate.<sup>1</sup> While time-resolved infrared spectroscopy is a powerful tool for investigating the kinetics of electron transfer and chemical transformations at the catalyst subunit, interpretation of the results requires knowledge of the possible catalytic intermediates. Therefore, we investigated the electrochemical and spectroscopic characterization of [Ru(dmb)<sub>2</sub>(CO)X]<sup>n+</sup> (dmb = 4,4'-dimethyl-2,2'-bipyridine, X = CO, CH<sub>3</sub>CN with n = 2; X = HCOO, COOH, H with n = 1) together with the photochemical reaction in Ar- and CO<sub>2</sub>-saturated CH<sub>3</sub>CN solution containing 1,3-dimethyl-2-phenyl-2,3-dihydro-1*H*-benzo[*d*]imidazole (BIH) as an electron donor and triethanolamine (TEOA) as a proton relay. When we know the properties of the possible intermediates of Ru mononuclear catalysts, that knowledge can be translated into the study of the supramolecular catalysts in the BIH/TEOA/CH<sub>3</sub>CN solution.

Electrochemical reduction of a series of Ru(dmb)<sub>2</sub>(CO)X<sup>n+</sup> (X = CO, CH<sub>3</sub>CN, HCOO) in TEOA-containing CH<sub>3</sub>CN solutions shows that the starting complexes convert to Ru(dmb)<sub>2</sub>(CO)H<sup>+</sup> under Ar. Furthermore, we found that TEOA itself reacts with CO<sub>2</sub> to form a Zwitterion, <sup>−</sup>O<sub>2</sub>C−OCH<sub>2</sub>CH<sub>2</sub>N<sup>⊕</sup>H(CH<sub>2</sub>CH<sub>2</sub>OH)<sub>2</sub> with *K*<sub>eq</sub> = 0.07 M<sup>−1</sup> in CH<sub>3</sub>CN. CO<sub>2</sub> insertion into one-electron reduced Ru−H is much faster with the Zwitterion. At this



meeting, we will discuss results with the mononuclear ruthenium carbonyl catalyst during the photocatalytic reduction of CO<sub>2</sub> and how the presence of TEOA impacts the formation of reaction intermediates. An important finding was that TEOA – a commonly used sacrificial electron donor in homogeneous photochemical experiments – plays a crucial role in CO<sub>2</sub> capture and formate selectivity.

We thank Dr Y. Tamaki and Prof. O. Ishitani at Tokyo Institute of Technology for providing us with the Ru(II)-Ru(II) supramolecular catalysts.

1. Tamaki, Y.; Ishitani, O. Supramolecular Photocatalysts for the Reduction of CO<sub>2</sub> *ACS Catal.* **2017**, *7*, 3394-3409.

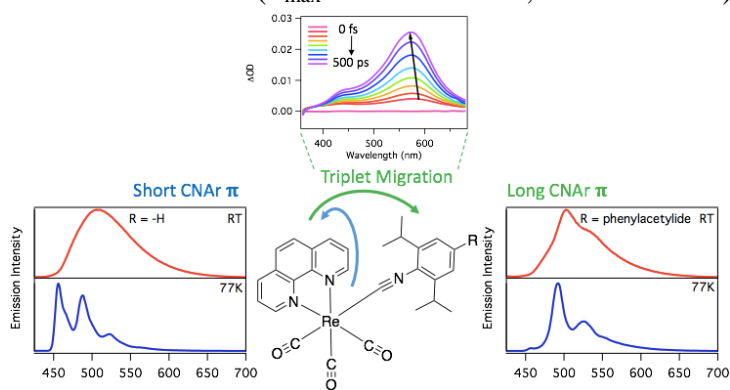
## Extremes in Photophysical Behavior from Re(I) MLCT Excited States

Hala Atallah, Chelsea M. Taliaferro, Joseph M. Favale, and Felix N. Castellano\*

Department of Chemistry  
North Carolina State University  
Raleigh, NC 27695-8204

A series of four transition metal complexes based on the Re(I) tricarbonyl phen template, with a lone ancillary arylisocyanide ligand (CNAr) were synthesized, yielding metal-organic chromophores of the generic molecular formula  $[\text{Re}(\text{phen})(\text{CO})_3(\text{CNAr})]^+$ . This series features varied degrees of  $\pi$ -conjugation length in the CNAr moiety, resulting in significant modulation in the resultant photophysical properties. All molecules possess long-lived (8 to 700  $\mu\text{s}$  at RT) and strongly blue-green photoluminescent excited states ( $\lambda_{\text{max}} = 500\text{-}518\text{ nm}$ ,  $\Phi = 14\text{-}64\%$ ).

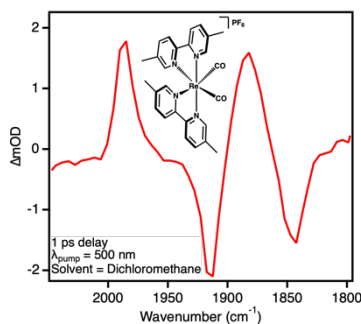
These chromophores have been photophysically investigated using static and dynamic spectroscopic techniques, the latter probed from ultrafast to supra-nanosecond time scales using transient absorption and photoluminescence. The combined experimental evidence, along with electronic structure calculations, illustrate that the arylisocyanide ligand is actively engaged in



manipulating excited state decay in three of these molecules, wherein the triplet metal-to-ligand charge transfer ( $^3\text{MLCT}$ ) state along with two distinct triplet ligand-centered ( $^3\text{LC}$ ) excited state configurations (phen and arylisocyanide) conspire to produce the resultant photophysical properties. A pair of molecules in this series also feature unique examples of inorganic excimer formation as evidenced by dynamic self-quenching in the corresponding photoluminescence intensity decays accompanied by the observation of a short-lived low-energy emission feature.

A comprehensive series of nine Re(I) diimine dicarbonyl complexes of the general molecular formula  $\text{cis-}[\text{Re}(\text{N}^{\wedge}\text{N})_2\text{CO}_2]^+$  were prepared and studied to systematically evaluate the photophysical consequences of various substituents resident on the diimine ligands ( $\text{N}^{\wedge}\text{N} = 2,2'$ -bipyridine and 1,10-phenanthroline derivatives). These panchromatic chromophores were structurally characterized, evaluated for their electrochemical and spectroelectrochemical properties, and finally investigated using static and dynamic photoluminescence, absorbance, and infrared spectroscopy from ultrafast to supra-nanosecond time scales. This presentation will detail these combined experimental results that report on the ultrafast

dynamics of this class of molecules for the first time using both electronic and vibrational spectroscopy. The MLCT excited state decay of these dicarbonyl molecules appears completely consistent with energy gap law behavior and the reduction in the number of CO subunits significantly attenuates nonradiative decay with respect to the tricarbonyl analogs.



## Kinetic Dispersion and Lateral Interactions Detected in Ferrocene-Modified Amorphous Carbon Electrodes Arise from Inherent Disorder in Carbon Materials

Jillian L. Dempsey, Debanjan Dhar, Brittany Huffman, Matthew Lockett,  
and Catherine McKenas  
Department of Chemistry  
University of North Carolina  
Chapel Hill, NC 27599-3290

Ultimately, molecular catalysts for fuel production must be integrated with photon-capturing materials for the generation of solar fuels. In addition to efficiently coupling light-harvesting and fuel-production, immobilization confines catalysts to the electrode surface, such that all catalysts are active. While recent work in the field has demonstrated that catalysts can be anchored to electrode and photoelectrode surfaces, the lack of accessible methodologies for characterizing kinetics and mechanism of surface-immobilized species has prevented rigorous quantification of their catalytic activity. To address this, recent work in our lab has focused on applying electroanalytical methods to quantify electron transfer and proton-coupled electron transfer reactivity of surface-anchored molecules. This poster will describe the chemical functionalization of amorphous carbon electrodes with ferrocene and characterization of interfacial electron transfer in these modified electrodes.

Ferrocene-modified amorphous carbon electrodes have been prepared via an *in situ* Grignard reaction with chlorine-terminated amorphous carbon films. Cyclic voltammograms of the ferrocene-modified carbon electrodes (Fc-(CH<sub>2</sub>)<sub>6</sub>-aC) show that surface coverages of up to  $1.2 \times 10^{-9}$  mol/cm<sup>2</sup> can be obtained. Plots of peak current vs. scan rate are anticipated to be linear for a surface-bound species, but data for the Fc-(CH<sub>2</sub>)<sub>6</sub>-aC electrodes exhibit curvature (Fig. 1). The extent of curvature varies as a function of surface coverage, suggesting non-uniform lateral interactions between the ferrocene groups across the film surface.

The aC-ferrocene electron transfer kinetics were quantified by both cyclic voltammetry and chronoamperometry. These data indicate a dispersion of heterogeneous electron transfer rate constants. Kinetic dispersion can arise from a distribution of monolayer structures that induce non-uniform ferrocene-ferrocene interactions. All together, these data suggest that ferrocene-modified amorphous carbon electrodes have a non-random surface distribution of electroactive ferrocene species, arising from the inherent disorder of the amorphous carbon films.

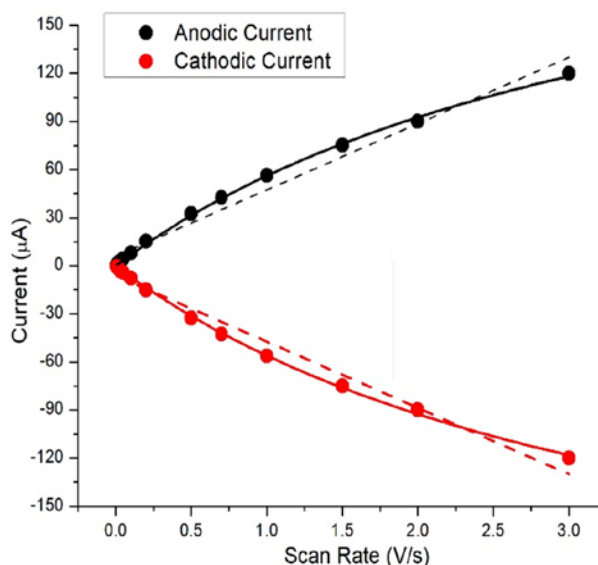


**Figure 1.** Peak current vs. scan rate for Fc-(CH<sub>2</sub>)<sub>6</sub>-aC electrodes show substantial curvature, indicative of non-uniform lateral interactions between ferrocene groups.

## Development of Robust Plasmonic and Excitonic Nanostructures for Investigation of Energy Conversion Dynamics in Hybrid Plexcitonic Model Systems

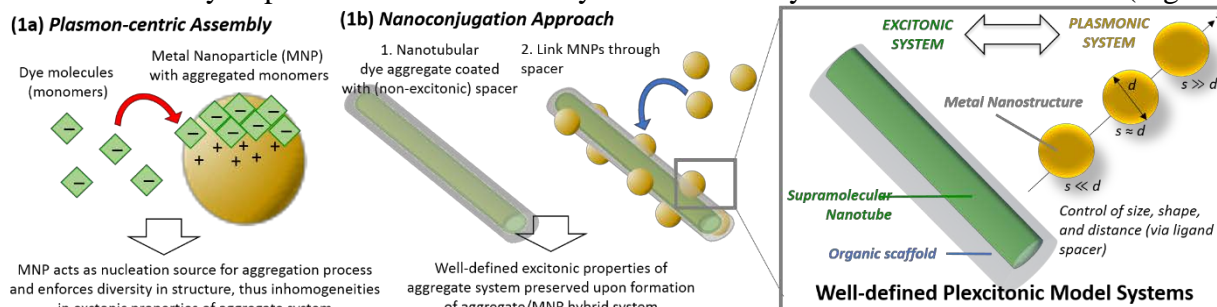
Christopher W. Leishman<sup>1</sup>, Nikunj Kumar Visaveliya<sup>1</sup>, Kara Ng<sup>1</sup>, Pooja Gaikwad<sup>1</sup>,  
Amedee des Georges<sup>2</sup>, Alexander Govorov<sup>3</sup>, and Dorthe M. Eisele<sup>1</sup>

(1) Chemistry, The City College of New York of The City University of New York (CUNY);

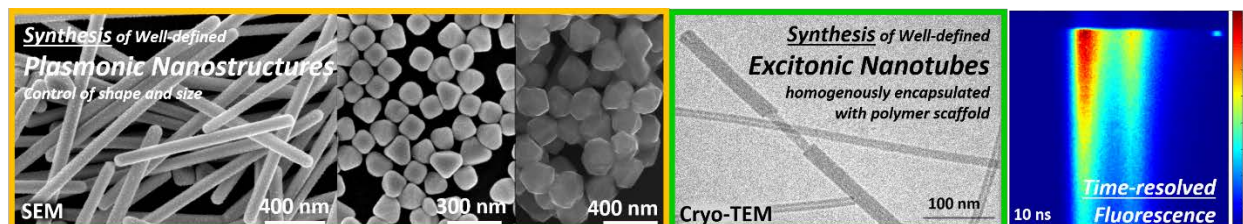
(2) Structural Biology Initiative, CUNY Advanced Science Research Center (ASRC);

(3) Physics, Ohio University at Athens

**Project's Motivation and Scope.** Excitonic and plasmonic nanoscale systems in close proximity show high potential for significant breakthroughs in energy related materials research. The interactions between these two kinds of nanostructures result in coupled optical transitions (plexcitons) having novel properties distinct from those of both excitons and plasmons or from the sum of their constituents (synergistic effects). The project's scope is to understand plasmon-exciton interactions in nanoscale systems with a focus on ultrafast dynamic aspects and the role of the hybrid system's architecture (*i.e.* shape and size of plasmonic nanostructure and its separation from the excitonic nanostructure). In contrast to recent research efforts, our project aims at a concerted treatment of hybrid nanosystems by bringing together both *Materials Research* and *Physical Research* approaches. To this end, we take a distinct approach to the material synthesis. Our research builds upon the classical *Plasmon-centric assembly* approach (Fig. 1a). We develop a *Nanoconjugation* approach for the synthesis of Hybrid Plexcitonic Model Systems: both components—the excitonic system and the plasmonic system—are treated on an even footing: in solution, the two components are synthesized separately, then functionalized by a spacer material and finally electrostatically linked with one another (Fig. 1b).



**Recent Key Results.** We developed methods for well-defined nanostructure synthesis, providing access to a diverse library of plasmonic nanostructures with morphology-controlled core-shell metal nanoparticles (*e.g.* Au@Ag, Au@Ag@Au, *etc.*) with tuned size, plasmon shift, and surface property tunability as well as with controlled shape (*e.g.* triangular prism, nanocube, pentagonal, hexagonal, octagonal, and elongated rods of different aspect ratios). We encapsulated excitonic nanotubes with a homogenous polymer scaffold (with tunable thickness) without altering the delicate supramolecular structure nor the exciton dynamics, but substantially increasing the system's stability as also revealed by our proof-of-concept dye-sensitized solar cell devices.



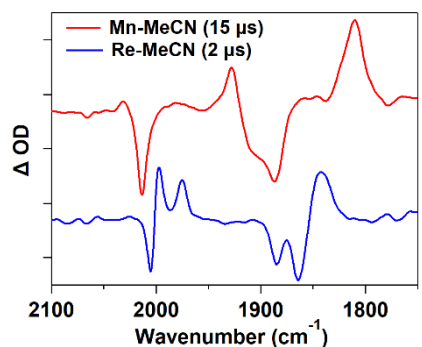
# Mechanistic Studies of Synergistic Metal-Ligand Cooperativity Promoted by a Ligand-Based Redox Couple

David C. Grills, Mehmed Z. Ertem, Etsuko Fujita

Chemistry Division, Brookhaven National Laboratory, Upton, NY 11973-5000

Mn- and Re-based polypyridyl complexes exhibit excellent activity and product selectivity for the photo- and electro-catalytic reduction of CO<sub>2</sub> to CO and/or formate. Following reductive activation of the precatalyst and CO<sub>2</sub>/H<sup>+</sup> binding, the catalytic cycle typically proceeds with the input of another electron, followed by proton-induced C–OH bond cleavage (*reduction-first* pathway). While the inverse, *protonation-first*, pathway requires less overpotential, it is rarely observed. In recent work on a Mn-based precatalyst,<sup>1</sup> we introduced Brønsted basic methoxy groups into the second coordination sphere of a sterically-bulky substituted bipyridyl (bpy) ligand. Their electronic influence, together with a weak allosteric hydrogen-bonding interaction, lowered the activation barrier for C–OH bond cleavage, providing access to the desirable *protonation-first* pathway, and saving up to 0.55 V in overpotential.

More recently,<sup>2</sup> we investigated electrocatalytic CO<sub>2</sub> reduction with [M(Me<sub>2</sub>OQN)(CO)<sub>3</sub>(CH<sub>3</sub>CN)] (Me<sub>2</sub>OQN<sup>−</sup> = 5,7-dimethyl-8-oxyquinolate; M = Mn (**Mn-MeCN**) or Re (**Re-MeCN**)). The non-innocent Me<sub>2</sub>OQN<sup>−</sup> ligand imparts unique behavior. For example, the onset of catalytic current is initiated with the input of one less equivalent of electrons relative to the bpy-based analogs. For **Re-MeCN**, this is attributed to the formal Me<sub>2</sub>OQN<sup>(•/−)</sup> redox couple contributing to each catalytic cycle in tandem with the formal Re<sup>(I/0)</sup> redox couple, facilitating in-situ generation of the active catalyst *upon one-electron reduction*. In contrast, **Mn-MeCN** requires a second reduction to activate the catalyst. However, in both cases the electron-rich Me<sub>2</sub>OQN<sup>−</sup> ligand facilitates a *protonation-first* pathway, thus representing a rare example of inner coordination sphere effects being used to access the *protonation-first* pathway. Several techniques, including pulse radiolysis coupled with time-resolved infrared spectroscopy (PR-TRIR), were used to gain structural insight into the electronic properties of the reduced



intermediates. In acetonitrile, the one-electron reduced form of **Re-MeCN** was shown to exist as an equilibrium mixture of the solvated complex, [Re-MeCN]<sup>•−</sup> and the five-coordinate species, [Re]<sup>•−</sup>, while for the Mn complex it exists mainly in the five-coordinate form, [Mn]<sup>•−</sup> (see PR-TRIR data to left). Chemical (Na/Hg) reduction in THF indicates that in this less coordinating solvent, the one-electron reduced Re complex exists mainly in the five-coordinate form, [Re]<sup>•−</sup>, which we will exploit to characterize the metallocarboxylate species, [Re-CO<sub>2</sub>]<sup>•−</sup>, by PR-TRIR in CO<sub>2</sub>-saturated THF.

1. Ngo, K. T.; McKinnon, M.; Mahanti, B.; Narayanan, R.; Grills, D. C.; Ertem, M. Z.; Rochford, J. *J. Am. Chem. Soc.* **2017**, *139*, 2604-2618.
2. McKinnon, M.; Ngo, K. T.; Sobottka, S.; Sarkar, B.; Ertem, M. Z.; Grills, D. C.; Rochford, J. *Organometallics* **2019**, *38*, 1317-1329.

**Acknowledgments:** We thank our collaborator, Prof. Jonathan Rochford (U. Mass, Boston), for the synthesis of precatalysts and their electrochemical analysis.

## Molecular Photoelectrocatalysts for Hydrogen Evolution

Bethany M. Stratakes, Tianfei Liu, Dean Bass and Alexander J. M. Miller  
Department of Chemistry  
University of North Carolina at Chapel Hill  
Chapel Hill, NC 27599-3290

Metal hydride complexes that directly absorb visible light to drive fuel-forming chemical reactions represent an intriguing class of molecules relevant to solar fuel synthesis. This project seeks to identify hydride complexes that can be generated electrochemically at mild potentials and that are capable of photochemical H<sub>2</sub> release or hydride transfer reactions. Promising candidates undergo photoelectrocatalytic testing and mechanistic examination to better understand the molecular design principles that enable photon-to-fuel energy storage.

A mechanistic study of the prototypical molecular photoelectrocatalyst, [Cp\*Ir(bpy)H]<sup>+</sup>, revealed a unique bimolecular “self-quenching” mechanism for H<sub>2</sub> evolution, which inspired the synthesis of a new generation of tethered bimetallic catalysts. Structure-function studies varying the linker revealed competing intra- and intermolecular H<sub>2</sub> release pathways, along with an intriguing array of aggregation phenomena that influence photoelectrocatalysis in water, Fig. 1.

Time-resolved spectroscopic studies are being undertaken to elucidate mechanistic differences between monometallic and bimetallic systems. While the monometallic system undergoes rate-limiting bimolecular electron transfer, fast intramolecular electron transfer in the bimetallic systems opens the door for interrogating reactive intermediates. Time-resolved UV-vis, IR, and X-ray absorption spectroscopies are enabled by a method for regenerating the hydride after each laser pulse, Fig. 2.

Recent research has focused on directing photochemistry towards hydride transfer. In one strategy, a catalyst is supported on mesoporous *nano*-ITO in order to disfavor bimetallic H<sub>2</sub> evolution pathways. Photoelectrocatalytic activity in water is retained, however, revealing a new *monometallic* H<sub>2</sub> release mechanism. Future studies will target hydride transfer in aprotic solvents. Another strategy uses a hydride acceptor as the solvent suppress H<sub>2</sub> evolution and promote hydride transfer. In dichloromethane solution, selective hydride transfer occurs to produce chloromethane.

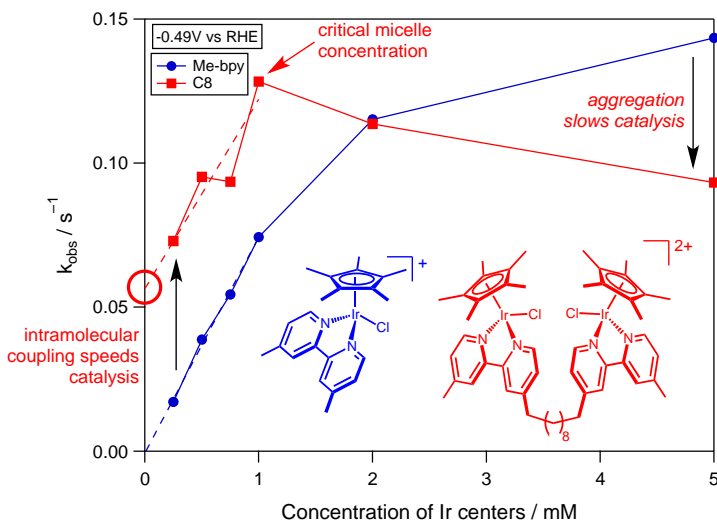


Fig. 1. Influence of competing pathways and aggregation on the rate constant ( $k_{\text{obs}}$ ) of H<sub>2</sub> evolution in aqueous photoelectrocatalysis.

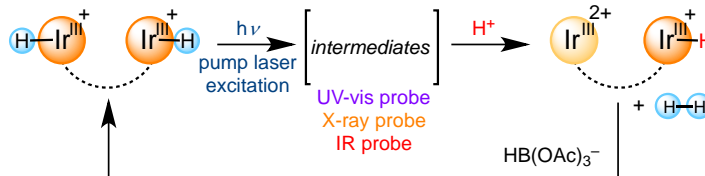


Fig. 2. Strategy for regeneration in time-resolved spectroscopies.

# Coherences in Photoinduced Electron Transfer Reaction: A Mechanistic Insight

Shahnawaz Rafiq, Bo Fu, Gregory D. Scholes  
Department of Chemistry  
Princeton University  
Princeton, NJ and 08544

Electron transfer is a ubiquitous process whose mechanism and dynamics are relevant to applications such as solar cells, molecular electronic devices, and various photoactivated processes. The past decade has seen tremendous advances in the possible role of quantum coherent effects in the photoinduced electron transfer processes in chemical, biological, and materials systems. The prevalence of such coherence effects holds a promise to increase efficiency and robustness of transport even in the face of strong energetic disorder. Coherence in electron transfer is firmly connected to adiabaticity, environment fluctuations and their timescales, intramolecular vibrations, so exploring these parameters could help us in first identifying the presence of coherent effects and then their potential functional relevance.

One of the bottlenecks in understanding the potential functional relevance of quantum coherent effects in solar photochemistry is identifying the experimental signature of the true coherent effect. So far, a rudimentary approach for such a correlation has been the observation of oscillatory time-domain signal in multi-pulse experiments. In our recent work on a donor-acceptor electron transfer system, oscillatory vibrational signatures act as a probe to report that the product of an electron transfer reaction can be *formed vibrationally coherent* even when *no coherence is generated in the reactant state*. This observation, wherein photoinduced electron transfer reaction itself creates a nonstationary vibrational wavepacket—possibly along a mode constituting the reaction coordinate—from a thermal population is proposed to be a *unique signature* of the coherent formation of an electron transfer product. Results supporting this claim will be discussed in the light of resonant mixing of the reactant-product diabatic states, electronic coupling, and ensuing evolution of the coherently generated wavepacket along different vibrational levels of an anharmonic potential. This work has strong implications towards understanding the role of coherences in that it provides a tangible signature of the coherently generated photoinduced electron transfer product in the presence of strong energetic disorder due to large reorganization energy.

In parallel with experimental effort, we are addressing and revisiting two fundamental problems about electron transfer reactions using a variety of state-of-the-art theoretical tools. One is in that how the coherence participates in the photo-induced electron transfer processes across a prototypical donor-bridge-acceptor system, where the role of high-frequency intramolecular vibrational mode will be highlighted and the number of bridge sites will be varied to explore a crossover from strong to weak electronic coupling between the donor and the acceptor. The second theoretical effort is to reveal the dephasing of the reactive mode wavepacket during a curve crossing process which has been widely recognized when monitoring the ultrafast electron transfer processes using pump-probe type techniques. These insights will help us understand the functional relevance of coherences in solar photochemistry.

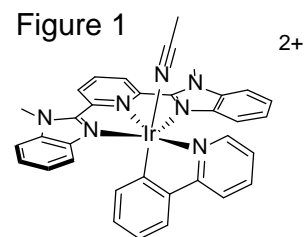
## Precise Mechanisms of CO<sub>2</sub> to CO Conversion Catalyzed by Iridium(III) Phenyl-Pyridine Photo- and Electrocatalysts

Gerald F. Manbeck, Mehmed Z. Ertem, Dmitry E. Polyansky, and Etsuko Fujita  
Chemistry Division, Energy & Photon Sciences Directorate  
Brookhaven National Laboratory  
Upton, NY 11973-5000

Pairing of light harvesting chromophores with molecular catalysts for multielectron small molecule transformations is a challenge in solar fuel production. A drastic simplification can be realized in the case of “self-sensitized” photocatalysis; however, efficient examples remain rare due to the limited number of transition metal complexes with the ability to function in visible light absorbing and catalytic capacities. Improvements in efficiencies among self-sensitized CO<sub>2</sub> reduction catalysts can be guided by thorough mechanistic investigations.

Iridium complexes supported by a planar tridentate ligand such as 2,2':6',2''-terpyridine (tpy) and an ortho-metallated 2-phenyl pyridine ligand (ppy), i.e. [Ir(tpy)(ppy)(CH<sub>3</sub>CN)]<sup>2+</sup>, represent recently discovered self-sensitized photocatalysts that reduce CO<sub>2</sub> selectively to CO with high quantum efficiency.<sup>1</sup> Unfortunately, the high initial efficiencies are counteracted by limited turnovers under many conditions. Recent reports have pursued the roles of isomerization, polymetallic interactions, and effect of light intensity on catalyst durability; however, many of the precise mechanistic steps and the deactivation pathways remain elusive.<sup>2,3</sup>

This poster will present detailed mechanisms of catalysis using a related complex, [Ir(bip)(ppy)(CH<sub>3</sub>CN)]<sup>2+</sup>, (bip = 2,6-bis(1-methyl)-1*H*-benzo[*d*]imidazole-2-yl)pyridine) (Figure 1), which is a modest photocatalyst, but provides well-defined voltammograms under catalytic conditions. Electrochemical investigations reveal the rate dependence on [Ir], [CO<sub>2</sub>], and [H<sub>2</sub>O], and illuminate several catalytic regimes whose mechanisms depend on the applied potential, the protonation state of intermediates, and the role of CO<sub>2</sub> or protons as the oxide acceptor in cleavage of a metallocarboxylate intermediate to form a metallocarbonyl complex. Selectivity for CO<sub>2</sub> reduction over proton reduction is maintained at water concentrations up to 30%; however, the formation of a hydride-bridge dimer is revealed as a deactivation pathway under these conditions. Our mechanistic proposals are supported by theoretical modeling of each pathway, by high resolution mass spectrometry, spectroelectrochemical infrared spectroscopy, and by X-ray absorption spectroscopy for characterization of catalyst electronic states. Based on these mechanistic details, we propose several catalyst designs to accelerate catalysis while prolonging longevity.



<sup>1</sup>Sato, S.; Morikawa, T.; Kajino, T.; Ishitani, O. *Angew. Chem. Int. Ed.* **2013**, 52, 988.

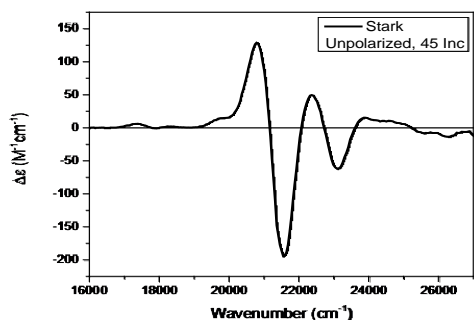
<sup>2</sup>Garg, K.; Matsubara, Y.; Ertem, M. Z.; Lewandowska-Andralojc, A.; Sato, S.; Szalda, D. J.; Muckerman, J. T.; Fujita, E. *Angew. Chem. Int. Ed.* **2015**, 54, 14128.

<sup>3</sup>Manbeck, G. F.; Garg, K.; Shimoda, T.; Szalda, D. J.; Ertem, M. Z.; Muckerman, J. T.; Fujita, E.; *Faraday Discuss.*, **2017**, 198, 301-317.

# Electron Transfer Dynamics in Efficient Molecular Solar Cells

Andrew Maurer, Eric Piechota, Victoria Davis, and Gerald J. Meyer  
Department of Chemistry  
University of North Carolina at Chapel Hill  
Chapel Hill, NC 27599

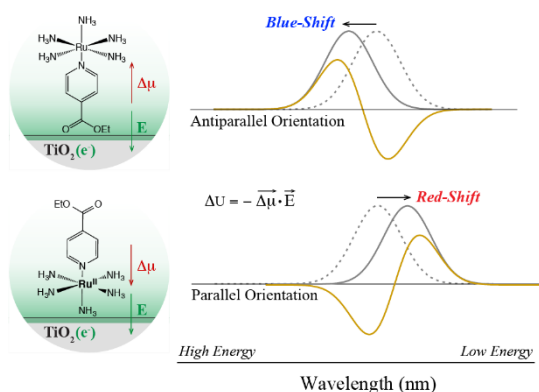
An objective of this Department of Energy supported research is to provide new mechanistic insight into surface mediated photochemical reactions at molecular-semiconductor interfaces. Our current research is focused on the role surface electric fields play in dye-sensitized electron transfer at oxide semiconductor interfaces. The surface fields are generated by excited state injection, electrochemical reduction, molecular dipoles, and/or ion surface adsorption. Molecular dyes report on the field magnitude and direction in a manner reminiscent of that used in traditional Stark spectroscopy. Pulsed laser excitation has been particularly valuable as it allows kinetic data for ion-migration (screening) and dye reorientation that occur in response to the transient electric field.



This poster presents a study designed to quantify the electric field created by excited state injection into TiO<sub>2</sub>. An early conclusion was that the electric field magnitude reported by dyes with carboxylic acid groups was larger than that for dyes with phosphonic acid binding groups. In this analysis, it was tacitly assumed that the photo-induced change in dipole moments was the same for the dyes. Hence an alternative interpretation is that the carboxylic acid containing dye simply has a larger dipole moment change upon light absorption. To distinguish between these possibilities, and to quantify dipole moment changes

for a wider variety of dyes, a traditional Stark apparatus has been constructed. Stark spectra like that shown display the expected second-derivative shape that yield dipole moments consistent with previous literature reports. Preliminary data indicates that the phosphonate groups are in fact better able to screen local fields than are carboxylate groups.

The compound [Ru(NH<sub>3</sub>)<sub>5</sub>(eina)]<sup>2+</sup> binds to TiO<sub>2</sub> weakly by either H bonding, with the amine groups, or through the ethyl ester group of the eina ligand shown. Pulsed light excitation results in spectral changes consistent with the dye flipping over. Interestingly, when the field was removed the dye molecules flip back over with dynamics that were time resolved. While an extensive literature exists for electric field 'poling' in polymers and liquid crystals, to our knowledge this represents the first demonstration of related behavior at a semiconductor interface. The implications of these findings for solar energy conversion will be discussed.



# Surface Chemistry and Heterogeneous Processes in Solar-Driven Pyridine-Catalyzed CO<sub>2</sub> Reduction

Denis Potapenko, Ari Gilman, and Bruce E. Koel  
Chemical and Biological Engineering  
Princeton University  
Princeton, NJ 08544

The utilization of atmospheric CO<sub>2</sub> as a renewable feedstock for liquid fuels is an important part of developing a sustainable energy infrastructure and reducing humanity's impact on the global climate. There have been several reports of improved efficiency over the use of semiconducting photocathodes when a dissolved pyridine co-catalyst is employed in the photoelectrocatalytic reduction of CO<sub>2</sub>. Our work aims to improve our fundamental understanding of these photoelectrocatalytic systems through UHV surface science experiments and in situ and operando spectroscopies. More specifically, we hope to determine the electronic and geometric structures of adsorbates relevant to photoelectrocatalytic CO<sub>2</sub> reduction on surfaces of gallium phosphide (GaP), a model III-V compound semiconductor photocathode material. To this end we have first investigated clean GaP (111) and (110) surfaces through STM, LEIS, and LEED. We have found that cycles of sputtering and annealing the surfaces can produce droplets of pure Ga metal. However, these droplets do not significantly impact experimental results in UHV. We have also studied chemistries of several small molecule adsorbates on the GaP surfaces using TPD and XPS techniques, including water, hydrogen, formaldehyde, methanol, formic acid, and pyridine. Methanol has been the most thoroughly investigated, and the results from theoretical calculations (by E.A. Carter and coworkers), TPD, IRRAS, and APPES indicate the formation of an adsorbed paired methanol-methoxy complex (Fig. 1). We are also making progress toward the use of operando ATR-FTIR to investigate the mechanisms of heterogeneous electrochemical reactions and adsorbed intermediate species at the interface of the photocathode and the aqueous electrolyte solution. The goal of these operando ATR-FTIR experiments is to determine how pyridine helps to catalyze photoelectrochemical CO<sub>2</sub> reduction.

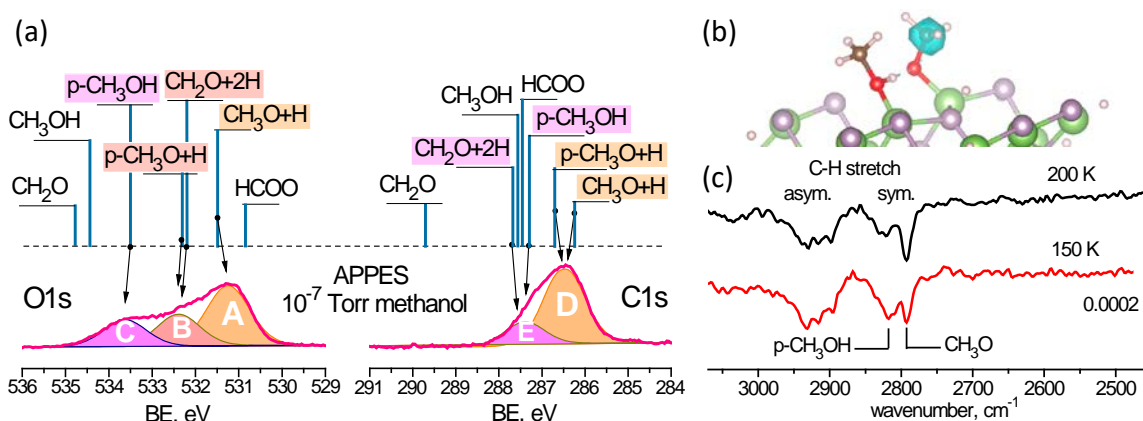


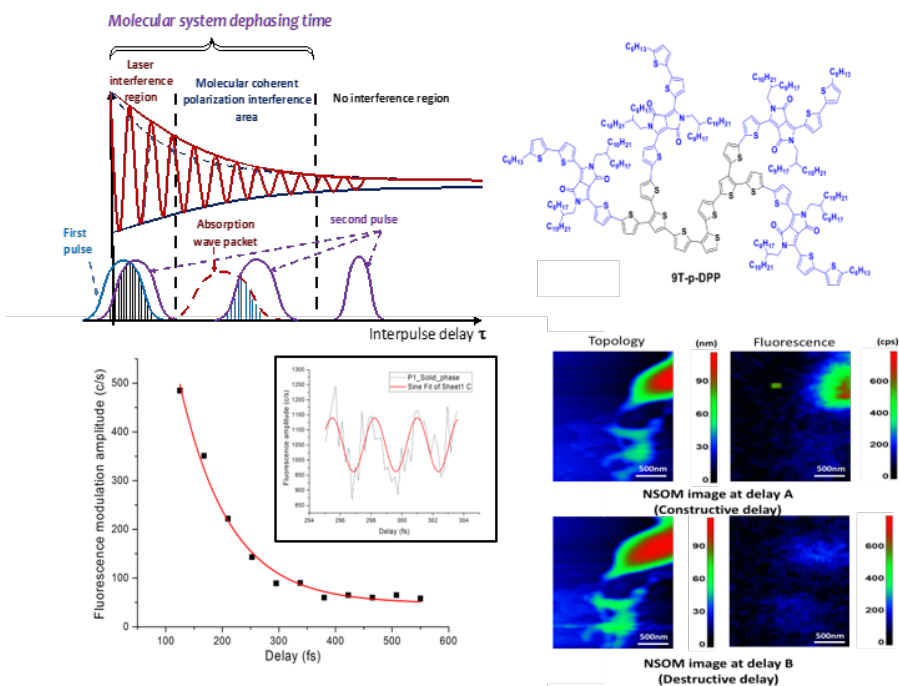
Figure 1. (a) APPES spectra from GaP(110) at 300 K in 10<sup>-7</sup> Torr methanol. Vertical lines above show the DFT calculated binding energies for various methanol-related surface species. (b) DFT-optimized paired methanol – methoxy complex (p-CH<sub>3</sub>OH – p-CH<sub>3</sub>O) on GaP(110) surface (by E.A. Carter and coworkers). (c) IRRAS spectra from methanol-saturated GaP(110) surface at 150 and 200 K.

# Coherent Energy and Charge Transport Processes in Photovoltaic Dendritic Molecular Systems Probed in Solution and in the Solid State

T. Goodson III

Department of Chemistry, Department of Macromolecular Science and Engineering, University of Michigan, Ann Arbor, Michigan 48109

This investigation is directed at the fundamental excitations in novel macromolecular organic materials towards efficient excitation transport and conversion performance. Dendritic molecules demonstrate a variety of directed excitation and electron transfer properties useful to photovoltaic applications. We have performed a time-resolved and nonlinear optical spectroscopy and microscopy of a novel organic dendrimer system in both solution and in the solid state. A functionalized oligothiophene dendritic system diketopyrrolopyrrole (DPP) groups was used in this study to probe intra- and inter-molecular energy and charge transfer properties of the three-dimensional macromolecular system in solution and in thin films. Linear and non-linear steady state analysis, fs-transient absorption, ultrafast fluorescence up-conversion spectroscopy, three-pulse photon echo peak shift (3PEPS) and time-resolved nonlinear near-field scanning optical microscopy (NSOM) are discussed in regards of the degree of intra- and inter-molecular coupling in solution and in the solid state. The NSOM nonlinear two-pulse interferometry approach allowed for the investigation of femtosecond (fs) coherent transport effects and dephasing dynamics in the solid state films with spatial resolution of  $\sim 40\text{nm}$ . Both coherent and incoherent energy transfer processes were observed in dendritic systems. A detailed comparison of the excitation dynamics showed differences in coherent charge and energy transfer dynamics in the solid state compared to solution-phase.



# Energetic Effects of Hybrid Organic/Inorganic Interfacial Architecture on Nanoporous Black Silicon Photoelectrodes

Ryan T. Pekarek,<sup>1,3</sup> Steven T. Christensen,<sup>2</sup> Jun Liu,<sup>2</sup> and Nathan R. Neale<sup>1</sup>

<sup>1</sup>Chemical and Nanoscale Sciences Center, <sup>2</sup>Materials Science Center NREL, Golden, CO 80401

<sup>3</sup>Department of Chemistry, The University of Texas at Austin, 2506 Speedway STOP A5300, Austin, Texas 78712, United States

Photoelectrochemical cells have been the subject of great interest in the research community as a route for fuel formation directly from sunlight. Interfacial layers are frequently employed on the surface of light-absorbing semiconductor photoelectrodes to enhance the activity and stability of the semiconductor. In this study, we consider the energetic effects of such layers on a nanoporous ‘black’ silicon photocathode. We construct hybrid organic/inorganic films by growing an oxide-nucleating molecular monolayer on the nanostructured Si surface and burying this molecular monolayer under TiO<sub>2</sub> deposited by atomic layer deposition. We examine the energetic effects of this hybrid interfacial architecture via our recently developed intensity-modulated high-frequency resistivity (IMHFR) impedance spectroscopy technique and quantify the change in thermodynamic flatband potential ( $V_{fb}$ ) as the oxide thickness is increased from 0–15 nm.

By comparing the IMHFR data with traditional voltammetry, we are able to deconvolute the thermodynamic and kinetic contributions that determine the observed proton reduction onset potential. We also study these photoelectrodes with Pt nanoparticles either (i) deposited on top of the molecular/TiO<sub>2</sub> interfacial layer or (ii) etched into the Si surface. In the first architecture, a beneficial positive shift in the thermodynamic  $V_{fb}$  is achieved from the Si|molecular|TiO<sub>2</sub>  $p$ - $n$  junction, but the lack of a direct Si|Pt contact results in large kinetic charge transfer losses (Figure 1). In contrast, the second architecture allows for facile charge transfer due to the direct Si|Pt contact but negates any beneficial thermodynamic effect of the molecular/TiO<sub>2</sub> bilayer. Despite the lack of thermodynamic effect of the hybrid molecular/TiO<sub>2</sub> interfacial layer, we find that there is still a significant kinetic benefit from this layer. This work demonstrates the sensitive nature of the thermodynamics and kinetics on the interfacial architecture and yields critical insights into the design of photoelectrochemical interfaces.

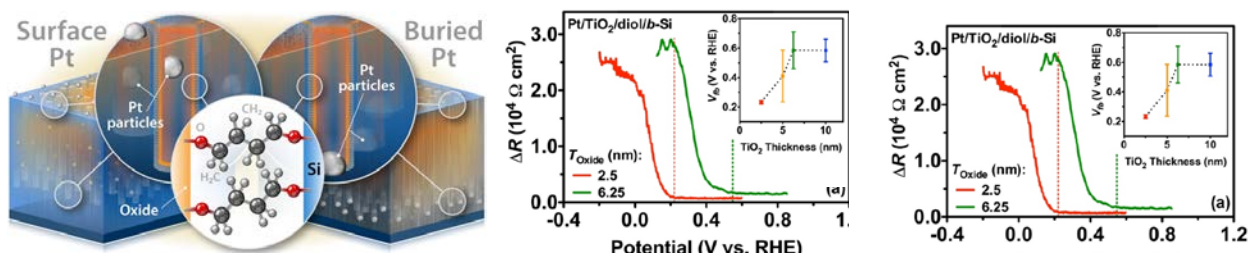


**Figure 1.** Left: The two architectures studied in this work: ‘Surface Pt’ (Pt/TiO<sub>2</sub>/diol/b-Si) and ‘Buried Pt’ (TiO<sub>2</sub>/diol/B-Pt/b-Si). Middle: Representative IMHFR plots of ‘surface Pt’ Pt/TiO<sub>2</sub> ( $x$  nm)/diol/b-Si where  $x = 2.5$  nm (red) and 6.25 nm (green). The inset depicts  $V_{fb}$  of samples where  $x = 2.5, 5, 6.25,$  and 10 nm. Right:  $\eta_{kin}$  ( $V_{fb} - V_{onset}$ ) of the samples shown in the middle panel.

R. T. Pekarek, S. T. Christensen, J. Liu, N. R. Neale, *Sustainable Energy & Fuels, Advance Article* (2019). <http://dx.doi.org/10.1039/C9SE00032A>

# Mechanistic Investigation of Oxygen Atom Transfer Pathway for Ru-based Water Oxidation Catalysts

Mehmed Z. Ertem, Javier J. Concepcion  
Chemistry Division, Energy & Photon Sciences,  
Brookhaven National Laboratory, Upton, NY 11973-5000

Water oxidation is at the heart of both natural and artificial photosynthesis. It is the ideal source of electrons and protons required to carry out reductive chemistry and store solar energy in the chemical bonds of the reduced products. Oxygen-Oxygen (O–O) bond formation is the key step of water oxidation as this first half of the reaction accounts for the larger part of the free energy requirement and catalytic rates are often limited by this step. Thus, a detailed mechanistic understanding of how it takes place is of paramount importance for the development of efficient water oxidation catalysts.

For Ru-based molecular water oxidation catalysts, water nucleophilic attack (WNA) (Fig. 1a) and interaction of two oxo moieties (I2M) (Fig. 1b) are well-established routes for O–O bond formation. The present work focuses on oxygen atom transfer (OAT) to nitrogen atoms of the coordinating ligands prior to O–O bond formation as an alternative pathway for catalytic oxygen evolution. We will present a detailed theoretical characterization of the electronic structures and energetics of competing O–O bond formation pathways (e.g., WNA and OAT) for  $[\text{Ru}(\text{dnp})(\text{py})_2(\text{OH}_2)]^{2+}$  (dnp = tetradentate 2-[6-(1,8-naphthyridin-2-yl)pyridin-2-yl]-1,8-naphthyridine and py is pyridine) complex (Figure 1c). The generality of OAT as an alternative pathway for O–O bond formation in water oxidation reactions will be discussed.

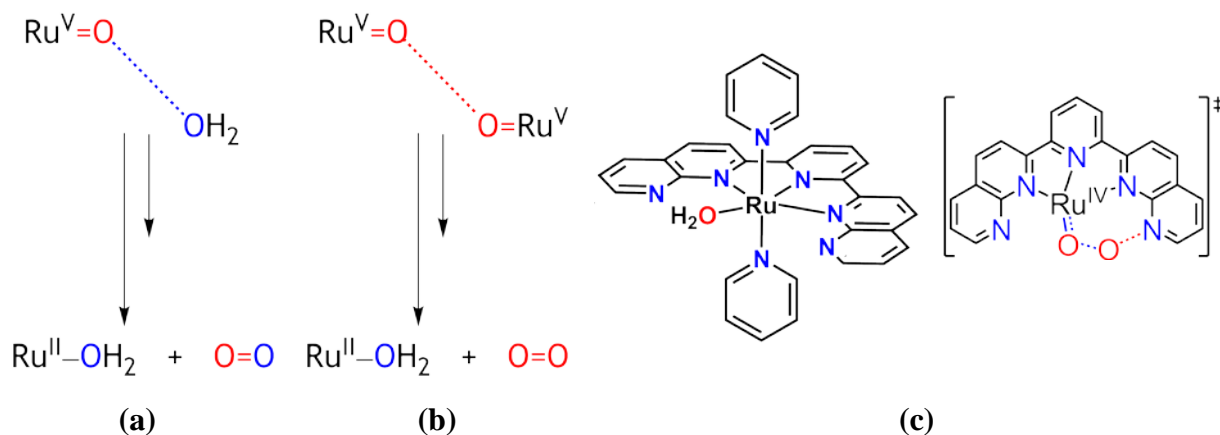


**Figure 1.** O–O bond formation via (a) water nucleophilic attack (WNA) and (b) interaction of two oxo moieties (I2M), (c)  $[\text{Ru}(\text{dnp})(\text{py})_2(\text{OH}_2)]^{2+}$  complex and oxygen atom transfer (OAT) route for O–O bond formation.

**Acknowledgments:** We thank Senior Chemist Emeritus James T. Muckerman (Brookhaven National Laboratory) for insightful discussions.

## Participant List – 41<sup>st</sup> Solar Photochemistry P.I. Meeting

Shane Ardo  
University of California, Irvine  
ardo@uci.edu

Neal Armstrong  
University of Arizona  
nra@email.arizona.edu

John B. Asbury  
Pennsylvania State University  
jasbury@psu.edu

Harry Atwater  
Caltech  
haa@caltech.edu

Robert A Bartynski  
Rutgers University  
bart@physics.rutgers.edu

Victor Batista  
Yale University  
victor.batista@yale.edu

Matt Beard  
National Renewable Energy Laboratory  
matt.beard@nrel.gov

David Beratan  
Duke University  
david.beratan@duke.edu

Louise Berben  
University of California Davis  
laberben@ucdavis.edu

Matt Bird  
Brookhaven National Laboratory  
mbird@bnl.gov

Jeff Blackburn  
National Renewable Energy Laboratory  
Jeffrey.blackburn@nrel.gov

David Bocian  
University of California, Riverside  
David.Bocian@ucr.edu

Shannon Boettcher  
University of Oregon  
swb@uoregon.edu

Stephen Bradforth  
University of Southern California  
bradfort@usc.edu

Kara Bren  
University of Rochester  
bren@chem.rochester.edu

Gary Brudvig  
Yale University  
gary.brudvig@yale.edu

Christine Caputo  
University of New Hampshire  
christine.caputo@unh.edu

Ian Carmichael  
Notre Dame Radiation Laboratory  
carmichael.1@nd.edu

Felix N. Castellano  
NC State University  
fncastel@ncsu.edu

Lin Chen  
Argonne National Lab/Northwestern Univ.  
lchen@anl.gov

Kyoung-Shin Choi  
University of Wisconsin  
kschoi@chem.wisc.edu

Javier J Concepcion  
Brookhaven National Laboratory  
jconcepc@bnl.gov

Bob Crabtree  
Yale University  
Robert.crabtree@yale.edu

Steve Cronin  
University of Southern California  
scronin@usc.edu

Jared Delcamp  
University of Mississippi  
delcamp@olemiss.edu

Jillian Dempsey  
University of North Carolina at Chapel Hill  
dempseyj@email.unc.edu

Dorthe M. Eisele  
CCNY-CUNY  
eisele@eiselegroup.com

Christopher Fecko  
DOE Office of Basic Energy Sciences  
christopher.fecko@science.doe.gov

Graham Fleming  
University of California, Berkeley  
grfleming@lbl.gov

Heinz Frei  
Lawrence Berkeley National Laboratory  
HMFrei@lbl.gov

Renee R Frontiera  
University of Minnesota  
rrf@umn.edu

Etsuko Fujita  
Brookhaven National Laboratory  
fujita@bnl.gov

Elena Galoppini  
Rutgers University-Newark  
galoppin@newark.rutgers.edu

Bruce Garrett  
DOE Office of Basic Energy Sciences  
bruce.garrett@science.doe.gov

Ted Goodson  
University of Michigan  
tgoodson@umich.edu

David Grills  
Brookhaven National Laboratory  
dcgrills@bnl.gov

Doug Grotjahn  
San Diego State University  
dbgrotjahn@sdsu.edu

Erik Grumstrup  
Montana State University  
erik.grumstrup@montana.edu

Lars Gundlach  
University of Delaware  
larsg@udel.edu

Devens Gust  
Arizona State University  
gust@asu.edu

Tom Hamann  
Michigan State University  
hamann@chemistry.msu.edu

Alex Harris  
Brookhaven National Laboratory  
alexh@bnl.gov

Dugan Hayes  
University of Rhode Island  
dugan@uri.edu

Craig L. Hill  
Emory University  
chill@emory.edu

Dewey Holten  
Washington University  
holten@wustl.edu

Frances A. Houle  
Lawrence Berkeley National Laboratory  
fahoule@lbl.gov

Libai Huang  
Purdue University  
libai-huang@purdue.edu

Joe Hupp  
Northwestern University  
j-hupp@northwestern.edu

Cynthia Jenks  
Argonne National Laboratory  
cjenks@anl.gov

Justin Johnson  
National Renewable Energy Laboratory  
justin.johnson@nrel.gov

Prashant  
University of Notre Dame  
pkamat@nd.edu

David Kelley  
"University of California, Merced"  
dfkelley@ucmerced.edu

Paul King  
National Renewable Energy Laboratory  
paul.king@nrel.gov

Christine Kirmaier  
Washington University  
kirmaier@wustl.edu

Victor Klimov  
Los Alamos National Laboratory  
klimov@lanl.gov

Bruce Koel  
Princeton University  
bkoel@princeton.edu

Todd Krauss  
University of Rochester  
krauss@chem.rochester.edu

Nate Lewis  
California Institute of Technology  
nslewis@caltech.edu

Gonghu Li  
University of New Hampshire  
gonghu.li@unh.edu

Tianquan Lian  
Emory University  
tlian@emory.edu

Jon Lindsey  
NC State University  
jlindsey@ncsu.edu

Ellen Matson  
University of Rochester  
matson@chem.rochester.edu

Elisa Miller-Link  
National Renewable Energy Laboratory  
elisa.miller@nrel.gov

Mark Lonergan  
University of Oregon  
lonergan@uoregon.edu

Stephen Maldonado  
University of Michigan  
smald@umich.edu

Tom Mallouk  
Penn State University  
tem5@psu.edu

Gerald Manbeck  
Brookhaven National Laboratory  
gmanbeck@bnl.gov

Dmitry Matyushov  
Arizona State University  
dmitrym@asu.edu

Jim McCusker  
Michigan State University  
jkm@chemistry.msu.edu

Gail McLean  
DOE Office of Basic Energy Sciences  
gail.mclean@science.doe.gov

Gerald Meyer  
University of North Carolina at Chapel Hill  
gjmeyer@email.unc.edu

Josef Michl  
University of Colorado  
josef.michl@colorado.edu

John R. Miller  
Brookhaven National Lab  
jrmiller@bnl.gov

Alex Miller  
University of North Carolina at Chapel Hill  
ajmm@email.unc.edu

Michael Mirkin  
Queens College-CUNY  
mmirkin@qc.cuny.edu

Tom Moore  
Arizona State University  
tmoore@asu.edu

Ana Moore  
Arizona State University  
amoore@asu.edu

Amanda Morris  
Virginia Tech  
ajmorris@vt.edu

Jim Muckerman  
Brookhaven National Laboratory  
muckerma@bnl.gov

Karen Mulfort  
Argonne National Laboratory  
mulfort@anl.gov

Jamal Musaev  
Emory University  
dmusaev@emory.edu

Nate Neale  
National Renewable Energy Laboratory  
nathan.neale@nrel.gov

Marshall Newton  
Brookhaven National Laboratory  
newton@bnl.gov

Daniel Nocera  
Harvard University  
dnocera@fas.harvard.edu

Arthur J Nozik  
"University of Colorado, Boulder and  
NREL"  
anozik@q.com

Colin Nuckolls  
Columbia University  
cn37@columbia.edu

Frank Osterloh  
University of California Davis  
fosterloh@ucdavis.edu

Bruce Parkinson  
University of Wyoming  
bparkin1@uwyo.edu

John W. Peters  
Washington State University  
jw.peters@wsu.edu

Oleg Poluektov  
Argonne National Laboratory  
Oleg@anl.gov

Dmitry Polyansky  
Brookhaven National Lab  
dep@bnl.gov

Oleg Prezhdo  
University of Southern California  
prezhdo@usc.edu

Sylwia Ptasinska  
Notre Dame Radiation Laboratory  
sptasins@nd.edu

Jeff Pyun  
University of Arizona  
jpyun@email.arizona.edu

Garry Rumbles  
National Renewable Energy Laboratory  
garry.rumbles@nrel.gov

Scott Saavedra  
University of Arizona  
saavedra@email.arizona.edu

Charles Schmuttenmaer  
Yale University  
charles.schmuttenmaer@yale.edu

Greg Scholes  
Princeton University  
gscholes@princeton.edu

Lance Seefeldt  
Utah State University  
lance.seefeldt@usu.edu

Diane Smith  
San Diego State University  
dksmith@sdsu.edu

Ming Lee Tang  
"University of California, Riverside"  
mltang@ucr.edu

Michael Therien  
Duke University  
michael.therien@duke.edu

Mark Thompson  
University of Southern California  
met@usc.edu

Randy Thummel  
University of Houston  
thummel@uh.edu

David Tiede  
Argonne National Laboratory  
tiede@anl.gov

Lisa Utschig  
Argonne National Laboratory  
utschig@anl.gov

Jao van de Lagemaat  
National Renewable Energy Laboratory  
jao.vandelagemaat@nrel.gov

Michael Wasielewski  
Northwestern University  
m-wasielewski@northwestern.edu

Benjamin Young  
Rhode Island College  
byoung@ric.edu

Xiaoyang Zhu  
Columbia University  
xyzhu@columbia.edu